

„Role of STAT3 N-terminal domain and GAS-site recognition in signaling and crosstalk with STAT1 and NF- κ B”

Von der Fakultät für Mathematik, Informatik und Naturwissenschaften der RWTH Aachen University zur Erlangung des akademischen Grades eines Doktors der Naturwissenschaften genehmigte Dissertation

vorgelegt von

Master of Science

Antons Martincuks

aus Riga, Lettland

Berichter: Professor Dr. Gerhard Müller-Newen
Universitätsprofessor Dr. Martin Zenke
Universitätsprofessor Dr. Bernhard Lüscher

Tag der mündlichen Prüfung: 23.01.2017

Diese Dissertation ist auf den Internetseiten der Universitätsbibliothek online verfügbar.

To my father (28.09.1961 – 26.01.2004)
Für meinen Vater (28.09.1961 – 26.01.2004)
Моему отцу (28.09.1961 – 26.01.2004)

Table of contents

Publications and coauthorships	2
Zusammenfassung	4
Abstract	5
I. Introduction	6
<u>1. Cellular signaling</u>	6
<u>2. JAK/STAT pathway</u>	7
2.1 History and pathway overview	7
2.2 Structure and functions of STAT proteins	9
2.3 IL-6/STAT3 signaling	11
2.3.1 IL-6 type cytokines	11
2.3.2 IL-6/STAT3 signal transduction	12
2.3.3 STAT3 in physiology and disease	14
2.3.4 The N-terminal domain of STAT3 in signaling	15
2.4 Crosstalk between STAT1 and STAT3	17
2.4.1 Opposing actions of STAT1 and STAT3	17
2.4.2 Crossregulation of IFN γ /STAT1 and IL6/STAT3 signaling	18
<u>3. STAT3 and NF-κB pathway crosstalk</u>	20
3.1 NF- κ B signaling overview	20
3.2 Canonical TNF α signaling	21
3.3 NF- κ B role in physiology and cancer	21
3.4 Structure and posttranslational modifications of p65	22
3.5 NF- κ B and STAT3 crosstalk	24
<u>4. Nucleocytoplasmic trafficking of proteins</u>	26
4.1 Molecular mechanism of nuclear import and export	26
4.2 Properties of importin- α adaptors	28
4.3 Nuclear trafficking of STAT1 and STAT3	29
<u>5. Aims of the study</u>	30
II. Materials and Methods	32
<u>1. Materials</u>	32
1.1 Chemicals and reagents	32
1.2 Plasmids	32
1.3 qPCR Primers	34
1.4 Mutagenesis primers	34

1.5 Genotyping primers	35
1.6 Antibodies	36
1.6.1 Primary antibodies	36
1.6.2 Secondary antibodies	36
1.7 Eukaryotic cell lines	37
1.7.1 Stably transfected cell lines	38
1.7.2 Growth medium	39
1.7.3 Cytokines and cytokine receptors	39
1.7.4 Transfection reagents	40
1.7.5 Other reagents	40
1.8 Prokaryotic cell lines	40
1.8.1 Cultivation	40
1.9 Antibiotics	41
 <u>2. Methods</u>	 42
2.1 Molecular biology methods	42
2.1.1 DNA restriction digest	42
2.1.2 Agarose gel electrophoresis	42
2.1.3 DNA fragment isolation	43
2.1.4 DNA fragment ligation	43
2.1.5 Transformation of competent E.Coli cells	43
2.1.6 Isolation of plasmid DNA	43
2.1.7 Measurement of DNA concentration	44
2.1.8 Plasmid DNA sequencing	44
2.1.9 Expression and purification of recombinant proteins	44
2.1.10 PCR– polymerase chain reaction	44
2.1.11 Quantitative PCR	46
2.1.11.1 RNA isolation and reverse transcription	46
2.1.11.2 qPCR	46
2.1.12 Site-directed mutagenesis	47
2.1.13 Genomic DNA isolation	47
2.2 Cell biology methods	48
2.2.1 Cell culture	48
2.2.2 Cell cryopreservation	48
2.2.3 Cell stimulation	49
2.2.4 Transient transfection of DNA	49
2.2.5 Stable transfection of DNA	49
2.2.5.1 Flp-In™ system	49
2.2.5.2 Flp-In™ T-Rex™ system	50
2.2.5.3 pMOWS system	50
2.2.6 Total cell protein extractions	50
2.2.7 Subcellular fractionation	51
2.2.8 Measurement of protein concentration	52
2.3 Biochemistry methods	52
2.3.1 SDS-Polyacrylamide-gel electrophoresis (SDS-PAGE)	52
2.3.2 Immunoblotting (Western-blot)	54
2.3.3 Coimmunoprecipitation	55
2.3.4 GST-pulldown	56
2.3.5 Electrophoretic mobility shift assay	56
2.4 Confocal laser scanning microscopy methods	58
2.4.1 Description	58

2.4.2 Microscope settings	58
2.4.3 Indirect immunofluorescence staining of cells	59
2.4.4 Live cell imaging	60
2.4.5 Quantification of nuclear STAT3-FP amounts	60
III. Results	61
<u>1. Characterization of stably transfected MEF Δ/Δ cells</u>	61
<u>2. The role of N-terminal domain and GAS-site recognition in STAT3 signaling</u>	65
2.1 Ligand-induced nuclear accumulation and DNA-binding ability of STAT3 are independent of each other.	65
2.2 STAT3 N-terminal domain deletion mutant remains in the cytoplasm in the form of activated dimers capable of GAS-element binding	68
2.3 STAT3 NTD is not required for binding to various importin- α isoforms	71
2.4 Nuclear export inhibition does not rescue impaired nuclear accumulation of (Δ N)STAT3	75
2.5 Basal nucleocytoplasmic shuttling does not require functional N-, SH2 or C-terminal domains	79
<u>3. STAT3-mediated regulation of STAT1 signaling</u>	81
3.1 Mutual intracellular crossregulation between STAT1 and STAT3 is asymmetric.	81
3.2 STAT3-mediated downregulation of IL-6-induced STAT1 activation relies on STAT3 transcriptional activity, but not on unique NTD functions.	84
<u>4. The crosstalk between NF-κB subunit p65 and STAT3</u>	89
4.1 Simultaneous visualization of p65 and STAT3 requires combined PFA and methanol treatment.	89
4.2 Absence of STAT3 has no significant effect on canonical TNF α -induced NF- κ B activation, nuclear translocation and target gene expression.	91
4.3 Absence of NF- κ B p65 subunit has no influence on IL-6-induced STAT3 signaling but leads to a decrease in STAT3 and STAT1 levels.	93
4.4 Inducible overexpression of STAT3 does not alter NF- κ B signaling, while total p65 increase leads to increased IL-6 induced STAT3 signaling and atypical STAT1 nuclear accumulation.	97
4.5 Weak interaction between NF- κ B p65 and STAT3 could be detected after TNF α , but not after IL-6 treatment.	100
<u>5. Characterization of STAT3-YFP knock-in mice.</u>	101
5.1 Generation and validation of transgenic mice.	101
5.2 Characterization of transgenic mice.	102
IV. Discussion	104
<u>1. STAT3-FP reproduces functional characteristics of endogenous STAT3</u>	105

<u>2. GAS-element-specific DNA recognition is dispensable for nuclear accumulation of STAT3</u>	106
<u>3. STAT3 N-terminal domain deletion mutant remains in the cytoplasm in the form of activated dimers capable of GAS-element binding</u>	108
<u>4. STAT3 NTD is not required for binding to various importin-α isoforms</u>	110
<u>5. Latent nucleocytoplasmic shuttling of STAT3 does neither require GAS-element recognition, nor functional N-terminal or SH2 domains</u>	113
<u>6. STAT3 downregulates gp130/STAT1 signaling via target gene expression</u>	116
<u>7. Canonical signaling of STAT3 and NF-κB are independent of each other but NF-κB supports expression and activation of STAT1 and STAT3</u>	122
<u>8. STAT3-YFP knock-in mice have been successfully generated</u>	127
 V. Summary and Outlook	 129
 VI. References	 135
 VII. Abbreviations	 156
 Acknowledgements	 165
 Curriculum Vitae (Deutsch)	 167
 Curriculum Vitae (English)	 169
 Eidesstattliche Erklärung	 171

„Research is what I'm doing when I don't know what I'm doing.”

Wernher von Braun

„A scientist in his laboratory is not only a technician: he is also a child placed before natural phenomena which impress him like a fairy tale.”

Marie Curie

„The human brain is an incredible pattern-matching machine.”

Jeff Bezos

Publications and coauthorships

Essential parts of this thesis are presented in following publications:

Martincuks A, Fahrenkamp D, Haan S, Herrmann A, Küster A, Müller-Newen G. Dissecting functions of the N-terminal domain and GAS-site recognition in STAT3 nuclear trafficking.
Cell Signal. 2016, 28(8):810-25.

Martincuks A, Andryka K, Küster A, Schmitz-Van de Leur H, Komorowski M, Müller-Newen G. Nuclear translocation of STAT3 and NF- κ B are independent of each other but NF-B supports expression and activation of STAT3.
Cell Signal. 2017, 32:36-47.

Martincuks A, Küster A, Schmitz-Van de Leur H, Müller-Newen G. STAT3-mediated regulation of gp130/STAT1 signaling relies on STAT3 transcriptional activity. (Manuscript in preparation)

Further publications:

Domoszlai T, Martincuks A, Fahrenkamp D, Schmitz-Van de Leur H, Küster A, Müller-Newen G. Consequences of the disease-related L78R mutation for dimerization and activity of STAT3.
J Cell Sci. 2014, 127(Pt 9):1899-910.

Schumacher A, Denecke B, Braunschweig T, Stahlschmidt J, Ziegler S, Brandenburg LO, Stope MB, Martincuks A, Vogt M, Görtz D, Camporeale A, Poli V, Müller-Newen G, Brümmendorf TH, Ziegler P. Angptl4 is upregulated under inflammatory conditions in the bone marrow of mice, expands myeloid progenitors, and accelerates reconstitution of platelets after myelosuppressive therapy.
J Hematol Oncol. 2015, 8:64.

Martin L, Peters C, Schmitz S, Moellmann J, Martincuks A, Heussen N, Lehrke M, Müller-Newen G, Marx G, Schuerholz T. Soluble Heparan Sulfate in Serum of Septic Shock Patients Induces Mitochondrial Dysfunction in Murine Cardiomyocytes. *Shock*. 2015, 44(6):569-77.

Martin L, Peters C, Heinbockel L, Moellmann J, Martincuks A, Brandenburg K, Lehrke M, Müller-Newen G, Marx G, Schuerholz T. The synthetic antimicrobial peptide 19-2.5 attenuates mitochondrial dysfunction in cardiomyocytes stimulated with human sepsis serum.
Innate Immunity. (Manuscript in revision)

Zusammenfassung

STAT3 (*signal transducer and activator of transcription 3*) ist ein ubiquitärer Transkriptionsfaktor, der in vielen biologischen Prozessen, wie Hämatopoese, Entwicklung und Immunantwort involviert ist. Eine Dysregulation der STAT3-Signaltransduktion ist bei der Entstehung und Progression von chronischen Entzündungen, Krebserkrankungen und Fibrose beteiligt.

Der erste Teil dieser Arbeit befasst sich mit den Funktionen der N-terminale Domäne (NTD) von STAT3 und der spezifischen DNS Bindung an GAS-Elemente bei der IL-6 vermittelten STAT3 Signalübertragung. Unsere Ergebnisse zeigen, dass GAS-Element Erkennung für den Zytokin-induzierten und basalen nukleären Import von STAT3 nicht essentiell ist. Demgegenüber zeigt die NTD-Deletionsmutante keine nukleäre Akkumulation nach IL-6 Stimulation und verbleibt im Zytoplasma in Form von phosphorylierten Dimeren, die imstande sind, GAS-Sequenzen zu erkennen. Die defekte Kerntranslokation von (Δ N)STAT3 konnte nicht durch fehlerhafte Assoziation mit α -Importin Molekülen erklärt werden. Außerdem konnten wir mechanistische Unterschiede zwischen aktivem und latentem nukleären Transport von STAT3 sowie zwischen aktivem Import von STAT3 und STAT1 aufzeigen.

Im zweiten Teil der Arbeit wurde die verstärkte Aktivierung von STAT1 nach IL-6 Stimulation in STAT3-defizienten Zellen analysiert. Unsere Befunde deuten auf eine STAT3 vermittelte Beschränkung der IL-6 induzierten STAT1 Aktivierung durch STAT3 Zielgenexpression und nicht durch spezifische Eigenschaften der NTD von STAT3 hin.

Im dritten Teil dieser Arbeit zeigten wir, dass STAT3 und NF- κ B keinen direkten gegenseitigen Einfluss auf die klassische Signalübertragung haben. Stattdessen korreliert die Expression der NF- κ B p65 Untereinheit mit der intrazellulären Gesamtmenge an STAT1 und STAT3.

Im letzten Teil der Arbeit wurden STAT3-YFP *knock-in* Mäuse als neues *in vivo* Untersuchungsmodell beschrieben und charakterisiert. Unsere Daten zeigten, dass transgene Mäuse erfolgreich generiert wurden und die YFP-Fluoreszenz mittels diverser Mikroskopietechniken nachgewiesen werden kann. Das STAT3-YFP *knock-in* Mausmodell kann für weiterführende Analysen der Funktionen von STAT3 *in vivo* genutzt werden.

Abstract

Signal transducer and activator of transcription 3 (STAT3) is a ubiquitous transcription factor involved in many biological processes, including hematopoiesis, development and immune response. Dysfunctional STAT3 signalling has been reported in many pathophysiological conditions such cancer, chronic inflammation and fibrosis.

In the first part of this work, we investigated the functions of the N-terminal domain and GAS-site recognition during IL-6-induced STAT3 signaling. Our results demonstrate the nonessential role of GAS-element recognition for both cytokine-induced and basal nuclear import of STAT3. In turn, deletion of the NTD markedly decreased nuclear accumulation upon IL-6 treatment resulting in a prolonged accumulation of phosphorylated dimers in the cytoplasm, at the same time preserving specific DNA recognition ability of the truncation mutant. Observed defect in nuclear localization could not be explained by flawed importin- α binding. Furthermore, our data indicated mechanistic differences between active and latent nuclear trafficking of STAT3, as well as between STAT1 and STAT3 active nuclear import.

In the second part of this thesis, we analyzed the excessive STAT1 activation in STAT3-deficient cells upon IL-6 treatment. Our findings show that STAT3-mediated regulation of IL-6-induced STAT1 signaling depends on STAT3 target gene expression, but not on isolated STAT3 NTD functions.

In the third part, we demonstrated that NF- κ B and STAT3 have no direct influence on each other canonical signaling pathways. Instead, the expression of NF- κ B subunit p65 correlates with total levels of STAT1 and STAT3.

In the final part of this work, we characterized a STAT3-YFP knock-in murine model as a potentially powerful tool for the visualization of STAT3 *in vivo*. Our data show that STAT3-YFP Knock-In mice have been successfully generated and that the YFP fluorescence can be detected by common microscopy techniques. The STAT3-YFP knock-in mice will be a valuable tool for deciphering the function of STAT3 *in vivo*.

I Introduction

1. Cellular signaling

Each biological organism consists of basic building blocks called cells which function as the elementary structural, functional, and biological units of life that can replicate independently. Each cell organizes its core intracellular processes into an infrastructure of various organelles separated by membranes. However, cells do not live in isolation. Intercellular communication is a fundamental feature of all unicellular and multicellular organisms and governs the proper development and function of every living organism [1].

In order to perceive and correctly respond to their microenvironment, cells utilize a complex system of communication named cell signaling that involves sending, receiving and processing of extracellular signals. Most signals are chemical ligands in nature and are recognized by specific receptors on or in target cells. When a signaling molecule binds to a receptor, it alters the activity of the receptor, triggering a change inside the cell that leads to a programmed response [2].

When an extracellular ligand activates a specific receptor located on the cell membrane, this receptor triggers a biochemical chain of events inside the cell termed intracellular signal transduction. Depending on the signal and cell type, the response may vary from altering metabolism, shape or gene expression profiles, to trigger differentiation, proliferation, apoptosis and other processes. The signal can be further amplified at any step and generate a massive response within a single cell [3].

Converting extracellular signals into cellular responses is not direct and generally involves several intermediate proteins or small molecules. Depending on receptor and intracellular molecules involved, several signal-transducing pathways have been described both in prokaryotes and eukaryotes [1-3]. Two examples of major signaling pathways are the evolutionary conserved JAK/STAT and NF- κ B pathways, which will be the main focus of this work.

2. JAK/STAT pathway

2.1 History and pathway overview

One class of secreted signaling molecules that control many biological processes is called cytokines. They regulate growth and differentiation of specific types of cells and are of particular importance in the immune system and blood cell formation. Cytokines are proteins which are secreted by different cells and are further classified according to their biological functions into interferons, interleukins, colony-stimulating factors, tumor necrosis factors and chemokines. The interferons (IFN) were originally discovered as agents that interfere with viral infections almost 60 years ago [4]. Further investigation into the exact molecular mechanism of interferon signaling more than 20 years ago led to the discovery of the JAK (Janus tyrosine kinase)-STAT (signal transducer and activator of transcription) pathway as a remarkably simple pathway for membrane to nucleus intracellular signal transduction [5].

The JAK/STAT pathway represents an evolutionary conserved signal transduction cascade mainly involved in hematopoiesis and immunity. During the last two decades, significant progress has been made in the identification of multiple STATs and regulatory proteins [6]. First, the Darnell group identified a protein complex named interferon-stimulated gene factor 3 (ISGF3) that was activated in the cytoplasm upon type I IFN stimulation and bound specific DNA elements called IFN stimulated response element (ISRE), which then led to transcriptional activation of IFN-dependent genes [7, 8]. ISGF3 was comprised of 113, 91, 84 and 48 kDa proteins, the 91 and 84 kDa proteins being two isoforms of the same protein generated through alternative splicing [8]. In parallel, a separate promoter for type II IFN-mediated transcriptional initiation was identified (gamma IFN-activated site, GAS) with a sequence different from ISRE [9]. The transcriptional complex bound to this sequence consists exclusively of the 91 kDa species, previously identified within the ISGF3 complex [10]. At this point, the name STAT1 was given to the 91 kDa protein and STAT2 to the larger 113 kDa protein within the ISGF3 complex [5]. A critical phosphorylation site at Y701 within STAT1 was identified as an essential

posttranslational modification for IFN-driven activation [10,11]. In subsequent years several other phosphotyrosine-containing DNA binding transcription factors were identified. In 1994 the laboratory of Friedemann Horn at the Institute for Biochemistry at RWTH Aachen, where this thesis was written, in parallel with the Kishimoto group identified and cloned the acute phase response factor (APRF) which is activated by interleukin-6 (IL-6) [12, 13]. This transcription factor, that also binds GAS elements, was later shown to be related to STAT1 and renamed STAT3 [14, 15]. Later on, STAT4 (activated by IL-12) [16, 17], differentially expressed STAT5A and STAT5B [18,19], as well as STAT6 (activated by IL-4) [20] were identified.

STATs are now considered as transcription factors that relay signals from activated receptors in the plasma membrane to the nucleus, where they regulate gene expression. According to the canonical model, inactive STAT proteins exist as latent monomers prior to stimulation and their activation requires dimerization via phosphotyrosine-SH2 domain interactions upon phosphorylation of a critical tyrosine residue by receptor-associated JAK kinases (Fig. 1.1). Upon ligand-binding, cytokine receptors undergo conformational changes that get JAKs into proximity of each other, allowing mutual activation by trans-phosphorylation. Activated JAKs phosphorylate cytokine receptors creating phospho-docking sites for STATs. STATs recruited to receptors are also phosphorylated by JAKs at a single tyrosine residue. Activated STATs dimerize followed by nuclear translocation and sequence-specific DNA-binding, resulting in gene transcription [21-23].

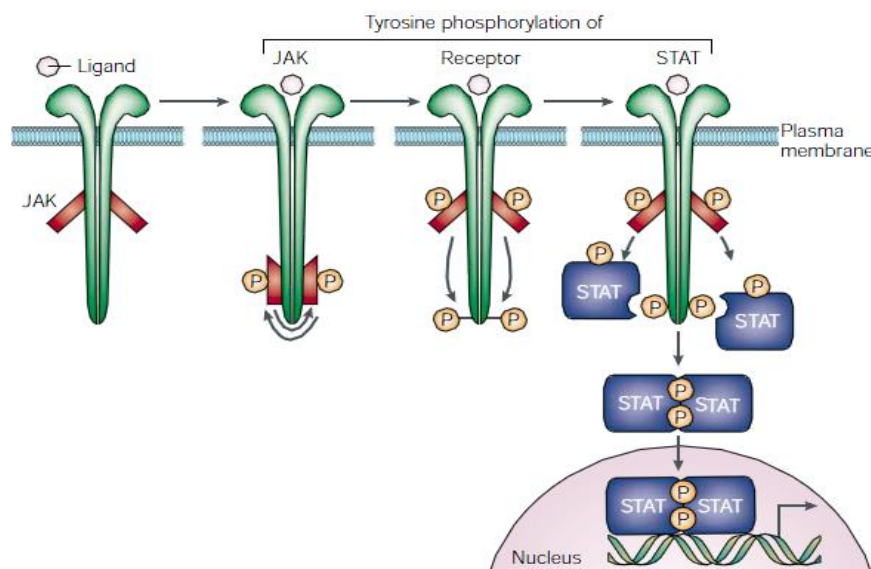


Fig. 1.1: Canonical JAK/STAT pathway. P – Tyrosine phosphorylation [21].

In recent years, various non-canonical aspects of JAK/STAT signaling have emerged, adding more complexity to this pathway [24]. Almost all unphosphorylated STAT proteins apart from a monomeric fraction exist as preformed or latent dimers in resting cells in the absence of the activating tyrosine phosphorylation [25]. Moreover, latent STAT proteins constitutively shuttle between nucleus and cytoplasm in the absence of cytokine stimulation [26, 27]. Unphosphorylated STATs (U-STATs) have been shown to drive specific gene expression by mechanisms distinct from those used by phosphorylated STATs [28] and act as transcriptional cofactors or corepressors [29, 30]. Furthermore, apart from cytokine receptors, STAT proteins can be activated by receptor tyrosine kinases (RTKs), several cytoplasmic kinases and G-protein-coupled receptors (GPCRs) [21, 31]. Finally, STAT3 has been demonstrated to have functions in regulation of mitochondrial respiration [32], stabilization of microtubules and cell migration [33]. Taken together, all these data demonstrate that JAK/STAT signaling is much more complex than previously thought.

2.2 Structure and functions of STAT proteins

In mammals seven structurally and functionally related STATs have been identified: STAT1, STAT2, STAT3, STAT4, STAT5A, STAT5B and STAT6. They range in size from 749 (STAT4) to 851 (STAT2) amino acids and share a similar structure that consists of seven conserved domains (Fig. 1.2) [34].

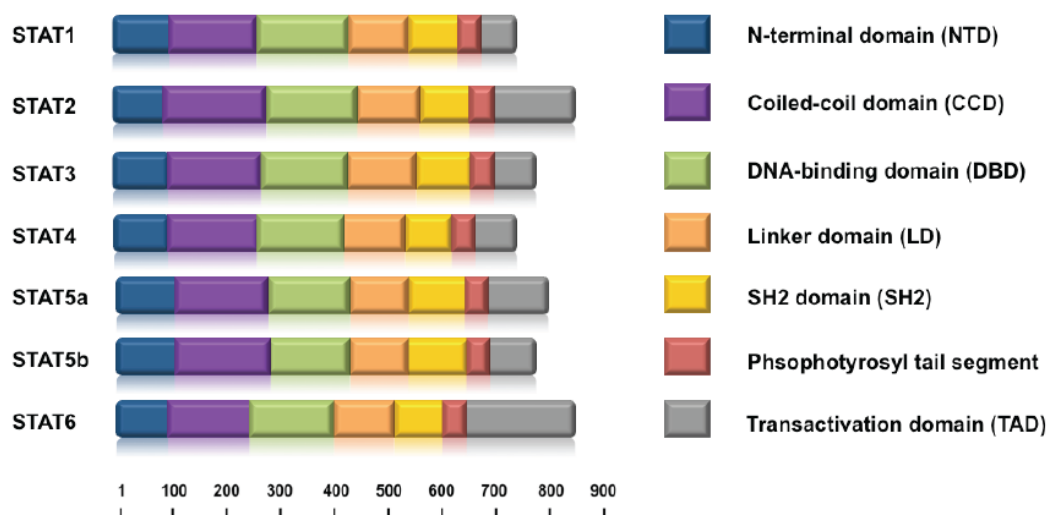


Fig. 1.2: Structural domains of STAT proteins [35].

N-terminal domains (amino-terminal, NH₂ domains, NTD) of STATs play major roles in oligomerization and nuclear accumulation. Coiled-coil domains (CCD) are essential for nuclear import/export cycle, as well as receptor binding. DNA-binding domains (DBD), as the name implies, direct DNA binding and are also involved in nuclear trafficking. Linker domains (LD) are cooperating in DNA binding, nuclear egress and transcriptional activity of STAT proteins. Src Homology 2 (SH2) domains are critical for receptor recruitment, dimerization and nuclear export. Phosphotyrosyl tails harbor critical tyrosine residues for stimulus-induced activation and dimerization, while transactivation domains (TAD) are important for dimerization, nuclear escape and full transcriptional activity of STATs. All domains are participating in physical interactions with other proteins [21, 22, 34].

Recent advances in measuring cell-specific transcriptomes and epigenomes together with gene-targeted mice revealed several thousands of genomic targets for STATs both in driving and repressing transcription [36]. Generation of STAT-deficient mice revealed many physiologically relevant actions of these molecules (Tab. 1.1) [31, 37].

Tab. 1.1: Phenotypes of STAT deficient mice

Genotype	Phenotype
STAT1 ^{-/-}	Viable and fertile, defective responses to type I and II interferons, increased susceptibility to tumorigenesis
STAT2 ^{-/-}	Viable and fertile, defective responses to type I interferons, reduced STAT1 levels in specific tissues
STAT3 ^{-/-}	Embryonic lethal, conditional knockouts have multiple defects in adult tissues (impaired survival and response to pathogens)
STAT4 ^{-/-}	Viable and fertile, defective IL-12-driven Th1 differentiation, increased susceptibility to intracellular pathogens
STAT5A ^{-/-}	Viable and fertile, defective mammary gland development and prolactin functioning
STAT5B ^{-/-}	Viable and fertile, defective growth and growth hormone signaling
STAT5A/B ^{-/-}	Viable but infertile, defective mammary gland development, growth and T-cell proliferation
STAT6 ^{-/-}	Viable and fertile, defective IL-4-driven Th2 differentiation, increased susceptibility to helminthic invasion

Unlike all other members of the *Stat* gene family, complete knockout of STAT3 leads to embryonic lethality in mice [38], while conditional tissue-specific gene targeting led to impairment of various functions in different cell types [39]. STAT3 is activated by a wide variety of cytokines, including the entire IL-6 (see section 1.2.3.1) and IL-10 (IL-10, IL-19, IL-20, IL-22, IL-24, IL-26) families, as well as G-CSF, leptin, IL-21, IL-27, various growth factors, oncogenes and other stimuli [22]. These data demonstrate that STAT3 has the most pleiotropic functions amongst all seven mammalian STAT proteins and might represent a primordial STAT protein [39]. Since the IL-6-type cytokines that signal through the ubiquitously expressed cytokine receptor gp130 are among best studied and potent physiological activators of STAT3 [40], IL-6/STAT3 signaling and its crosstalk with other signaling pathways will be the main topic of this work.

2.3 IL-6/STAT3 signaling

2.3.1 IL-6 type cytokines

The family of IL6-type cytokines consists of several proteins with molecular masses of about 20 kDa: IL-6, IL-11, IL-27, IL-31, IL-35, LIF (leukemia inhibitory factor), OSM (oncostatin M), CNTF (ciliary neurotrophic factor), CT-1 (cardiotrophin-1), CLC (cardiotrophin-like cytokine) and NP (neuropoietin). They are important mediators involved in the regulation of the acute-phase response to injury and infection, hematopoiesis, liver and neuronal regeneration, bone metabolism, embryonal development and fertility (Fig. 1.3).

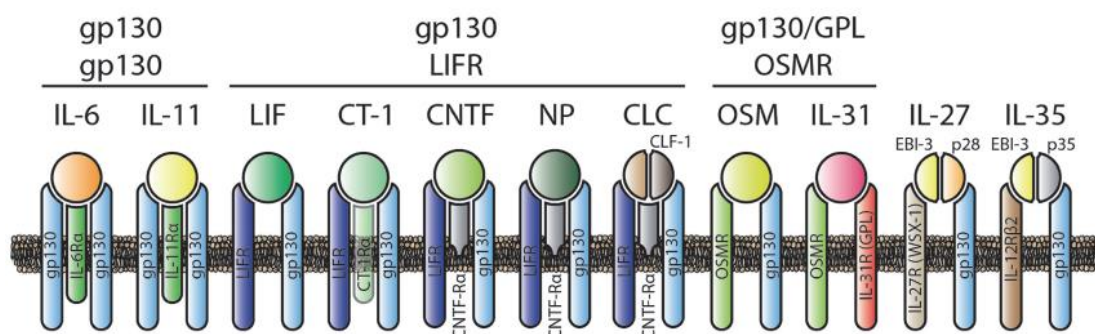


Fig. 1.3: IL-6-type cytokine receptor complexes. All complexes (except for IL-31) contain at least one gp130 subunit. IL6 and IL-11 bind to homodimeric complexes, other members of IL-6 family bind heterodimers [41].

Receptors of the IL-6-type cytokines consist of non-signaling ligand binding α -receptors (for example IL-6R α , also known as gp80) and the signal transducing receptors (gp130, LIFR, and OSMR), which bind to JAKs and become tyrosine phosphorylated upon ligand stimulation [40, 42, 43].

Glycoprotein 130 is a common subunit of the receptor complexes for almost all cytokines of the IL-6 family, serving at least ten cytokines with the help of other eight receptors forming homo- and heterodimers [44]. Although gp130 is ubiquitously expressed, the number of cells that respond to IL-6-type cytokines is limited, because the expression of the ligand binding subunits (α -receptors) is more tightly regulated. Apart from membrane-bound receptor complexes soluble forms of IL-6-type receptors have been described. They modulate local and systemic responses to cytokines and are formed either by shedding of membrane-bound receptors or by translation from an alternatively spliced mRNA [40].

2.3.2 IL-6/STAT3 signal transduction

In resting cells STAT3 molecules exist as monomers, as well as homodimers or heterodimers with STAT1 [25, 45-47]. Moreover, like all members of the STAT family, unphosphorylated STAT3 (U-STAT3) continuously shuttles in and out of the nucleus without any stimulus or upstream activation [48-50], being able to regulate gene transcription [28].

Cytokine receptor gp130 forms complexes with JAK1, JAK2 and TYK2 [36], with JAK1 being the essential kinase for IL-6-dependent signaling [51]. Upon IL-6 stimulation, STAT3 molecules are recruited via their SH2 domains to phospho-YXXQ motifs of gp130 and become phosphorylated at the critical Y705 residue. Then, phosphorylated STAT3 proteins form activated homodimers or heterodimers with STAT1 and translocate into the nucleus with the help of active transport, where it binds to GAS elements and regulates the expression of a specific set of genes [40]. Whether specific GAS recognition is required for activated STAT3 to accumulate in the nucleus of cytokine stimulated cells remains unclear.

Of note, dimer to monomer ratio of STAT3 species does not change significantly after stimulation [47, 50, 52] and both preformed and activated STAT3 dimers exist in a similar parallel orientation in contrast to latent antiparallel dimers of STAT1 and STAT5 [53]. Moreover, nuclear accumulation of STAT3 in response to cytokine stimulation is achieved not only by active dimer translocation to the nuclei, but also by reduced nuclear export and overall shuttling, as demonstrated in living cells [49]. STAT3 phosphorylation and DNA binding decrease after 30 min of IL-6 stimulation via negative feedback and reach control levels after 60 min [54, 55].

Among STAT3-induced genes, suppressor of cytokine signaling 3 (SOCS3) is a classical negative feedback inhibitor that specifically affects signaling mediated by IL-6 and gp130 by acting on the JAKs and receptor [56, 57]. Apart from SOCS3 there are other ways to terminate IL-6-induced STAT3 signaling via protein tyrosine phosphatases, the protein inhibitor of activated STAT3 (PIAS3) and other proteins. After DNA binding and transcription initiation STAT3 is dephosphorylated and either degraded or exits the nucleus via CRM1-mediated export into the cytoplasm until the next activation event occurs (Fig.1.4) [40, 48, 49, 58].

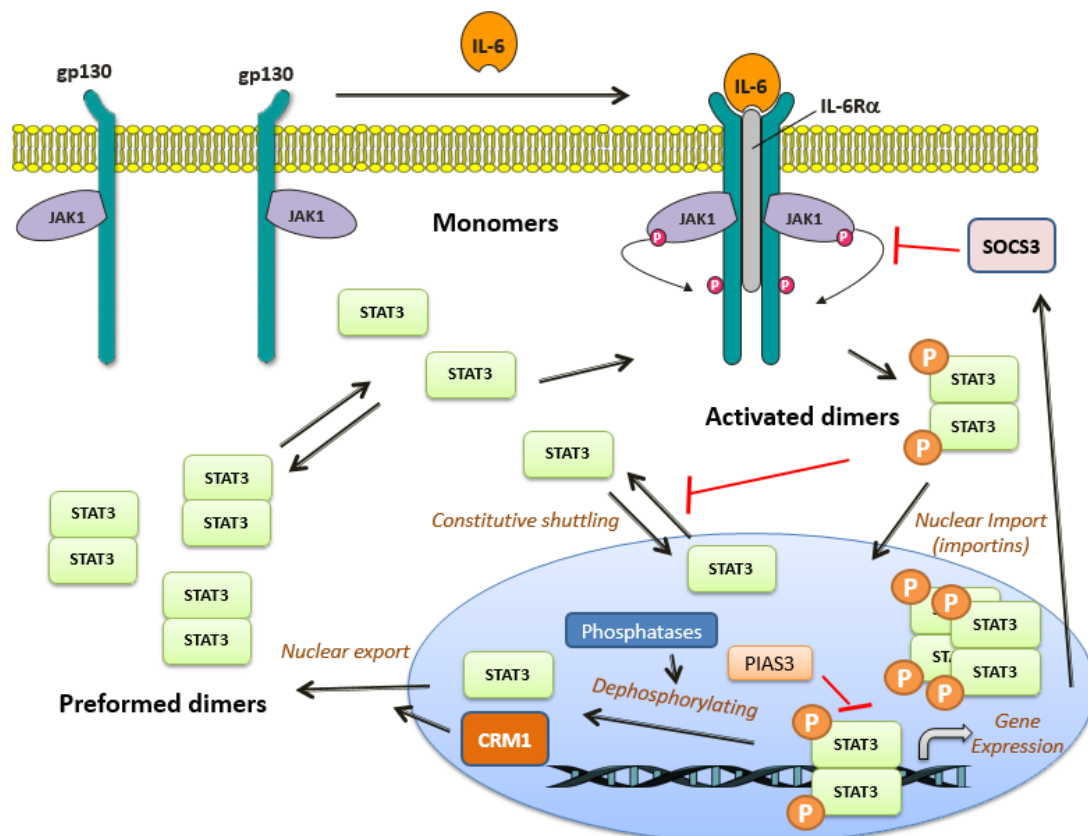


Fig. 1.4: In-depth IL6/STAT3 Signaling model.

2.3.3 STAT3 in physiology and disease

STAT-induced genes have distinctive response elements within their promoters. Biochemical studies have determined that the GAS element TTCN₂₋₄GAA consensus sequence defines the optimal binding site for all STATs, and STAT3 favors n=2 spacing within elements [59]. Global chromatin surveys showed that STAT3 binds at least 3,000 different gene promoters [60] and conditional knockout experiments demonstrated a crucial role for STAT3 in acute phase gene expression, embryonic development, differentiation, anti-apoptotic and pro-survival gene expression [21, 37, 39, 61]. Tissue-specific ablation revealed a prominent role of STAT3 in a wide variety of physiological processes summarized in Tab. 1.2.

Tab. 1.2: Phenotypes of tissue-specific STAT3 ablation [39]

STAT3^{-/-} Cells	Phenotype
Keratinocytes	Impaired 2nd hair cycle, wound repair and keratinocyte migration
Mammary cells	Delayed mammary involution, opposing role to STAT5
Hepatocytes	Impaired acute phase response
Neurons	Impaired survival after damage
T cells	Impaired IL-6 dependent survival and differentiation
Monocytes/Neutrophils	Enhanced inflammatory response and chronic inflammation

STAT3 activation within immune cells is associated with immunosuppression, promoting the immune evasion of the tumor, differentiation of macrophages toward the anti-inflammatory M2 phenotype and the decrease of functional dendritic cells [62]. On the other hand, IL-6- or IL-23-driven STAT3 signaling is critical for inflammatory Th17 cell differentiation in mice and humans [63, 64]. Moreover, In B-cells STAT3 positively regulates an early step in development by promoting differentiation and survival [65]. Finally, although platelets lack nuclei and transcriptional activity, STAT3 has been shown to promote platelet aggregation by enhancing collagen-induced signaling as a scaffold protein [66]. This dual role in diverse and even opposed physiological processes can be explained in part by the induction of distinct sets of target genes by STAT3 in different cells [39, 61].

Dysfunctional STAT3 signaling has been described as having a leading role in cancer progression, chronic inflammation and autoimmune diseases [67, 68]. Prolonged activation of STAT3 has been detected in several types of human cancers, including all the major carcinomas (breast, colon, gastric, lung, head and neck, skin, pancreas, prostate) as well as some hematologic tumors [69]. IL-6-STAT3 signaling is a major pathway for cancer progression having a key role in regulating many target genes central for cancer inflammation in the tumor microenvironment. Moreover, numerous STAT3-regulated genes encode cytokines and growth factors, the receptors of which in turn reactivate STAT3 signaling, thereby promoting a stable feedforward loop [68]. However, a tumor suppressing role for STAT3 has also been described [70, 71] and, depending on the mutational profile, STAT3 has been found to act both as a tumor suppressor and as an oncogene in primary brain tumors [72], which makes the exact role of STAT3 in cancer progression very complex.

Inhibition of STAT3 can reverse tumor growth while having few effects in normal cells under experimental conditions, which implicated STAT3 as a significant target for therapy [60, 69]. Over the years, SH2 domain interaction and specific DNA recognition seem to be the most targetable properties of STAT3 for the development of new anti-cancer drugs [73]. Recently, the N-terminal domain (NTD) of STAT3 has also been proposed as a promising therapeutic target for cancer therapy [74].

2.3.4 The N-terminal domain of STAT3 in signaling

NTDs are involved in many important aspects of STAT signaling, including oligomerisation and protein-protein interactions [21]. Interestingly, these domains appear later in evolution and it has been proposed that the NTDs development expanded STAT functions by allowing more flexibility on DNA binding [75]. Structural data suggests that NTDs can fold independently [76] and are tightly involved in homotypic dimerization of STAT proteins [77]. Despite high sequence similarity, NTD-driven homodimer formation of STAT1, STAT4 and STAT3 have different dissociation constants, STAT3 having the lowest homotypic affinity of them all [78].

STAT3 NTD (aa 1-124) was first shown to be essential for tetramerisation at the $\alpha 2$ -*macroglobulin* gene promoter, which is required for the maximal IL-6-induced transcriptional activation [79]. It was originally suggested that the NTD of STAT3 is dispensable for cytokine-induced nuclear accumulation and those gene expression that does not require tetramerisation, such as *socs3* [80]. However, further investigations unveiled a more prominent role of the NTD for STAT3 signal transduction. First, our group previously demonstrated that the NTD of STAT3 is critical for preformed dimer formation, but is dispensable for basal nucleocytoplasmic shuttling, indicating that dimerization of unphosphorylated STAT3 is not required for latent nuclear import [52]. Second, the NTD has been shown to be essential for interaction with p300 and subsequent STAT3 acetylation [81], as well as complex formation with APE1, which is required for stable chromatin association in the IL-6-dependent hepatic acute phase response [82]. Third, monoubiquitination of an evolutionary conserved lysine located in the NTD of STAT3 is critical for recruitment of BRD4, a component of the active PTEFb complex in RNA Pol II-mediated transcriptional elongation [83].

In embryonic fibroblasts of STAT3 KO mice reconstituted with a NTD-deleted STAT3 mutant ((Δ N)STAT3), the truncated transcription factor was unable to efficiently induce both STAT3-mediated reporter activity and endogenous mRNA expression [84]. A recent study demonstrated decreased induction of many STAT3-regulated genes upon NTD deletion despite similar levels of tyrosine 705 phosphorylation in response to LIF treatment [85]. Moreover, the NTD of STAT3 is required for dominant-negative activity of the STAT3-Y705F mutant [86] and selective pharmacological inhibition of STAT3 NTD induced apoptotic death in cancer cells [87]. Finally, although NTD deletion mutants can bind GAS DNA sequences in an EMSA assay [52, 79], it was demonstrated that NTD deletion resulted in an unexpected defect in cytokine-induced nuclear accumulation of STAT3 [52], suggesting a potential role for the NTD in active nuclear import of the phosphorylated STAT3 dimer. Taken together, these findings point to a more prominent role of NTD in STAT3 signaling that needs further investigation.

2.4 Crosstalk between STAT1 and STAT3

2.4.1 Opposing actions of STAT1 and STAT3

Opposing roles of STAT1 and STAT3 in physiology and disease represent another noteworthy aspect of JAK/STAT signaling. While STAT3 activation usually promotes cell survival, proliferation, motility and immunosuppression, STAT1 signaling mostly leads to apoptotic, anti-proliferative and immune responses. Despite high sequence similarity and being activated downstream of common cytokine and growth factor receptors, their actions are reciprocally regulated. An imbalance in their expression or activation status may redirect cytokine signals in either direction, which can have significant consequences [88-90].

STAT1 is a central player in IFN signaling, mediating signals of both type I (IFN α , IFN β) and type II (IFN γ) interferons, which are involved in cell growth regulation and antiviral response. Type I IFNs lead to both STAT1 and STAT2 activation triggering ISGF3 transcriptional complex formation and binding to ISRE sequences. In turn, IFN γ triggers prolonged STAT1 activation via IFN-gamma receptor (IFNGR), STAT1/STAT1 homodimer formation and GAS element binding within interferon-inducible genes [21]. Of note, both type I and II IFNs also activate STAT3, albeit less efficiently [91]. IFN γ /STAT1 pathway prevents the expansion of normal and tumor cells via pro-apoptotic and anti-proliferative gene induction and pro-survival gene downregulation [88, 92]. At the same time, STAT1 activation directly induces pro-inflammatory gene expression, antigen presentation and development of Th1 lymphocytes. Thus, STAT1 acts as tumor suppressor and enhances anti-tumor immunity [88-90].

In turn, STAT3 signaling upon either IL-6 and IL-10 stimulation promotes proliferation and inhibits apoptosis by inducing specific target genes. STAT3 signaling plays a major role in anti-inflammatory responses, including downregulation of antigen-presentation and deactivation of myeloid cells, which results in the escape of neoplastic cells from immune surveillance. In contrast to STAT1, STAT3 is mainly considered as an oncogene, because activated STAT3 can mediate cellular

transformation by itself and its constitutive activation is reported in nearly 70% of solid and hematological tumors [89, 93]. Opposing roles of STAT1 and STAT3 in oncogenesis are summarized in Fig. 1.5.

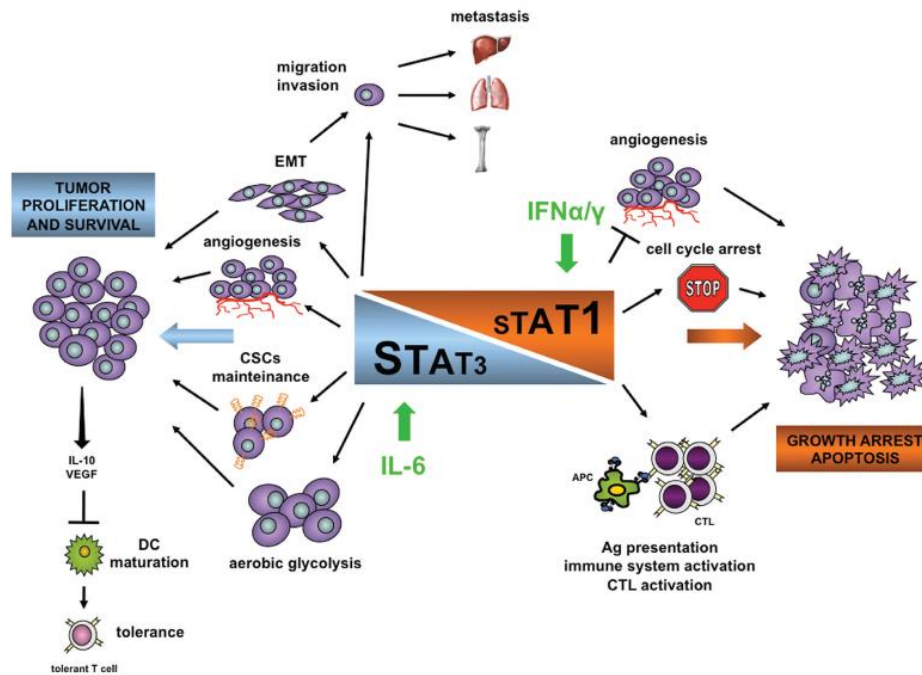


Fig. 1.5: Opposite effects of STAT1 and STAT3 in cancer development [90]

2.4.2 Crossregulation of IFN γ /STAT1 and IL6/STAT3 signaling

As discussed above, IFN γ /STAT1 and IL-6/STAT3 have opposing actions in cell proliferation, apoptosis and inflammatory processes. However, several reports show that STAT1 and STAT3 may combine with the same docking sites within both IFNGR and gp130 [40, 94]. Preferential binding of STAT1 and STAT3 to IFNGR and gp130 after IFN γ and IL-6 stimulation, respectively, can be explained by different affinities of STAT proteins to both receptors. After IFN γ treatment, STAT1 had a much higher affinity for the phospho-Y419 motif in IFNGR1 than STAT3 [95], while upon IL-6 stimulation STAT3 is able to bind flexible phospho-YXXQ motifs (Y767, Y814, Y905 and Y915) in gp130, whereas STAT1 is recruited only to the more restricted consensus sequences phospho-YXPQ (Y905, Y915) [40]. Although STAT1 is transiently activated upon IL-6 type cytokine stimulation, this gp130-mediated activation leads to much less efficient STAT1 phosphorylation and nuclear

translocation compared to IFN γ treatment, while STAT3 activation is more sustained [96, 97]. On the other hand, STAT3 is phosphorylated transiently in response to IFN γ in wild-type murine embryonic fibroblasts (MEF) and human follicular dendritic cell-like cells but only STAT1 is essential for proper signaling and relevant target gene upregulation [94, 98]. Interestingly, IFN γ stimulation did not show any detectable STAT3 activation in HUVEC and U4C-JAK1 cells [97, 99], suggesting that atypical STAT3 phosphorylation upon IFN γ treatment is cell-lineage specific.

In addition, experiments with STAT-deficient cells provided interesting results that may add to the understanding of mutual crossregulation between STAT1 and STAT3. First, IL-6 induced an IFN γ -like response in STAT3 $^{-/-}$ MEFs, including increased and prolonged STAT1 phosphorylation and DNA association [100]. Next, activation of STAT3 after IFN γ stimulation was also much stronger and more sustained in STAT1 $^{-/-}$ MEFs [94]. Furthermore, STAT3 knockout cells displayed enhanced gene expression and antiviral activity in response to IFN α and IFN β treatment [101], while constitutively active STAT1 (STAT1C) attenuated IL-6-induced STAT3 activation in multiple myeloma cells [102]. Taken together, all these observations suggest an intrinsic mutual crossregulation between STAT1 and STAT3 signaling, which deserves further clarification. A simplified model of IFN γ /STAT1 and IL-6/STAT3 signaling crosstalk is presented in Fig. 1.6.

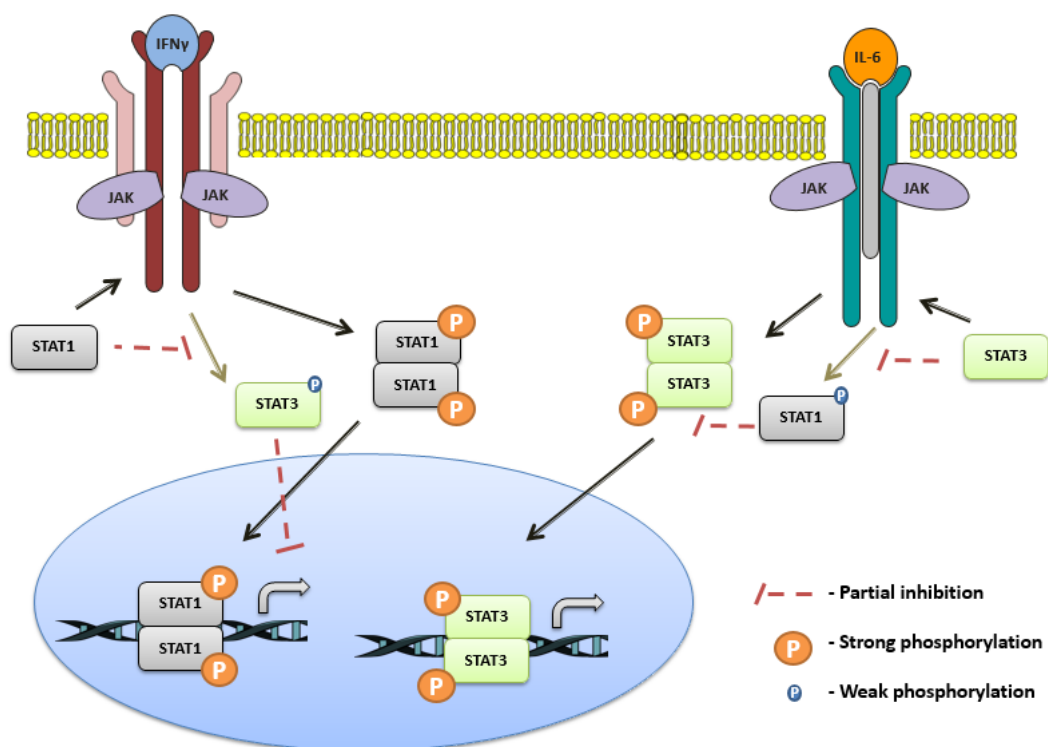


Fig. 1.6: IFN γ /STAT1 and IL-6/STAT3 cross-regulation

3. STAT3 and NF- κ B pathway crosstalk

3.1 NF- κ B signaling overview

The pleiotropic transcription factor nuclear factor kappa B (NF- κ B) is a crucial regulator of many physiological and pathophysiological processes, including control of adaptive and innate immune responses, inflammation, proliferation, apoptosis and tumorigenesis. NF- κ B is found in essentially all cell types and is a collective name for inducible dimeric transcription factors composed of members of the Rel family of DNA-binding proteins that recognize a common sequence motif. Found in *Drosophila* and molluscs, the NF- κ B signaling appeared early in evolution, regulates an exceptionally large number of genes and has been intensively investigated for over two decades. [103-107]. Several signaling pathways are known that lead to activation of NF- κ B (Fig. 1.4):

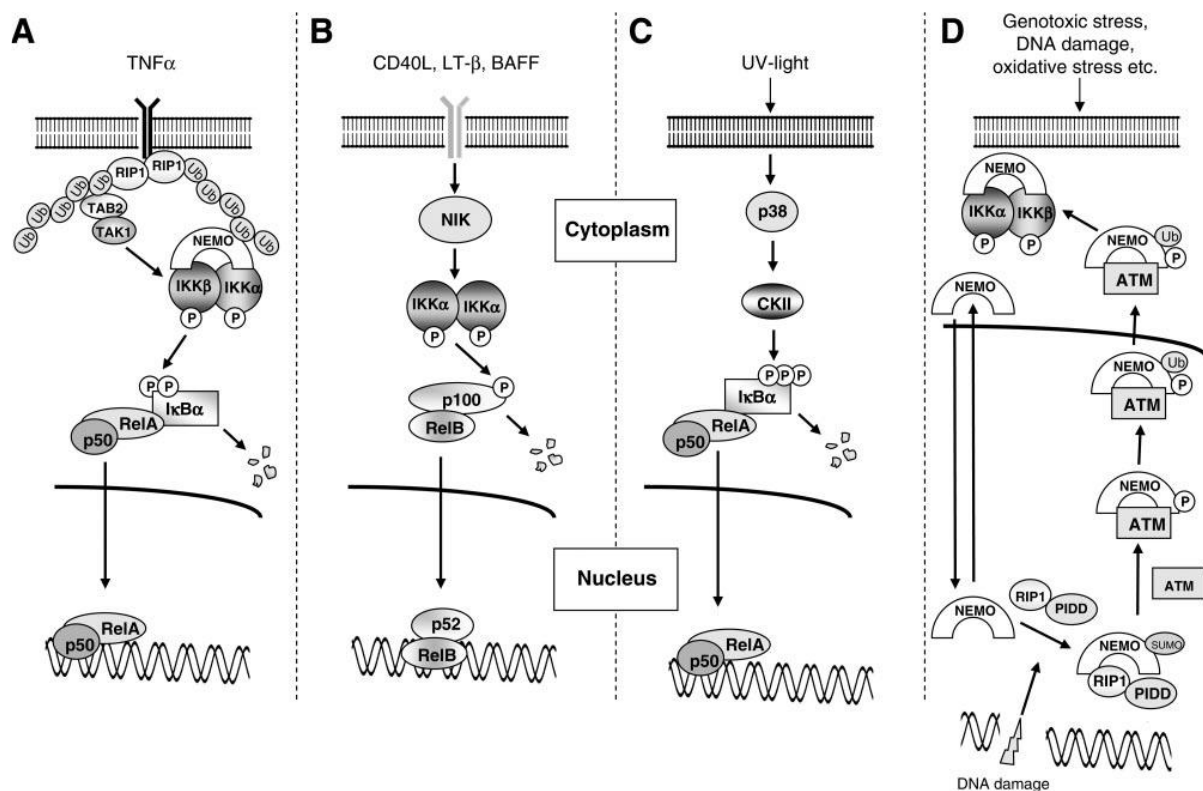


Fig. 1.7: Major NF- κ B activating pathways. A. Canonical NF- κ B activation by TNF α . The classical p65/p50 heterodimer translocates into the nucleus to induce gene expression. B. Alternative or non-canonical NF- κ B activation pathway. RelB/p52 heterodimer translocates into the nucleus. C,D Atypical NF- κ B activation. Triggered via UV and p38 MAP kinase (C) or via genotoxic stress (D) [106].

3.2 Canonical TNF α signaling

For the purpose of this work I will only focus on the classical or canonical NF- κ B activating pathway in response to TNF α stimulation via TNF-receptors (TNFR) (Fig. 1.7 A). NF- κ B is maintained in an inactive form by sequestration in the cytoplasm through interaction with inhibitors of kappa B alpha (I κ B α). Stimulation of TNFRs with their cognate ligands activates TNFR-associated factor (TRAF) proteins and subsequently TGF β -activated kinase 1 (TAK1), which phosphorylates and activates I κ B kinase complex (IKK). The IKK complex consists of three components - the kinases IKK α and IKK β and the noncatalytic, regulatory IKK γ or NF- κ B essential modulator (NEMO). While IKK α is also found in the nucleus where it is recruited to the promoter regions of NF- κ B dependent genes and contributes to the stimulation of gene expression, IKK β is mostly found in the cytoplasm, where it phosphorylates I κ B α at serines 32 and 36, resulting in K48-linked poly-ubiquitination of I κ B α by the SCF- β TrCP ubiquitin-ligase complex and degradation by the proteasome. Proteolytic degradation of I κ B α immediately leads to and is required for NF- κ B nuclear translocation (Fig. 1.4A) [103-107]. Following degradation of I κ B α , the liberated NF- κ B dimers move to the nucleus and bind to promoter and enhancer regions, which typically bear κ B sites with the consensus sequence GGGRNWYYCC (N - any base, R - purine; W - adenine or thymine and Y - pyrimidine) [108]. The DNA-binding specificity and affinity are determined by the composition of NF- κ B dimers [109]. NF- κ B-dependent re-synthesis of I κ B α proteins as part of a negative feedback loop and additional mechanisms then lead to NF- κ B dimer dissociation and CRM1-dependent nuclear export [110, 111]. Remarkably, NF- κ B/I κ B α complexes shuttle between cytoplasm and nucleus of nonactivated cells similarly to STATs and this process leads to a basal transcriptional activity of NF- κ B [112].

3.3 NF- κ B role in physiology and cancer

NF- κ B transcription factor has been implicated in a variety of functions (Fig. 1.8), including innate immunity, which represents a first line of defense against invading pathogens. During this process, NF- κ B-mediated transcription of genes encoding

cytokines, chemokines, antimicrobial peptides, and specific enzymes helps to fight against invading bacteria, fungi and viruses. Adaptive immunity also employs NF- κ B-dependent functions, which contribute to secondary lymphoid organ development and the maturation and activation of immune cells, such as B and T cells. NF- κ B also tightly controls the cell proliferation via cell-cycle regulators [105-107]. The Stark lab has demonstrated that TNF α induced NF- κ B signaling induced the expression of 1225 genes in human mammary epithelial cells [113].

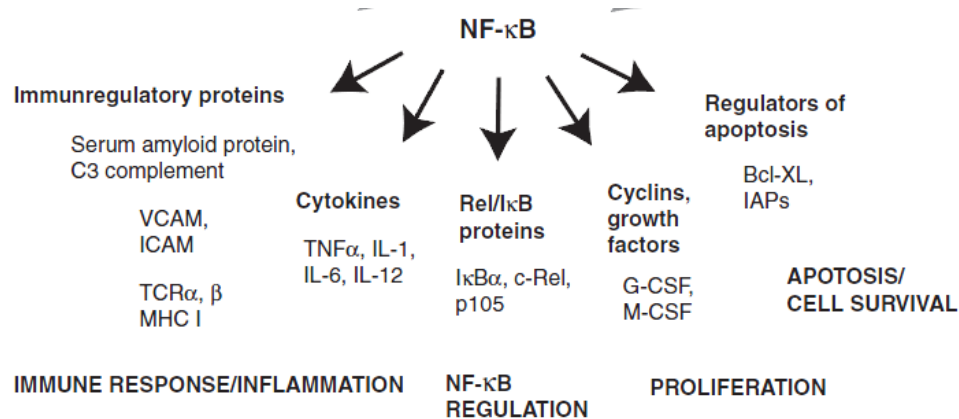


Fig. 1.8: Overview of NF- κ B target genes. [114].

Aberrant NF- κ B signaling positively affects tumorigenesis through the expression of genes involved in cell proliferation, angiogenesis, metastasis, inflammation and escape from apoptosis (pro-survival genes) as identified in both tissue samples and cell lines [115]. However, recent publications provide evidence that, in contexts where pro-survival signals derive from other oncogenes, NF- κ B activity exerts a tumor-suppressor function instead, for example by improving sensitivity to cytotoxic chemotherapy [116], or acting as a tumor suppressor itself [117]. Similarly to STAT3, the opposing roles of NF- κ B in oncogenesis, promoting tumorigenesis on one hand and acting as a tumor suppressor on the other, exemplify the complexity of NF- κ B signaling [115, 116].

3.4 Structure and posttranslational modifications of p65

In mammalian cells, the transcription factor NF- κ B family consists of five different DNA-binding proteins (Fig. 1.7 A): p65 (RelA), RelB, c-Rel, p50/p105 (NF- κ B1) and

p52/p100 (NF- κ B2). Together they constitute a dozen of different homo- or heterodimer combinations (Fig. 1.9A). NF- κ B family members all share a conserved 300-amino acid Rel homology domain (RHD) that is located toward the N-terminus of the protein and is required for dimerization, interaction with I κ B proteins, nuclear translocation, and binding to DNA. All known NF- κ B family dimers are shown in figure 1.9 A. Depending on the cell type and environment, a specific subset of dimers may be present inside the cell. Normally, p65/RelA dimers are ubiquitously expressed and this combination is regarded as the classical NF- κ B complex [119]. Induction, amplitude and duration of NF- κ B signaling are determined by differential cofactor interactions and post-translational modifications of this transcription factor.

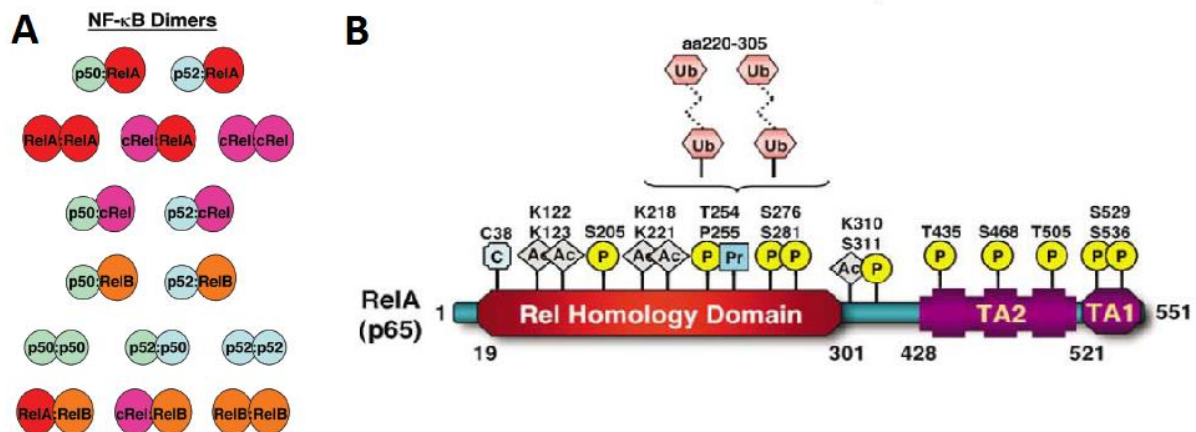


Fig. 1.9: NF- κ B dimers and p65 structure and posttranslational modifications. A. Five NF- κ B polypeptides via homo- and hetero-dimerization can form 15 homo- or heterodimer complexes. The top four rows show transcriptional activators, the fifth row indicates transcriptional repressors, and the bottom row shows dimers that are not able to bind DNA [119]. B. RelA/p65 posttranslational modifications. P – phosphorylation, Pr – prolyl isomerization, Ac – acetylation, Ub – ubiquitination, C – cysteine modification [120].

The most well studied NF- κ B family subunit is p65 (65-kDa) or RelA. In addition to the RHD it contains two C-terminal TADs, which mediate transcription of NF- κ B target genes.

A lot of information has been obtained about post-translational modifications of the p65 subunit, which is modified by phosphorylation, acetylation, prolyl isomerization, nitrosylation and ubiquitination (Fig. 1.9B) [120]. Some of these modifications occur in the cytoplasm and can also stimulate NF- κ B translocation to the nucleus. Different pathway activators or receptors induce diverse modifications of RelA. For example, in response to LPS p65 is phosphorylated at serine 276 (S276) by the protein kinase A in a complex with I κ Ba in the cytoplasm [121], but in response to TNF α S276

phosphorylation occurs in the nucleus by mitogen- and stress-activated protein kinase 1 (MSK1) [122]. Phosphorylation at S276 is required for NF- κ B transcriptional activity, as revealed in a knock-in mouse model expressing a p65 protein with a serine 276 to alanine mutation [123]. S311 has been shown to be phosphorylated *in vivo* in response to TNF- α and an inactivating mutation of that residue severely impairs p65 transcriptional activity [124]. S468 phosphorylation has been described as both enhancing and repressing p65 transcriptional activity depending on cell-type and activating stimuli [125, 126]. Finally, the most extensively described activating phosphorylation occurs at S536 within the TAD, which results in a reduced affinity between p65 and I κ B α [104, 106] and structural mutation of p65 serine 536 to alanine inhibited I κ B α polyubiquitination and degradation [127].

3.5 NF- κ B and STAT3 crosstalk

In recent years, a functional crosstalk between STAT3- and NF- κ B-mediated signal transduction pathways has been described to play a central role in cancer progression [60] and acute phase response in the liver [128]. Numerous types of interactions between NF- κ B and STAT3 have been observed, including an overlapping set of target genes, physical association, competition or cooperation at gene promoters and others (Fig. 1.10) [60, 129]. It becomes more evident that both NF- κ B and STAT3 play a central role in the context of inflammation induced cancer by controlling distinct functions in cancer cells and the surrounding microenvironment, especially in immune cells that infiltrate tumors [130].

Since both factors control the expression of several thousand genes, many of those gene groups are being controlled by the cooperation of both factors. For example, the Stark lab reported 123 genes in human mammary epithelial cells that are dependent on both NF- κ B and STAT3, including *RANTES*, *IL-6*, *IL-8*, *IFN β* and *ICAM-1*, all of which have promoter regions that bind STAT3 and also have κ B sites. [131]. Some of the genes actually require both factors bound to promoters in order to initiate transcription, such as C-reactive protein (*CRP*) and serum amyloid A (*SAA*) genes [132, 133]. In turn, transcription of the inducible nitric oxide synthase (*iNOS*) is suppressed upon STAT3/NF- κ B complex formation [134].

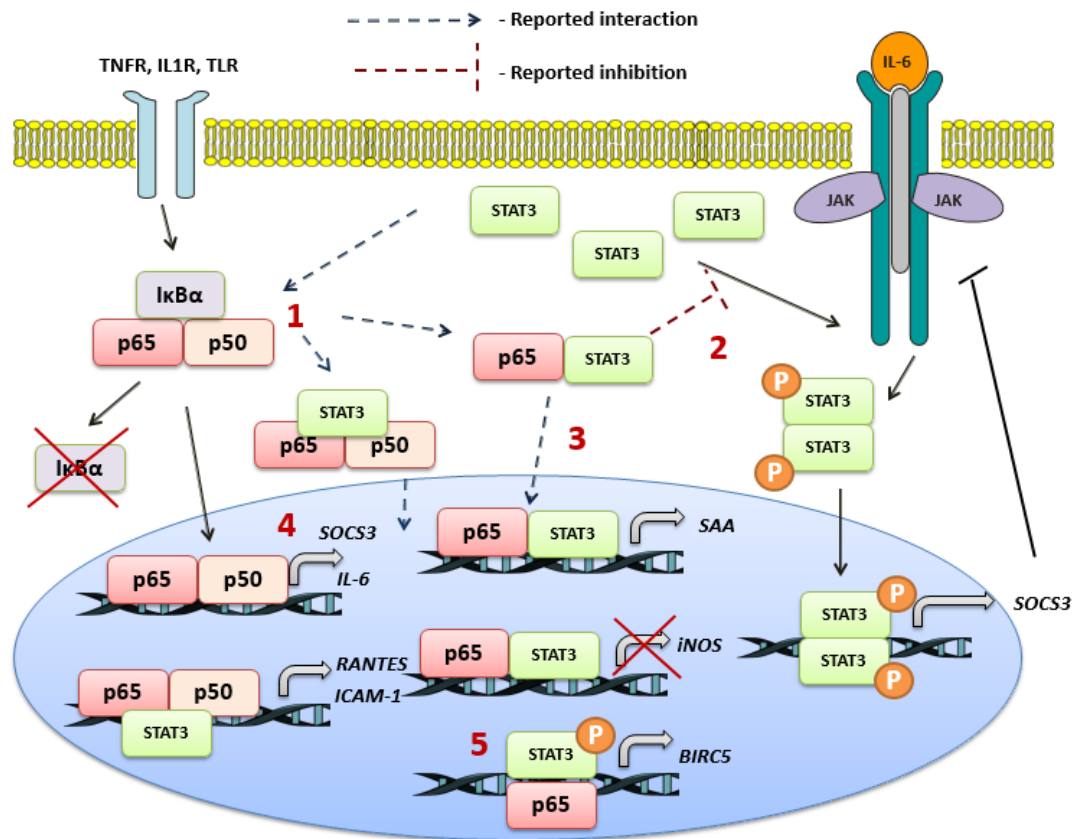


Fig. 1.10: Summarizing scheme of the most studied interactions between gp130 induced STAT3 activation and the NF-κB signaling. 1. Unphosphorylated STAT3 competes with IκB and binds unphosphorylated NF-κB dimers resulting in nuclear import and gene expression (*RANTES*). 2,3. Newly formed STAT3/p65 complex either inhibits STAT3 phosphorylation (2) or translocates into nucleus (3) to activate (*SAA*) or repress (*iNOS*) genes. 4 NF-κB induces either inhibitor (*SOCS3*) or activator (*IL-6*) of STAT3 signaling. 5. STAT3 recruits p300 histone acetyltransferase, thereby prolonging nuclear retention of p65 and protumorigenic gene expression (*BIRC5*).

Apart from functional crosstalk and overlapping target genes, several NF-κB family members, in particular p65 and p50, have been demonstrated to physically interact with STAT3. The consequences of these interactions are different and depend on cell type and localization [128, 131]. However, a coherent picture of how both factors can directly influence each other's signaling has not emerged. On the one hand, STAT3 was required for RhoA-induced NF-κB gene transcription, while nuclear accumulation of p65 subunit was reported to be impaired in STAT3 deficient cells upon both Rho and TNFα stimulation [135, 136]. In contrast, an augmented nuclear p65 presence and increased expression of typical NF-κB target genes upon STAT3 depletion was observed in A549 lung cancer cells [137], glioblastoma cells [138] and primary mouse pneumocytes [139]. Little is known about the effect of p65 deletion or overexpression on STAT3 activity and how exactly both factors influence each others canonical signaling, which requires further investigation.

4. Nucleocytoplasmic trafficking of proteins

Compartmentalization between nucleus and cytoplasm within eukaryotic cells appeared during evolution in order to isolate genetic information and provide spatial separation between transcription and translation. This led to development of complex regulatory mechanisms controlling gene expression and selective transport between the nuclear and cytoplasmic compartments to maintain the distinctive composition of each [140].

4.1 Molecular mechanism of nuclear import and export

Macromolecules that are larger than app. 40 kDa require active transport across the nuclear membrane through nuclear pore complexes (NPCs) using soluble transport factors or carrier molecules that continuously shuttle between the cytoplasm and nucleus [141]. NPCs represent big macromolecular complexes that perforate the nuclear envelope and form the channel for the bidirectional exchange of molecules between the cytoplasm and nucleus [142] and are constructed from multiple copies of proteins collectively called nucleoporins [143]. There are several nuclear transport pathways, most of which use a family of carrier molecules collectively called β -karyopherins, with import carriers called importins and export carriers called exportins [140].

Many proteins are imported using the classic nuclear protein import cycle involving importin- β with various importin- α molecules as adaptors. Protein cargo is recognized via its nuclear localization signal (NLS) by specialized adaptor importins- α followed by binding to importin- β . The latter allows passage of the whole cargo/ α / β complex through the NPC by interaction with nucleoporins. Subsequent cargo release occurs within the nucleus after interaction with RanGTP, which dissociates the import complex. Importin- β complexed with RanGTP is transported back to the cytoplasm, while importin- α molecules are exported in conjunction with the β -karyopherin CAS and RanGTP. Subsequently, cytoplasmic Ran GTPase activating protein (RanGAP) stimulates the Ran GTPase, generating RanGDP that dissociates from the importins and thereby releases them for another import cycle (Fig. 1.11A) [140].

In turn, the primary nuclear export pathway involved in transporting the majority of proteins back to cytoplasm uses chromosome region maintenance 1 (CRM1, exportin 1 or XPO1). CRM1 is a ubiquitous transport receptor protein that recognizes its cargo via a hydrophobic nuclear export signal (NES) peptide sequence. The hydrophobic NES of the cargo protein binds to a hydrophobic groove of CRM1 containing an active site cysteine 528. Then, together CRM1 and cargo form a trimeric complex with RanGTP, which provides directionality of the transport. Similarly to nuclear import, after the CRM1/RanGTP/cargo complex is exported to the cytoplasm, RanGTP is hydrolyzed to RanGDP by RanGAP and RanBP1, the trimeric complex dissociates and the cargo protein is released into the cytoplasm. CRM1 and RanGDP are then recycled back into the nucleus through the NPC for another export cycle (Fig. 1.11B) [144-146]. Actinobacterial toxin leptomycin B (LMB), as well as myxobacterial cytotoxins, named ratjadones (RATs), specifically bind CRM1 and inhibit nuclear export via alkylating C528 residue [147].

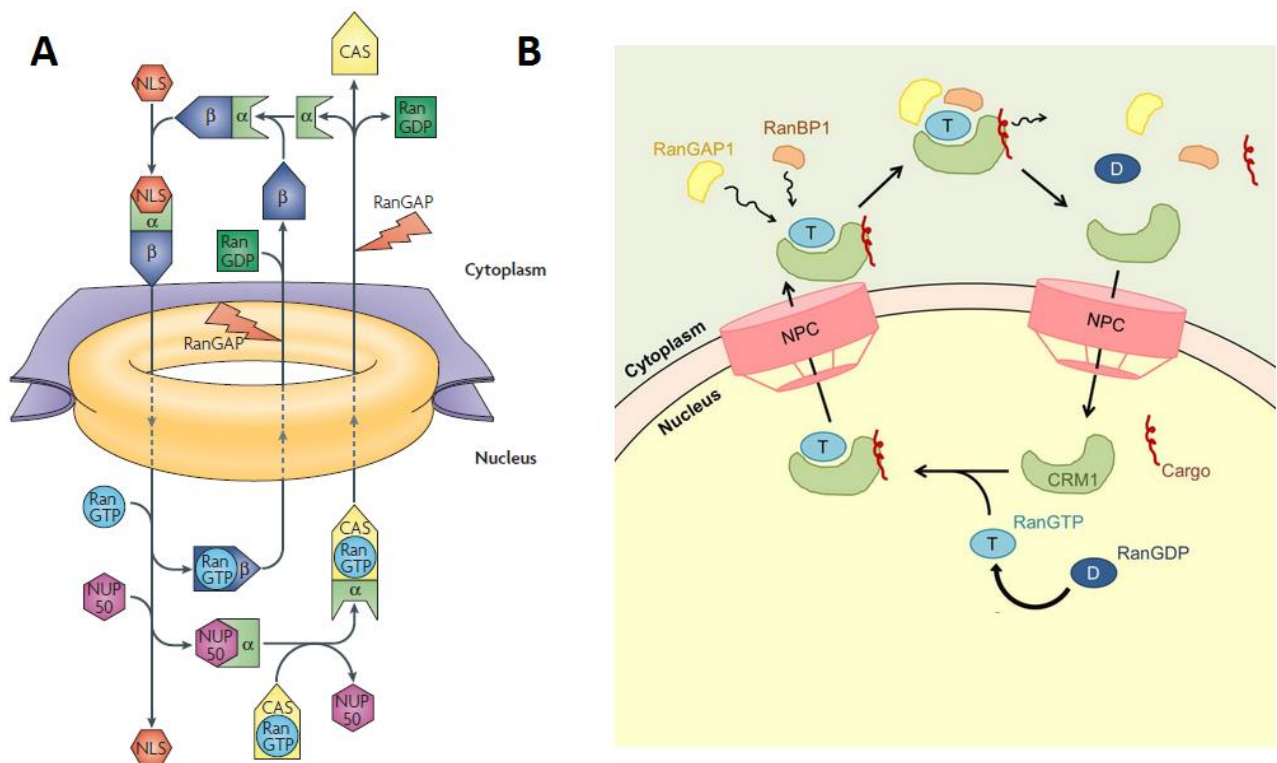


Fig. 1.11: Overview of nuclear protein import and export. A. Classical nuclear import pathway [140]. B. CRM1 nuclear export cycle [146].

4.2 Properties of importin- α adaptors

Importin- β is encoded by a single gene in all eukaryotic organisms, while seven isoforms of importin- α ($\alpha 1$, $\alpha 3$, $\alpha 4$, $\alpha 5$, $\alpha 6$, $\alpha 7$ and $\alpha 8$) are expressed in higher eukaryotes. Such diversity is required for the notable importin- α substrate specificity *in vivo* [148]. NLS recognition is crucial for the formation of the import complex and, normally, importin- α recognizes the classical NLS, which consists of either one (monopartite) or two (bipartite) stretches of basic amino acids (Fig. 1.12B) [140].

Importin- α molecules consist of a flexible N-terminal importin- β binding (IBB) domain, ten armadillo (ARM) motifs, and an acidic C-terminal domain. ARM repeats generate a banana-shaped structure with NLS-binding sites. The major binding site for monopartite NLS represent ARM repeats 1-4, while the minor site is located at ARM repeats 6-8 (Fig. 1.12A). Bipartite NLS sequences occupy the major site with the larger basic cluster and the minor site with smaller basic cluster. The N-terminal domain of importin- α binds to importin- β via the importin- β binding domain (IBB) and has an auto-inhibitory function masking the NLS binding site of importin- α in the absence of importin- β (Fig. 1.12C) [149-151]. Hence, importin- α constructs without IBB domain (Δ IBB) have a higher affinity for NLSs than full-length proteins [152].

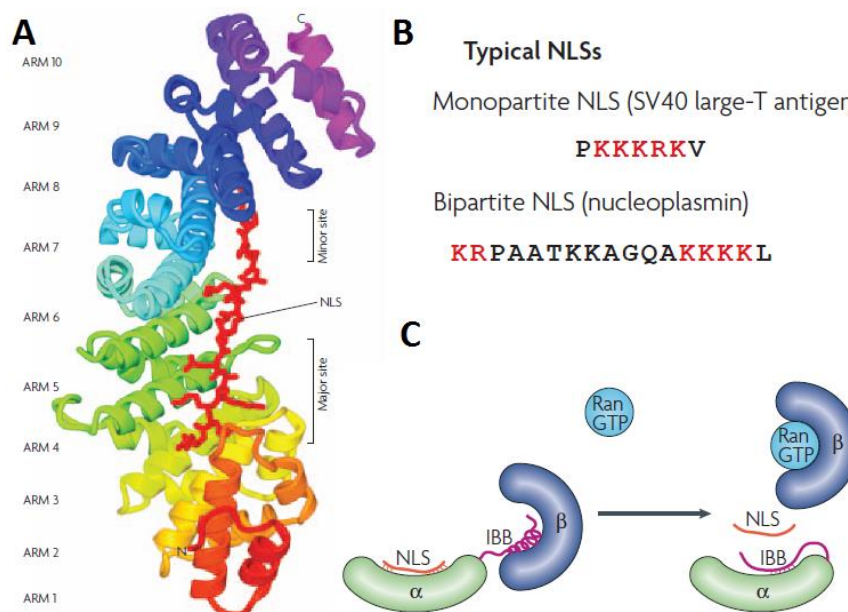


Fig. 1.12: Importin- α adapter properties [140]. A. Structure of the nucleoplasmin NLS (red) bound to importin- α . B. Classic NLSs based on one (monopartite) or two (bipartite) clusters of basic residues. C. Schematic illustration of the autoinhibitory role of the IBB domain.

4.3 Nuclear trafficking of STAT1 and STAT3

Among all seven mammalian STATs, STAT1 nuclear trafficking has been most extensively studied. The importin- α 5/NPI-1/KPNA1 isoform and not importin- α 1/Rch1 has been shown to be essential for STAT1 nuclear translocation as a result of IFN γ stimulation [24, 153]. However, unlike most substrates that carry a classical NLS and bind to importin- α s (such as NF- κ B binding to importin- α 1 [154]), the activated STAT1 dimer binds to importin- α 5 in a nonconventional manner without the involvement of the IBB domain and a classical NLS. Instead, STAT1 requires the importin- α 5 C-terminal acidic tail, where a local unfolding of ARM repeat 10 is mediated by a single conserved residue Y476 within importin- α 5 molecule. Introducing a glycine at this position disturbs STAT1 association with importin- α 5 *in vitro*, suggesting that phosphorylated STAT1/importin- α 5 complex assembly is dependent on the intrinsic flexibility of ARM 10 [155]. This nonconventional binding is targeted by Ebola virus VP24 protein that competes for specific binding to ARMs 8–10 of importin- α 5 with phosphorylated STAT1. This competitive mechanism of VP24 still allows conventional NLS-containing proteins to bind importins- α , thus specifically blocking only STAT1 antiviral activity and leaving other cellular processes intact [156].

Currently, there is no consensus in the literature as to what importin- α isoforms are required for STAT3 nuclear import. The laboratory of Nancy Reich has demonstrated that STAT3 interacted with α 3 and α 6 importins *in vitro* independent of its tyrosine 705 phosphorylation state [157]. In contrast, other group demonstrated STAT3 association with α 1, α 3 and α 5 importins only after OSM stimulation [158]. Furthermore, the group of Xinmin Cao demonstrated stimulation-dependent binding to α 5 and α 7 importins of both STAT1 and STAT3 *in cellulo* and *in vitro* [159]. Finally, other study showed an *in-vitro* STAT3 binding to α 1, α 3, α 6 and α 7 importins [160]. Proper importin binding and nuclear import requires intact NTD and CCD domains of STAT3 [52, 157, 158]. Given that STAT3 has a prominent role in physiology and progression of many diseases, the exact molecular mechanism of STAT3 nuclear import warrants further studies.

5. Aims of the study

STAT3 is a ubiquitous transcription factor involved in many biological processes, including hematopoiesis, inflammation and cancer progression. Dysregulated STAT3 signaling has been described to be crucial for cancer progression, chronic inflammation and autoimmune diseases, making it a promising therapeutic target. However, in order to develop successful therapeutics, the exact molecular mechanisms of physiologic and pathologic STAT3 signaling must be characterized. Among those are STAT3 nuclear import and specific DNA recognition.

Our group have previously shown an intact GAS element binding capability of N-terminally truncated STAT3 ((Δ N)STAT3), despite an apparent defect in nuclear accumulation of this mutant [52]. In the first part of this thesis, we have investigated the roles of GAS-element-specific DNA-binding and NTD in STAT3 nuclear trafficking, the role of STAT3 NTD in binding to importin- α adaptors and subsequent IL-6-induced STAT3 nuclear translocation, as well as structural requirements for constitutive nucleocytoplasmic shuttling of latent STAT3 and whether basal nuclear import uses the same mechanisms as cytokine-mediated active nuclear accumulation. For this purpose we used STAT3 knockout MEF cells (MEF Δ/Δ or STAT3 $^{-/-}$) stably reconstituted with different STAT3 constructs with fluorescent tags. Ectopically expressed STAT3-YFP as well as STAT3-CFP-YFP have been previously shown to mirror the subcellular distribution of endogenous STAT3 [52, 53, 58].

In addition, STAT3 has been shown to crosstalk with other signaling pathways, most notably NF- κ B and STAT1. Despite the fact that STAT1 and STAT3 are closely related and share many activating stimuli, they both have opposing roles in many biological processes, such as proliferation, apoptosis, inflammation and anti-tumor immune responses [90]. In addition, studies on STAT-deficient cells demonstrated the existence of reciprocal STAT1/STAT3 regulatory mechanisms that deserve further investigations [94, 100-102]. In the second part of this work, we used STAT3- and STAT1-deficient MEFs to further elucidate possible cross-regulation mechanisms.

Finally, a growing body of research indicates functional cross-talk between NF- κ B and STAT3 that mostly is evident during acute phase protein expression and inflammation-induced tumorigenesis [60, 128]. However, a coherent picture of whether NF- κ B and STAT3 can directly influence each other's signaling upon TNF α and IL-6 treatment respectively has not yet emerged. Hence, the main aim of the third part of the study is to concentrate on the involvement of NF- κ B p65 in IL-6-induced STAT3 activation, nuclear accumulation and gene expression, as well as on the reciprocal role of STAT3 in canonical TNF α -induced NF- κ B signaling using p65- and STAT3-deficient MEF along with inducible expression of the transcription factors in HeLa cells.

II. Materials and Methods

Materials and methods are described according to standard protocols used in the Institute of Biochemistry and Molecular Biology at RWTH Aachen University and modified regarding individual differences in experimental procedures.

1. Materials

1.1 Chemicals and reagents

All chemicals and reagents were prepared according to *pro analysi* quality standards. All water solutions were prepared using double distilled water (ddH₂O, Merck).

1.2 Plasmids

Name	Description
pcDNA5/FRT/TO special (pcDNA5)	Eukaryotic expression vector under the control of CMV promoter that contains a modified multiple cloning site, ampicillin and hygromycin resistance, tetracycline-inducible expression cassette and a FRT site for stable transfection
pOG44	Eukaryotic expression vector containing the cDNA of Flp-recombinase for stable transfection
pMOWS	Hybrid retroviral vector encoding puromycin resistance cassette under SV40-promoter for transgene expression in murine cells (generous gift from Prof. Jürgen Scheller, Heinrich-Heine University, Germany, described in [161]).
pMOWS-STAT3-YFP(NTD)	Hybrid retroviral vector encoding the N-terminal domain of murine STAT3 (aa 1-123) fused to YFP tag
pMOWS-p65-YFP	Hybrid retroviral vector encoding the avian p65 (RelA) fused to YFP tag

Name	Description
pMOWS-p65-YFP(S276A)	Hybrid retroviral vector encoding the avian p65 (RelA) point mutant S276A fused to YFP tag
pMOWS-p65-YFP(S311A)	Hybrid retroviral vector encoding the avian p65 (RelA) point mutant S311A fused to YFP tag
pMOWS-p65-YFP(S468A)	Hybrid retroviral vector encoding the avian p65 (RelA) point mutant S468A fused to YFP tag
pMOWS-p65-YFP(S536A)	Hybrid retroviral vector encoding the avian p65 (RelA) point mutant S536A fused to YFP tag
pGEX-GST-importin- α 5	Full-length GST-tagged human importin alpha 5 (KPNA1) cloned into pGEX-4T3 vector for bacterial expression (a kind gift of Prof. Susana de la Luna, The Centre for Genomic Regulation, Spain)
pGEX-GST-importin- α 5 Δ IBB	GST-tagged human importin alpha 5 (KPNA1) with deleted IBB domain (aa 58-538) cloned into pGEX-4T1 vector for bacterial expression
pGEX-GST-importin- α 1 Δ IBB	GST-tagged human importin alpha 1 (KPNA2) with deleted IBB domain (aa 62-529) cloned into pGEX-4T1 vector for bacterial expression (a kind gift of Prof. Susana de la Luna)
pGEX-GST-importin- α 3 Δ IBB	GST-tagged human importin alpha 3 (KPNA4) with deleted IBB domain (aa 59-521) cloned into pGEX-4T1 vector for bacterial expression (a kind gift of Prof. Susana de la Luna)
pGEX-GST-importin- α 6 Δ IBB	GST-tagged human importin alpha 6 (KPNA5) with deleted IBB domain (aa 58-536) cloned into pGEX-4T1 vector for bacterial expression (a kind gift of Prof. Susana de la Luna)
pGEX-GST-importin- α 7 Δ IBB	GST-tagged human importin alpha 7 (KPNA6) with deleted IBB domain (aa 61-536) cloned into pGEX-4T1 vector for bacterial expression (a kind gift of Prof. Susana de la Luna)
pGEX-GST-importin- α 5 (Y476G)	Full-length GST-tagged human importin alpha 5 (KPNA1) with point mutation Y476G cloned into pGEX-4T3 vector for bacterial expression
pGEX-GST-importin- β 1	Full-length GST-tagged human importin beta 1 (KPNB1) cloned into pGEX-4T1 vector for bacterial expression (human importin beta 1 cDNA obtained from BioCat, Germany, #BC003572-TCH1003-GVO-TRI)

Name	Description
pcDNA5-STAT3-CFP-YFP(L78R)	Eukaryotic expression vector encoding murine STAT3 point mutant L78R fused to CFP and YFP tags
pcDNA5-STAT3-YFP(mSNICQ)	Eukaryotic expression vector encoding murine STAT3 with amino acids ⁴⁶⁵ SNICQ ⁴⁶⁹ substituted to ⁴⁶⁵ GSSGS ⁴⁶⁹ fused to YFP tag
pcDNA5-STAT3-CFP-YFP(Δ TAD)	Eukaryotic expression vector encoding murine STAT3 point mutant L78R fused to CFP and YFP tags

1.3 qPCR Primers

Name	Sequence/Company
Murine <i>socs3</i> sense	5'- CCG CGG GCA CCT TTC-3'
Murine <i>socs3</i> antisense	5'- TTG ACG CTC AAC GTG AAG AAGT - 3'
Murine <i>ikba</i> sense	5'- CTC CCC CTA CCA GCT TAC CT -3'
Murine <i>ikba</i> antisense	5'- TAG GGC AGC TCA TCC TCT GT - 3'
Murine <i>gusB</i>	QT00176715 (Qiagen)

1.4 Mutagenesis primers

Mutation	5'-3' Sequences
STAT3 mSNICQ FP	GGAAGTTCCGGAAGTATGCCAAATGCTTGGGC
STAT3 mSNICQ RP	ACTTCCGGAAGTTCGATCACCACAACTGGCAA
STAT3 Δ TAD FP	AAGCACCTGACCCTTAGG
STAT3 Δ TAD RP	ACAGGTGACCACTTGGTCTTCAAGTAC

Mutation	5'-3' Sequences
p65 S276A FP	GCTGCGGCGGCCTGCCGACCGGGAGC
p65 S276A RP	GCTCCCGGTCGGCAGGCCGCCGCAGC
p65 S311A FP	CATATGAGACCTTCAAGGCCATCATGAAGAAGAG
p65 S311A RP	CTCTTCTTCATGATGGCCTTGAAGGTCTCATATG
p65 S468A FP	GTTACACAGACCTGGCAGCCGTCGACAACTCC
p65 S468A RP	GGAGTTGTCGACGGCTGCCAGGTCTGTGAAC
p65 S536A FP	GAT GAA GAC TTC TCC GCC ATT GCG GAC ATG G
p65 S536A RP	CCA TGT CCG CAA TGG CGG AGA AGT CTT CAT C
importin- α 5 Y476G FP	GCTTTGATTGAAGAAGCTGGTGGTCTGGATAAAATTGAG
importin- α 5 Y476G RP	CTCAATTTTATCCAGACCACCAGCTTCTTCAATCAAAGC
importin- α 1 Δ IBB FP	CGTAGAATTCATGTCTCCGCTGCAGGAAAC
importin- α 1 Δ IBB RP	GGGAGCTGCATGTGTCAGAG
importin- α 3 Δ IBB FP	CGTAGGATCCATGGACTCTGATATAGATGGTGATTATAG
importin- α 3 Δ IBB RP	GGGAGCTGCATGTGTCAGAG
importin- α 5 Δ IBB FP	CGTAGAATTCATGGAAGAAGAAGTTATGTCAGATGG
importin- α 5 Δ IBB RP	GGGAGCTGCATGTGTCAGAG
importin- α 6 Δ IBB FP	CGTAGAATTCATGTCTATGCTTGAAAGTCCTATAC
importin- α 6 Δ IBB RP	GGGAGCTGCATGTGTCAGAG
importin- α 7 Δ IBB FP	CGTAGAATTCATGGCCATGTTGATAGTCTTCTC
importin- α 7 Δ IBB RP	CACTGCTCGAGTTATAGCTGGAAGCCCTCC

1.5 Genotyping primers

Name	Sequence
EX20B	5'- GCG GGC CAT CCT AAG CAC AAAG-3'
EX21B	5'- CCT CCT TGG GAAT GTC GGGG- 3'
IN20B	5'- CAC CTG CCG CAA ATG TAT TAA CG-3'

1.6 Antibodies

1.6.1 Primary antibodies

Name	Species	Cat. Number/Company	Application
α -pY705-STAT3	rabbit	9131/Cell Signaling	Polyclonal, IB
α -pY705-STAT3 (D3A7)	rabbit	9145/Cell Signaling	Monoclonal, IF
α -pY701-STAT1	rabbit	7649/Cell Signaling	Monoclonal, IB
α -pY1022/1023-JAK1	rabbit	3331/Cell Signaling	Polyclonal, IB
α -pS536-p65	rabbit	3033/Cell Signaling	Monoclonal, IB
α -pS32-IkB α	rabbit	2859/Cell Signaling	Monoclonal, IB
α -STAT3	mouse	9139/Cell Signaling	Monoclonal, IB, IF
α -STAT3	mouse	sc-7179X/SantaCruz	Polyclonal, EMSA
α -STAT1	rabbit	sc-346/SantaCruz	Polyclonal, IB
α -STAT1	rabbit	HPA000982/Sigma-Aldrich	Polyclonal, IF
α -JAK1	rabbit	610231/BD Transduction Lab	Monoclonal, IB
α -p65	rabbit	4764/Cell Signaling	Monoclonal, IB, IF
α -IkB α (L35A5)	mouse	4814/Cell Signaling	Monoclonal, IB
α -dsRed	rabbit	632496/Clontech Lab	Polyclonal, IB
α -GFP	goat	600-101-215/Rockland	Polyclonal, IB, IP
α -GST	mouse	sc-138/SantaCruz	Monoclonal, IB
α -GAPDH	mouse	sc-32233/SantaCruz	Monoclonal, IB
α -Lamin A/C	goat	sc-6215/SantaCruz	Polyclonal, IB
α -STAT5	rabbit	sc-836/SantaCruz	Polyclonal, IB

1.6.2 Secondary antibodies

Name	Species	Cat. Number/Company	Application
α -rabbit-IgG/HRP	goat	00052233/DAKO,	Polyclonal, IB
α -goat-IgG/HRP	rabbit	00045307/DAKO	Polyclonal, IB
α -mouse-IgG/HRP	rabbit	00046035/DAKO	Polyclonal, IB

Name	Species	Cat. Number/Company	Application
α -rabbit-IgG/Alexa Fluor®555	donkey	A-31572/Thermo Fischer Scientific	Polyclonal, IF
α -mouse-IgG/Alexa Fluor®488	donkey	A-21202/Thermo Fischer Scientific	Polyclonal, IF

1.7 Eukaryotic cell lines

Name	Description
HeLa 229	Adherent human cervical carcinoma cell line.
HeLa T-REx™	Stably transfected HeLa cells with FRT-sequence for the creation of stable cell lines and tetracycline repressor for inducible gene expression (R714-07, Life Technologies)
Hek293 T-REx™	Stably transfected Hek293 cells with FRT-sequence for the creation of stable cell lines and tetracycline repressor for inducible gene expression
MEF	Adherent murine embryonic fibroblasts
MEF Δ/Δ (STAT3 $-/-$)	Adherent murine embryonic fibroblasts, STAT3 deficient (generous gift from Prof. Valeria Poli, University of Turin, Italy, described in [100])
MEF p65 $-/-$	Adherent murine embryonic fibroblasts, p65 deficient (generous gift from Prof. Lienhard Schmitz, Justus-Liebig-University, Germany, described in [162])
MEF STAT1 $-/-$	Adherent murine embryonic fibroblasts, STAT1 deficient (generous gift from Prof. Michał Komorowski, Institute of the Fundamental Technological Research, Poland, described in [163])
MEF Δ/Δ FRT	Adherent STAT3 deficient murine embryonic fibroblasts with FRT-sequence for the creation of stable cell lines
Plat-E	Platinum retroviral packaging cell line based on the Hek293T cell line
ESC	Wild-type murine embryonic stem cells
ESC STAT3-YFP	E14 murine embryonic STAT3-YFP knock-in stem cells, generated in cooperation with Prof. Valeria Poli, University of Turin, Italy

1.7.1 Stably transfected cell lines

Name	Transfected plasmid	Supplementation
MEF Δ/Δ STAT3-CFP-YFP	pcDNA5-STAT3-CFP-YFP (generated by M.Vogt)	500 ng/ml hygromycin
MEF Δ/Δ STAT3-CFP-YFP(Δ NTD)	pcDNA5- Δ NSTAT3-CFP-YFP (generated by M.Vogt)	500 ng/ml hygromycin
MEF Δ/Δ STAT3-CFP-YFP(R609Q)	pcDNA5-STAT3-CFP-YFP(R609Q) (generated by M.Vogt)	500 ng/ml hygromycin
MEF Δ/Δ STAT3-YFP(K685R)	pcDNA5- STAT3-YFP(K685R) (generated by A. Herrmann)	500 ng/ml hygromycin
MEF Δ/Δ STAT3-CFP-YFP(Δ NLS)	pcDNA5-STAT3- CFP-YFP(Δ NLS) (generated by M.Vogt)	500 ng/ml hygromycin
MEF Δ/Δ STAT3-CFP-YFP(Δ NES)	pcDNA5-STAT3- CFP-YFP(Δ NES) (generated by M.Vogt)	500 ng/ml hygromycin
MEF Δ/Δ STAT3-YFP(mSNICQ)	pcDNA5- STAT3-YFP(mSNICQ) (generated by A. Herrmann)	500 ng/ml hygromycin
MEF Δ/Δ STAT3-CFP-YFP(L78R)	pcDNA5- STAT3-CFP-YFP(L78R)	500 ng/ml hygromycin
MEF Δ/Δ STAT3-CFP-YFP(Δ TAD)	pcDNA5-STAT3- CFP-YFP(Δ TAD)	500 ng/ml hygromycin
MEF Δ/Δ STAT3-YFP(NTD)	pMOWS-STAT3-YFP(NTD)	1 μ g/ml puromycin
MEF p65 $-/-$ p65-YFP	pMOWS-p65-YFP	1 μ g/ml puromycin
MEF p65 $-/-$ p65-YFP(S276A)	pMOWS-p65-YFP(S276A)	1 μ g/ml puromycin
MEF p65 $-/-$ p65-YFP(S311A)	pMOWS-p65-YFP(S311A)	1 μ g/ml puromycin
MEF p65 $-/-$ p65-YFP(S468A)	pMOWS-p65-YFP(S468A)	1 μ g/ml puromycin
MEF p65 $-/-$ p65-YFP(S536A)	pMOWS-p65-YFP(S536A)	1 μ g/ml puromycin
HeLa T-REx TM STAT3-GFP	pcDNA5-STAT3-GFP (generated by N. Rinis)	100 ng/ml hygromycin and 10 μ g/ml blasticidin
HeLa T-REx TM p65-dsRed	pcDNA5-p65-dsRed (generated by N. Rinis)	100 ng/ml hygromycin and 10 μ g/ml blasticidin
HeLa T-REx TM p65	pcDNA5-p65	100 ng/ml hygromycin and 10 μ g/ml blasticidin
HeLa T-REx TM dsRed	pcDNA5-dsRed	100 ng/ml hygromycin and 10 μ g/ml blasticidin

Name	Transfected plasmid	Supplementation
Hek293 T-REx TM STAT3-YFP	pcDNA5- STAT3-YFP (generated by A. Mohr)	100 ng/ml hygromycin and 10 µg/ml blasticidin
Hek293 T-REx TM STAT3-YFP(ΔNTD)	pcDNA5- STAT3-YFP(ΔNTD)	100 ng/ml hygromycin and 10 µg/ml blasticidin
Hek293 T-REx TM STAT3-YFP(R609Q)	pcDNA5- STAT3-YFP(R609Q)	100 ng/ml hygromycin and 10 µg/ml blasticidin

1.7.2 Growth medium

Name	Description
DMEM, low glucose, GlutaMAX TM	Normal growth medium (Gibco, Invitrogen)
Opti-MEM®, reduced serum medium	For use with cationic lipid transfection reagents during transient DNA transfection (Gibco, Invitrogen)

1.7.3 Cytokines and cytokine receptors

Name	Description	Source
IL-6	Human recombinant IL-6 cytokine	Prepared as described previously [164]
sIL-6Rα	Human recombinant soluble IL-6 receptor	Prepared as described previously [165]
IFNγ	Murine recombinant IFN gamma	Purchased from Peprotech (#315-05)
IFNγ	Human recombinant IFN gamma	Purchased from Immunotools (11343536)
TNFα	Human recombinant TNF alpha	Purchased from Peprotech (#300-01A)

1.7.4 Transfection reagents

Name	Description
TransIT®-LT1	DNA transfection reagent, for transient and stable transfection of HeLa and Hek293 cells (Mirus, USA)
FuGENE®	DNA transfection reagent, for stable transfection of MEF cells (Promega, USA)

1.7.5 Other reagents

Name	Company
FCS (fetal calf serum)	Cytogen, USA
Trypsin (0.05%)/EDTA (0.02%)	Lonza, Belgium

1.8 Prokaryotic cell lines

Name	Mutations
<i>E.Coli</i> JM83	F ⁻ ara Δ (lac-proAB) rpsL (Str ^r) [ϕ 80 d lac Δ (lacZ)M15]
<i>E.Coli</i> DH5 α	F ⁻ endA1 glnV44 rhi-1 recA1 relA1 gyrA96 deoR nupG ϕ 80dlacZ Δ M15 Δ (lacZYA-argF)U169, hsdR17(r _K ⁻ m _K ⁺), λ -
<i>E.Coli</i> BL21(DE3)pLysS	F ⁻ ara ompT hsdS _B (r _B ⁻ m _B ⁻) gal dcm (DE3) pLysS (Cam ^R)

1.8.1 Cultivation

Recombinant *E.Coli* strains were cultivated in LB (Luria-Bertani, Roth) medium with supplemented ampicillin (100 mg/l).

LB (Luria-Bertani) medium:

10 g/L Tryptone
5 g/L Yeast extract
10 g/L NaCl

For long-term storage bacterial cells with plasmid of interest were stored at -80°C with 20% glycerin.

1.9 Antibiotics

Name	Description
Ampicillin	Solvent: water, stock concentration 100 mg/ml (Roth)
Doxycyclin	Solvent: water, stock concentration 1 mg/ml (Sigma-Aldrich)
Hygromycin B	Solvent: water, stock concentration 100 mg/ml (Invivogen)
Zeocin	Solvent: water, stock concentration 100 mg/ml (Invitrogen)
Blasticidin	Solvent: water, stock concentration 10 mg/ml (Invitrogen)
Puromycin	Solvent: water, stock concentration 10 mg/ml (Invitrogen)
Penicillin/Streptomycin	Solvent: water, stock concentration 10 000 units penicillin and 10 mg/ml streptomycin (Sigma-Aldrich)
Leptomycin B	Solvent: ethanol, stock concentration 20µg/ml (Enzo Life Sciences)

2. Methods

2.1 Molecular biology methods

2.1.1 DNA restriction digest

Digestion with restriction endonucleases was carried out according to the restriction enzyme manufacturer's instructions. Plasmid DNA or PCR product were mixed to a total volume of 20 µl for analytical digest and 40 µl for preparative digest. The reaction mixture was incubated at 37°C for 45-60 minutes for analytical digest and 90 minutes for preparative digest. During digestion with two restriction endonucleases an appropriate buffer was selected to ensure optimal reaction conditions and at least 75% efficiency of both enzymes. Restriction enzymes were purchased from New England Biolabs (NEB). DNA fragments were then analyzed via agarose gel electrophoresis.

2.1.2 Agarose gel electrophoresis

Agarose gel electrophoresis is used for the separation of DNA fragments according to their size. The DNA samples were mixed with 0.1 volumes of 10x loading buffer and loaded onto a 1% ethidium bromide agarose gel in 1x TAE buffer. DNA was visualized with a UV light source and photographed. To estimate the size of the linear double-stranded DNA fragments the 1 Kb Plus DNA ladder (Invitrogen) was used.

1 x TAE:

40 mM Tris base
20 mM Acetic acid
1 mM EDTA

10 x DNA loading buffer:

40% Ficoll 400.000
0.4% Xylencyanol blue
0.4% Bromophenol blue

2.1.3 DNA fragment isolation

After preparative digest the desired bands were excised from the agarose gel with a clean scalpel and purified using Qiaquick gel extraction kit (Qiagen), according to the manufacturer's instructions. DNA fragment was eluted in water for chromatography (Merck) for further use.

2.1.4 DNA fragment ligation

The purified double stranded DNA fragments were ligated into the linearized plasmids with T4 DNA Ligase (400 000 U/ml, NEB). A ligation reaction mixture consists of 1 µl T4 DNA ligase, 2 µl of 10 × ligation buffer, an appropriate molar ratio of linearized vector DNA and purified insert DNA fragment (1:3) filled up to a total volume of 20 µl. Reaction mixture was incubated at room temperature for 60-90 minutes and then transformed into competent *E.coli* cells.

2.1.5 Transformation of competent *E.Coli* cells

50 µl of frozen competent *E.Coli* JM83 or DH5α cells were thawed on ice 15 minutes before use. Plasmid DNA (1-5 ng) or 10-20 µl of the ligation mixture was mixed with competent cells and then incubated on ice for 30 minutes. Cells were heat shocked at 42°C for 90 seconds, and then placed on ice for 120 seconds. Transformation mixture was spread over a selective (ampicillin, 100 mg/l) LB-agar plate. The plate was incubated overnight at 37°C. The positive clones were then screened for positive ones using QIAprep® Spin Miniprep kit according to manufacturers instructions for small-scale plasmid DNA isolation and subsequent PCR analysis.

2.1.6 Isolation of plasmid DNA

For large-scale plasmid DNA purification 250 ml LB medium containing ampicillin (100 mg/l) were inoculated with 100 µl of selective LB medium containing positive clone cells and incubated overnight at 37°C with vigorous shaking. Bacterial cells

were then harvested by centrifugation (6000 RPM) for 15 minutes at 4°C. Pelleted bacteria were resuspended and large-scale plasmid extractions were performed using HiSpeed® Plasmid Maxi kit from QIAGEN according to the manufacturer's protocol. DNA was eluted in 0.5-1 ml water for chromatography (Merck).

2.1.7 Measurement of DNA concentration

The DNA concentration was calculated based on the value of OD_{260nm} measured with a spectrophotometer (Nano-Drop™ ND-1000, Peqlab). The OD_{260nm}/OD_{280nm} ratio yielded a determination of DNA purity. For pure DNA, this ratio must be approximately 1.8-2.0.

2.1.8 Plasmid DNA sequencing

Sequencing of newly constructed DNA plasmids was performed by MWG-Biotech AG (Martinsried). 1 µg of plasmid DNA was mixed with 1.5 µl sequencing-primer (10 pmol/µl) and water for chromatography (Merck) ad 15 µl.

2.1.9 Expression and purification of recombinant proteins

GST-fusion proteins were expressed in *E. coli* BL21(DE3)pLysS and purified by affinity chromatography on Protino® Glutathione Agarose 4B (Macherey-Nagel, Germany) according to standard protocols.

2.1.10 PCR – polymerase chain reaction

In order to specifically amplify single DNA sequences a widely used molecular biology technique called polymerase chain reaction (PCR) was used. PCR uses four deoxyribonucleotide triphosphates (dNTPs), a heat-stable Taq-DNA Polymerase (NEB) and two specific oligonucleotides (primers), which hybridize to sense and antisense strands of the template fragment. PCR consists of three basic steps: denaturation, annealing and elongation, repeated 20-30 times. Two different protocols were used for isolated plasmid DNA and for transgenic mice genotyping.

For DNA insert generation and specific DNA element detection a standard PCR protocol was used:

(Per sample)

Template DNA	5 ng
Forward/reverse primer (MWG Biotech)	15 pmol each
2,5 mM dNTP mix (Qiagen)	2 μ l
10x Thermo Polymerase Buffer (NEB)	2.5 μ l
Taq Polymerase (5 U/ μ l, NEB)	1.0 U
H ₂ O	ad 25 μ l

The following PCR program was used for amplification:

Initial denaturation	98 °C	20 s	
Denaturation	94 °C	10 s	} 30 cycles
Annealing	48 °C	20 s	
Elngation	72 °C	22 s	
Final elngation	72 °C	300 s	

For genotyping of STAT3-YFP Knock-in mice isolated gDNA was amplified with EX20B-EX21B and EX20B-IN20B (see II.1.5) primer combinations for knock-in or wild-type genotype detection respectively using this PCR reaction mixture:

(Per sample)

Isolated gDNA	2 μ l
10 pmol Forward/Reverse primers (MWG Biotech)	1.5 μ l each
2,5 mM dNTP mix (Qiagen)	1.5 μ l
5x Green GoTaq® Flexi Buffer (Promega)	5 μ l
25 mM MgCl ₂ (Promega)	2 μ l
DMSO	2 μ l
Taq Polymerase (5 U/ μ l, NEB)	0.5 μ l
H ₂ O	9 μ l

The following PCR program was used for isolated gDNA from mice:

Initial denaturation	94 °C	300 s	
Denaturation	94 °C	30 s	} 30 cycles
Annealing	60 °C	30 s	
Elnigation	72 °C	30 s	
Final elngation	72 °C	300 s	

The annealing temperature is correlated with the melting temperature (T_M) of the primers depending on their A/T-G/C content. This was calculated using following formula: $T_M = (C + G) \times 4 + (A + T) \times 2$.

2.1.11 Quantitative PCR

2.1.11.1 RNA isolation and reverse transcription

Approximately 2×10^6 MEF cells were stimulated according to experimental setup, collected in ice-cold PBS and spun down in an Eppendorf centrifuge at 3500 RPM for 5 min at 4°C. Resulting pellets were lysed in RLT buffer containing β -mercaptoethanol for RNase inhibition and RNA isolation was performed using Qiagen RNeasy® Mini Kit according to manufacturers instructions. RNA was eluted in RNase-free water and concentration was measured using a Nanodrop spectrophotometer (Thermo Scientific). For reverse transcription 1 μ l RNA per sample was reverse transcribed using Qiagen Omniscript® RT Kit according to suppliers protocol. After this, cDNA samples were diluted 1:4 and analyzed by qPCR.

2.1.11.2 qPCR

The qPCR measurements were done using the SensiMix SYBR Kit (#QT650-02, Bioline, UK) on the Rotor-Gene Q 2plex (#9001550, Qiagen) according to manufacturer's protocol. For each sample 2 μ l of reverse transcribed cDNA was mixed with forward and reverse primers for specific genes of interest (see II.1.3) at a concentration of 10 pmol/ μ l. Expression was normalized to the housekeeper gene *mGUSB*. The relative expression ratio was calculated by the $\Delta\Delta C_t$ method [166],

plotted using GraphPad Prism 6 software and statistically evaluated by Student's *t*-test. A *P* value of less than 0.05 was considered significant.

2.1.12 Site-directed mutagenesis

PCR-based site directed mutagenesis for point mutant generation was performed with QuickChange® mutagenesis kit (Agilent Technologies USA). Online QuickChange® primer design tool was utilized for proper primer selection (see II.1.4).

(Per sample)

Template DNA	10-25 ng
Forward/reverse primer (MWG Biotech)	11 pmol each
2,5 mM dNTP mix (Qiagen)	2 µl
Quicksolution (Agilent)	2 µl
10x Pfu Ultra Polymerase Buffer (Agilent)	5 µl
Pfu Ultra Polymerase (2.5 U/µl, Agilent)	1 µl
H ₂ O	ad 25 µl

Following PCR program was used for amplification:

Initiation	95 °C	60 s	
Denaturation	95 °C	50 s	} 19 cycles
Annealing	60 °C	50 s	
Elongation	68 °C	720 s	
Final elongation	68 °C	660 s	

2.1.13 Genomic DNA isolation

The gDNA from murine embryonic stem cells was isolated using QIAamp® DNA Mini Kit (Qiagen) according to manufacturer's protocols (Spin Protocol). For crude gDNA isolation from animal material, tail tips from newborn mice were incubated in 50 mM NaOH at 96-98 °C for 60 minutes with constant shaking, cooled down on ice for 2 minutes and subsequently neutralised by adding 1 M Tris-HCl (pH 8.5) with 10 mM EDTA. Samples were stored at -20 °C.

2.2 Cell biology methods

2.2.1 Cell culture

Adherent cells were grown in DMEM medium supplemented with 10% fetal calf serum and 1% penicillin/streptomycin at 37°C in a humidified atmosphere containing 5% CO₂. For passaging cells were washed once with phosphate buffered saline (PBS), treated with trypsin/EDTA solution and incubated at 37°C for 5 minutes. The detached cells were diluted with warm DMEM culture medium and split into new flasks. Cells were kept either in standard TC Dish 100 (#83.3902, Sarstedt, Germany) for growth and expansion, or in Falcon® 6 Well Tissue Culture Plates (#353046, Corning, USA) for different experimental procedures.

<u>PBS:</u>	137 mM	NaCl
	2.7 mM	KCl
	8.1 mM	Na ₂ HPO ₄
	1.5 mM	KH ₂ PO ₄

2.2.2 Cell cryopreservation

For long-term storage 90% confluent cells were detached, spun down at 1,000 RPM for 5 minutes and resuspended in medium containing 20% FCS and 10% DMSO. The cell suspension was transferred into cryotubes (1 ml in each) and placed into Styrofoam box with isopropanol at -80 °C overnight for slow temperature reduction. Afterwards, cells were transferred and stored at -150 °C freezer. For thawing, frozen cells were placed in a 37 °C water bath and subsequently transferred onto a 10 cm dish containing 10 ml of preheated medium.

2.2.3 Cell stimulation

Cytokine and soluble receptors were mixed in pre-warmed growth medium DMEM and added to the cells at various time periods at 37°C and 5% CO₂ prior to protein extraction, fixation or RNA isolation procedures or during live cell imaging.

2.2.4 Transient transfection of DNA

Transient transfection was performed when adherent cells reached a density of 60-70% confluence. Plasmid DNA and *TransIT*[®]-LT1 transfection reagent (Mirus, USA) were mixed in pre-warmed OptiMEM[®] reduced serum medium in a 3:1 ratio (μl of reagent/μg of DNA) and added to the cells, according to the manufacturer's instructions.

2.2.5 Stable transfection of DNA

2.2.5.1 Flp-In[™] system

Flp-In[™] System (Invitrogen, USA) was utilized for generation of stably transfected MEF Δ/Δ cell lines. For this purpose, cells were transfected with pFRT/lacZeo vector containing a FRT(Flp recombination target)-sequence for stable genome integration via Zeocin selection. Multiple cloning site vectors (pcDNA5/FRT/TO) containing fluorescent fusion protein constructs were then co-transfected in resulting MEF Δ/Δ FRT cells with pOG44 plasmid encoding Flp-Recombinase for stable integration via homologous recombination. Positive clone selection was performed with 1 mg/ml hygromycin. Afterwards, YFP-positive cells were enriched via fluorescence-activated cell sorter (FACS) at the Institute of Molecular Pathobiochemistry, Experimental Gene Therapy and Clinical Chemistry (RWTH Aachen).

2.2.5.2 Flp-In™ T-Rex™ system

For generation of cell lines that inducibly express genes of interest, zeocin and blasticidin-resistant HeLa-T-REx™ and Hek293 T-REx™ cells containing pcDNA6/TR vector for constitutive tetracycline-repressor (*tetR*) expression were stably transfected with pcDNA5/FRT/TO vectors in the same way, as described in 2.2.5.1 and selected via 300 µg/ml hygromycin and 10 µg/ml blasticidin supplementation. The stable clones contained the gene of interest under the control of tetracycline-operators (TetO₂) and the expression was induced by doxycycline (1-20 ng/ml) treatment.

2.2.5.3 pMOWS system

MEF STAT1^{-/-} and p65^{-/-} cells were retrovirally transduced utilizing pMOWS system [167]. In short, the genes of interest were cloned into the retroviral pMOWS expression vectors and transiently transfected into Hek293-derived PlatE retrovirus packaging cells. On the next day, the culture medium was replaced by increased serum growth medium containing 30% FCS and viruses were harvested as supernatants 24 hours after medium change. For the infection of MEF cells, virus-containing medium was given to the cells and selection was performed with 1 µg/ml puromycin for the next seven days.

2.2.6 Total cell protein extractions

For the isolation of total cellular lysates, cells were collected from the flask with the scraper in ice cold PBS and spun down at 4°C and 3500 RPM for 5 minutes. Resulting cell pellets were resuspended in 50-300 µl (depending on total cell amount) RIPA lysis buffer and left for at least 30 minutes on ice. Protease and phosphatase inhibitors were always added fresh to the lysis buffer (RIPA +/+) prior to use.

<u>RIPA Lysis Buffer:</u>	50 mM	Tris/HCl, pH 7,4
	150 mM	NaCl

0,5%	Nonidet P-40
1 mM	EDTA
1 mM	NaF
15%	Glycerol

<u>Protease inhibitors:</u>	2 µg/ml	Aprotinin (Sigma,USA)
	1 µg/ml	Leupeptin (Sigma, USA)
	0,5 mM	EDTA
	0,25 mM	PMSF

<u>Phosphatase inhibitor:</u>	1 mM	NaVO ₃
-------------------------------	------	-------------------

After removal of cell debris by 10 minutes of full-speed centrifugation at 4°C the supernatant containing total cell lysates was collected and stored in Eppendorf tubes at -20°C for further experiments.

2.2.7 Subcellular fractionation

Subcellular fractionation is a separation of karyoplasm (nucleoplasm) from cytoplasm. After washing with ice-cold PBS, cells were collected by centrifugation (3,500 RPM, 5 min 4°C). The pellet was resuspended in 100-200 µl hypotonic lysis buffer and incubated on ice for 15 min. After centrifugation (2,000 RPM, 10 min, 4°C) the supernatant containing cytosolic protein fraction was placed in separate Eppendorf tubes, centrifuged at maximum speed for additional 10 minutes to remove cell waste and stored at -20°C for further experiments. The remaining pellet containing nuclear protein fraction was resuspended in 500 µl nuclear isolation buffer, incubated on ice for 5 min and centrifuged (3,500 RPM, 5 min, 4°C) three times. After the last centrifugation the remaining pellet was resuspended in 50 µl nuclear lysis buffer, incubated on ice for 30 min and centrifuged (13,200 RPM, 10 min, 4°C). After centrifugation the supernatant representing nuclear protein fraction was collected in separate Eppendorf tubes and stored at -20°C for further experiments.

<u>Hypotonic lysis buffer:</u>	10 mM	Tris/HCl, pH 7,5
--------------------------------	-------	------------------

	10 mM	NaCl
	3 mM	MgCl ₂
<u>Nuclear isolation buffer:</u>	0,5%	Nonidet P-40
	10 mM	Tris/HCl, pH 7,5
	10 mM	NaCl
	3 mM	MgCl ₂
<u>Nuclear lysis buffer:</u>	2%	Triton X-100
	20 mM	Tris/HCl, pH 7,5
	280 mM	NaCl
	10 mM	NaF

Protease inhibitors were added prior to use as described for total protein extractions.

2.2.8 Measurement of protein concentration

Protein concentrations were measured in a solution according to a spectroscopic analytical procedure, called Bradford protein assay, which is based on an absorbance shift of the dye Coomassie Brilliant Blue G-250 from 465 nm to 595 nm upon binding to protein. The OD_{595nm} value of this dye is directly proportional to the concentration of soluble proteins. To measure the concentration of protein after total cell protein extraction or subcellular fractionation 3 µl of protein solution was diluted with 1 ml of 20% dye reagent concentrate (BioRad) and incubated at room temperature for 5 minutes. Absorbance was measured at 595 nm.

2.3 Biochemistry methods

2.3.1 SDS-Polyacrylamide-gel electrophoresis (SDS-PAGE)

SDS-PAGE (Sodium dodecyl sulfate polyacrylamide gel electrophoresis) is a method to separate proteins based on the length of their polypeptide chains, which governs

the electrophoretic mobility of proteins within a polyacrylamide gel. The amphiphilic SDS destroys secondary and tertiary protein structures, maintaining the proteins as

negatively charged polypeptide chains. The SDS-PAGE system contains two gels: a stacking gel with a low level of crosslinkage and low pH to sweep up proteins in a sample between two moving boundaries and a separation gel of higher pH and crosslinkage, where the proteins are separated. During this work only 10% separation gels were used.

<u>Separation gel:</u>	10%	Acrylamid
	375 mM	Tris/HCl, pH 8,8
	0,1%	SDS
	0,02%	TEMED
	0,1%	APS

<u>Stacking gel:</u>	5%	Acrylamid
	125 mM	Tris/HCl, pH 6,8
	0,1%	SDS
	0,02%	TEMED
	0,1%	APS

Probes derived from cellular extractions containing equal amounts of protein (20-30 µg) were denatured by heating at 95°C for 10 minutes in 4 x Laemmli buffer and then centrifuged immediately for 30 seconds at 13,200 RPM, at 4°C. After centrifugation probes were loaded on a SDS polyacrylamide gel in a running system filled with SDS running buffer. To determine the size of proteins and monitor the progress of an electrophoretic run the first well was loaded with 5 µl molecular weight marker PageRuler™ (#26616, Thermo Scientific). The gel was running at room temperature at 20-30 mA until the blue loading dye reached the bottom of the gel.

<u>4x Laemmli Buffer:</u>	40%	Glycerin
	8%	SDS
	250 mM	Tris/HCl, pH 6,8
	0,4%	Bromphenolblue

20%	β -Mercaptoethanol
-----	--------------------------

<u>SDS Running Buffer:</u>	1,5%	Tris-Base, pH 8,3
	7,2%	Glycin
	0,5%	SDS

2.3.2 Immunoblotting (Western-blot)

Western-blotting is a method of transferring separated proteins from SDS-PAGE in an electrical field from the gel onto a membrane for subsequent analysis. The proteins were transferred to an Amersham™ Hybond™ polyvinylidene difluoride (PVDF) membrane (#10600023, GE Healthcare, Germany) by semi-dry blotting using Anode I, Anode II and Cathode buffers:

<u>Anode buffer I:</u>	300 mM	Tris-Base, pH 10,4
------------------------	--------	--------------------

<u>Anode buffer II:</u>	25 mM	Tris-Base, pH 10,4
-------------------------	-------	--------------------

<u>Cathode buffer:</u>	25 mM	Tris-Base, pH 10,4
	40 mM	ϵ -Aminocaproic acid
	0,01%	SDS

To prevent non-specific background binding of the primary and/or secondary antibodies to the membrane, PVDF membrane was blocked after blotting for at least 30 minutes in TBS-T solution containing 10% bovine serum albumin (BSA) (#11930.04, Serva, Germany). After blocking, the membrane was rinsed with TBS-T buffer under agitation at room temperature for 5 minutes, the primary antibody diluted in TBS-T (1:1000) with 5% BSA was added and incubated overnight at 4°C under constant agitation. After the incubation the primary antibody was removed, membrane was washed three times for 10 minutes and the secondary antibody diluted in TBS-T (1:2000) was added for at least 60 minutes.

<u>TBS-T buffer:</u>	20 mM	Tris/HCl, pH 7,4
----------------------	-------	------------------

137 mM	NaCl
0,1%	Tween® 20

After another washing steps in TBS-T, the bound proteins were then detected using the ECL detection system Immobilon™ Western (Millipore, USA) and LAS-4000mini (Fujifilm) biomolecular imager. For protein counterstaining bound antibodies and an active HRP on the blot were removed by stripping: the membrane was placed in 10 ml stripping buffer containing freshly added 78 µl β-Mercaptoethanol and incubated at 70°C for 25-30 minutes. The incubation step was followed by blocking with 10% BSA solution and two washing steps in TBS-T. Afterwards, another primary antibody was added and the process repeated as described above.

<u>Stripping buffer:</u>	2%	SDS
	62,5 mM	Tris/HCl, pH 6,7

Quantification of immunoblotting results was conducted using MultiGauge v3.2 (Fujifilm, Japan) software, plotted using GraphPad Prism 6 software and statistically evaluated by Student's *t*-test.

2.3.3 Coimmunoprecipitation

Coimmunoprecipitation (Co-IP) is a common technique to analyze protein-protein interactions *in vitro*. Total cell lysates were prepared in RIPA +/- buffer as described in II.2.2.6 with a subsequent prolonged centrifugation step (30 minutes, 13,200 RPM at 4°C) for higher total protein yield. 30 µl of packed Protein G Sepharose beads (GE Healthcare, Germany) and 1 µg of the α-GFP antibody (#30694; Rockland, USA) per sample were incubated for 6 h at 4°C under permanent rotation. Resulting antibody-beads complexes were resuspended in RIPA buffer and spun down (5 minutes, 2,000 RPM at 4°C) three times. After incubation with 1,000 µg of total cell lysates overnight in RIPA +/- buffer at 4°C, bound complexes were washed three times with RIPA +/- buffer, boiled at 95°C for 10 minutes with 10 µl 4x Laemmli Buffer and analyzed by SDS-PAGE and immunoblotting.

2.3.4 GST-pulldown

The GST-pulldown assay was used to study protein-protein associations *in vitro*. For this purpose, various purified GST fusion importins were absorbed to S-linked glutathione agarose (#G4510, Sigma-Aldrich, USA) at 4°C overnight under constant rotation. For each sample, 50 µl of the agarose beads and 1 µg of purified importin molecules fused to GST-tag at the N-terminus were used. After washing with RIPA buffer three times, beads were incubated overnight with 1,000 µg of whole cell lysates in RIPA +/+ buffer. Afterwards, beads were washed three times with RIPA +/+ buffer, boiled 10 minutes at 95°C in 10 µl of 4x Laemmli buffer and bound proteins were separated on 10% SDS-PAGE and subjected to immunoblotting analysis with the indicated antibodies.

2.3.5 Electrophoretic mobility shift assay

Electrophoretic mobility shift assay (EMSA) is a common affinity electrophoresis method to study protein–DNA interactions. A double-stranded sis-inducible element (SIE) oligonucleotide from the *c-fos* promoter (m67SIE: 5'-GATCCGGGAG GGATTTACGG GAAATGCTG-3') was radioactively labelled by filling in 5'-protruding ends with 2 µl of Klenow enzyme (EP0051, 1 U/µl, Fermentas) and 2.5 µl [α -³²P]dATP (0.37 MBq/µl, Hartmann Analytic) in labeling buffer for 30 minutes at 37°C and radioactively labeled oligonucleotides were purified by QIAquick® Nucleotide Removal Kit (Qiagen) according to supplier's protocol. Radioactivity was measured by BetaScout 2007 liquid scintillation tester (PerkinElmer, USA). Subsequently, total cell lysates containing 10 µg protein (adjusted to total volume of 10.5 µl) in RIPA +/+ buffer were incubated with about 10 fmol (10,000 cpm) of labelled oligonucleotides in EMSA sample buffer for 10 minutes at room temperature. The DNA–protein complexes were separated on a 4.5% polyacrylamide gel in 0.25% TBE buffer at 220 V for 5 hours. Afterwards, the gel was fixed in fixation buffer for 15 minutes and dried on a gel dryer (Biotec Fischer) for 3 hours at 75°C. The phosphosignal was captured by Storage Phospho-Screen (Molecular Dynamics) at room temperature overnight and detected with a Typhoon-9410 fluorescence scanner (GE Healthcare, Germany) by excitation with a 633 nm laser line. For gel supershift total cell lysates were

incubated with 2.5 μ l of specific α -STAT3 antibody (sc-7179X) for 1 hour prior to gel loading.

<u>Labeling buffer:</u>	12.63%	Buffer M
	10 mM	dGTP/dCTP/dTTP
	1%	BSA
<u>5x Gelshift buffer:</u>	50 mM	Hepes/KOH, pH 7.8
	5 mM	EDTA
	25 mM	MgCl ₂
	50%	Glycerol
<u>EMSA sample buffer (per sample):</u>	2 μ l	1% BSA
	4 μ l	5x Gelshift buffer
	0.2 μ l	0.5 M DTT
	0.2 μ l	0.2 M PMSF
	1 μ l	Poly dIdC
	0.2 μ l	[α - ³² P]dATP-oligo (10,000 cpm)
	ad 9.5 μ l	ddH ₂ O
<u>5x TBE Buffer:</u>	1 M	Tris
	830 mM	Boric acid
	10 mM	EDTA, pH 8.3
<u>4.5% polyacrylamide gel:</u>	6.75 ml	40% Acryl-Bisacrylamide (19:1)
	3 ml	5x TBE buffer
	4.5 g	Glycerol
	200 μ l	20% APS
	40 μ l	TEMED
	47.75 ml	ddH ₂ O
<u>Fixation buffer:</u>	10%	Methanol
	10%	Acetic acid

2.4 Confocal laser scanning microscopy methods

2.4.1 Description

For the investigation of fluorescently labeled probes a confocal laser scanning microscope (LSM) was used. Confocal microscopy uses a pinhole and point illumination to eliminate out-of-focus light from the probe to increase optical resolution and contrast of images. It assembles the pixel information into images by scanning the probe point by point and line by line. Optical sectioning allows the reconstruction of three-dimensional structures from the obtained images.

2.4.2 Microscope settings

The investigation of subcellular distribution of immunostained and fluorescently labeled proteins was performed with a confocal laser scanning microscope LSM 710, (Carl Zeiss, Germany) using Zen 2012 software (Zeiss, Germany). The following setup was used for different fluorescent tags (Tab. 2.1):

Tab. 2.1: The microscope setup during fluorescence signal detection

Fluorescent dye	eYFP	Alexa Fluor®555	Alexa Fluor®488	DRAQ5™
Laser	Argon	DPSS 561-10	Argon	HeNe633
Excitation	514nm, 2%	561 nm, 2%	488 nm, 2%	633 nm, 2%
Pinhole	89.9	89.9	89.9	89.9
Main beam splitter	458/514	458/561	488	458/514/561/633
Emission Range	519-555 nm	562-655 nm	493-555 nm	661-759 nm

For all samples an image size of 1024×1024 pixels was used in 12-bit format with four times averaging and 1.5-2.5 zoom. Imaging was carried out using the LD C-Apochromat 40x /1.1 W Korr M27 water immersion objective.

2.4.3 Indirect immunofluorescence staining of cells

Cells were seeded and grown directly on glass coverslips (18 mm, Thermo Scientific) in a 12 well plate under standard growth conditions. According to experimental procedure cells were stimulated prior to fixation for different time periods. After removing the growth medium and washing two times with PBS⁺⁺ buffer, cells were fixed either with 3.7% PFA or ice-cold 100% methanol at room temperature for 20 minutes for one-step fixation, or with combined treatment of 3.7% PFA at room temperature for 15 minutes in the dark and subsequent ice-cold 100% methanol at 20°C for 10 minutes. After washing with PBS⁺⁺, cells were permeabilized with PBST⁺⁺ buffer for 5 minutes in the dark, quenched with 50 mM NH₄Cl diluted in PBST⁺⁺ for 5 minutes at room temperature to attenuate autofluorescence and blocked with PBST⁺⁺ containing 5% BSA for 1 hour at room temperature to prevent unspecific binding of antibodies. Primary antibodies were diluted 1:50 in PBST⁺⁺ with 1% BSA and applied to the cell-containing coverslips overnight at 4°C by placing coverslips upside-down onto parafilm with 30 µl antibody dilution drops. Afterwards, coverslips were dipped three times in PBST⁺⁺ buffer with 1% BSA and similarly stained with Alexa Fluor® 555 anti-rabbit alone or with Alexa Fluor® 488 anti-mouse antibody dilutions (1:1,000) for 90-120 minutes at 4°C. Subsequently, cell nuclei were stained with DRAQ5™ (Biostatus, UK) at 1:1,000 dilution for additional 20 minutes at 4°C.

<u>PBS⁺⁺</u>		PBS
	1 mM	MgCl ₂
	0,1 mM	CaCl ₂
<u>PBST⁺⁺</u>		PBS
	1 mM	MgCl ₂
	0,1 mM	CaCl ₂
	0,1%	Triton X-100

Finally, immunostained coverslips were mounted with Immu-Mount (Thermo Scientific) on glass slides and kept in the dark to prevent bleaching.

2.4.4 Live cell imaging

Stably transfected MEF Δ/Δ cells were plated 24 hours prior to imaging on 35-mm glass-bottomed dishes (Ibidi, Germany) in 300 μ l normal growth medium. Cells were imaged at 37°C and 5% CO₂ in an XL-LSM Incubator (PeCon, Germany) mounted on the stage of a Zeiss LSM 710. To prevent evaporation, the objective was immersed with Immersol™ fluid instead of water (Carl Zeiss, Germany).

2.4.5 Quantification of nuclear STAT3-FP amounts

The images of stably transfected MEF Δ/Δ cells were taken in real-time using Time Series function (1 image per minute) of Zen 2012 for 45 minutes during a live-cell imaging experiment. In order to quantify nuclear accumulation of fluorescent fusion proteins, the Profile function of Zen 2012 software was utilized to plot mean fluorescence intensities across the nuclear compartments of analyzed cells (Fig. 2.1). Changes in nuclear YFP fluorescence were measured within the same cells (n=10-20 cells per sample) before and 40 minutes after cytokine treatment.

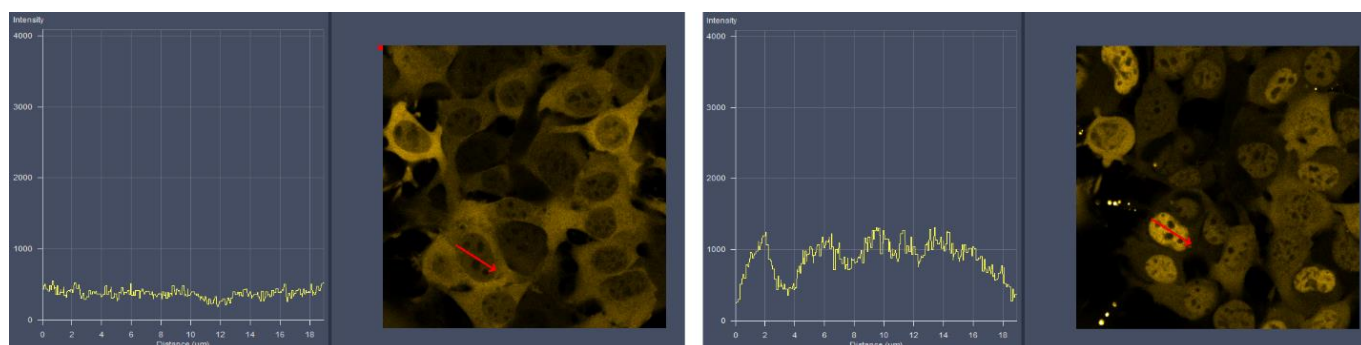


Fig. 2.1: Demonstration of the profile function of Zen 2012 software.

Mean fluorescent intensity was plotted using the GraphPad Prism 6 software (GraphPad Software, USA) and changes were statistically evaluated by Student's *t*-test. A *P* value of less than 0.05 was considered significant.

III.Results

1. Characterization of stably transfected MEF Δ/Δ cells

A focal point of this work is the analysis of STAT3 activation and nuclear translocation by confocal microscopy. For this purpose, we have chosen STAT3-deficient mouse embryonic fibroblasts (MEF Δ/Δ) stably reconstituted with STAT3 constructs fused to a fluorescent protein (STAT3-FP) as a well-established system for studying the importance of STAT3 domains for signaling. Although total knockout of STAT3 led to early embryonic lethality in mice [38], conditional gene targeting has been successfully used to study STAT3 functions in specific tissues and cells [168, 169] and STAT3 knockout MEF Δ/Δ have been established [100]. Our group has previously generated MEF Δ/Δ cells stably reconstituted with a wild-type (WT) STAT3-FP construct using the Flp-InTM system (Figure 3.1 A, B) [52]. In order to confirm functionality of the STAT3-FP construct, we analyzed four critical steps of STAT3 activation: tyrosine 705 phosphorylation, nuclear accumulation, GAS-element binding and transcription of immediate early target genes.

IL-6 treatment of MEF Δ/Δ (WT)STAT3-FP cells for 30 minutes resulted in STAT3 Y705 phosphorylation similarly to wild-type MEFs. In turn, MEF Δ/Δ cells demonstrated complete absence of STAT3 in whole cell lysates as expected (Fig. 3.1C). STAT3 subcellular localization upon IL-6 stimulation was analyzed in a live-cell imaging experiment. Similarly to endogenous STAT3 [52], STAT3-FP accumulated in the nuclei of IL-6 treated cells reaching its peak at 30 minute time point (Fig. 3.1D). Moreover, stable reconstitution of STAT3-FP reversed the absence of socs3 mRNA upregulation in MEF Δ/Δ cells to the same extent as in wild-type MEFs (Fig. 3.1E). Upon IL-6 stimulation of (WT)STAT3-FP cells three major DNA complexes were detected by electrophoretic mobility shift assay (EMSA) (Fig. 3.1F) that are composed of STAT3-FP homodimers (S3/S3), STAT3-FP/STAT1 (S3/S1) heterodimers and STAT1 homodimers respectively, as expected for wild-type STAT3 [170]. A supershift experiment with a STAT3 specific antibody confirmed that the observed bands upon IL-6 stimulation represent indeed STAT3 homodimer and

STAT3/STAT1 heterodimer populations. Combined, these data validate fluorescently labeled STAT3 for mimicking endogenous STAT3 activation for further experiments.

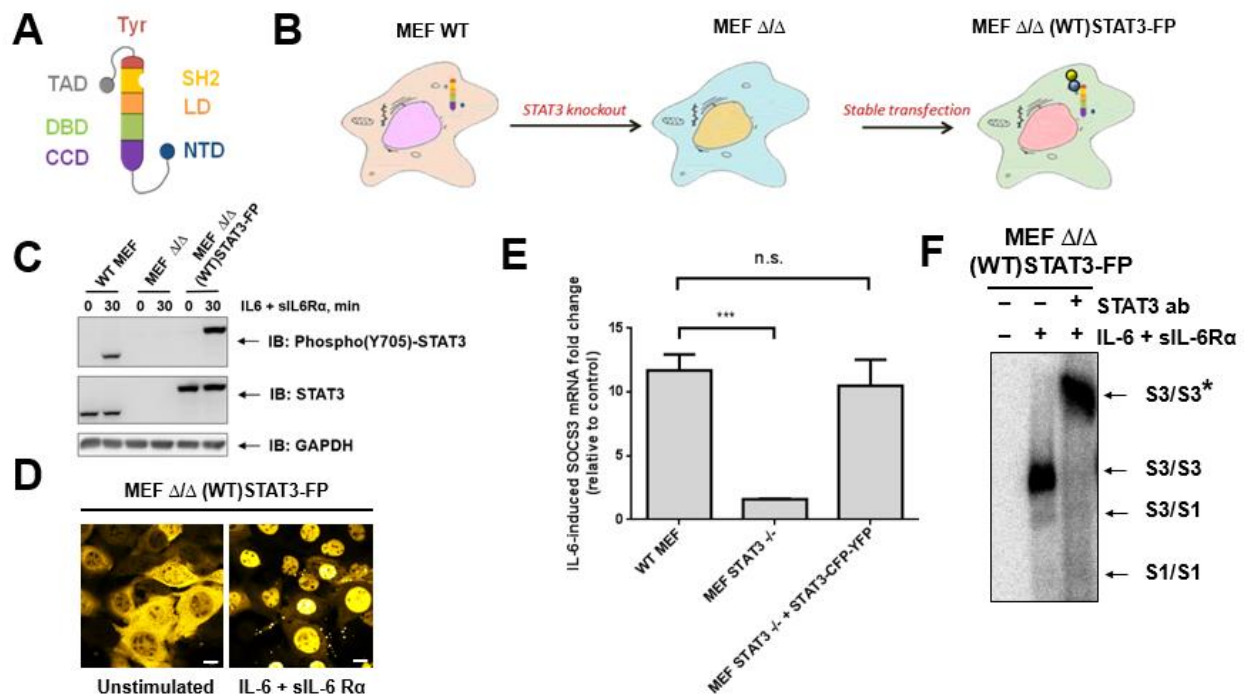


Fig. 3.1: Characterization of fluorescently labeled wild-type STAT3 construct. A. STAT3 monomer structure with flexible NTD and TAD domains. B. Scheme of wild-type (MEF WT), STAT3 deficient (MEF Δ/Δ) and stably reconstituted (MEF Δ/Δ (WT)STAT3-FP) MEF cells. C. Analysis of STAT3 tyrosine 705 phosphorylation. Indicated cell lines were stimulated with 20 ng/ml IL-6 and 500 ng/ml sIL-6R α for 30 minutes or left untreated. Total cell lysates were prepared and analyzed by immunoblotting with the indicated antibodies. GAPDH immunodetection served as a loading control. D. Real-time nuclear translocation of WT STAT3 fusion proteins upon IL-6 stimulation. MEF Δ/Δ cells stably reconstituted with (WT)STAT3 fused to CFP-YFP double tags were observed by confocal live-cell imaging. Cells were either left untreated (left) or stimulated with 20 ng/ml IL-6 and 500 ng/ml soluble IL-6R (sIL-6R α) for 30 (right). Scale bars represent 10 μ m. E. SOCS3 mRNA expression increases upon IL-6 treatment. WT MEF, MEF Δ/Δ , and MEF Δ/Δ (WT)STAT3-FP cells were treated with 20 ng/ml IL-6 and 500 ng/ml soluble IL-6R (sIL-6R α) for 60 minutes. Whole cellular mRNA was isolated, and the expression of *socs3* was measured by RT-qPCR. Expression was normalized to the housekeeper protein mGUSB. Data are representative of four independent experiments. *** $p < 0.0005$. n.s. = not significant. F. IL-6 induced DNA-binding of STAT3 fusion proteins. MEF Δ/Δ (WT)STAT3-FP cells were stimulated with 20 ng/ml IL-6 and 500 ng/ml sIL-6R α for 30 minutes or left untreated, subsequently total cell lysates were analyzed by an EMSA assay using a STAT1/STAT3 specific GAS element corresponding to a mutated sequence from the *c-fos* promoter (m67SIE). Explain S1/S1 etc. * Supershifted STAT3 band upon addition of a STAT3 antibody prior to gel loading.

Our group has previously published results with MEF Δ/Δ cells stably transfected with N-terminal deletion ((Δ N)STAT3-FP) and point-mutated putative nuclear localization sequences ((Δ NLS)STAT3-FP) or nuclear export sequences ((Δ NES)STAT3-FP) within STAT3 [52]. During this project we have used several fluorescently labelled STAT3 mutant constructs, an overview of which can be found in Fig. 3.2A.

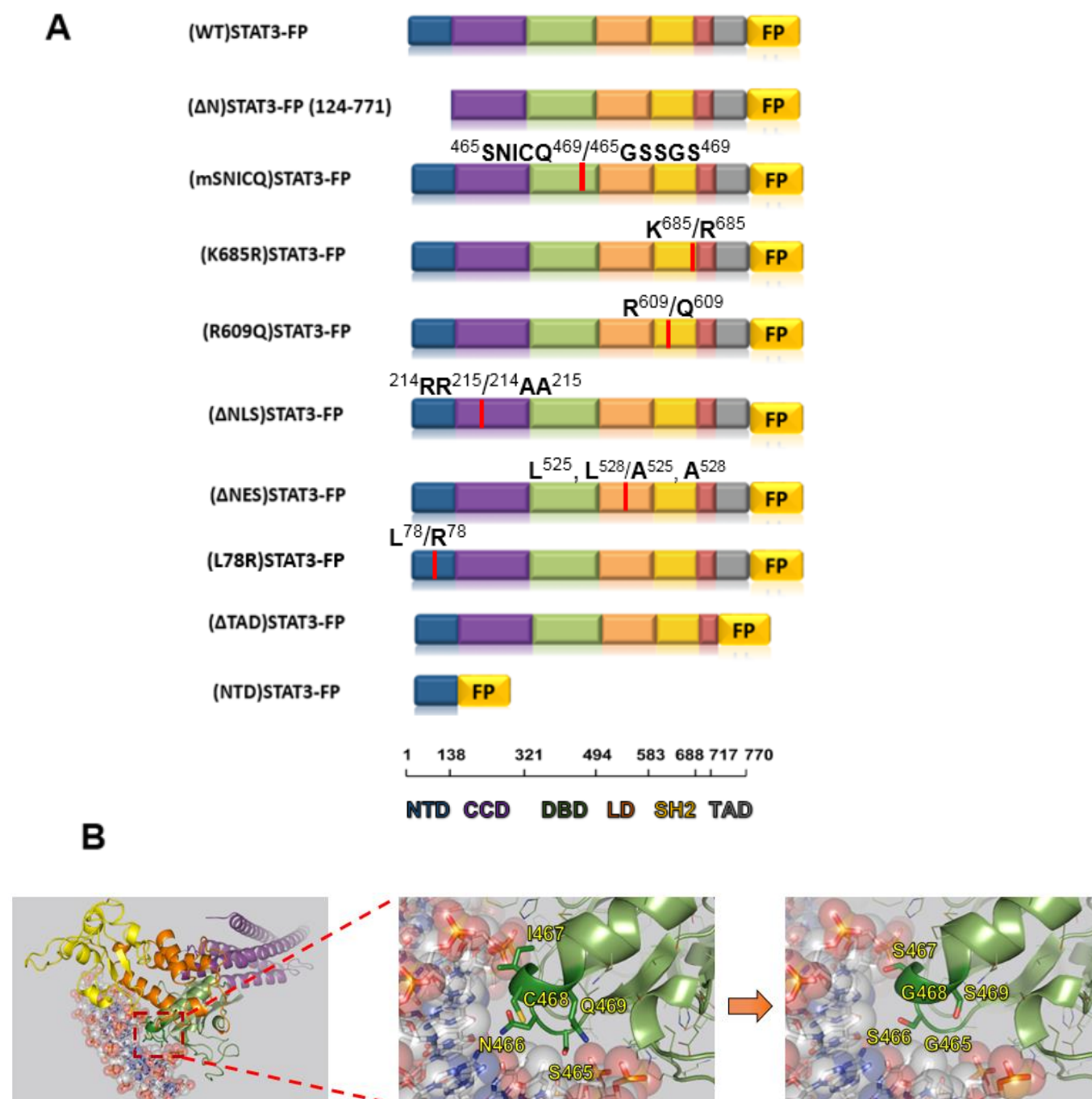


Fig. 3.2: Overview of STAT3 constructs used in this work. A. Graphical representation of conserved domains of STAT3–FP and mutant constructs used for the generation of stable cell lines. Red bars show the positions of the relevant mutations. FP, fluorescent proteins; NTD, N-terminal domain; CCD, coiled-coil domain; DBD, DNA-binding domain; SH2, src-homology 2 domain; TAD, transactivation domain. B. STAT3 DNA binding abrogation scheme. Left: Ribbon diagram of STAT3 bound to DNA (only one STAT3 of the STAT3 dimer is shown; PDB accession number: 1BG1) [172]. The DNA-binding SNICQ-sequence of STAT3 (center) and the mutated GSSGS sequence (right) are highlighted in dark green with amino acid side chains of these motifs represented as rod models. The DNA helix recognized by STAT3 (5'TGCATTTCCCGTAAATCT3') is represented as rod model and van der Waals radii of the atoms are indicated as transparent spheres. Graphic representation and introduction of point mutations were performed using the PyMOL software (PyMOL Molecular Graphics System, Version 1.7.4 Schrödinger, LLC).

Presented mutated STAT3–fluorescent protein (FP) constructs were then stably transfected in MEF Δ/Δ cells and analyzed during the subsequent parts of this work. (R609Q)STAT3-FP represents a STAT3 molecule with dysfunctional SH2 domain that cannot bind to the receptor and therefore cannot be activated by a cytokine [50, 86]. The K685R mutation interferes with STAT3 acetylation on the critical lysine 685 residue and has a negative impact on cytokine-induced stable dimer formation [171]. Furthermore, a C-terminal deletion mutant ((Δ TAD)STAT3-FP) and the isolated STAT3 NTD ((NTD)STAT3-FP) constructs were stably expressed in MEF Δ/Δ cells for further functional analysis of N- and C-terminal ends of STAT3.

In order to analyze connection between GAS recognition and nuclear accumulation of STAT3, we have created an artificial STAT3 (mSNICQ)STAT3-FP mutant that is not able to specifically recognize GAS elements in order to analyze functional role of DNA binding in STAT3 subcellular localization and signaling. In order to abrogate specific STAT3 DNA-binding we mutated one of the four STAT3 loops that contact the DNA double helix. We introduced mutations into the $\alpha 5$ loop of the DNA-binding domain as this loop provides the most intensive DNA contacts and contains critical determinants for the specific recognition of the consensus DNA sequence (Fig. 3.2B, left) according to crystal structure of STAT3 dimer bound to DNA [172]. Within the SNICQ sequence (Fig. 3.2B, center) residues S465, N466 and Q469 provide the most important contacts, most of them consisting of hydrogen bonds. Among these amino acids, N466 is of particular importance and provides both polar and hydrophobic interactions with DNA, which are crucial for consensus sequence recognition. More specifically, it contacts T₁, T₂ and the guanine base of the G:C base pair at position 3 of the motif T₁T₂C₃C₄C₅G₆T₇A₈A₉. C468 contributes to DNA-binding by forming a hydrophobic pocket together with the methylene groups of S465, N466 and Q469 in which the methyl groups of two thymines (T₁, T₂) are accommodated [172]. In order to reduce STAT3-DNA contacts (both hydrogen bonds and the mentioned hydrophobic contacts) N466, I467 and Q469 were mutated to serine to shorten the side chains while maintaining the polar characteristic of the $\alpha 5$ loop. Furthermore, S465 and C468 were mutated to glycine to further reduce the contacts to DNA. As visualized at the right of Fig. 3.2B, the introduction of these mutations should abrogate STAT3 DNA-binding.

2. The role of N-terminal domain and GAS-site recognition in STAT3 signaling

2.1. Ligand-induced nuclear accumulation and DNA-binding ability of STAT3 are independent of each other.

Upon activation, STATs undergo phosphorylation-dependent dimerization and accumulate in the nucleus, where they bind to DNA and regulate gene transcription [21]. We have previously shown that despite the ability to bind DNA in electrophoretic mobility shift assay phosphorylated STAT3 dimers lacking the N-terminal domain show defective nuclear accumulation upon stimulation [52]. We were interested, whether (mSNICQ)STAT3 can still be imported in the nucleus upon stimulation despite its inability to bind to GAS sequences. For this purpose, MEF Δ/Δ cells stably transfected with different STAT3-FP constructs were stimulated with IL-6 and soluble IL-6R α . Changes in STAT3 subcellular localization were assessed in a live-cell imaging experiment with quantification of nuclear fluorescence (Fig. 3.3 A, B).

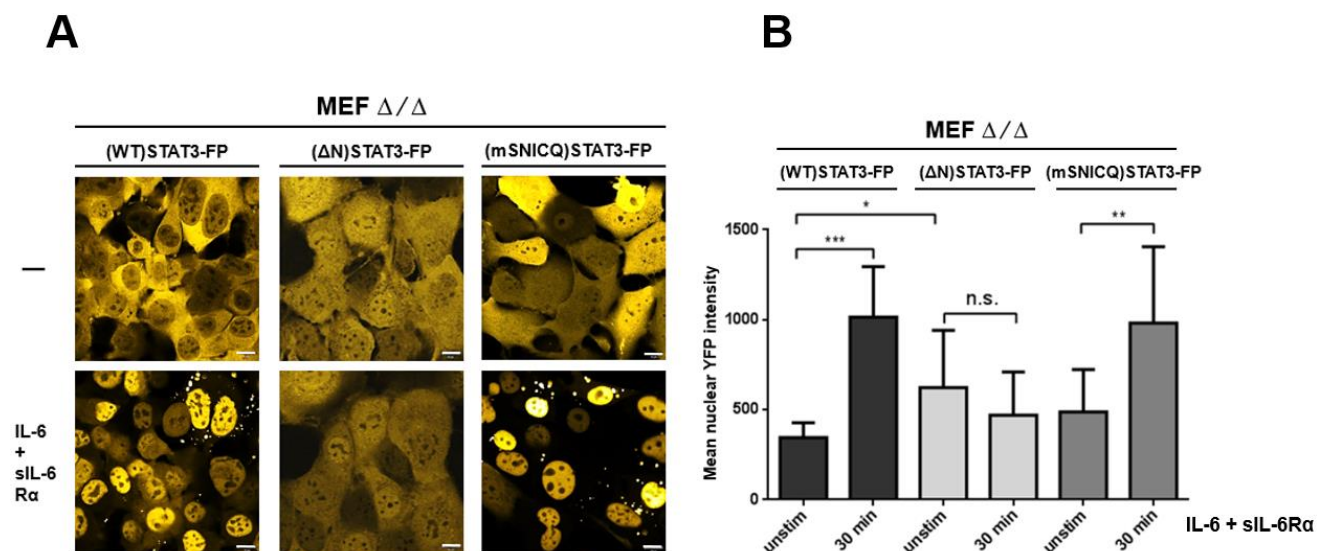


Fig. 3.3: IL-6-induced real-time nuclear translocation of STAT3 fusion proteins. A. MEF Δ/Δ fibroblasts stably transfected with (WT)STAT3 or (Δ N)STAT3 with CFP-YFP double tags or (mSNICQ)STAT3 with YFP tag constructs were observed by confocal live-cell imaging. Cells were stimulated with 20 ng/ml IL-6 and 500 ng/ml soluble IL-6R (sIL-6R α) for 30 minutes or left untreated. Scale bars represent 10 μ m. B. Quantification of the nuclear presence of fluorescently labeled STAT3 constructs in MEF Δ/Δ cells (means \pm SD of n=15 cells per sample). ***p < 0.0005. **p < 0.005. *p < 0.05. n.s. = not significant.

Upon stimulation, wild-type STAT3-FP showed rapid nuclear translocation, while NTD deletion mutant did not or only poorly accumulate in the nucleus, as described earlier [52]. The mSNICQ mutant, however, entered the nucleus with similar kinetics to wild-type. Thus, disruption of the DNA-binding interface of STAT3 does not impair nuclear accumulation.

The same stably transfected MEF Δ/Δ cells were also used to analyze DNA-binding, STAT1 association and tyrosine 705 phosphorylation of (Δ N)STAT3-FP and (mSNICQ)STAT3-FP in comparison to STAT3-FP wild-type (Fig. 3.4A). Additionally, expression of the STAT3 immediate early target gene *socs3* upon IL-6 stimulation was quantified in order to analyze transcriptional activity of FP constructs (Fig. 3.4B).

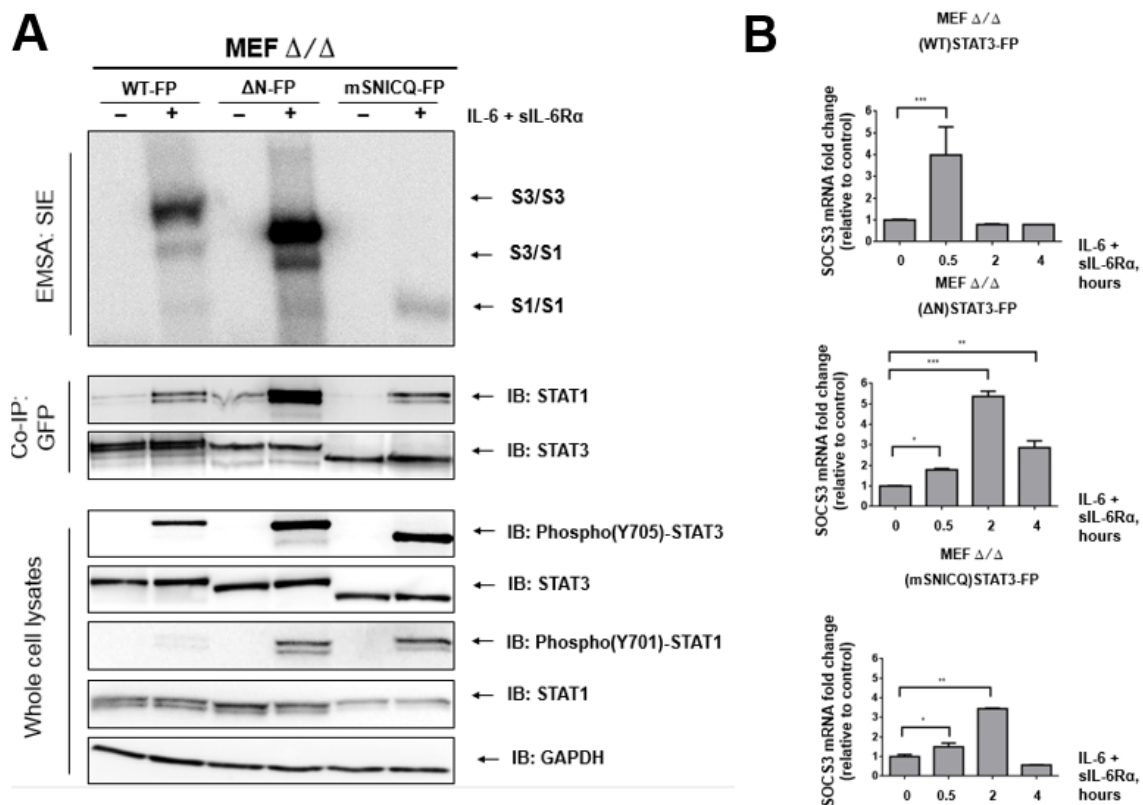


Fig. 3.4: Analysis of STAT3-FP construct activation, heterodimer formation, GAS-recognition and transcriptional activity. A. IL-6 induced DNA-binding, STAT1 binding and activation of STAT3 fusion proteins. Indicated cells were stimulated with 20 ng/ml IL-6 and 500 ng/ml sIL-6R α for 30 minutes or left untreated, subsequently total cell lysates were prepared and analyzed either in an electrophoretic mobility shift assay using hybridized 32 P-labelled SIE oligonucleotides, coimmunoprecipitation (Co-IP) experiment with the antibody against GFP or by Western blotting using indicated antibodies. * Supershifted STAT3 band upon addition of a STAT3 antibody prior to gel loading. (B) IL-6-inducible *socs3* mRNA expression. MEF Δ/Δ cells stably transfected with fluorescent (WT)STAT3-FP, (Δ N)STAT3-FP or (Δ SNICQ)STAT3-FP mutants were treated with 20 ng/ml IL-6 and 500 ng/ml sIL-6R α for indicated times. Whole cellular mRNA was isolated, and the expression of *socs3* was measured by RT-qPCR. Expression was normalized to the housekeeper gene *mGUSB*. The relative expression ratios were calculated by the $\Delta\Delta$ Ct method [166]. Data are representative of three independent experiments. ***p < 0.0005. **p < 0.005. *p < 0.05.

As for (WT)STAT3-FP, (Δ N)STAT3-FP showed a similar pattern of DNA binding with three different homo- and heterodimer populations, but the signals from all three complexes were increased, suggesting an increased activation potential of this mutant compared to wild-type, given the equal protein expression in cellular lysates. As predicted, the STAT3 mutant with disrupted DNA-binding interface could not recognize the GAS sequence and only STAT1 homodimers were detected upon IL-6 stimulation in cells stably expressing the (mSNICQ)STAT3-FP construct. All three STAT3-FP constructs form heterodimers with STAT1 and are tyrosine phosphorylated at the position 705 after IL-6 stimulation. Similarly to EMSA, (Δ N)STAT3-FP is more sensitive to the stimulus and binds stronger to STAT1 than wild-type, while (mSNICQ)STAT3-FP expression and phosphorylation levels remained comparable. Moreover, both (Δ N)STAT3-FP and (mSNICQ)STAT3-FP expressing cells, but not (WT)STAT3-FP, showed an increased STAT1 activation upon IL-6 treatment. Despite its inability to bind DNA, (mSNICQ)STAT3-FP was still able to form homodimers and heterodimers with wild-type STAT3-FP (data not shown).

To investigate how the NTD deletion and DNA-binding interface mutations affect the expression of the STAT3 target gene *socs3*, cells were stimulated with IL-6 for 30, 120 and 240 minutes, total mRNA was isolated and analyzed via real-time qPCR (Fig. 1D). As expected, significant upregulation of *socs3* mRNA was detected after 30 minutes of stimulation as an immediate early gene response within the cells expressing (WT)STAT3-FP. After 2 or 4 hours total levels of *socs3* mRNA did not significantly differ from unstimulated cell population. Both (Δ N)STAT3-FP and (mSNICQ)STAT3-FP failed to induce significant *socs3* upregulation after 30 minutes to the same extent as wild-type. Increase of *socs3* mRNA compared to unstimulated control was observed after 2 hours in cells expressing the mutated constructs, which may be explained by other transcription factor involvement, such as abnormally activated STAT1. Taken together, our data demonstrate that the NTD deletion mutant is capable to bind DNA but not to accumulate in the nucleus, while the mSNICQ mutant demonstrates the diametrically opposed capability to undergo rapid nuclear translocation upon stimulation without being able to bind GAS-elements. Both mutants were defective in the early induction of *socs3* gene expression.

2.2. STAT3 N-terminal domain deletion mutant remains in the cytoplasm in the form of activated dimers capable of GAS-element binding

To further explore the consequences of defective nuclear translocation of the STAT3 NTD deletion mutant, we analyzed its activation kinetics compared to wild-type. It has been shown for STAT1 that the deletion of the NTD resulted in a constitutively phosphorylated phenotype and inability to be dephosphorylated by phosphatases *in vivo* [173], as well as absence of IFN α -induced nuclear accumulation [174]. MEF Δ/Δ cells, stably expressing (WT)STAT3-FP and (Δ N)STAT3-FP fusion proteins, were pulse stimulated with IL-6 for 20 minutes, left untreated for up to 4 hours and total cell lysates were subjected to either EMSA or immunoblotting (Fig. 3.5).

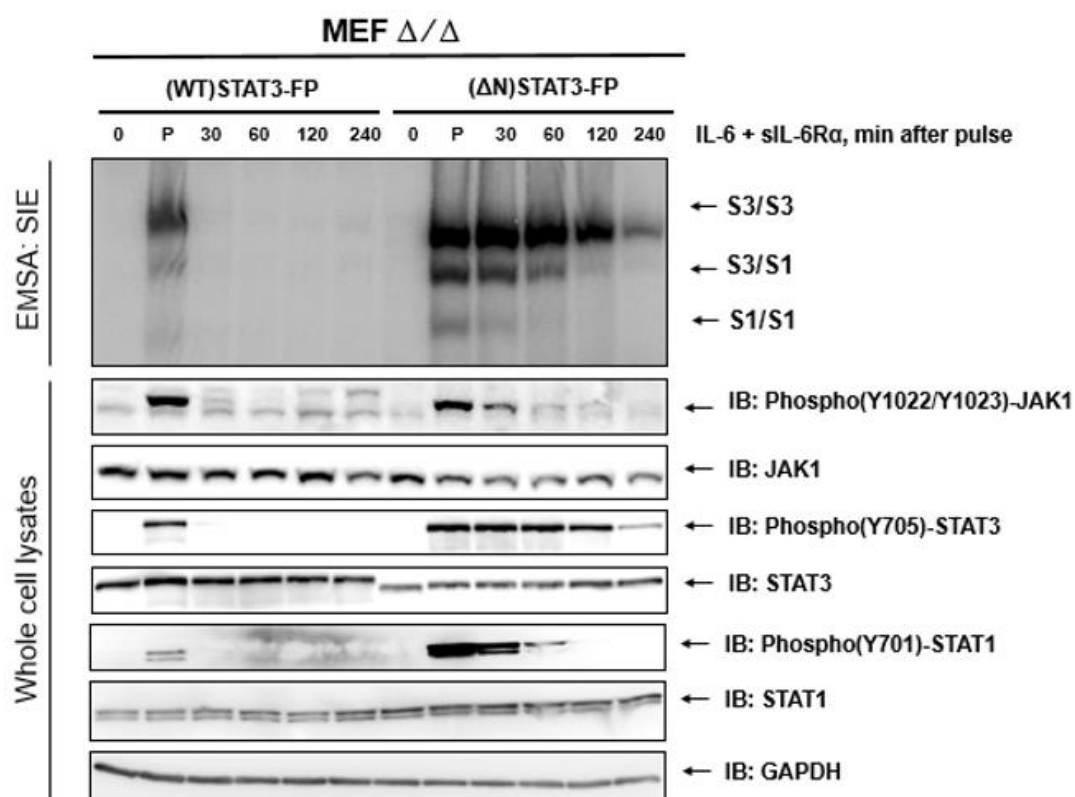


Fig. 3.5: IL-6 induced DNA-binding/dissociation rate and deactivation of the wild-type and Δ N STAT3 fusion proteins. Cells were pulse-stimulated with 20 ng/ml IL-6 and 500 ng/ml sIL-6R α for 20 minutes, washed with PBS, supplied with fresh medium and left untreated for up to 240 minutes. Total cell lysates were prepared at the indicated time points and analyzed either in an electrophoretic mobility shift assay using hybridized 32 P-labelled m67SIE oligonucleotides or by Western blotting using the antibodies indicated. GAPDH immunostaining served as a loading control.

While the wild-type fusion protein showed rapid dephosphorylation of tyrosine 705 and dissociation from DNA already 30 minutes after stimulus elimination, (Δ N)STAT3 remained in the form of phosphorylated dimers for more than 4 hours after cytokine removal. Furthermore, STAT1 activation in cells expressing (Δ N)STAT3-FP was markedly elevated. Apart from (Δ N)STAT3-FP homodimers, (Δ N)STAT3-FP/STAT1 heterodimers were bound to radioactive DNA probes for at least 2 hours in contrast to cells, expressing (WT)STAT3-FP. This augmented activity of (Δ N)STAT3 was not correlated with JAK1 activation. Tyrosine phosphorylation of JAK1 in (Δ N)STAT3-FP cells was only slightly prolonged for 30 minutes after stimulus removal and correlates only with increased STAT1 activation in the mutant cell line.

Next, we applied indirect immunofluorescence to analyze the subcellular distribution of activated (Δ N)STAT3-FP dimers after 30 minutes of stimulation (Fig. 3.6). As expected, phosphorylated (WT)STAT3-FP molecules were localized primarily in the nucleus. In contrast, phosphorylated dimers of the STAT3 NTD deletion mutant are trapped in the cytoplasm.

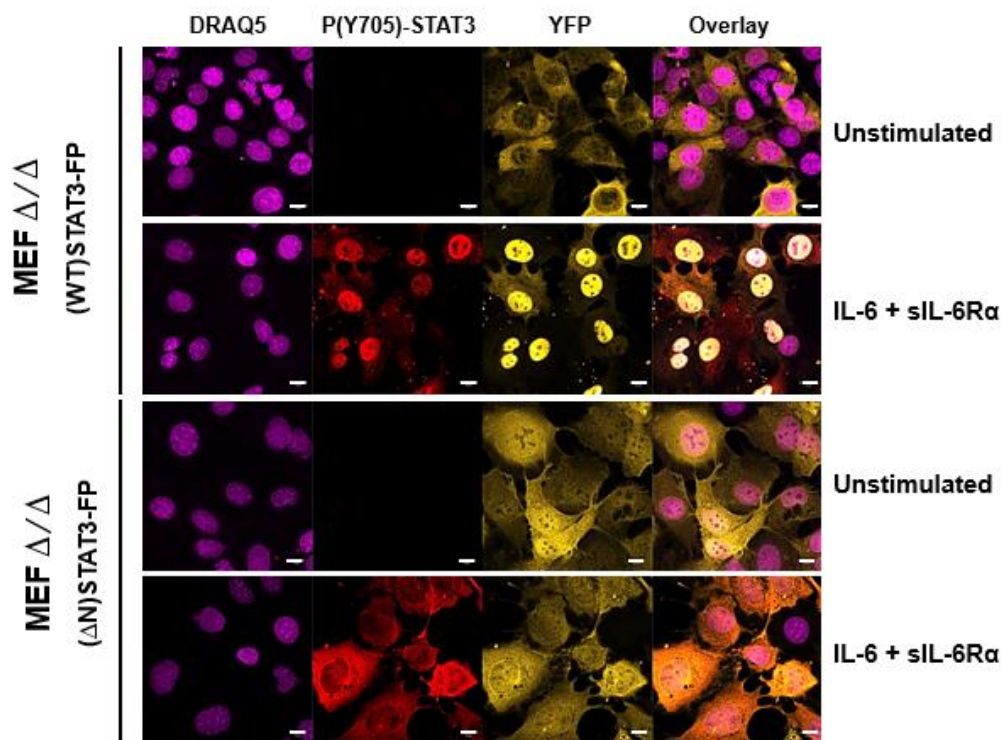


Fig. 3.6: Immunofluorescence studies of MEF Δ/Δ fibroblasts stably transfected with (WT)STAT3-FP or (Δ N)STAT3-FP constructs. Cells were stimulated with 20 ng/ml IL-6 and 500 ng/ml sIL-6R α for 30 minutes or left untreated, fixed, permeabilized and stained using a phospho(Y705)STAT3 antibody, followed by incubation with a secondary Alexa Fluor-555 conjugated antibody and DRAQ5 nuclear marker. Scale bars represent 10 μ m.

The stably transfected MEF Δ/Δ cells were also used to compare the IL-6 treatment sensitivity of (Δ N)STAT3-FP with (WT)STAT3-FP (Fig. 3.7A). Deletion of the N-terminal domain in the mutant resulted in an increased sensitivity of the protein to IL-6 stimulation at low concentrations of the cytokine (1-5 ng/ml) compared to wild-type.

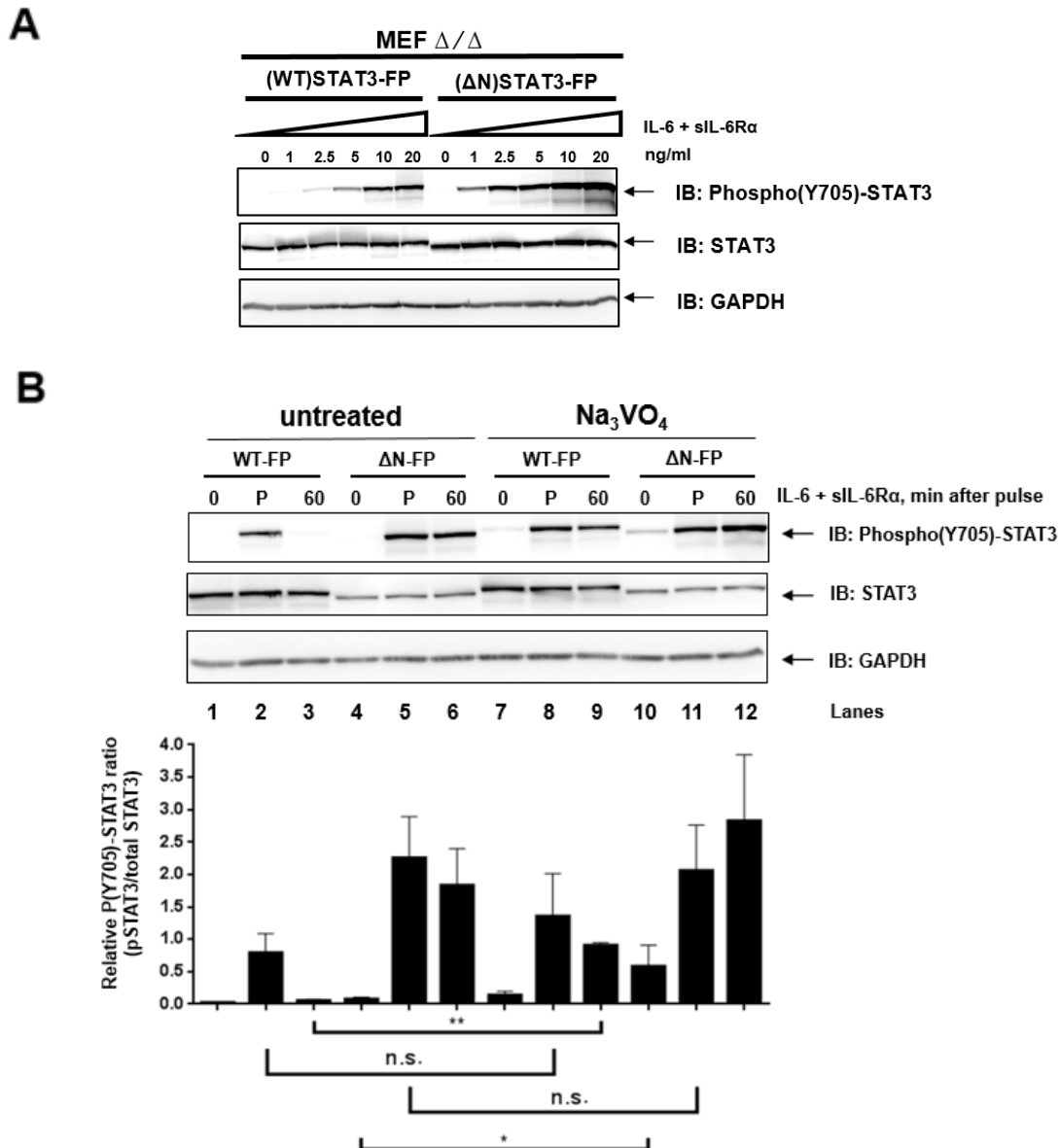


Fig. 3.7: IL-6 sensitivity and phosphatase inhibition. A. STAT3 activation in stably transfected (WT)STAT3-FP and (Δ N)STAT3-FP cells. Cells were stimulated with indicated concentrations of IL-6 and 500 ng/ml sIL-6R α for 30 minutes or left untreated. Total cell lysates were prepared and analyzed by Western blotting using the antibodies indicated. B. Effect of phosphatase inhibition on (WT)STAT3-FP or (Δ N)STAT3-FP deactivation. MEF Δ/Δ stably transfected with (WT)STAT3-FP or (Δ N)STAT3-FP were incubated with 1 mM sodium orthovanadate for 1 hour or left untreated. Then cells were pulse-stimulated with 20 ng/ml IL-6 and 500 ng/ml sIL-6R α for 20 minutes, washed with PBS, supplied with fresh medium and left untreated for 60 minutes. Finally total cell lysates were prepared and analyzed by Western blotting using the antibodies indicated. Immunoblots from three independent experiments were quantified using Fujifilm MultiGauge v3.2 software. **p < 0.005. *p < 0.05. n.s. = not significant.

Since prolonged activation of (Δ N)STAT3-FP was not attributed to prolonged JAK1 activity, a possible role of tyrosine phosphatases for this effect was investigated. If the lack of dephosphorylation of (Δ N)STAT3-FP was due to ineffective access of tyrosine phosphatases which may only be active in the nucleus, phosphatase inhibition via sodium orthovanadate would be expected to produce the same prolonged activation effect for (WT)STAT3-FP. Stably transfected MEF Δ/Δ cells were pretreated with or without sodium orthovanadate for 1 hour, pulse stimulated with IL-6 and left for 60 minutes, as described previously. Total cell lysates were analysed by immunoblotting and results from three independent experiments were quantified (Fig. 3.7B). Indeed, phosphatase inhibition produced the same prolonged p-STAT3 signal for the wild-type fusion protein as seen for NTD deletion mutant. Moreover, elimination of tyrosine phosphatase activity had no statistically significant influence on (WT)STAT3-FP and (Δ N)STAT3-FP ligand-dependent phosphorylation intensity, but it led to an increase in basal phosphorylation, suggesting that phosphatases are able to act on (Δ N)STAT3-FP only in the unstimulated state. These findings indicate that the conserved NTD is indispensable for cytokine-induced nuclear accumulation and subsequent dephosphorylation.

2.3. STAT3 NTD is not required for binding to various importin- α isoforms

Presence of the conserved NTD of STAT1 is required for its association with importin- α 5 and subsequent nuclear translocation [175]. Here we asked, whether the same holds true for STAT3 NTD and its interaction with α -importins. For this purpose, we expressed 5 human GST-tagged importins (α 1, α 3, α 5, α 6 and α 7) with deleted IBB domain to eliminate possible autoinhibition [149]. Expressed proteins were absorbed to GST-beads and incubated with total cell lysates from IL-6 stimulated MEF Δ/Δ cells stably expressing (WT)STAT3-FP. Resulted protein complexes were analyzed via SDS-PAGE and subsequent immunoblotting (Fig. 3.8A). Activated (WT)STAT3-FP was shown to bind importins α 5 (strongest), α 3 and α 7, but not the other importins and GST protein alone.

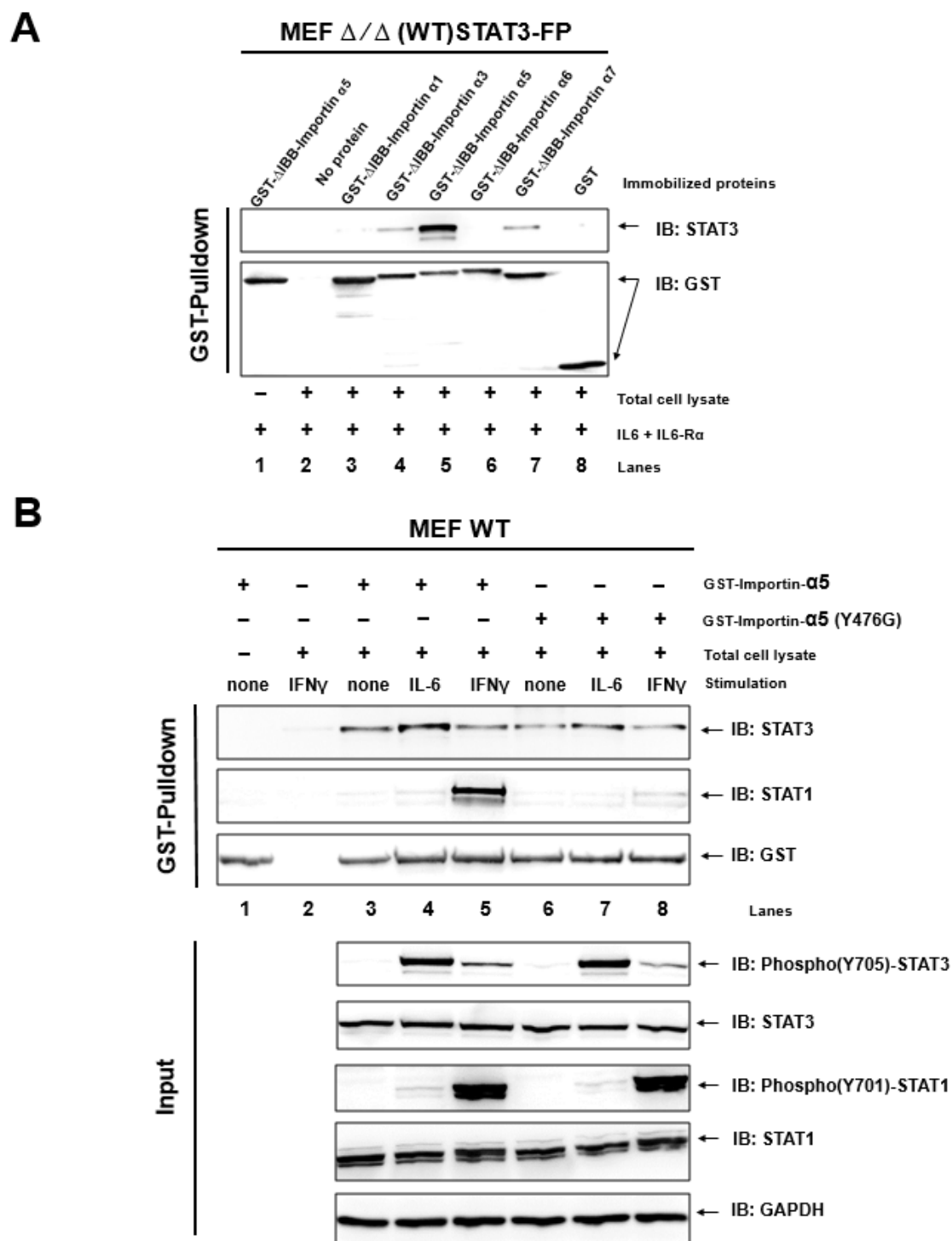
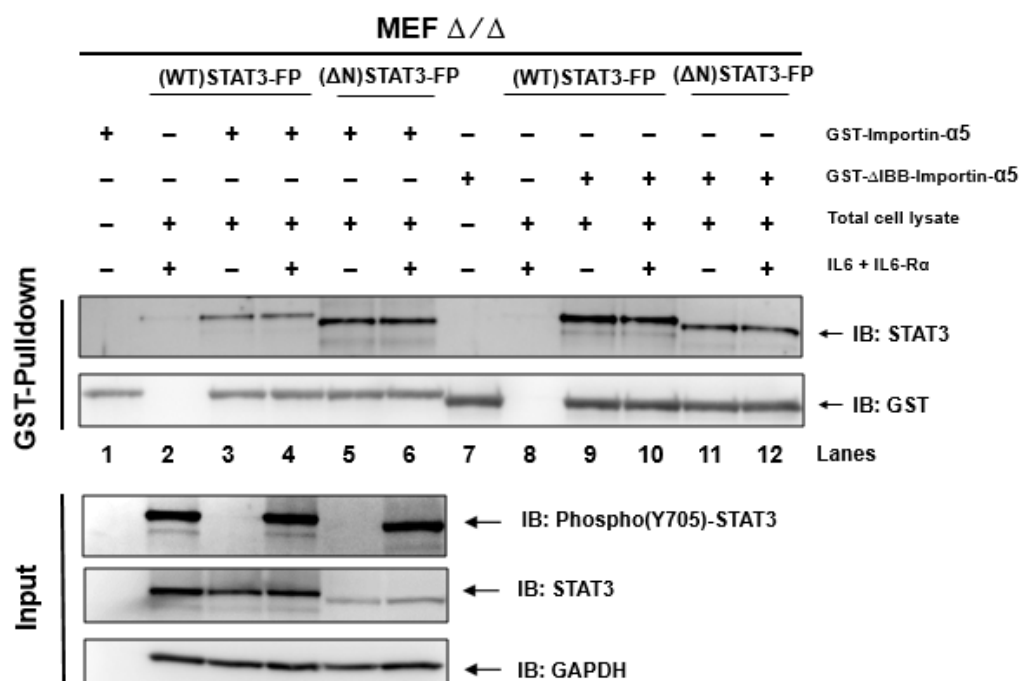
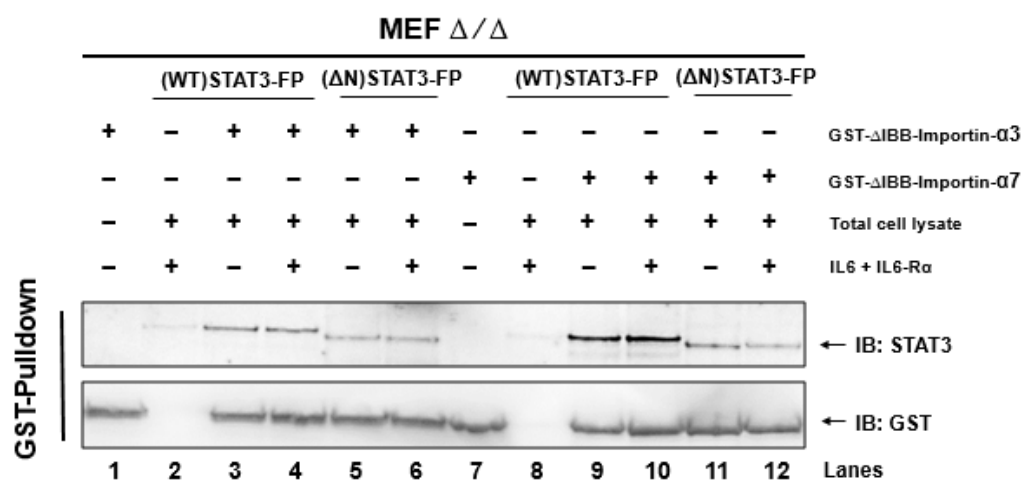
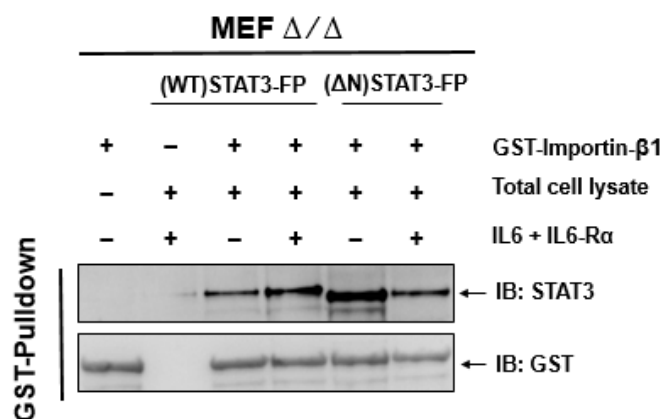


Fig. 3.8: STAT3 binding to α -importins *in-vitro* A. Wild-type STAT3-FP fusion protein binding to different importins analyzed by GST pull-down assay. Indicated GST-importin fusion proteins were coupled to GST-beads and incubated with total protein extracts of MEF Δ/Δ cells stably transfected with (WT)STAT3-FP construct and stimulated with 20 ng/ml IL-6 and 500 ng/ml sIL-6R α for 20 minutes. Precipitated complexes were separated on 10% SDS-PAGE and subjected to Western blotting using the antibodies indicated. Lanes 1, 2 and 8 served as internal controls for specific interactions between STAT3-FP and importin molecules. B. Endogenous STAT3 and STAT1 protein binding to importin- $\alpha 5$ constructs analyzed by GST pull-down assay. GST-importin- $\alpha 5$ or mutated GST-importin- $\alpha 5$ (Y476G) proteins bound to GST-beads were incubated with total protein extracts of wild-type MEF cells that were stimulated with either 20 ng/ml IL-6 and 500 ng/ml sIL-6R α or 20 ng/ml IFN γ for 20 minutes. Precipitated complexes were analyzed by Western blotting using the antibodies indicated similarly to Fig.3A. Lanes 1 and 2 served as internal controls for specific interactions between STAT1, STAT3 and importin- $\alpha 5$ molecules.

To support the finding that STAT3 binding to GST fusion proteins is specific to STAT3 and not fluorescent tags, we performed the pulldown experiment with lysates of wild-type MEF cells. For STAT1 importin- α 5 binding *in vitro* has been shown to be phosphorylation-dependent and mutation of a single conserved tyrosine at position 476 to glycine within importin- α 5 abolished STAT1 binding [155]. To analyze, whether the same applies to STAT3/importin- α 5 interaction, we stimulated MEF cells with IL-6 and IFN γ and incubated lysates with full-length importin- α 5 or mutated importin- α 5(Y476G) GST-fusion proteins (Fig. 3.8B). Afterwards, we analyzed binding of both STAT1 and STAT3 to GST-importin- α 5 constructs by immunoblotting. Our results confirmed previously published stimulus-dependent STAT1 binding to wild-type importin- α 5, while binding to the Y476G mutant was almost completely eliminated. In contrast, endogenous STAT3 could be precipitated from lysates of both unstimulated and IL-6 or IFN γ stimulated cells. Furthermore, the tyrosine 476 substitution had no detrimental effect on STAT3 association, suggesting distinct molecular recognition mechanisms for STAT1 and STAT3 by importin- α 5.

To examine, whether the conserved NTD is required for binding to importin- α 5, we stimulated MEF Δ/Δ cells stably expressing (WT)STAT3-FP and (Δ N)STAT3-FP constructs with IL-6 or left them untreated. Total cell lysates were incubated with GST-agarose beads coupled with both full-length importin- α 5 and IBB truncation mutant fusion proteins and STAT3 association was investigated via immunoblotting (Fig. 3.9A). Both (WT)STAT3-FP and (Δ N)STAT3-FP were able to co-precipitate independently of IL-6 stimulation or presence of the autoinhibitory IBB domain. Weaker STAT3 bands from (Δ N)STAT3-FP lysates always correlated with lower amounts of total STAT3 in these cells compared to cells stably expressing (WT)STAT3-FP. GST- Δ IBB-importin- α 3 and GST- Δ IBB-importin- α 7 containing beads also precipitate STAT3 independent of IL-6 stimulation and presence of the NTD, albeit to a lesser extent than importin- α 5 (Fig. 3.9B).

Moreover, binding to importin- β 1 showed a similar pattern with slightly increased association in unstimulated state for (Δ N)STAT3-FP (Fig. 3.9C). These data demonstrate that in contrast to STAT1, STAT3 *in vitro* associates with importin alpha isoforms independently of phosphorylation and NTD presence.

A**B****C**

See next page for legend

Fig. 3.9: STAT3 binding to α -importins *in-vitro* A. IL-6-induced wild-type STAT3 and NTD deletion mutant binding to either full-length or IBB deletion constructs of importin- α 5 analyzed by GST pull-down assay. GST-importin- α 5 and GST-(Δ IBB)importin- α 5 recombinant proteins were coupled to GST-beads and incubated with total protein extracts of MEF Δ/Δ cells stably transfected with either (WT)STAT3-FP or (Δ N)STAT3-FP constructs. Cells were stimulated with 20 ng/ml IL-6 and 500 ng/ml sIL-6R α for 20 minutes or left untreated and total cell lysates were incubated with GST-beads that contained GST-importin- α 5 and GST-(Δ IBB)importin- α 5 proteins. Precipitated complexes were analyzed by Western blotting using the antibodies indicated. Lanes 1 and 7 contained no lysates, while lanes 2 and 8 had no GST fusion protein on beads, which served as internal controls for specific interactions between STAT3-FP and importin- α 5 molecules. For input analysis 30 μ g of total cell lysates were analyzed via immunoblotting using same antibodies. B. IL-6-induced wild-type STAT3 and NTD deletion mutant binding to importin- α 3 or importin- α 7 proteins analyzed by GST pull-down assay. Same setup as described for Fig.4B was used for the analysis of precipitated protein complexes. Similar to Fig. 3.9 A, lanes 1, 2, 7 and 8 served as internal controls. C. IL-6-stimulated wild-type STAT3 and NTD deletion mutant binding to importin- β 1 analyzed by GST pull-down assay. Same setup as described for Fig.3.9 A,B was used for the analysis of precipitated protein complexes.

2.4. Nuclear export inhibition does not rescue impaired nuclear accumulation of (Δ N)STAT3

STAT1, STAT3 and other STATs are present in the nucleus to some extent even in the absence of the activating stimuli [26, 27, 49]. As evidence for the existence of a “basal” nucleocytoplasmic shuttling, nuclear accumulation of unphosphorylated STAT3 was observed upon disruption of a steady state of constant nuclear import and export via leptomycin B (LMB)-mediated exportin-1 (CRM1) inhibition [48]. In order to validate these data with our fluorescent constructs, MEF Δ/Δ cells transfected with (WT)STAT3–FP were pulse-stimulated with IL-6 and soluble IL-6R α for 20 minutes and left untreated for up to 4 hours after stimulus removal with or without 5 ng/ml LMB. STAT3 subcellular localization was monitored in a live-cell imaging experiment (Fig. 3.10A). Additionally, STAT3-FP intracellular distribution in the presence of LMB was monitored without any stimuli for 16 hours (Fig. 3.10B). As expected, in response to IL-6 stimulation fluorescently labeled STAT3 molecules showed distinct nuclear accumulation, which was reversed after stimulus removal. However, upon nuclear export inhibition STAT3-FP molecules remained present in the nuclei of stimulated cells even 4 hours after stimulus removal. Moreover, LMB treatment alone led to an increase in nuclear STAT3-FP without any stimuli clearly demonstrating the presence of cytokine-independent nuclear trafficking. Thus, STAT3 nuclear egress upon cytokine stimulation is completely dependent on CRM1,

whereas nuclear export of unphosphorylated STAT3 partially relies on classical CRM1-mediated nuclear export.

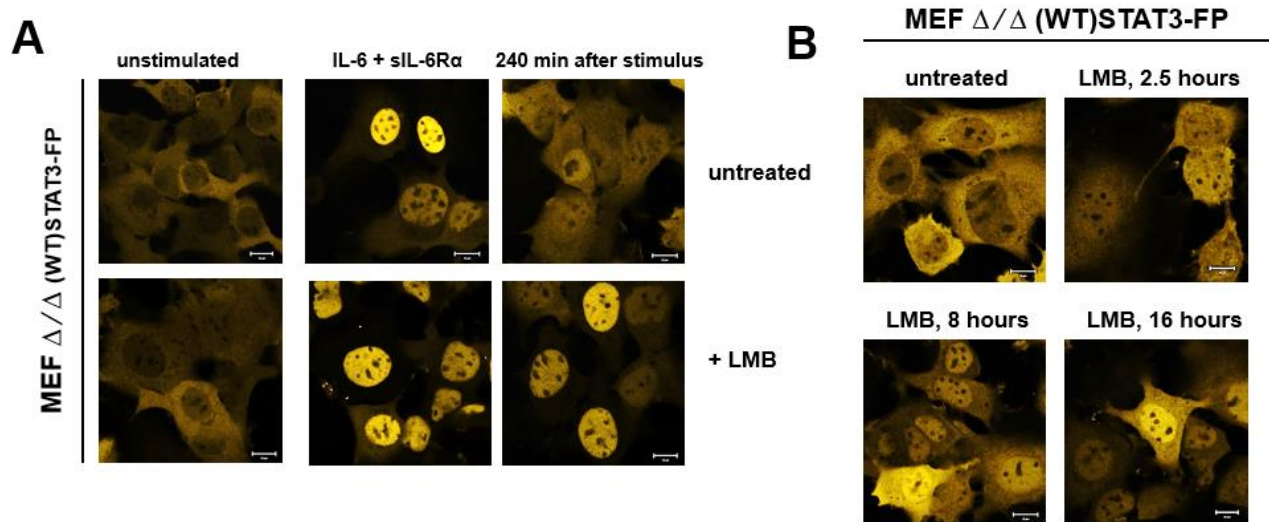


Fig. 3.10: CRM1-mediated nuclear export inhibition effect on STAT3 subcellular localization A. MEF Δ/Δ (WT)STAT3 cells were stimulated with 20 ng/ml IL-6 and 500 ng/ml soluble IL-6R (sIL-6R α) for 30 minutes, washed with PBS and left in fresh medium for up to 240 minutes without or with 5 ng/ml LMB. B. MEF Δ/Δ (WT)STAT3 cells were incubated with 5 ng/ml LMB and observed using a confocal microscope for up to 16 hours. Scale bars represent 10 μ m.

To rule out the possibility that previously observed (Δ N)STAT3-FP defect in nuclear accumulation might be due to rapid nuclear export of phosphorylated (Δ N)STAT3-FP species, (Δ N)STAT3-FP transfected cells were either treated with LMB, IL-6 and soluble IL-6R α or all three reagents together for 4 hours and subcellular distribution of fluorescently labeled proteins was monitored in real time in a live-cell imaging experiment (Fig. 3.11A). (Δ N)STAT3-FP, in contrast to IL-6 treatment (upper panel), demonstrates significant nuclear accumulation in LMB-treated cells (middle panel). Furthermore, (Δ N)STAT3 accumulated in the nuclei of the resting cells much faster than wild-type (data not shown). However, combined treatment with IL-6 and LMB did not result in enhanced nuclear presence of (Δ N)STAT3-FP compared to LMB treatment alone (lower panel), suggesting that inhibited nuclear accumulation of (Δ N)STAT3 stems from defect in nuclear import, rather than nuclear retention.

Next, we wanted to analyze the influence of LMB treatment and the resulting partial nuclear accumulation of (Δ N)STAT3-FP on dephosphorylation and subcellular localization compared to (WT)STAT3-FP. We pulse stimulated LMB-treated or untreated MEF Δ/Δ (WT)STAT3-FP and MEF Δ/Δ (Δ N)STAT3-FP cells with IL-6 and analyzed STAT3 dephosphorylation kinetics via immunoblotting (Fig. 3.11B).

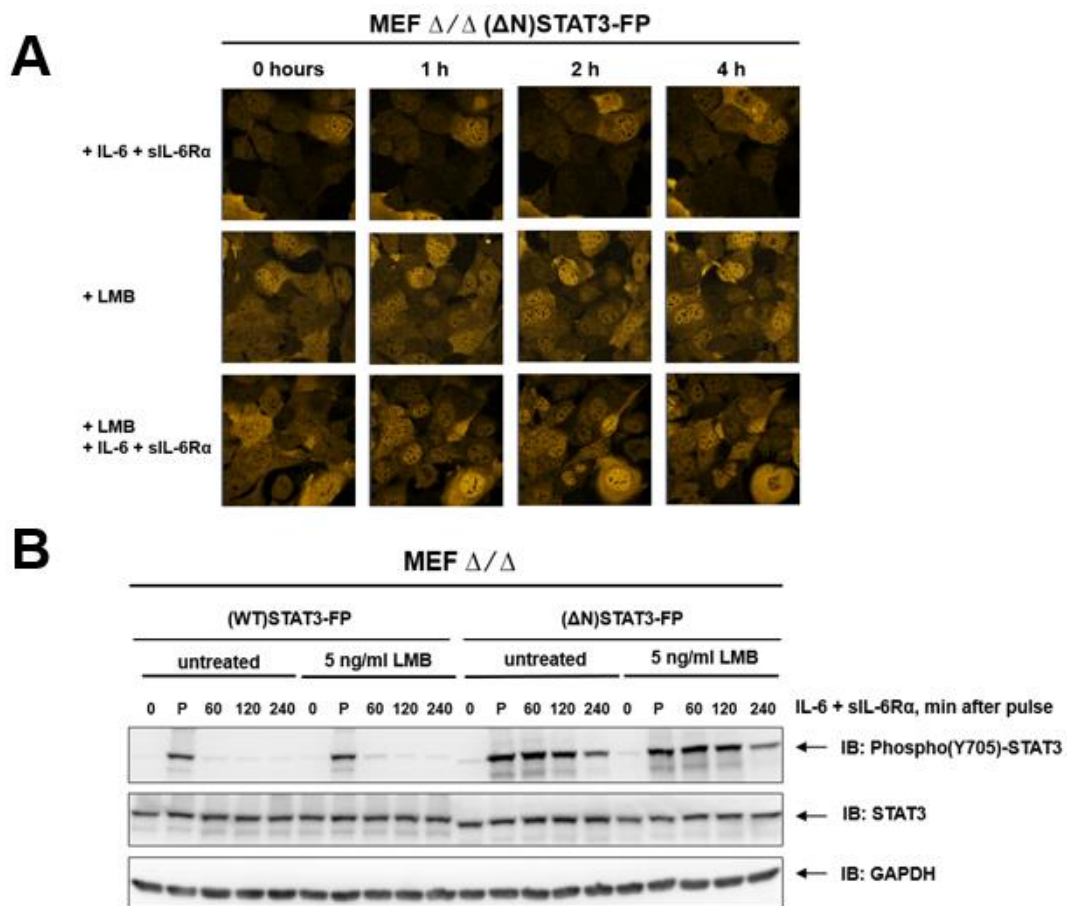


Fig. 3.11: CRM1-mediated nuclear export inhibition effect on (Δ N)STAT3-FP subcellular localization and dephosphorylation kinetics of WT and (Δ N)STAT3. A. Subcellular localization of (Δ N)STAT3-FP upon nuclear export inhibition. MEF Δ/Δ (Δ N)STAT3 cells were incubated with 5 ng/ml LMB, 20 ng/ml IL-6 and 500 ng/ml soluble IL-6R (sIL-6R α) or both for indicated time periods and monitored in live-cell imaging experiment. B. Effect of nuclear export inhibition on (WT)STAT3-FP or (Δ N)STAT3-FP deactivation. Cells were pulse-stimulated with 20 ng/ml IL-6 and 500 ng/ml sIL-6R α for 20 minutes with or without prior 10 ng/ml LMB treatment, washed with PBS, supplied with fresh medium either with or without 10 ng/ml LMB and left untreated for up to 240 minutes. Total cell lysates were prepared at the indicated time points and analyzed by Western blotting using the antibodies indicated.

Our results indicate that nuclear localization upon CRM1-dependent export inhibition had no significant effect on both (WT)STAT3-FP and (Δ N)STAT3-FP phosphorylation-dephosphorylation cycles (compare with Fig. 3.5).

Finally, we were interested whether CRM1-mediated nuclear export inhibition affect cytoplasmic localization of phosphorylated (Δ N)STAT3-FP dimers seen in Fig. 3.6. Indirect immunofluorescence of LMB-treated or untreated MEF Δ/Δ (WT)STAT3-FP and MEF Δ/Δ (Δ N)STAT3-FP cells was performed after 20 minutes of IL-6 stimulation and 180 minutes after cytokine removal (Fig. 3.12A). Mean nuclear YFP signal was additionally quantified (Fig. 3.12B).

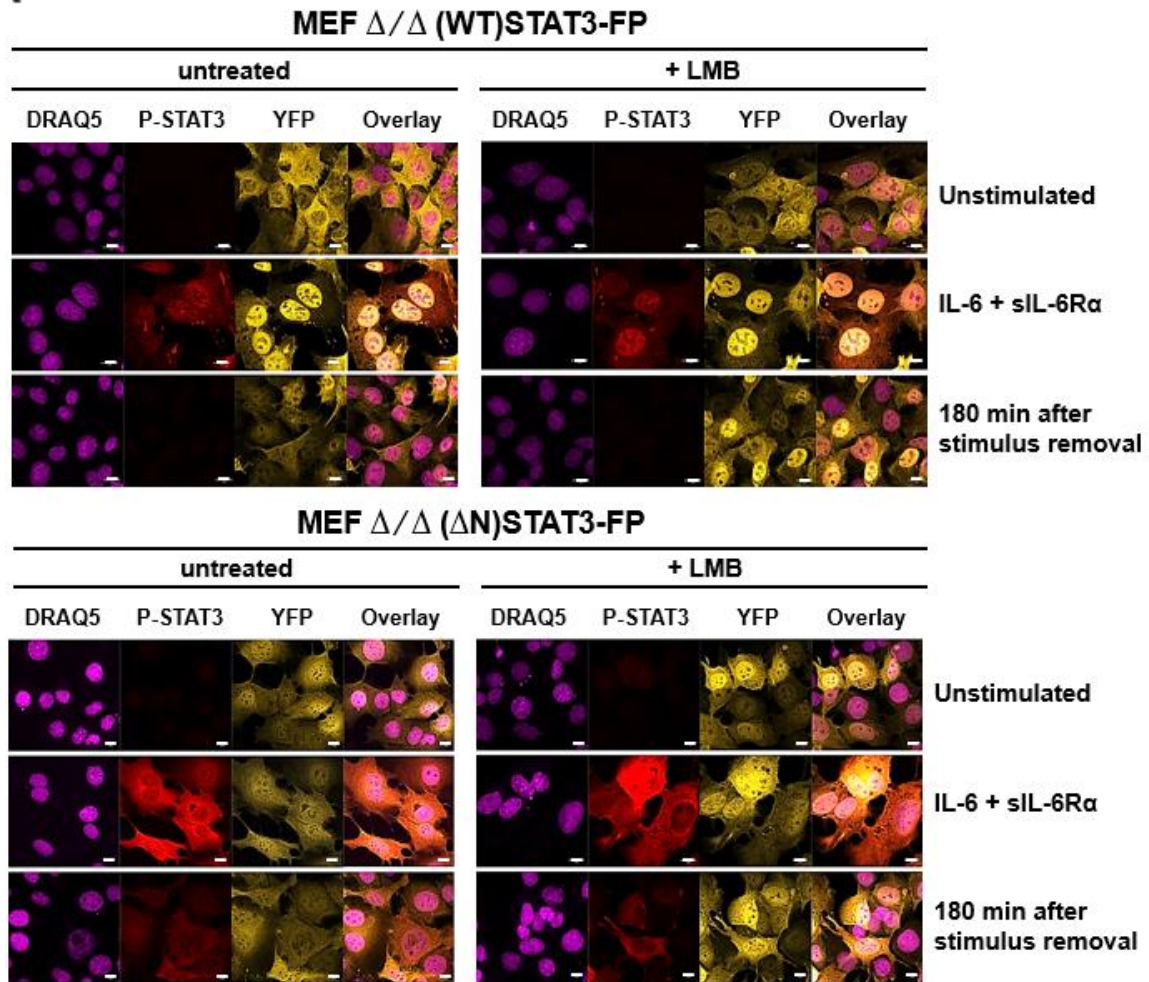
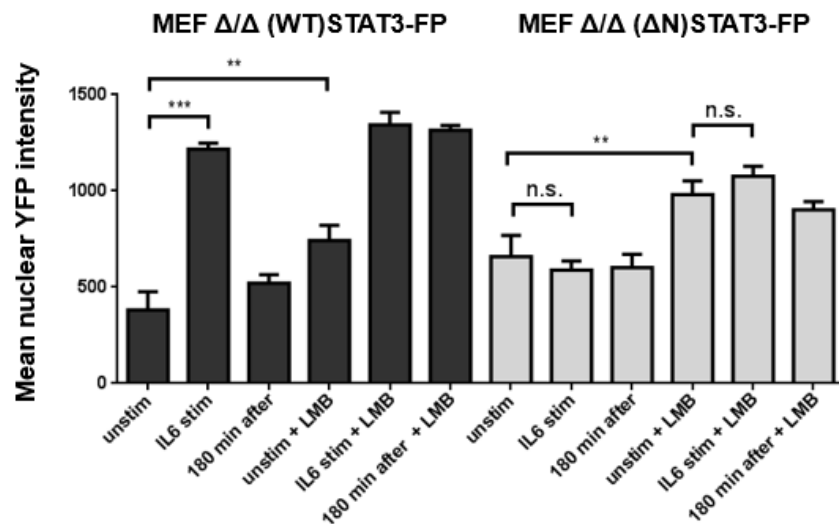
A**B**

Fig. 3.12: Subcellular localization of phosphorylated (Δ N)STAT3-FP dimers upon nuclear export inhibition. A. Immunofluorescence studies of MEF Δ/Δ fibroblasts stably transfected with (WT)STAT3-FP or (Δ N)STAT3-FP constructs. Cells were preincubated with LMB for 3 hours or left untreated, then stimulated with 20 ng/ml IL-6 and 500 ng/ml sIL-6R α for 30 minutes, fixed, permeabilized and stained using a phospho(Y705)STAT3 antibody, followed by incubation with a secondary Alexa Fluor-555 conjugated antibody and DRAQ5 nuclear marker. Scale bars represent 10 μ m. B. Mean nuclear presence of fluorescently labeled STAT3 constructs in MEF Δ/Δ cells analyzed above (means \pm SD of n=10 cells per sample). ***p < 0.0005. **p < 0.005. n.s. = not significant.

Upon LMB treatment (WT)STAT3-FP is efficiently dephosphorylated but remains nuclear even after 180 minutes after cytokine treatment, while phosphorylated (Δ N)STAT3-FP dimers remain largely cytoplasmic even in LMB treated cells. Both (WT)STAT3-FP and (Δ N)STAT3-FP demonstrate statistically significant nuclear accumulation in the nuclei of resting LMB-treated cells. These data indicate that nuclear export inhibition had no significant effect on impaired cytokine-induced (Δ N)STAT3-FP nuclear accumulation and phosphorylated (Δ N)STAT3-FP dimers are trapped in the cytoplasm as a result of impaired nuclear import.

2.5. Basal nucleocytoplasmic shuttling does not require functional N-, SH2 or C-terminal domains

Since both latent (WT)STAT3-FP and (Δ N)STAT3-FP accumulate in the nucleus of resting cells upon 4 hours of CRM1-mediated nuclear export inhibition, we were interested whether other STAT3 mutations could interfere with basal nuclear trafficking of STAT3. Nucleocytoplasmic shuttling of mutated putative NES ((Δ NES)STAT3-FP) and NLS ((Δ NLS)STAT3-FP) sequences within STAT3 have been previously analyzed [52]. Additionally, we have generated MEF Δ/Δ cells stably expressing C-terminally truncated (Δ TAD)STAT3-FP (aa 1-709) and (K685R)STAT3-FP containing a point-mutation of an acetylated lysine residue within SH2 domain, that has been reported to be critical for cytokine-induced dimerization of STAT3 [171]. Along with the DNA-binding deficient (mSNICQ)STAT3-FP mutant, we incubated MEF Δ/Δ cell lines stably expressing different STAT3 mutants with 5 ng/ml LMB for 4 hours and observed changes in subcellular localization in a live-cell imaging experiment (Fig. 3.13A). As expected, latent (WT)STAT3-FP accumulates in the nucleus of the resting cells upon 4 hours of CRM1-mediated nuclear export inhibition. Moreover, all mutated constructs also showed significant increase in nuclear presence after 4 hours of CRM1-dependent nuclear export abrogation. To analyze whether functional SH2 domains of STAT3 are of importance for basal nucleocytoplasmic trafficking, the construct for the expression of (R609Q)STAT3-FP with a non-functional SH2 domain was generated. R609Q mutation leads to unresponsiveness to cytokine treatment due to impaired receptor recruitment of

STAT3 and abrogates preformed dimer formation [50, 53, 86]. MEF Δ/Δ cells stably transfected with this construct were analyzed in a live-cell imaging experiment upon either IL-6 or LMB treatment and changes in mean nuclear YFP signal were quantified (n=15 cells) (Fig. 3.13B). (R609Q)STAT3-FP demonstrates nuclear accumulation only in resting cells upon nuclear export blockage and not after IL-6 stimulation. Taken together, our data suggest that the basal nucleocytoplasmic shuttling of inactive STAT3 underlies a different mechanism than ligand-dependent active nuclear import and does not require receptor recruitment, DNA-binding, preformed dimer formation, functional N-terminal, transactivation and SH-2 domains.

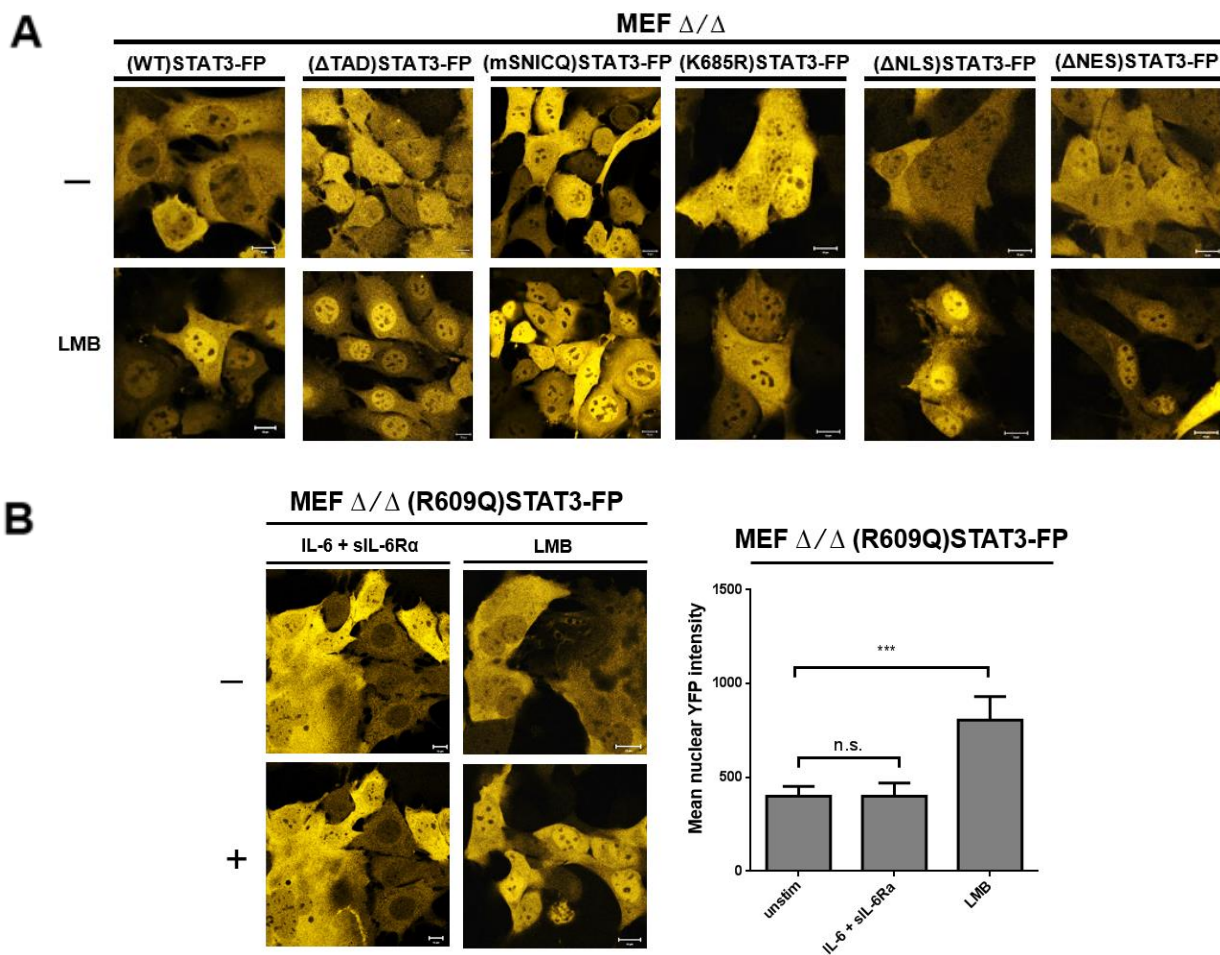


Fig. 3.13: LMB-induced nuclear accumulation of different STAT3-FP constructs. A. LMB-induced basal nuclear accumulation of (WT)STAT3-FP, (Δ TAD)STAT3-FP, (mSNICQ)STAT3-FP, (K685R)STAT3-FP, (Δ NLS)STAT3-FP or (Δ NES)STAT3-FP fusion proteins. MEF Δ/Δ cells stably transfected with the indicated fluorescent constructs were treated with 5 ng/ml LMB for 4 hours and observed in real-time live-cell confocal imaging. Scale bars represent 10 μ m. B. IL-6- or LMB-induced influence on subcellular localization of (R609Q)STAT3-FP fusion protein. Left panel: MEF Δ/Δ cells stably transfected with (R609Q)STAT3-FP were treated with either 20 ng/ml IL-6 and 500 ng/ml siIL-6R α for 20 minutes or 5 ng/ml LMB for 4 hours and observed in real-time live-cell confocal imaging. Scale bars represent 10 μ m. Right panel: Quantification of the (R609Q)STAT3-FP nuclear presence in MEF Δ/Δ cells (means \pm SD of n=15 cells per sample). ***p < 0.0005. n.s. = not significant.

3. STAT3-mediated regulation of STAT1 signaling

3.1. Mutual intracellular crossregulation between STAT1 and STAT3 is asymmetric.

Our data showed an enhanced STAT1 activation through phosphorylation of Y701 in MEF Δ/Δ (Δ N)STAT3-FP and (mSNICQ)STAT3-FP in comparison to STAT3-FP wild-type (Fig. 3.4A). Previously, enhanced STAT1 activation upon IL-6 stimulation was observed in STAT3-deficient MEF cells [100]. In turn, in STAT1-deficient MEFs STAT3 was abnormally activated upon IFN γ treatment [94]. To verify these observations we have used STAT1- and STAT3-deficient MEFs in order to study signaling of STAT3 and STAT1 in the absence of STAT1 and STAT3, respectively, via immunoblotting (Fig. 3.14).

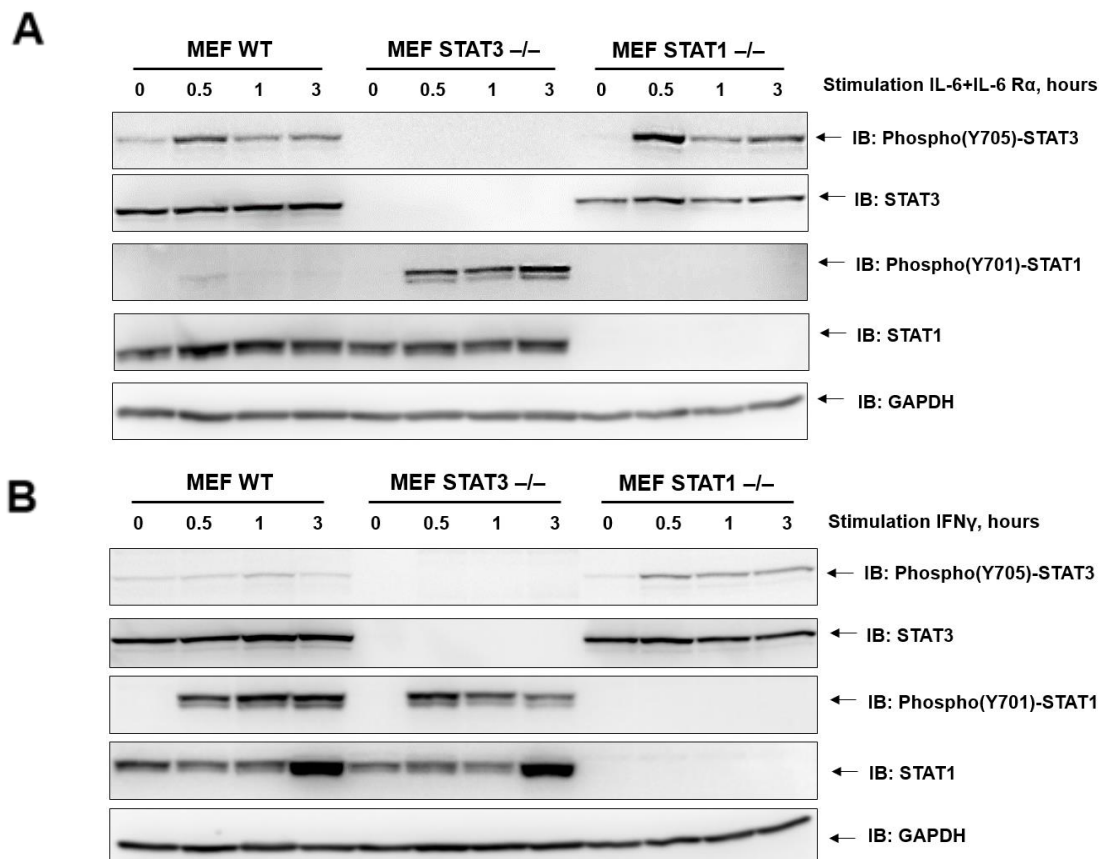
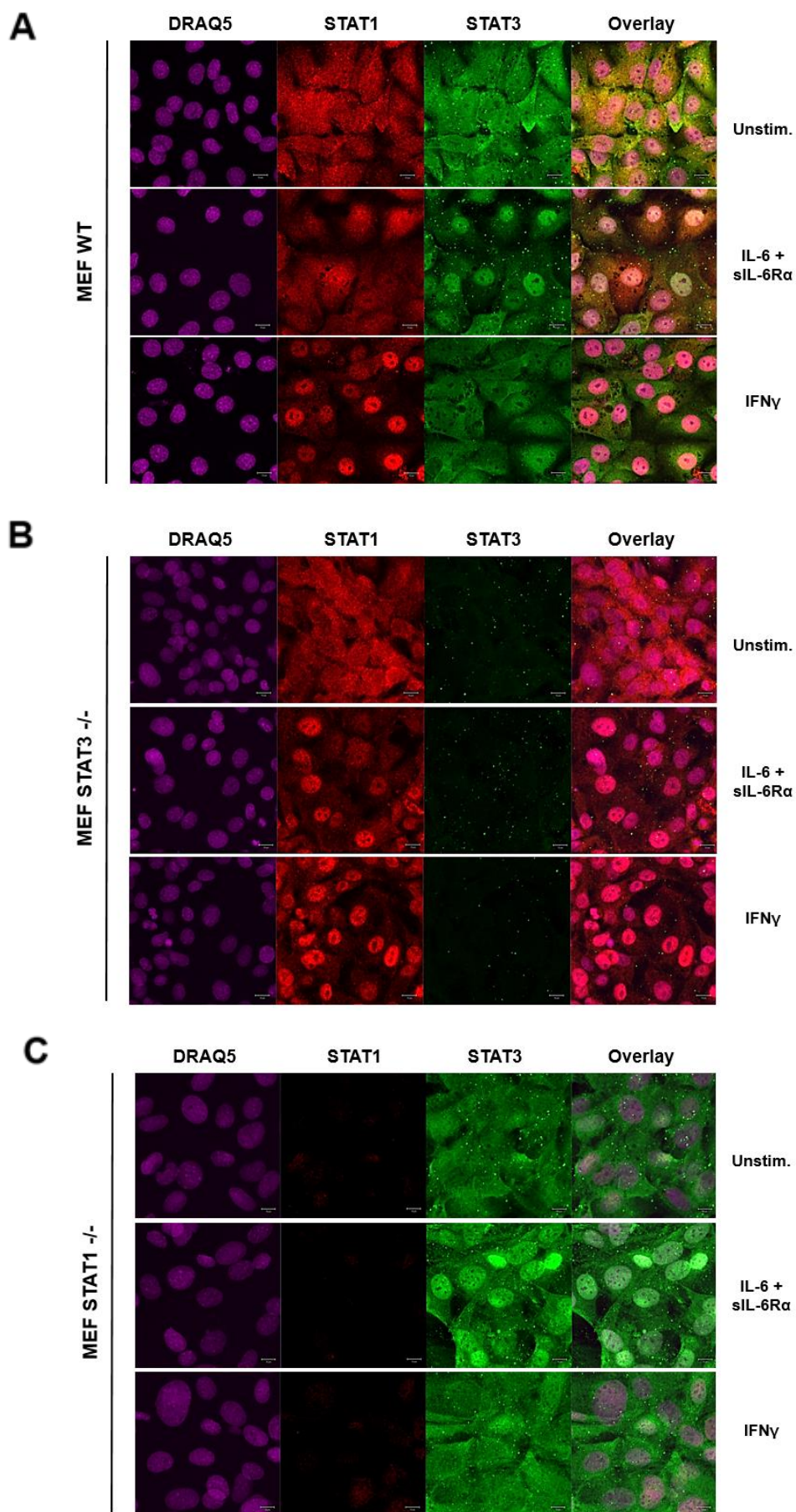


Fig. 3.14: Analysis of STAT3 and STAT1 activation in WT, STAT3 $-/-$ and STAT1 $-/-$ cell lines. A. IL6-induced activation of STAT3 and STAT1. Indicated cell lines were stimulated with 20 ng/ml IL-6 and 500 ng/ml sIL-6R α for different time periods. Total cell lysates were prepared and analyzed by Western blotting using the antibodies indicated. B. IFN γ -induced activation of STAT3 and STAT1. Indicated cell lines were stimulated with 20 ng/ml IFN γ for different time periods. Total cell lysates were prepared and analyzed by Western blotting using the antibodies indicated.

STAT1 and STAT3 deficiency has a significant impact on IL-6 induced activation of STAT3 and STAT1, respectively (Fig. 3.14A). Compared to WT MEF cells, the Y705 phosphorylation of STAT3 is increased after 30 minutes of IL-6 stimulation of STAT1-deficient cells, while STAT1 Y701 phosphorylation upon IL-6 treatment is markedly enhanced and prolonged in STAT3 $-/-$ cells as reported previously [100]. In turn, IFN γ stimulation led to slightly increased activation of STAT3 in STAT1 $-/-$ cells in contrast to WT MEF, whereas STAT3 absence, although not affecting IFN γ -induced upregulation of total STAT1 after 3 hours of stimulation, led to decreased Y701 phosphorylation during later time points of stimulation (Fig. 3.14B). The absence of STAT3 and STAT1 bands in STAT3 $-/-$ and STAT1 $-/-$ verified the knockout background of analyzed cells.

Next, to analyze the subcellular distribution of STAT3 and STAT1 in STAT1 $-/-$ and STAT3 $-/-$ MEFs, respectively, cells were fixed and analyzed via indirect immunofluorescence (Fig. 3.15). As expected for wild-type MEFs, STAT3 translocate to the nucleus after 30 minutes of IL-6 and not IFN γ stimulation, whereas STAT1 showed nuclear accumulation only in IFN γ -treated cells (Fig. 3.15A). Furthermore, increased and prolonged IL-6-induced STAT1 activation in STAT3 $-/-$ cells is accompanied by increased nuclear presence of STAT1 similar to IFN γ stimulated cells (Fig. 3.15B). In contrast, marginally increased STAT3 Y705 phosphorylation in STAT1 $-/-$ cells did not result in atypical STAT3 nuclear accumulation after 30 minutes of IFN γ treatment (Fig. 3.15C). Canonical nuclear accumulation of STAT1 upon IFN γ treatment and STAT3 after IL-6 stimulation was not significantly affected by the ablation of the other transcription factor. Conclusively, these experiments showed that STAT1 and STAT3 deficiencies lead to asymmetric effects on one another, STAT3 $-/-$ cells showing atypical STAT1 activation and nuclear translocation upon IL-6 stimulation, but minor increase in STAT3 phosphorylation in IFN γ -treated STAT1 $-/-$ cells does not lead to detectable subsequent nuclear accumulation.

Fig. 3.15: Nuclear translocation of STAT1 and STAT3 following IL-6 and IFN γ treatment of WT, STAT3 $-/-$ and STAT1 $-/-$ MEF. A. Subcellular localization of STAT1 and STAT3 in WT MEF. WT MEF cells were stimulated with 20 ng/ml IL-6 and 500 ng/ml sIL-6R α or 20 ng/ml IFN γ for 30 minutes, fixed with methanol and incubated with primary STAT1 and STAT3 antibodies, followed by immunostaining with Alexa Fluor-555 and Alexa Fluor-488 antibodies, respectively, as well as DRAQ5 nuclear marker. Scale bars represent 10 μ m. B, C. Subcellular localization of STAT1 and STAT3 in STAT3 $-/-$ and STAT1 $-/-$ MEF. Cells were treated and prepared in the same way as WT MEF.



See previous page for legend

3.2. STAT3-mediated downregulation of IL-6-induced STAT1 activation relies on STAT3 transcriptional activity, but not on unique NTD functions.

Previous reports demonstrated that presence of STAT3 downregulates IL-6-induced STAT1 activation, modulates gp130 signaling toward an IL-6-type rather than an IFN γ -type response, and, notably, negatively regulates IFN α/β -induced gene expression and antiviral activity [100, 101]. Initial findings indicated the involvement of STAT3 transcriptional activity and the expression of specific target genes (such as *socs3*) in this regulatory mechanism [176], however isolated STAT3 NTD fragment alone could suppress IFN α/β response directly in a manner independent of STAT3 function as a transcriptional factor [101]. In order to address the roles of NTD and transcriptional potential of STAT3 in regulating atypical IL-6-induced STAT1 signaling, gain-of-function and loss-of-function approaches were used.

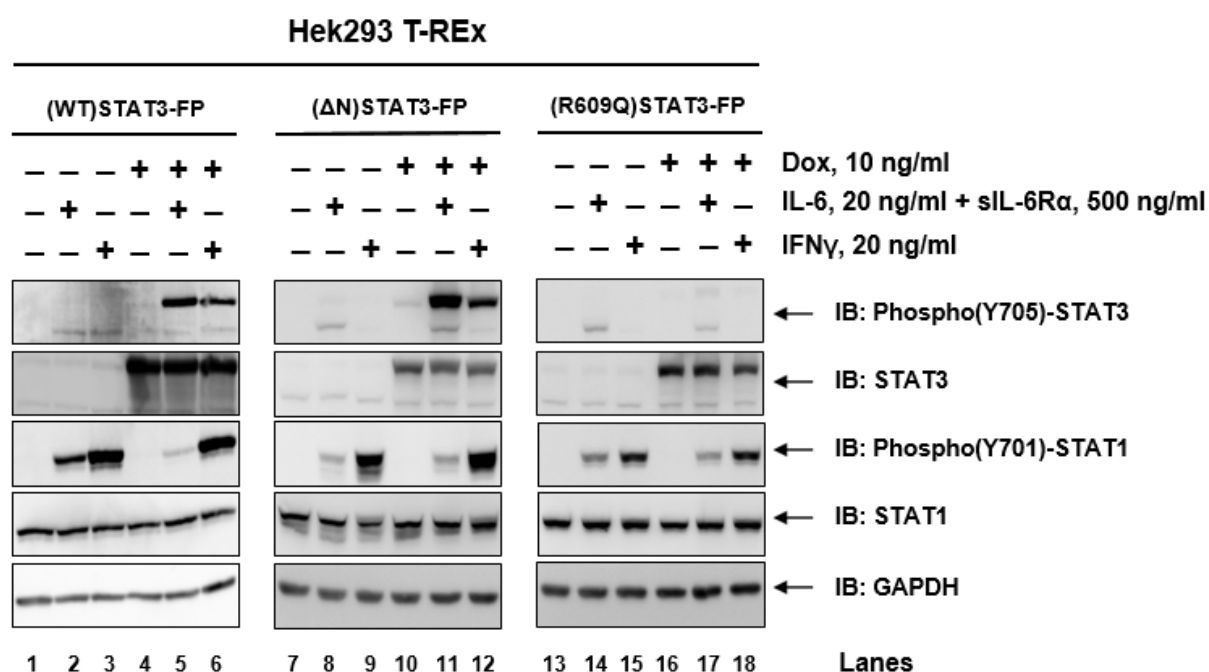


Fig. 3.16: STAT1 and STAT3 phosphorylation upon IL-6 and IFN γ stimulation. Hek293 T-Rex stably transfected with WT STAT3-FP, (ΔN)STAT3-FP and (R609Q)STAT3-FP constructs were left untreated or treated with 10 ng/ml doxycycline for 24 h to induce expression of the gene of interest. Subsequently, cells were stimulated with 20 ng/ml IL-6 and 500 ng/ml sIL-6R α or 20 ng/ml IFN γ for 30 minutes and total cell lysates were prepared and analysed by immunoblotting using antibodies indicated. GAPDH served as a loading control.

First, we stably transfected full-length STAT3-FP, (Δ N)STAT3-FP and (R609Q)STAT3-FP constructs in Hek293 Flp-In T-REx cells that inducibly express genes of interest upon doxycycline treatment, stimulated induced and non-induced cells with either IL-6 or IFN γ and analyzed the activating tyrosine phosphorylation of STAT3 and STAT1 via immunoblotting (Fig. 3.16). Overexpression of wild-type STAT3-FP upon doxycycline induction led to decreased phosphorylation of endogenous STAT1 upon IL-6 stimulation compared to non-induced controls (lanes 2 and 5), while IFN γ -induced STAT1 activation remained unchanged, confirming the ability of full-length STAT3 to regulate STAT1 signaling upon IL-6 treatment. Induction of (Δ N)STAT3-FP and (R609Q)STAT3-FP construct expression did not significantly affect STAT1 tyrosine 701 phosphorylation upon both IL-6 and IFN γ treatment, indicating that N-terminal deletion and SH2 domain mutants of STAT3 lost the ability to regulate STAT1.

To further substantiate the involvement of STAT3 NTD in STAT1 signaling regulation, we used stably reconstituted STAT3 $-/-$ MEF (MEF Δ/Δ) cells described in section III.2 of this thesis. In order to validate the role of wild-type STAT3 in modulating gp130 signaling, we stimulated WT, MEF Δ/Δ and MEF Δ/Δ (WT)STAT3-FP with IL-6 and analyzed STAT1 tyrosine phosphorylation (Fig. 3.17A). Immunoblotting results revealed that the abnormal STAT1 activation seen in MEF Δ/Δ can be reversed by stable restoration of WT-STAT3-FP in these cells. Of note, higher total (WT)STAT3-FP amounts also led to an increase in total STAT1 levels.

We have previously published that N-terminal deletion and somatic mutation L78R prevent the formation of preformed STAT3 dimers [52, 53]. In order to analyze whether latent dimer formation plays a role in regulation of STAT1 signaling, we compared IL-6-induced STAT1 activation in WT, MEF Δ/Δ and MEF Δ/Δ stably expressing (WT)STAT3-FP, (Δ N)STAT3-FP and (L78R)STAT3-FP constructs. Additionally, we transfected MEF Δ/Δ cells with the isolated STAT3 NTD ((NTD)STAT3-FP) fluorescent fusion protein in order to study the impact of NTD alone on STAT1 activation. All six cell lines were stimulated with IL-6 and IFN γ as a positive control for canonical STAT1 signaling and phosphorylation of STAT3 and STAT1 was analyzed (Fig. 3.17B).

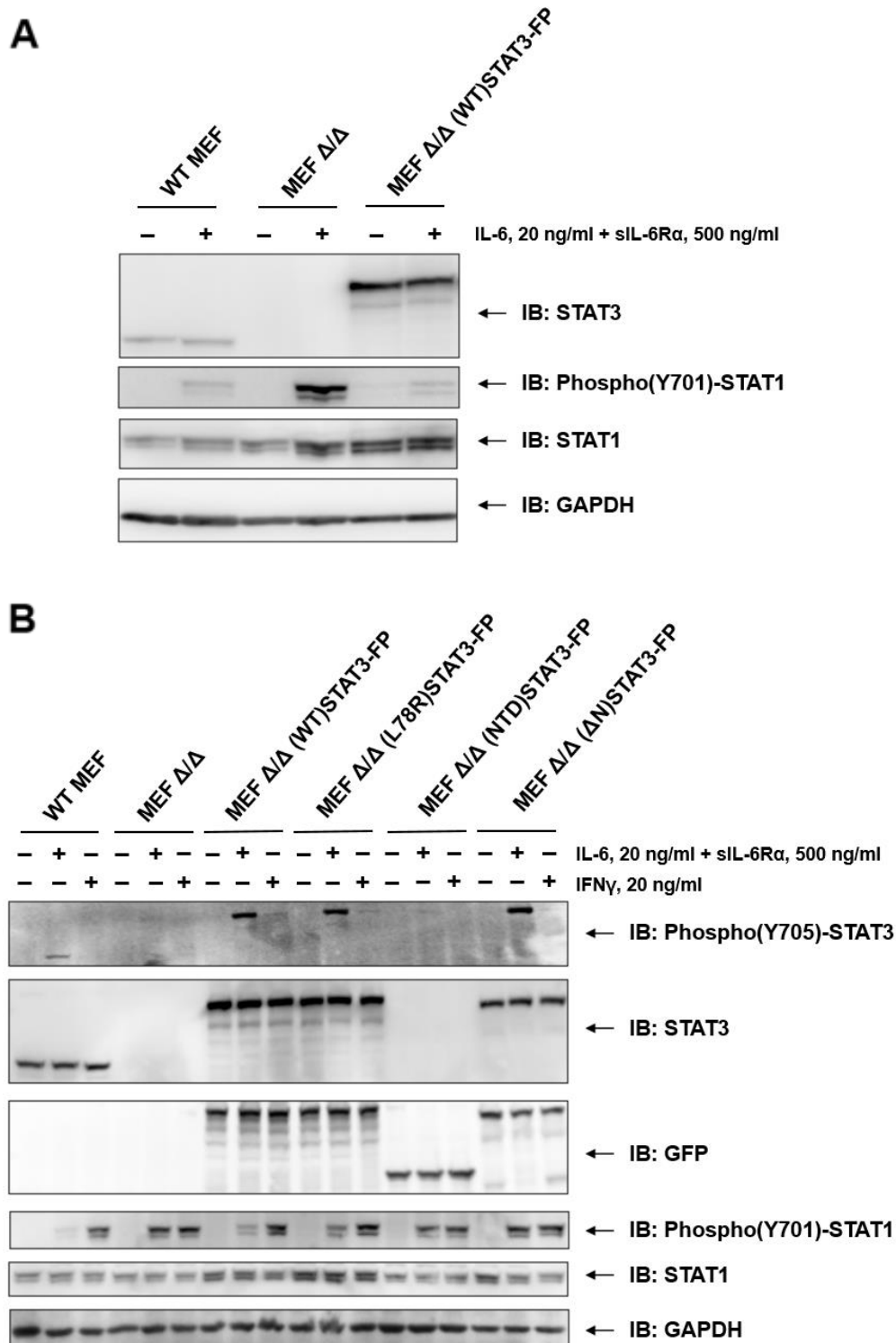


Fig. 3.17: STAT1 and STAT3 phosphorylation upon IL-6 and IFN γ stimulation in reconstituted MEF cells. A. STAT3 limits IL-6 induced STAT1 activation. Indicated cell lines were stimulated with 20 ng/ml IL-6 and 500 ng/ml sIL-6R α and total cell lysates were analysed by immunoblotting using indicated antibodies. B. Effect of different STAT3 mutants on IL-6 induced STAT1 activation. Indicated cell lines were stimulated with 20 ng/ml IL-6 and 500 ng/ml sIL-6R α or 20 ng/ml IFN γ for 30 minutes and total cell lysates were analysed by immunoblotting using antibodies as indicated. GAPDH served as a loading control.

As expected, N-terminal deletion of STAT3 led to a similar increase in STAT1 phosphorylation on tyrosine 701 as seen in STAT3-deficient MEF Δ/Δ cells upon IL-6 treatment, indicating that the NTD is important for STAT3-mediated regulation of STAT1 signaling. In turn, both (WT)STAT3-FP and (L78R)STAT3-FP expressing cell lines demonstrated weaker STAT1 phosphorylation upon IL-6 stimulation in comparison to IFN γ , indicating that preformed dimer formation ability of STAT3 is not essential for crossregulation of STAT1. Moreover, although reported to be sufficient for antiviral response suppression [101], the isolated NTD of STAT3 did not downregulate IL-6 induced STAT1 activation, suggesting that STAT3 NTD alone is not sufficient for regulation of STAT1 phosphorylation.

To support these findings, atypical nuclear translocation of STAT1 observed in STAT3 $-/-$ cells upon IL-6 treatment was analyzed in the presence of ectopically expressed (WT)STAT3-FP, (Δ N)STAT3-FP and (NTD)STAT3-FP constructs. Indirect immunofluorescence experiments revealed that nuclear accumulation of endogenous STAT1 in IL-6-stimulated cells was abolished upon stable expression of full-length (WT)STAT3-FP, but not (Δ N)STAT3-FP or (NTD)STAT3-FP (Fig. 3.18). IFN γ -induced STAT1 nuclear presence was not affected by any of the constructs (data not shown).

Conclusively, the results obtained from Hek293-Trex cell lines stably overexpressing STAT3 and stably transfected MEF Δ/Δ indicate that intracellular STAT3 redirects gp130 signaling towards IL-6-type, rather than IFN-type response by suppressing STAT1 activation and signaling. Furthermore, although deletion of the N-terminal domain inhibited STAT3-mediated regulation of STAT1 activation, immunoblotting and immunofluorescence studies with isolated (NTD)STAT3-FP did not confirm the specific role of STAT3 NTD in this process. Since both (Δ N)STAT3-FP and (mSNICQ)STAT3-FP cell lines showed defective transcriptional activity and increased STAT1 phosphorylation at the same time, these observations indicate that modulation of STAT1 activity upon gp130 signaling relies mainly on STAT3-induced target gene expression and not on specific STAT3 NTD properties. In agreement with these data, the early downregulation of IL-6-induced STAT1 phosphorylation in the presence of STAT3 required *de novo* protein synthesis, as demonstrated by an inhibition of translational elongation via cycloheximide [176].

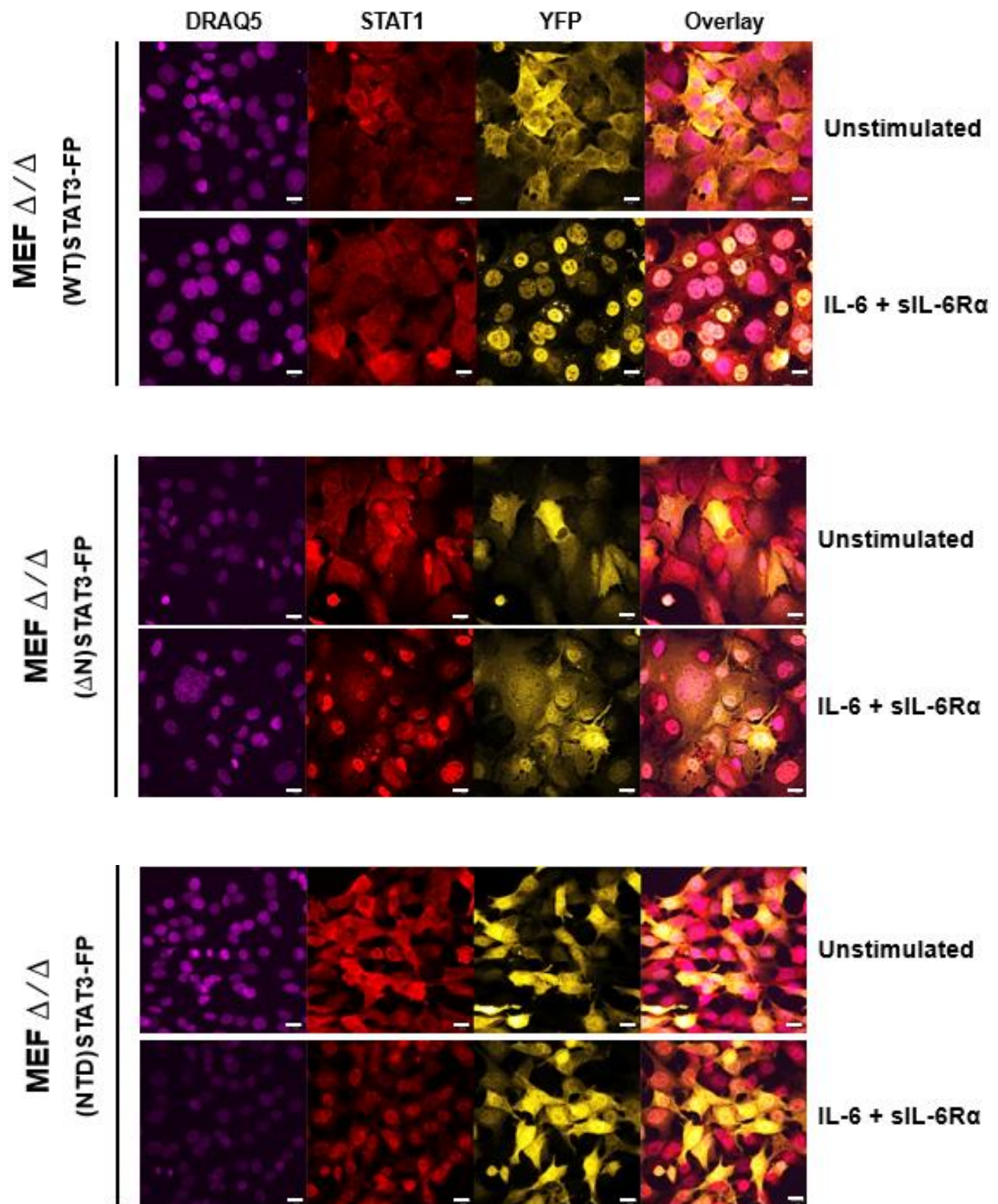


Fig. 3.18: Immunofluorescence studies of endogenous STAT1 subcellular localization in MEF Δ/Δ stably transfected with (WT)STAT3-FP, (Δ N)STAT3-FP or (NTD)STAT3-FP constructs. Indicated cells were stimulated with 20 ng/ml IL-6 and 500 ng/ml sIL-6R α for 30 minutes or left untreated, fixed, permeabilized and stained using a primary α -STAT1 antibody, followed by incubation with a secondary Alexa Fluor-555 conjugated antibody and DRAQ5 nuclear marker. Scale bars represent 10 μ m.

4. The crosstalk between NF- κ B subunit p65 and STAT3

4.1. Simultaneous visualization of p65 and STAT3 requires combined PFA and methanol treatment.

There is no consensus in the literature as to how STAT3 and NF- κ B subunit p65 influence each others nuclear translocation and signaling in general [135-139]. In order to analyze nuclear translocation of endogenous p65 and STAT3 we developed and optimized protocol for simultaneous visualization of both factors via indirect immunofluorescence. Our group previously showed IL-6-induced nuclear accumulation of endogenous STAT3 using methanol fixation and immunofluorescence staining of MEF [52]. However, paraformaldehyde fixation has been reported to be better suited for visualization of NF- κ B p65 localization by immunofluorescence [177]. In order to find optimal conditions to analyse both p65 and STAT3 subcellular localization in parallel, the two conditions of fixation were compared. HeLa cells were treated for 30 min with TNF or IL-6 to induce nuclear translocation of endogenous p65 or STAT3, respectively, or left untreated. TNF α -induced nuclear accumulation of p65 was clearly visible in paraformaldehyde fixed cells but hardly detectable upon methanol fixation (Fig. 3.19A). However, paraformaldehyde fixation is not suited for the analysis of cytokine-induced nuclear accumulation of STAT3 because already in unstimulated cells the bulk of STAT3 appeared nuclear (Fig. 3.19B). In order to resolve these problems, we applied a combined protocol of paraformaldehyde fixation followed by methanol treatment and after immunofluorescence staining assessed the subcellular localization of both factors by confocal microscopy (Fig. 3.19C). Under these conditions, STAT3 shows uniform distribution in resting state and nuclear accumulation upon IL-6 stimulation as observed in live cell imaging of (WT)STAT3-FP, but not TNF α treatment. In turn, p65 appears cytoplasmic in unstimulated cells and enters the nucleus after TNF α but not after IL-6 stimulation. These results demonstrate that a combined paraformaldehyde and methanol fixation protocol is best suited for parallel analysis of cytokine-induced nuclear translocation of endogenous NF- κ B and STAT3 via indirect immunofluorescence.

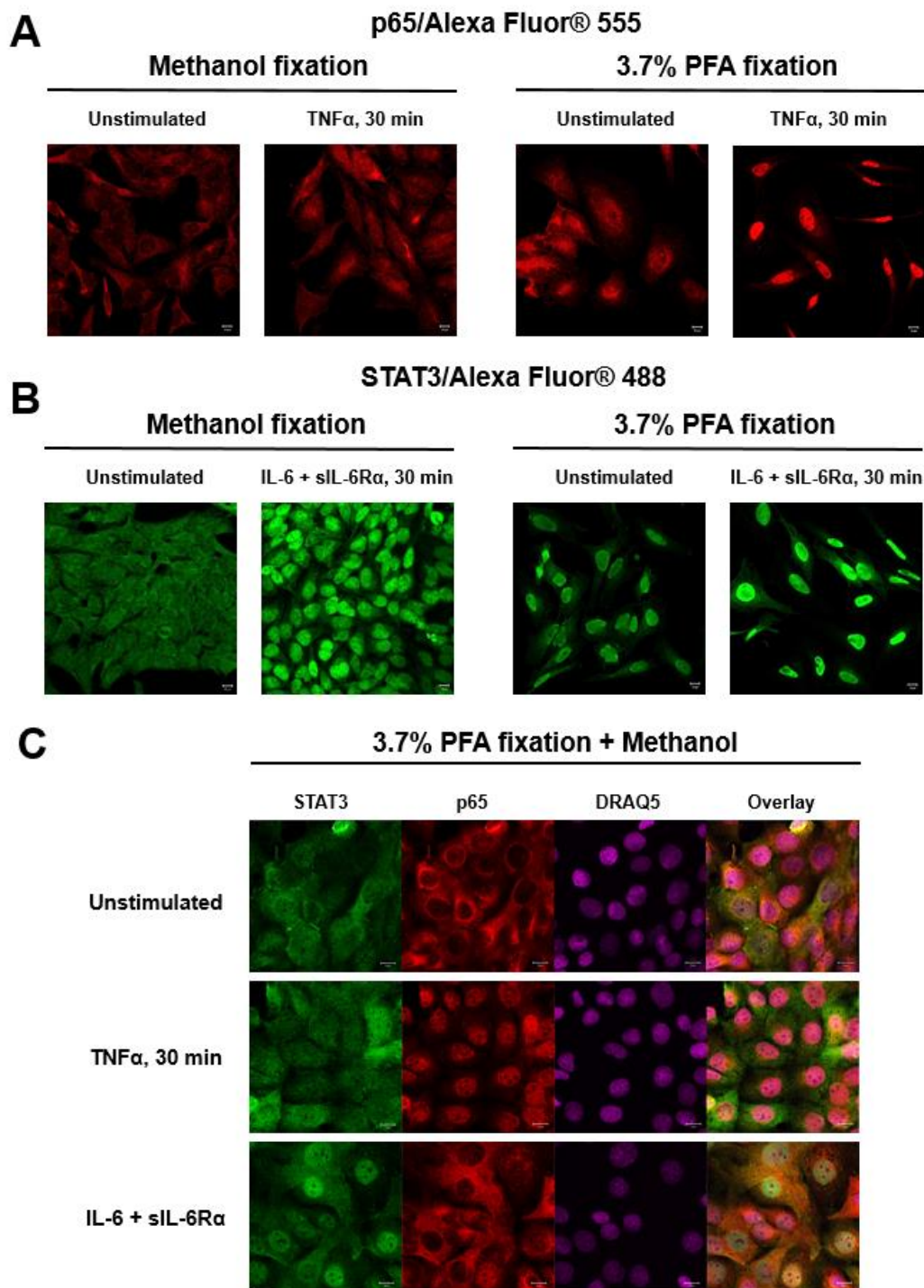


Fig. 3.19: Nuclear translocation of NF- κ B and STAT3 following cytokine treatment after PFA, methanol or combined PFA-methanol treatment. A. Indirect immunofluorescence of p65 subcellular localization following 3.7% paraformaldehyde (PFA) or methanol fixation. HeLa cells were stimulated with 10 ng/ml TNF α for 30 minutes or left untreated, fixed either with 3.7% PFA or methanol, permeabilized and stained using a p65 antibody, followed by incubation with a secondary Alexa Fluor-555 conjugated antibody. B. Indirect immunofluorescence of STAT3 subcellular localization following 3.7% PFA or methanol fixation. Cells were stimulated with 20 ng/ml IL-6 and 500 ng/ml soluble IL-6R (sIL-6R α) for 30 minutes or left untreated, fixed either with 3.7% PFA or methanol, permeabilized and stained with primary STAT3 and secondary Alexa Fluor-488 antibodies. C. Simultaneous visualization of p65 and STAT3 subcellular localization following combined 3.7% PFA and methanol treatment. Cells were stimulated or left untreated as indicated, incubated with primary p65 and STAT3 antibodies, followed by immunostaining with Alexa Fluor-555 and Alexa Fluor-488 antibodies, respectively, as well as DRAQ5 nuclear marker. Scale bars represent 10 μ m.

4.2. Absence of STAT3 has no significant effect on canonical TNF α -induced NF- κ B activation, nuclear translocation and target gene expression.

In wild-type MEF, upon TNF α treatment serine 536 phosphorylation of p65 peaked after 5 minutes of stimulation, while I κ B α was degraded after 15 minutes and returned to normal levels at 60 minutes time point, representing canonical NF- κ B signaling [178]. It has been reported that STAT3 ablation or blockade affects NF- κ B signaling [137-139]. Using STAT3 knockout MEF, we analysed the impact of STAT3 deletion on canonical NF- κ B activation. STAT3 $^{-/-}$ cells were stimulated with TNF α for indicated time points and compared with similarly treated WT MEF.

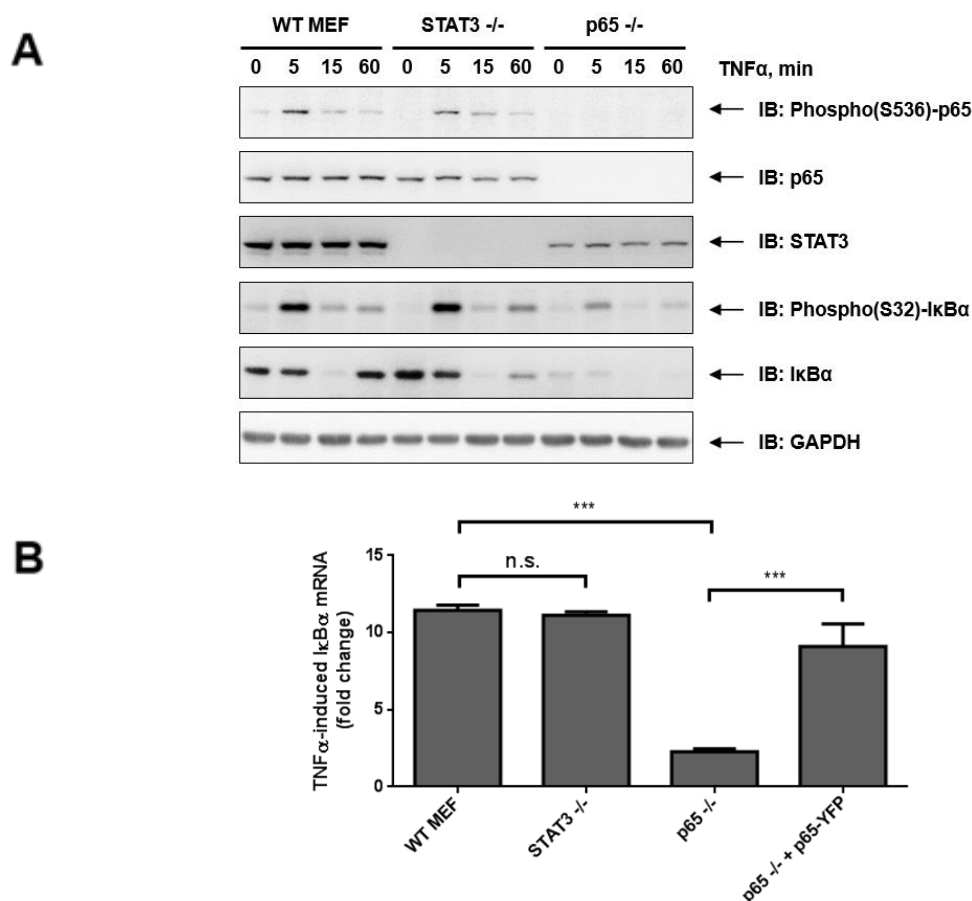


Fig. 3.20: NF- κ B activation and target gene expression in wild-type, STAT3 $^{-/-}$ and p65 $^{-/-}$ MEF upon TNF α stimulation. A. Analysis of p65 serine 536 phosphorylation and I κ B α phosphorylation and degradation. Cell lines were stimulated with 10 ng/ml TNF α for 5, 15 and 60 minutes or left untreated. Total cell lysates were analysed by immunoblotting with the indicated antibodies. B. I κ B α mRNA expression upon TNF α treatment. Wild-type MEF, STAT3 $^{-/-}$, p65 $^{-/-}$ cells, as well as p65 $^{-/-}$ cells stably transfected with a fluorescent p65-YFP construct were treated with 10 ng/ml TNF α for 45 minutes. The expression of *ikba* was measured by RT-qPCR and normalized to mGUSB. Data are representative of three independent experiments. *** $p < 0.0005$. n.s. = not significant.

As seen in Fig. 3.20A, STAT3-deficient cells showed essentially the same pattern of p65 S536 phosphorylation kinetics, I κ B α S32 phosphorylation and degradation in response to TNF α stimulation. Cells deficient in endogenous p65 served as a negative control and showed lower total I κ B α and, interestingly, also lower STAT3 levels. Analysis of GAPDH levels demonstrated equal loading of all lanes. Next, we assessed expression changes of the canonical NF- κ B target gene *ikba* upon TNF α treatment. As shown by quantitative real time PCR, the fold change of TNF α -induced *ikba* mRNA in wild-type and STAT3 deficient fibroblasts is comparable (Fig. 3.20B). Moreover, in p65 deficient MEF *ikba* mRNA upregulation was impaired and stable transfection of p65-YFP fusion protein in these cells reversed the effect, confirming p65 involvement in *ikba* expression.

Finally, we compared p65 nuclear translocation in WT and STAT3^{-/-} MEF using confocal microscopy and subcellular fractionation approaches. Nuclear entry of p65 was unaltered after 30 minutes of TNF α stimulation in STAT3-deficient cells compared with WT MEF, as seen by immunofluorescence and immunoblotting of nuclear fractions (Fig. 3.21). Taken together, our data show that STAT3 knockout has no major effect on TNF α -induced canonical NF- κ B signaling in MEF.

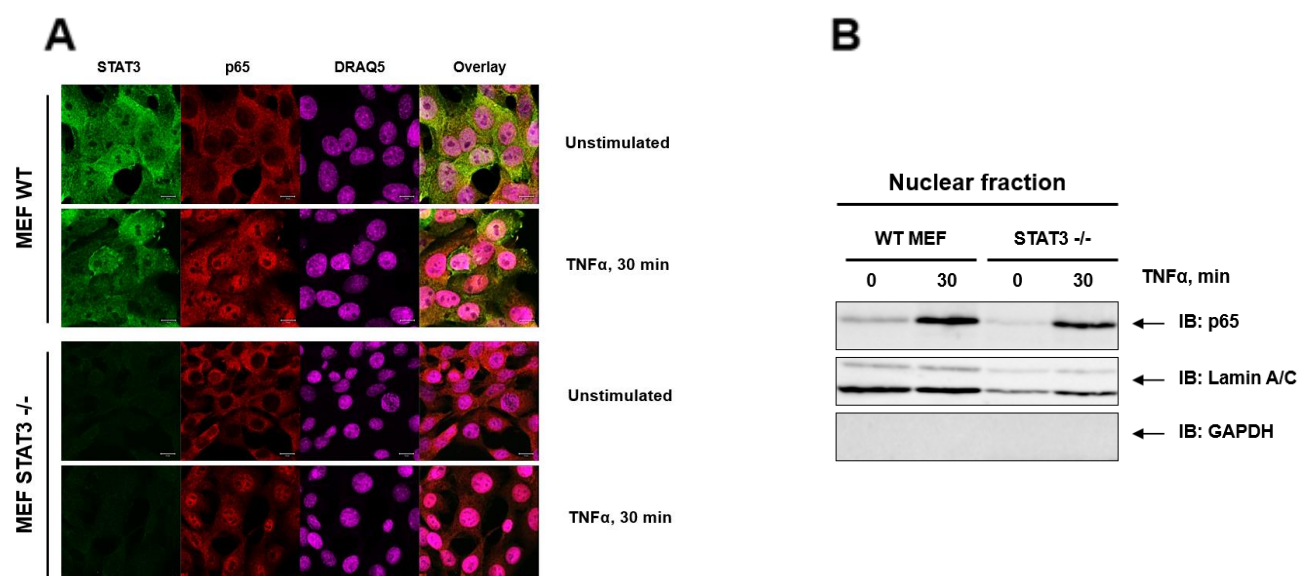


Fig. 3.21: NF- κ B nuclear translocation in wild-type, STAT3^{-/-} and p65^{-/-} MEF upon TNF α stimulation. A. Subcellular localization of p65 and STAT3 after stimulation with 10 ng/ml TNF α for 30 minutes. Indicated cell lines were fixed with combined PFA/methanol treatment, incubated with primary p65 and STAT3 antibodies, followed by immunostaining with Alexa Fluor-555 and Alexa Fluor-488 antibodies, respectively, as well as DRAQ5 nuclear marker. Scale bars represent 10 μ m. B. Analysis of p65 nuclear accumulation by cell fractionation. Wild-type and STAT3^{-/-} MEF were stimulated with 10 ng/ml TNF α for 30 minutes, followed by nuclear extract preparation and immunoblotting with p65 antibody. Lamin A/C served as nuclear fraction loading control, GAPDH served as cytoplasmic marker.

4.3. Absence of NF- κ B p65 subunit has no influence on IL-6-induced STAT3 signaling but leads to a decrease in STAT3 and STAT1 levels.

To further explore the observation of lower total STAT3 levels in p65^{-/-} MEF (Fig. 3.20A) and to analyse the influence of p65 on canonical STAT3 signaling, we stimulated wild-type and p65 deficient cells with IL-6 for 30 minutes and assessed STAT3 tyrosine 705 phosphorylation via immunoblotting, as well as expression of the STAT3 target gene *socs3* upon p65 deletion (Fig. 3.22).

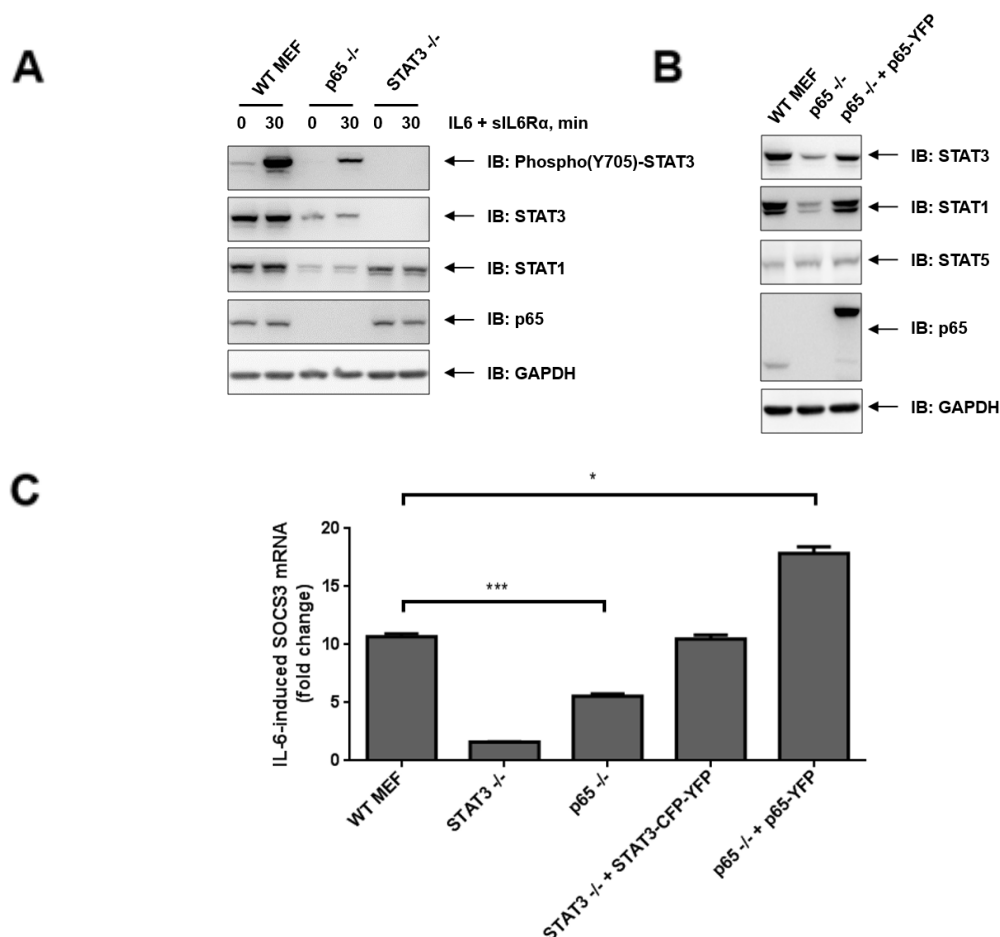


Fig. 3.22: NF- κ B nuclear translocation in wild-type, STAT3^{-/-} and p65^{-/-} MEF upon TNF α stimulation. A. Analysis of STAT3 tyrosine 705 phosphorylation. Cell lines were stimulated with 20 ng/ml IL-6 and 500 ng/ml soluble IL-6R (sIL-6R α). Total cell lysates were analysed by immunoblotting with the indicated antibodies. B. Analysis of total STAT1, STAT3 and STAT5 levels upon p65-YFP reconstitution. Total cell lysates of WT, p65^{-/-} and p65^{-/-} MEF stably transfected with p65-YFP were prepared and immunoblotted with the indicated antibodies. C. Increase in SOCS3 mRNA expression upon IL-6 treatment. Wild-type MEF, STAT3^{-/-}, p65^{-/-} cells, as well as STAT3^{-/-} MEF stably transfected with STAT3-CFP-YFP and p65^{-/-} cells stably transfected with p65-YFP construct were treated with 20 ng/ml IL-6 and 500 ng/ml soluble IL-6R (sIL-6R α) for 60 minutes. Whole cellular mRNA was isolated, and the expression of *socs3* was measured by RT-qPCR. Data are representative of three independent experiments. *p < 0.0005. ***p < 0.0005.

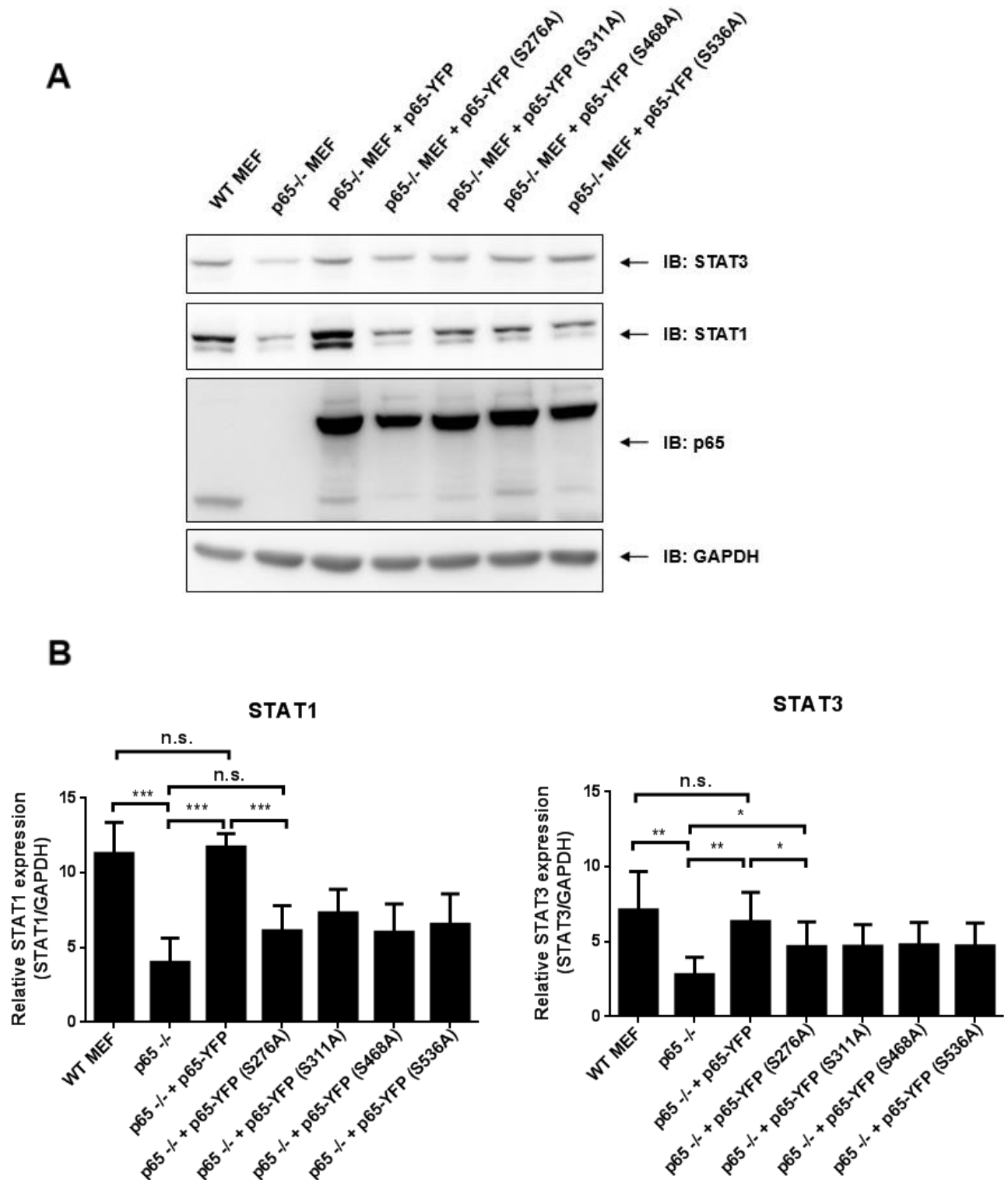


Fig. 3.23: Effect of several p65 mutants on STAT3 and STAT1 expression.. A. Analysis of STAT3 and STAT1 expression via immunoblotting. Whole cell lysates of indicated cell lines stably expressing mutated p65-YFP constructs were analysed with antibodies indicated. B. Quantification of total STAT1 and STAT3 levels from cell lines analyzed above. Immunoblots from three independent experiments were quantified using Fujifilm MultiGauge v3.2 software. *p < 0.05. **p < 0.005. ***p < 0.0005. n.s. = not significant.

Both phosphorylation and total levels of endogenous STAT3 were decreased in p65 knockout cells compared to wild-type (Fig. 3.22A). Furthermore, total levels of STAT1 were also downregulated by p65 absence. To examine whether lower levels of STAT1 and STAT3 were not an off-target effect of genetic manipulations in p65^{-/-} cells, we stably transfected these cells with a construct expressing p65-YFP and observed that total amounts of STAT1 and STAT3 recovered and were comparable to wild-type, confirming the role of p65 in STAT1 and STAT3 expression (Fig. 3.22B). In turn, total STAT5 levels remained unchanged across all three cell lines. Detection of GAPDH verified equal protein loading in both blots.

As expected, IL-6 treatment led to an approximately 10-fold increase in *socs3* mRNA in wild-type MEF and this effect was absent in STAT3^{-/-} cells. In turn, p65 knockout led to an almost 2-fold decrease in *socs3* upregulation probably due to lower total STAT3 levels. In line with this interpretation, stable expression of STAT3-CFP-YFP in STAT3^{-/-} cells restored *socs3* expression. In p65^{-/-} MEF reconstituted with p65-YFP *socs3* mRNA upregulation in response to IL-6 was even increased compared to wild-type cells (Fig. 3.22C).

Having shown that stable wild-type p65-YFP reconstitution supports the recovery of total STAT1 and STAT3 in p65 deficient MEFs, serine to alanine mutants of p65-YFP were analyzed in order to identify the necessary phosphorylation site and validate p65 transcriptional activity for this observation (Fig. 3.23A). MEF p65^{-/-} cells were stably transfected with the indicated p65-YFP mutants and total STAT1 and STAT3 were analysed via immunoblotting. The STAT recovery potential of p65 mutants was compared to WT, p65^{-/-} and wild-type p65-YFP counterparts. Immunostaining experiments revealed that mutation of the key serine at position 276 had comparable impact to p65-deficient cells on total STAT1 and levels. It has been shown, that phosphorylation of p65 at serine 276 is the major phosphorylation site of p65 and its phosphorylation is essential for p65-dependent cellular responses [179], indicating that STAT1 and to a lesser extent STAT3 protein amounts depend on p65 activation and transcriptional activity. While effects of S311A, S468A and S536A mutations on STAT1 expression were less significant, total levels of STAT3 showed only minor decrease upon all four point-mutant construct expression (Fig. 3.23B).

To assess the influence of p65 knockout on STAT3 nuclear import, we stimulated cells with IL-6 for 30 minutes and detected STAT3 nuclear accumulation by confocal microscopy and immunoblotting of nuclear fractions. Despite lower total STAT3 fluorescence signal, p65^{-/-} MEF showed prominent nuclear accumulation of endogenous STAT3 similar to wild-type cells (Fig. 3.24A). The same pattern was observed in nuclear extracts (Fig. 3.24B).

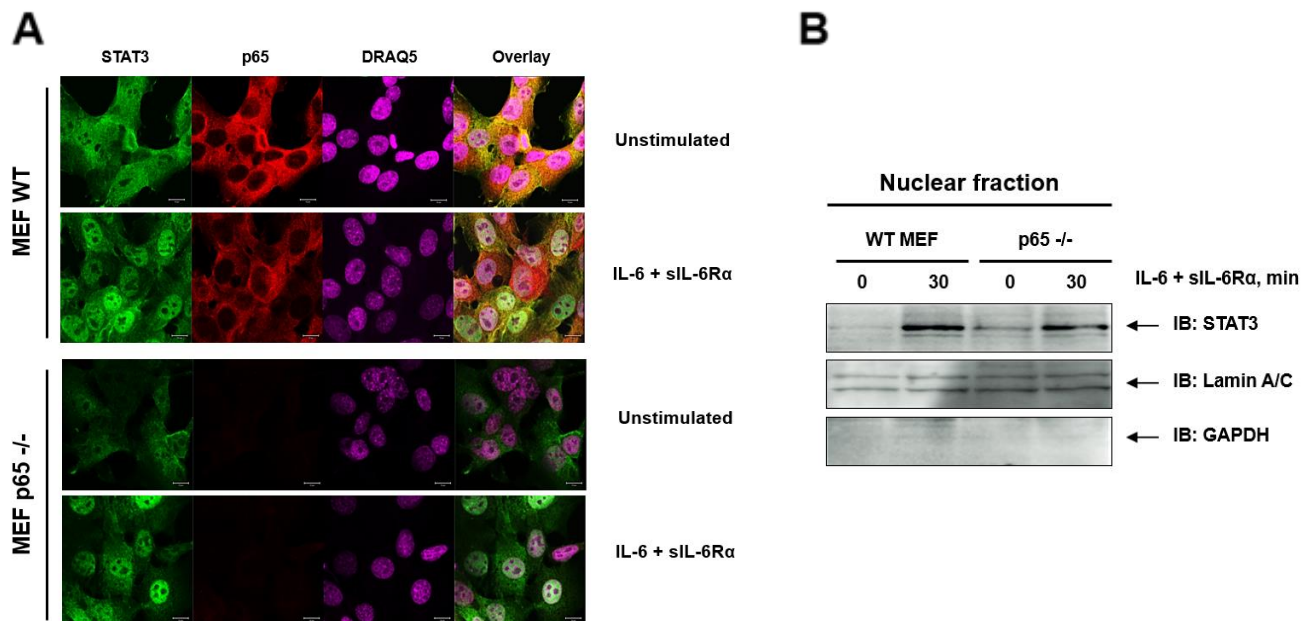


Fig. 3.24: NF-κB nuclear translocation in wild-type, STAT3^{-/-} and p65^{-/-} MEF upon TNFα stimulation. A. Subcellular localization of p65 and STAT3 after stimulation with 10 ng/ml TNFα for 30 minutes. Indicated cell lines were fixed with combined PFA/methanol treatment, incubated with primary p65 and STAT3 antibodies, followed by immunostaining with Alexa Fluor-555 and Alexa Fluor-488 antibodies, respectively, as well as DRAQ5 nuclear marker. Scale bars represent 10 μm. B. Analysis of p65 nuclear accumulation by cell fractionation. Wild-type and STAT3^{-/-} MEF were stimulated with 10 ng/ml TNFα for 30 minutes, followed by nuclear extract preparation and immunoblotting with p65 antibody. Lamin A/C served as nuclear fraction loading control, GAPDH served as cytoplasmic marker.

These findings show that upon p65 knockout IL-6-induced STAT3 activation is unaffected but total STAT3 levels are decreased resulting in diminished expression of STAT3 target genes upon IL-6 stimulation. In summary, our data show that STAT3 has very little influence on canonical NF-κB signaling involving the p65 subunit, while presence of p65 has significant impact on total amounts of transcribed STAT1 and STAT3 proteins, but not STAT5. To further explore these observations, in the next part we analyzed the effect of overexpression of both factors on each others signaling.

4.4. Inducible overexpression of STAT3 does not alter NF- κ B signaling, while total p65 increase leads to increased IL-6 induced STAT3 signaling and atypical STAT1 nuclear accumulation.

Since we observed no effect of STAT3 knockout on NF- κ B activation, we analysed whether overexpression of STAT3 has any influence on NF- κ B signaling. For this purpose a HeLa Flp-In T-REx system was utilized, which allows for conditional expression of the gene of interest upon doxycycline induction. HeLa T-REx cells were stably transfected with a STAT3-eGFP expression vector and both induced and non-induced cells were stimulated with TNF α for 30 and 60 minutes or left untreated. Cytoplasmic and nuclear extracts were prepared and analysed by immunoblotting using indicated antibodies (Fig. 3.25).

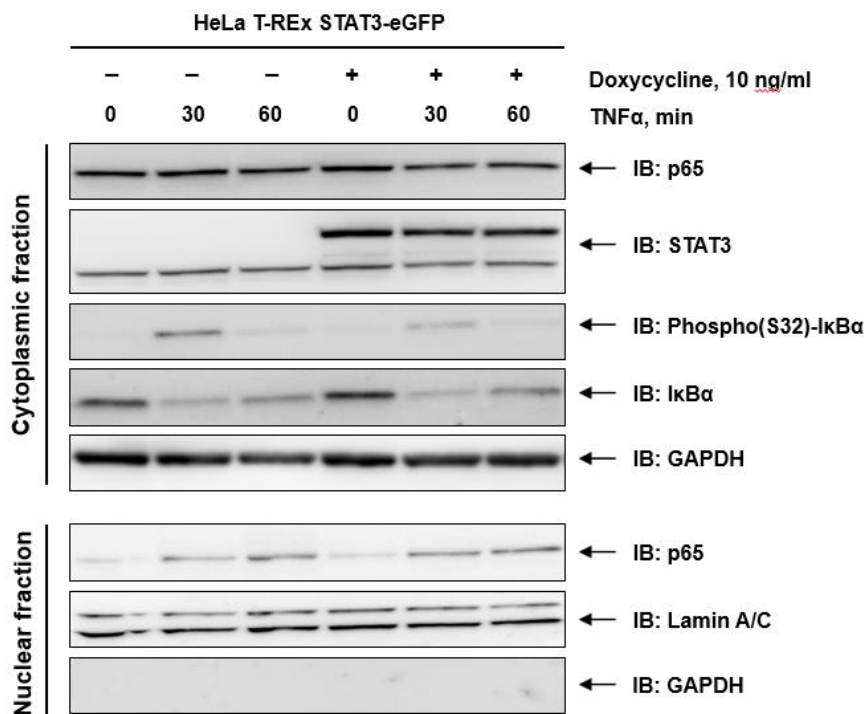


Fig. 3.25: Activation and nuclear translocation of p65 after STAT3-eGFP overexpression. HeLa Flp-In T-REx cells stably transfected with STAT3-eGFP fluorescent fusion protein were left untreated or induced with 10 ng/ml doxycycline for 24 h to induce the expression of the transgene. Subsequently, cells were stimulated with 10 ng/ml TNF α for indicated time points and cytosolic and nuclear extracts were prepared and analysed by immunoblotting with the indicated antibodies. Antibodies against GAPDH and Lamin A/C were used as cytoplasmic and nuclear loading controls respectively.

As shown in Fig. 3.25, I κ B α phosphorylation and degradation, as well as p65 nuclear translocation were comparable with or without overexpressed STAT3. Additional STAT3 bands with lower electrophoretic mobility than endogenous STAT3 demonstrate the inducible expression of the fluorescent fusion protein. Detection of GAPDH and Lamin A/C verified the cytoplasmic and nuclear fractions.

We could restore total STAT3 and STAT1 levels upon p65-YFP reconstitution in p65^{-/-} cells (Fig. 3.22B), which led to an overcompensation of socs3 mRNA expression upon IL-6 treatment compared to wild-type MEF (Fig. 3.22C). To further substantiate this finding we studied the effect of p65 overexpression on expression and activation of endogenous STAT3 in inducible HeLa Flp-In T-Rex stably transfected with p65-dsRed. Doxycycline induced and non-induced cells were either stimulated with IL-6 or left unstimulated and cytosolic and nuclear fractions were prepared.

Immunoblotting revealed a considerable increase in tyrosine phosphorylation of STAT3 in cells overexpressing p65-dsRed upon IL-6 stimulation (Fig. 3.26A). Moreover, endogenous STAT1 shows an atypical nuclear presence upon IL-6 treatment when p65 is overexpressed, confirming the influence of p65 levels on both STAT3 and STAT1. However, in contrast to MEF, p65-dsRed overexpression does only slightly alter total STAT3 and STAT1 protein amounts in HeLa cells, as judged by immunoblotting of cytoplasmic fraction (Fig. 3.26A). In order to prove, that p65-dsRed overexpression effect on STAT3 overactivation is p65 dependent, we created two additional inducible HeLa Flp-In T-REx cell lines stably transfected with p65 or dsRed. These cells were stimulated with IL-6 or left unstimulated with or without doxycycline induction and total cell lysates were analyzed by immunoblotting. Only in cells expressing p65 STAT3 showed increased IL-6-induced phosphorylation upon doxycycline induction (Fig. 3.26B), confirming that the effect observed in Fig. 3.26A is not due to dsRed induction or doxycycline treatment itself. Staining of p65 and dsRed affirms inducible expression of these proteins and GAPDH immunodetection verifies equal loading. Taken together, inducible p65 overexpression in HeLa cells leads to an increased STAT3 activation and uncharacteristic STAT1 nuclear presence upon IL-6 stimulation. Next, we analyzed physical interaction between the two factors upon IL-6, TNF α or combined treatment.

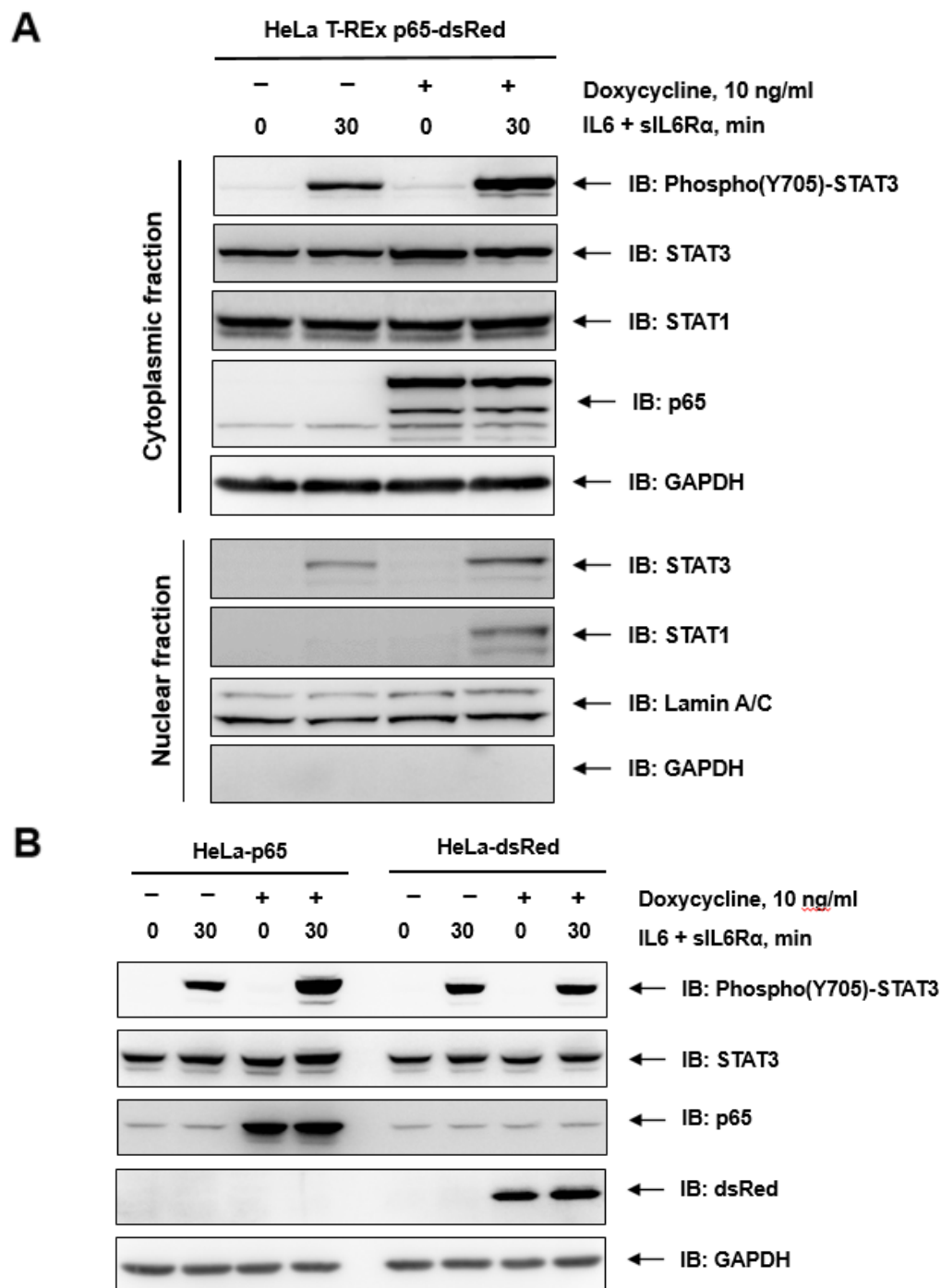


Fig. 3.26: STAT3/STAT1 activation and total levels after p65-dsRed overexpression. A. STAT3 activation and nuclear translocation of STAT1 and STAT3 after p65-dsRed overexpression. HeLa Flp-In T-REx cells stably transfected with p65-dsRed fluorescent fusion protein were left untreated or induced with 10 ng/ml doxycycline for 24 h to induce the expression of the transgene. Subsequently, cells were stimulated with 20 ng/ml IL-6 and 500 ng/ml soluble IL-6R (sIL-6R α) for 30 minutes and cytosolic and nuclear extracts were prepared and analysed by immunoblotting with the indicated antibodies. Antibodies against GAPDH and Lamin A/C were used as cytoplasmic and nuclear loading controls, respectively. B. STAT3 activation after overexpression of dsRed and p65. HeLa Flp-In T-REx cells stably transfected with p65 or dsRed were left untreated or induced with 10 ng/ml doxycycline for 24 h to induce the expression of the transgene. Subsequently, cells were stimulated with 20 ng/ml IL-6 and 500 ng/ml soluble IL-6R (sIL-6R α) for 30 minutes and total cell lysates were prepared and analysed by immunoblotting with the indicated antibodies. GAPDH served as a loading control respectively.

4.5. Weak interaction between NF- κ B p65 and STAT3 could be detected after TNF α , but not after IL-6 treatment

Several reports demonstrated physical interactions of p65 and STAT3 upon IL-1 β -induced NF- κ B activation [128, 134] and combined activation of STAT3 and p65 by IGF-1 and TNF α respectively [180]. To assess, whether STAT3 and p65 form complexes upon TNF α and IL-6 treatments, we stimulated MEF Δ/Δ (WT)STAT3-FP cells with TNF α , IL-6 or both factors for indicated time periods and analyzed p65 binding to (WT)STAT3-FP via co-immunoprecipitation. Heterodimer formation of STAT3 with STAT1 served as a positive control (Fig. 3.27). The stimulation of cells with TNF α resulted in a weak interaction of (WT)STAT3-FP with p65 but not STAT1, while IL-6 treatment resulted only in STAT1 association. Interestingly, combined IL-6 and TNF α treatment resulted in weaker STAT1/(WT)STAT3-FP binding compared to IL-6 treatment alone, as well as p65/(WT)STAT3-FP interaction only after two hours of stimulation compared to TNF α treatment. These results suggest that p65 interacts with STAT3 upon NF- κ B activating stimuli and not IL-6 treatment alone.

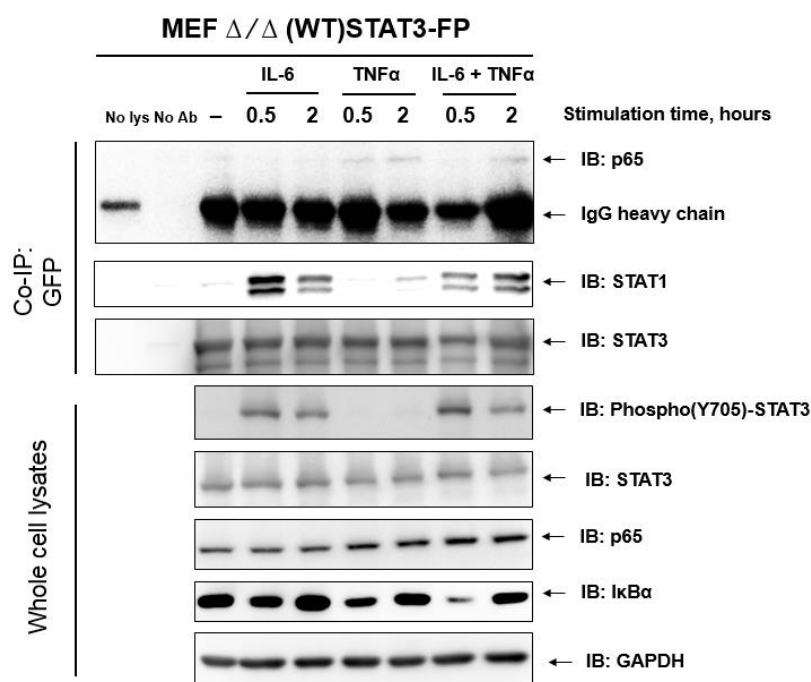


Fig. 3.27: Co-immunoprecipitation of STAT3 with p65 and STAT1 upon IL-6 and TNF α treatment. MEF Δ/Δ (WT)STAT3-FP cells were stimulated as indicated and total cell lysates were prepared, subjected to co-immunoprecipitation with α -GFP antibody and analyzed via immunoblotting with indicated antibodies (top). First two lanes in Co-IP blot served as internal controls containing no cell lysate or no α -GFP antibody, respectively. 20 μ g of whole cell lysates served as an input control (bottom).

5. Characterization of STAT3-YFP knock-in mice

5.1. Generation and validation of transgenic mice.

Activation of STAT3, which involves its phosphorylation and nuclear accumulation, has been observed in several pathophysiological conditions such as cancer, chronic inflammation and autoimmunity. We and other groups have successfully used fluorescently labelled STAT3 for dissecting previously unknown aspects of STAT3 signaling and functions [48-50, 52, 53, 58]. In order to apply this tool *in vivo*, we have generated a STAT3-YFP knock-in murine model, expressing fluorescently labelled STAT3 (STAT3 α -isoform) under the control of the endogenous STAT3 promoter, as a potentially powerful tool for the visualization of STAT3 *in vivo* using common and advanced microscopy techniques.

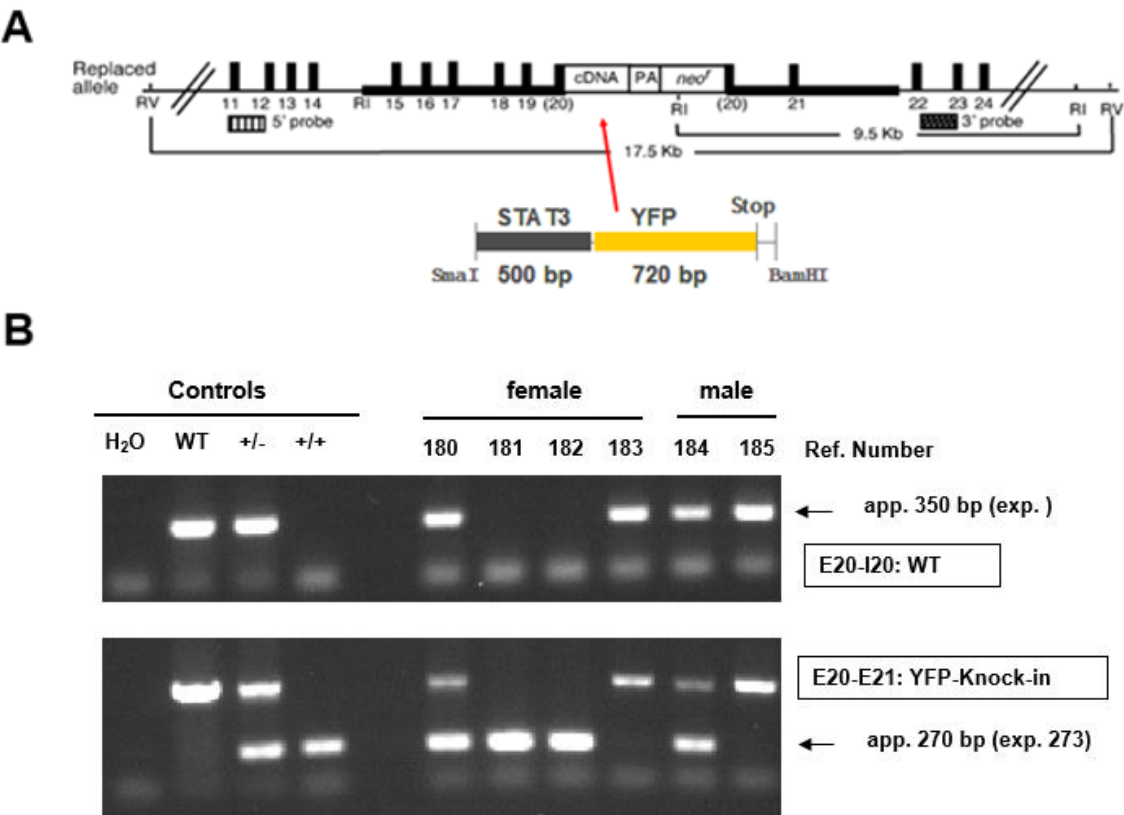


Fig. 3.28: Generation and validation of STAT3-YFP knock-in mice. A. Overview of the strategy for STAT3-YFP insertion via homologous recombination. B. STAT3-YFP knock-in mice genotyping. Upper and lower gels show PCR amplicons for wild-type and knock-in alleles, respectively, for any given mice. Animal sex and numbers are indicated at the top. Isolated gDNA from WT, STAT3-YFP heterozygous (+/-) and homozygous (+/+) embryonic stem cells (ESC) were used as an amplicon controls. Expected (exp.) and observed (app.) amplicon sizes are indicated with black arrows.

After cloning of the targeting construct in our lab, transgenic animals were generated by homologous recombination by the group of Valeria Poli (University of Turin, [100, 176]). The YFP cDNA was inserted behind the C-terminal region of Stat3 α at chromosome 11 and fused in frame with exon 20, provided with a polyadenylation site and placed within two homology regions together with a neomycin resistance cassette (Fig. 3.28A). Subsequently, frozen embryos of transgenic mice were transferred to Institute for Laboratory Animal Science and Experimental Surgery at RWTH Aachen University (Aachen, Germany) and C57BL/6 mice were used for embryo transplantation. Animal genotype was analyzed by PCR using specific primer combinations (See II.1.5) for wild-type and knock-in allele (Fig. 3.28B). During this thesis a total of 235 transgenic animals were genotyped. Both heterozygous and homozygous transgenic animals demonstrated no obvious aberrations in their phenotype, viability and mating potential.

5.2. Characterization of transgenic mice.

To verify the proper expression of STAT3-YFP *in vivo*, we performed cytospin of spleen cells from a homozygous STAT3-YFP knock-in mouse and YFP signal of fixed cells was detected using confocal microscopy (Fig. 3.29A). Also, spleen cell lysates were prepared and STAT3-YFP protein expression was analyzed in Western blot analysis (Fig. 3.29B). As expected, immunoblotting demonstrated an endogenous STAT3 band at 90 kDa in lysates from WT animal. Two STAT3 bands corresponding to endogenous STAT3 and STAT3-YFP were detected in spleen cells from heterozygous animal and one STAT3-YFP band at around 110 kDa in lysates from homozygous mouse. The results from these experiments verified STAT3-YFP protein expression in heterozygous and homozygous STAT3-YFP knock-in mice.

Additionally, primary hepatocytes of wild-type, heterozygous and homozygous mice were isolated from livers of 10 weeks old animals via two-step *in-situ* collagenase perfusion method by the group of Ralf Weiskirchen [181], fixed with 3.7% PFA and subjected to confocal microscopy analysis (Fig. 3.29C). Microscopy verified the proper expression of STAT3-YFP protein in primary hepatocytes from heterozygous

and homozygous mice. The stronger signal in homozygous STAT3-YFP knock-in cells indicates a gene dosage effect.

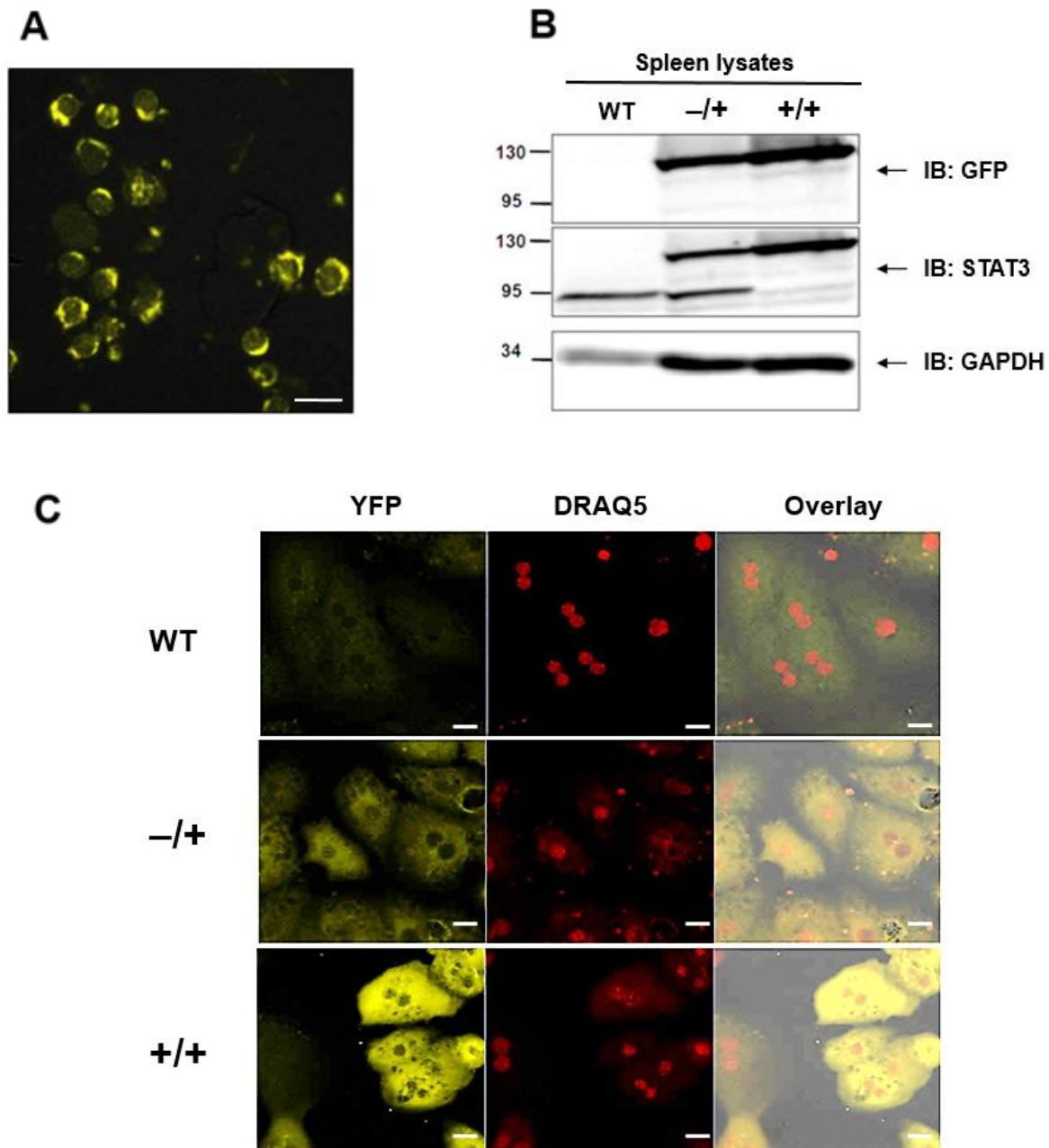


Fig. 3.29: Characterization of transgenic STAT3-YFP knock-in mice. A. Confocal microscopy of fixed spleen cells from STAT3-YFP knock-in homozygous mice. B. Western blot of spleen cell lysates from WT, heterozygous and homozygous STAT3-YFP knock-in mice performed with the indicated antibodies. WT - wild type; -/+ – knock-in heterozygous; +/+ – knock-in homozygous. C. Confocal microscopy of isolated primary hepatocytes from indicated animals (left). DRAQ5 was used as a nuclear marker. Scale bars represent 10 μ m.

In conclusion, the herein demonstrated results indicate that STAT3-YFP knock-in mice were successfully generated and that the expression of STAT3-YFP can be detected by immunoblotting and confocal microscopy, as well as flow cytometry and 2-photon microscopy (data not shown).

IV. Discussion

The JAK-STAT signaling module constitutes a fundamental intracellular signal transduction pathway that relays numerous signals of crucial importance for development and homeostasis in animals. The JAK-STAT system has evolved early in metazoa and exists already in the slime mold *Dictyostelium discoideum* and in the fruit fly *Drosophila melanogaster* [75, 182]. The genomes of mammals encode four JAKs (JAK1, JAK2, JAK3, Tyk2) and seven STATs (STAT1, 2, 3, 4, 5A, 5B, 6). The JAK-STAT pathway is of central importance for the transmission of signals from numerous cytokine and growth factors, which are essential determinants for the generation of blood and immune cells as well as the regulation of various processes in other tissues of the organism [21-23, 36, 37].

STAT3, a pleiotropic transcription factor that is the most studied member in the STAT family, is involved in many physiological processes including embryonic development, hematopoiesis and immunity. Extracellular ligands such as cytokines and growth factors activate STAT3 by specific binding to transmembrane receptors and the subsequent activation of receptor-associated and cytoplasmic tyrosine kinases [21, 22, 39]. According to the canonical model, upon activation STAT3 monomers are phosphorylated at the critical tyrosine 705 residue, form homo- or heterodimers and translocate to the nucleus, where they regulate gene expression. Under physiological conditions STAT3 activation is a tightly controlled transient process, which involves negative regulators such as SOCS3, PIAS3, phosphatases and other proteins [40]. Recently, various non-canonical aspects of STAT3 signaling have emerged [24]. Latent STAT3 already forms homodimers or heterodimers with STAT1 [25, 45-47] and constantly shuttles in and out of the nucleus [48-50]. Unphosphorylated STAT3 can bind to DNA and drive gene expression in a distinct manner from phosphorylated STAT3, as well as functionally interacts with other transcription factors, such as NF- κ B [131].

To date persistent activation of STAT3 has been observed in many pathophysiological conditions such as malignant transformation and tumorigenesis; fibrosis in kidney, lung, and liver; rheumatoid arthritis, Alzheimer's disease, psoriasis,

autoimmune and cardiovascular diseases [67-69, 183]. Therefore, STAT3 inhibitors are currently under intense development in many therapeutic fields.

In order to suppress STAT3 signaling, direct STAT3 inhibitors usually target one of three structural domains of STAT3: SH2 domain, DNA-binding (DBD) domain or N-terminal (NTD) domain [73, 74, 183]. Hence, the main focus of this work was to further elucidate the roles of NTD, DBD and SH2 domains in cytokine-induced and latent STAT3 signaling mechanisms, as well as to gain further insight into STAT3 crosstalk with STAT1 and NF- κ B transcription factors.

1. STAT3-FP reproduces functional characteristics of endogenous STAT3 cells

In the past, fluorescent fusion proteins of STAT3 (STAT3-YFP and STAT3-CFP-YFP) have been successfully used by our group to study subcellular localization and intracellular dynamics of STAT3 [49, 52, 53, 58, 184]. Fluorescent fusion proteins of all other mammalian STATs have also been successfully generated and characterized [185-190]. STAT3-deficient MEF cells developed by Poli and colleagues [100] stably transfected with wild-type STAT3-FP ((WT)STAT3-FP) were reported to mimic endogenous STAT3 tyrosine 705 phosphorylation and cytokine-induced nuclear translocation [52, 58].

To further validate MEF Δ/Δ STAT3-FP cells as a useful tool for studying STAT3 signaling, GAS-recognition and immediate early STAT3 target gene expression were analyzed in addition to tyrosine phosphorylation and nuclear accumulation of (WT)STAT3-FP (Fig. 3.1). The results of these experiments revealed that in line with published observations for endogenous STAT3 [170], the IL-6-induced activation (WT)STAT3-FP leads to formation of three major DNA complexes: STAT3-FP homodimers (S3/S3), STAT3-FP/STAT1 (S3/S1) heterodimers and STAT1 homodimers. Moreover, IL-6 stimulation of both WT MEF and MEF Δ/Δ STAT3-FP cells resulted in comparable 10-fold *socs3* mRNA upregulation, as it has been reported previously [191]. Thus, (WT)STAT3-FP stably expressed in STAT3-deficient MEF Δ/Δ cells is a functional transcription factor that faithfully reproduces important functional characteristics of endogenous STAT3 (cytokine-induced phosphorylation,

nuclear translocation, DNA-binding and transcriptional activity) and fluorescently labeled STAT3 constructs can be used for further analysis of STAT3 signaling.

2. GAS-element-specific DNA recognition is dispensable for nuclear accumulation of STAT3

Like for all other members of the STAT family, upon extracellular ligand treatment STAT3 activation involves tyrosine phosphorylation, dimerization, nuclear translocation and subsequent binding to specific DNA sequences [21]. Apart from this canonical activation model STAT3 has been also shown to shuttle permanently between cytoplasm and nucleus independently of cytokine treatment. However, the molecular mechanisms of STAT3 nuclear trafficking are not yet defined. In the first major part of this work, we were interested, if nuclear accumulation of cytokine-activated STAT3 requires GAS-element-specific DNA-binding, to assess the role of the N-terminal domain in STAT3 nuclear trafficking and whether latent nucleocytoplasmic shuttling uses the same nuclear import machinery as cytokine-induced nuclear accumulation.

For STAT1 several DNA-binding mutants do not recognize specific GAS sequences, but many of them retain the ability to accumulate in the nucleus upon cytokine-dependent activation [192]. In turn, nuclear accumulation of STAT5B upon growth hormone stimulation was abrogated by disrupting specific STAT5B-DNA-binding [193]. In order to assess whether STAT3 nuclear accumulation relies on specific DNA-binding we have generated an artificial STAT3 mutant that does not recognize the consensus DNA sequence. For this purpose we have chosen to target the amino acid sequence ⁴⁶⁵SNICQ⁴⁶⁹ in the $\alpha 5$ loop of the STAT3 DNA-binding domain. Hypomorphic mutations of S465, N466 and Q469 that lead to a disruption of STAT3 signaling have been reported in patients with hyperimmunoglobulinemia E syndrome (HIES) [194], where serine 465 mutation to phenylalanine leads to abrogated DNA binding and *socs3* upregulation upon cytokine stimulation despite intact nuclear translocation [195]. The residue C468 has been previously shown to be alkylated by a selective STAT3 small molecule inhibitor C48, which resulted in abrogation of DNA-binding [196]. The asparagine at position 466 has also been involved in interaction with one of the compounds that disturb STAT3-DNA interaction in nuclear extracts

[197]. In agreement with these data, we disrupted the DNA-binding interface while maintaining the polar properties of this loop by introducing five amino acid substitutions: S465G, N466S, I467S, C468G and Q469S (Fig. 3.2B).

Indeed, the mSNICQ mutant was not able to bind a radioactively labelled m67SIE probe in EMSA assay despite its intact ability to become phosphorylated on tyrosine 705 and form heterodimers with STAT1 upon IL-6 stimulation (Fig. 3.4A). Nevertheless, (mSNICQ)STAT3-FP rapidly accumulated in the nucleus upon IL-6 stimulation (Fig. 3.3) similarly to (WT)STAT3-FP. Interestingly, despite intact stimulus-dependent (mSNICQ)STAT3-FP/STAT1 heterodimer formation in co-immunoprecipitation assay, only STAT1/STAT1 homodimer bands were detected by EMSA in cells stably expressing (mSNICQ)STAT3-FP construct upon stimulation, indicating that both monomeric partners within a STAT3/STAT1 heterodimer require intact DNA-binding interfaces for cytokine-driven GAS-element recognition. In contrast, (Δ N)STAT3-FP was unable to accumulate in the nucleus upon cytokine treatment (Fig. 3.3) while still being able to recognize GAS sites and form tyrosine-phosphorylated dimers (Fig. 3.4A), as reported previously [52, 79].

Upregulation of the immediate early endogenous STAT3 target gene *socs3* was significantly reduced for both mutants after 30 minutes but still present with delayed kinetics (Fig. 3.4B). Delayed *socs3* upregulation explain the contradicting (Δ N)STAT3-driven gene induction results in two different publications [80, 84]. Although (Δ N)STAT3-FP failed to accumulate in the nucleus upon stimulation, the NTD truncation mutant of STAT3 has been previously shown to inducibly associate with the *socs3* promoter in a two-step ChIP assay [84], suggesting that despite deficient nuclear accumulation (Δ N)STAT3-FP might still be able to induce STAT3 target genes as a homodimer or (Δ N)STAT3-FP/STAT1 heterodimer, albeit less efficiently than the wild-type. On the other hand, the *socs3* gene promoter is capable of binding both STAT1 and STAT3 and both factors at least in part mediate *socs3* upregulation by leukemia inhibitory factor [191]. Moreover, *socs3* induction by IFN γ in human fibrosarcoma, human lung adenocarcinoma and wild-type MEFs is STAT1-dependent [198]. Given that STAT1 has been previously shown to induce STAT3 target genes upon IL-6 type cytokine treatment with delayed kinetics in the absence of STAT3 [199, 200], increased STAT1 activation observed in (Δ N)STAT3-FP and

(mSNICQ)STAT3-FP expressed cells (Fig. 3.4A) can account for delayed IL-6-induced socs3 induction despite dysfunctional STAT3 signaling.

Taken together, our data indicates that for successful immediate target gene induction both nuclear accumulation and specific GAS sites recognition are required. However, IL-6-induced active nuclear import and nuclear accumulation of STAT3 are not regulated by the availability of GAS binding sites. The same observation has been made for IFN γ -induced STAT1 signaling [201]. The authors propose other mechanisms than GAS-element binding of STAT1 for intact nuclear localization. A recent publication reported the ability of latent STAT3 to bind an AGG-element with the consensus sequence AGGN₃AGG without involvement of a functional DNA-binding domain [202]. This DNA-binding activity might not be relevant for activated STAT3.

3. STAT3 N-terminal domain deletion mutant remains in the cytoplasm in the form of activated dimers capable of GAS-element binding

A recent study demonstrated that deletion of the first 126 amino acids of STAT3 resulted in significant reduction of LIF-induced expression of STAT3 target genes as a result of decreased STAT3 binding to their regulatory regions [85]. One alternative explanation for the impact of N-terminal domain deletion on target gene transcription can be its functional role in STAT3 nuclear accumulation. In our study, (Δ N)STAT3 remains phosphorylated and is able to bind specific DNA sequences for up to 4 hours after stimulus removal (Fig. 3.5). Moreover, phosphorylated dimers of (Δ N)STAT3 localize primarily to the cytosol in contrast to wild-type, as demonstrated by immunofluorescence (Fig. 3.6) and this cytoplasmic trapping cannot be rescued by inhibition of CRM1-dependent nuclear export (Fig. 3.12).

It has been shown that NTDs are involved in dephosphorylation of STATs. STAT1 dephosphorylation requires NTD-mediated spatial reorientation of phosphorylated dimers [203], while point-mutations within the N-terminal domains of STAT1 and STAT5A/B led to defective dephosphorylation of these molecules upon cytokine stimulation [204]. Furthermore, prolonged phosphorylation and DNA-binding, as well

as the inability to accumulate in the nucleus upon stimulation has been also demonstrated for the NTD deletion mutant of STAT1 [173, 174]. STAT1 lacking the N-terminal domain was constitutively phosphorylated on tyrosine 701 and was more sensitive to cytokine-induced activation [173].

In our study (Δ N)STAT3-FP was more sensitive to lower cytokine concentrations than (WT)STAT3-FP, however, in contrast to STAT1, deletion of NTD did not induce STAT3 activation without any stimulus (Fig. 3.7A). Enhanced sensitivity of (Δ N)STAT3 cannot be explained by its inability to form unphosphorylated dimers, since somatic point mutation of leucine 78 to arginine also causes defects in latent dimer formation, but this mutant is not as sensitive as (Δ N)STAT3 [53]. (Δ N)STAT3 prolonged phosphorylation also cannot be explained by NTD requirement for extensive spatial reorientation of the monomers, reported for STAT1 [200], because both latent and active monomers of STAT3 have been shown to have parallel orientation in contrast to STAT1 [53, 205]. Therefore, prolonged phosphorylation of (Δ N)STAT3 homodimers might be a consequence of cytoplasmic retention.

STAT1 and STAT3 activation in response to IL-6 has been shown to rely mainly on JAK1 kinase [51]. Being that JAK1 activation was only slightly elongated and correlated only with prolonged STAT1 phosphorylation in cells stably expressing (Δ N)STAT3-FP (Fig. 3.5), the prolonged phosphorylation profile of STAT3 N-terminal truncation mutant could not be explained by prolonged reactivation at the receptor alone. For STAT1 it has been demonstrated, that the N-terminal domain appears to regulate association with the nuclear phosphatase TC45 (the nuclear isoform of the T-cell protein tyrosine phosphatase (TC-PTP)) and subsequent STAT1 dephosphorylation [204]. The same phosphatase is also involved in STAT3 deactivation [206] and we hypothesized, that instead of constant reactivation, prolonged phosphorylation may be induced by the inability of (Δ N)STAT3 to interact with phosphatases.

Inhibiting cellular phosphatases with sodium vanadate resulted in prolonged tyrosine 705 phosphorylation for (WT)STAT3-FP upon IL-6 pulse stimulation for up to 1 hour similar to (Δ N)STAT3-FP in cells without vanadate treatment (Fig. 3.7B), indicating that lack of NTD results in phosphatase inability to dephosphorylate STAT3.

However, the NTD does not mediate STAT3-TC45 physical interaction, since the presence of only linker, SH2 and transactivation domains of STAT3 is sufficient for phosphatase binding [207]. TC45-mediated STAT3 dephosphorylation also requires the small proteins GdX and SIPAR that convert TC45 into a STAT3-specific phosphatase and enhance complex formation, though again not the N-terminal domain, but DNA-binding and linker domains of STAT3 are important for physical association with GdX and SIPAR [208, 209]. Basal phosphorylation of wild-type STAT3 and to a greater extent (Δ N)STAT3 was elevated upon vanadate treatment (Fig. 3.7B), suggesting that some cytoplasmic phosphatases are still able to act on NTD truncation mutant of STAT3 in resting cells. These findings suggest that the activated dimers of STAT3 NTD truncation mutant are not able to interact with nuclear TC45 due to defect in their nuclear localization.

Recently, DUSP2, a member of dual-specificity phosphatase (DUSP) family, has been reported to negatively regulate Th17 development by dephosphorylating STAT3 on tyrosine 705 and serine 727 residues. Furthermore, STAT3 N-terminal domain was essential for its interaction with DUSP2 [210]. However, since DUSP2 is expressed exclusively in immune cells [211] and in MEF cells there is no detectable DUSP2 protein expression [212], it is unlikely that in our system (Δ N)STAT3-FP fails to be dephosphorylated due to lost ability to interact with DUSP2. Nevertheless, MEF cells abundantly express DUSP5 phosphatase [212], which belongs to the same type II DUSPs and has a structure similar to DUSP2 [213]. Moreover, STAT3 binds to the promoter regions of human DUSP5 in HepG2 and A549 cells [214]. Taken together, these data suggests DUSP5 as a potential candidate phosphatase for STAT3 dephosphorylation which requires the NTD.

4. STAT3 NTD is not required for binding to various importin- α isoforms

Next, we assessed whether the inability of (Δ N)STAT3 to accumulate in the nucleus upon IL-6 treatment is caused by defective binding to α -importins. STAT1 nuclear import in IFN γ -stimulated cells relies mainly on importin- α 5/NPI-1 [153] and the NTD of STAT1 is required for association with importin- α 5 [175]. Of note, no difference of STAT1 phosphorylation and nuclear accumulation was detected between wild type

and importin- α 5-deficient MEFs [215], suggesting that importin- α 5 is preferred rather than required by phosphorylated STAT1 dimers for nuclear import. Because STAT1 and STAT3, but not STAT5A, have been reported to similarly bind to importins α 5 and α 7 upon cytokine stimulation in different cell lines [159] we hypothesized that STAT3 N-terminal domain deletion can lead to a defect in α -importin association, as observed for STAT1.

In agreement with the above mentioned data, wild-type STAT3-FP precipitated together with importins α 5 and α 7, as well as α 3, importin- α 5 association being the strongest (Fig. 3.8A). Importin binding specifically to STAT3 molecules and not to fluorescent tags was confirmed by co-precipitation of endogenous STAT3 with GST-importin- α 5 from wildtype MEFs (Fig. 3.8B). Association with importin- α 5 has also been described to be important for axonal retrograde transport of STAT3 [216]. Unexpectedly, in our hands STAT3 binding to importin- α 5, as well as α 3 and α 7, was not dependent on IL-6 stimulation (Fig. 3.8B, 3.9A and B). Stimulus independent STAT3 association with importin- α 3 (Δ IBB) has been proposed as possible explanation for STAT3 nuclear presence without cytokine treatment [157]. Moreover, both (WT)STAT3-FP and (Δ N)STAT3-FP also associated with nuclear carrier importin- β 1 *in-vitro* independently of IL-6 stimulation (Fig. 3.9C), which has also been reported previously [160, 217]. To date, there is no unified model as to how and under which stimulation conditions STAT3 interacts with importin molecules [157-160]. Additionally, both STAT1 and STAT3 latent nuclear import have been shown to be independent of energy or transport carriers [218], which warrants further studies in order to elucidate the exact nuclear import mechanism for STAT proteins.

In our hands full-length importin- α 5 binds endogenous STAT1 only upon IFN γ stimulation and this association is abolished by the critical tyrosine mutation Y476G in importin- α 5, faithfully reproducing previously published observations [155]. But endogenous STAT3 binds to both wild-type and Y476G-mutated GST-fusion importin- α 5 molecules independently of stimulation, pointing to mechanistic differences in nuclear import of STAT1 and STAT3 (Fig. 3.8B). Moreover, STAT3 bound both full-length and Δ IBB truncation mutant of importin- α 5 (Fig. 3.9A), suggesting that STAT3 nuclear translocation also does not rely on classical NLS recognition by α -importins, as similarly reported for STAT1 [155]. In contrast to

STAT1 [175], deletion of the NTD of STAT3 had no detrimental effect on importin- α 5, - α 3 and - α 7 binding (Fig. 3.9A and B). Conclusively, our results show that despite similar independence from canonical importin alpha binding *in-vitro* via a classical NLS, mechanistical aspects of STAT3 association with importin alpha isoforms is distinct from that proposed for STAT1.

The exact role of STAT3 NTD in active nuclear import is still unclear. The NTD of STAT3 may be involved with other than α -importin protein-protein interactions. For instance, STAT3 nuclear import has been shown to be also dependent on RanGTP [214], as well as on the small GTPase Rac1 and the GTPase-activating protein for Rho family GTPases MgcRacGAP [219]. As further evidence for the essential role of the NTD for active nuclear import, the tumor suppressor ARHI is able to downregulate STAT3 transcriptional activity by blocking nuclear translocation of phosphorylated STAT3 via direct interaction with the NTD of STAT3 and prevention of STAT3-importin complex formation [220, 221]. Furthermore, several other STAT3 interacting proteins have been identified over the last two decades involved in both promoting and repressing STAT3 signaling (see Conclusions and Outlook section) and N-terminal deletion of STAT3 may affect the association with some of them.

It is likely that the NTD is required for the correct conformation of full-length activated STAT dimers necessary for nuclear import and proper STAT phosphorylation-dephosphorylation cycles. Phosphorylation-induced conformational changes of STAT5A/B led to both local SH2-domain and long-distance structural rearrangements within other domains, affecting the entire structure of STAT5 [222]. Given that interactions of a phosphotyrosine 705-peptide with the SH2 domain caused structural and dynamic changes in LD and DBD domains of STAT3 [223], N-terminal deletion might have an inter-domain allosteric effect on other STAT3 domains, which leads to observed defects in cytokine-induced nuclear accumulation and subsequent dephosphorylation. In summary, the exact molecular mechanisms responsible for cytoplasmic trapping and subsequent defective dephosphorylation of phosphorylated (Δ N)STAT3-FP dimers remain ill-defined and require further analysis. In this context, we decided to analyze the role of CRM1-mediated nuclear export of STAT3.

5. Latent nucleocytoplasmic shuttling of STAT3 does neither require GAS-element recognition, nor functional N-terminal or SH2 domains

Re-export of STAT3 from the nucleus back to the cytoplasm after stimulation is dependent on CRM1, a LMB-sensitive export protein [48, 49, 58]. We hypothesized that (Δ N)STAT3-FP may still be imported properly in the nucleus, which is then followed by rapid nuclear export causing the observed lack of nuclear accumulation. In order to test this hypothesis, we decided to block CRM1-mediated nuclear export using Leptomycin B (LMB) and to monitor STAT3-FP subcellular distribution via confocal microscopy. As demonstrated previously [48], STAT3 nuclear export was effectively blocked by LMB treatment, leading to predominantly nuclear localization of (WT)STAT3-FP even after 4 hours after stimulus removal compared to untreated control (Fig. 3.10A).

Additionally, LMB treatment of cells leads to partial nuclear accumulation of unphosphorylated STAT3, confirming continuous STAT3 trafficking in and out of the nucleus in the absence of cytokine treatment (Fig. 3.10B). Our group had previously shown that both basal nuclear import and latent nuclear export of fluorescently labeled STAT3 were markedly reduced upon IL-6 stimulation and that latent nucleocytoplasmic shuttling of STAT3 is much slower than cytokine-induced nuclear translocation [49]. In line with these observations, LMB treatment of unstimulated cells led to slow and only partial (WT)STAT3-FP nuclear localization compared to rapid IL-6-induced nuclear accumulation (Fig. 3.12B).

Confocal live-cell imaging showed that (Δ N)STAT3-FP also accumulated in the nuclei of unstimulated cells upon LMB treatment (Fig. 3.11A). However, CRM1-mediated nuclear export blockage in combination with IL-6 did not lead to improved nuclear accumulation of (Δ N)STAT3-FP as compared to LMB treatment alone. Previously, we have demonstrated that (Δ N)STAT3-FP shuttles between the nucleus and the cytoplasm of resting cells despite its inability to form latent dimers and to accumulate in the nucleus upon IL-6 stimulation. Moreover, upon LMB treatment (Δ N)STAT3-FP accumulated in the nuclei much faster than (WT)STAT3-FP (data not shown), which

is in agreement with our previous observation that the NTD deletion mutant shuttled more rapidly than STAT3 wild-type [52]. Thus, the previously observed lack of (Δ N)STAT3-FP nuclear accumulation upon cytokine stimulation is not due to rapid CRM1-mediated nuclear egress.

Interestingly, inhibition of CRM1-mediated nuclear export had no significant effect on (WT)STAT3-FP dephosphorylation kinetics (Fig. 3.11B) despite nuclear export inhibition and prolonged nuclear retention in LMB-treated cells. Thus, we conclude that main phosphatases acting on activated STAT3 dimers localize predominantly in the nuclear compartment and CRM1-mediated nuclear export of STAT3 is not required for Y705 dephosphorylation after cytokine stimulation.

Likewise, inhibition of CRM1-mediated nuclear export had no significant effect on both prolonged (Δ N)STAT3-FP phosphorylation (Fig. 3.11B) and cytoplasmic trapping of activated dimers (Fig. 3.12A and B), indicating that phosphorylated (Δ N)STAT3-FP dimers are not entering the nucleus as efficiently as (WT)STAT3-FP, rather than not being retained and exported back to cytoplasm. Given that (Δ N)STAT3-FP cannot form latent dimers prior to cytokine stimulation [52] and activated dimers are still mainly cytosolic even after nuclear export blocking, we conclude that LMB-induced nuclear accumulation in cells stably expressing (Δ N)STAT3-FP is achieved predominantly through latent monomers.

Furthermore, since activated dimers of (Δ N)STAT3-FP are unable to localize in the nucleus upon cytokine treatment despite increased and prolonged tyrosine 705 phosphorylation, but latent (Δ N)STAT3-FP monomers still can accumulate upon blocking of CRM1-mediated export, our data indicates that cytokine-induced active nuclear import of STAT3 is different from basal nucleocytoplasmic shuttling. The same has been shown for STAT1 [224]. Both unphosphorylated STAT1 and STAT3 have been shown to enter the nucleus in the absence of cytosolic proteins, such as importins, whereas tyrosine-phosphorylated STAT1 dimers required both metabolic energy and added cytosol for nuclear import [218].

Although unphosphorylated STATs have been shown to regulate expression of specific target genes [30, 131], the exact purpose and functional connection between

preformed dimer formation and constitutive nucleocytoplasmic shuttling of STAT proteins remains unclear. We have previously published that although NTD deletion leads to complete absence of latent STAT3 dimers, it does not impede basal nuclear import, indicating that preformed dimers are not required for nucleocytoplasmic shuttling of STAT3 [52]. Also, both (Δ N)STAT3-FP and (L78R)STAT3-FP mutants that exist as pure monomers in the latent state show similar uniform distribution across nucleus and cytoplasm in live-cell imaging experiments prior to stimulation compared to predominantly cytoplasmic localization of (WT)STAT3-FP [52, 53, Fig. 3.3A]. Based on the observations that (Δ N)STAT3-FP with inhibited latent dimerization shuttles faster [52] and accumulates in the nuclei of resting cells in response to LMB more rapidly than (WT)STAT3-FP, as well as parallel cytoplasmic trapping of activated (Δ N)STAT3-FP dimers despite nuclear accumulation of (Δ N)STAT3-FP monomers upon CRM1-mediated nuclear export inhibition (Fig. 3.12A and B), we propose that the nuclear fraction of unphosphorylated STAT3 in resting cells consists predominantly of monomers and not preformed dimers.

Confocal live-cell imaging showed that (WT)STAT3-FP and (Δ N)STAT3-FP similarly accumulated in the nuclei of unstimulated stably transfected MEF cells upon LMB treatment (Fig. 4A), confirming the notion, that basal nuclear import does not require the N-terminal domain. Afterwards, we wanted to analyze whether disruption of previously reported putative NLS [225] or NES [48] of STAT3, lack of specific DNA-binding, mutation of critical lysine residue 685 or C-terminal deletion has any influence on basal nuclear import of STAT3. Confocal live-cell imaging revealed that previously identified putative NLS and NES sequences of STAT3, intact acetylation of lysine 685, specific GAS-recognition and TAD domain of STAT3 are not required for basal nuclear accumulation of latent STAT3 in resting cells upon CRM1-mediated nuclear export inhibition (Fig. 3.13A).

As a final point, we decided to assess possible roles for SH2 domains in basal nuclear transport using fluorescent fusion protein of STAT3 with a non-functional SH2 domain [226] (Fig. 3.13B). (R609Q)STAT3-FP failed to accumulate in the nucleus after IL-6 treatment but localized in the nucleus after 4 hours of blocking CRM1-mediated nuclear export, showing that a functional SH2 domain is also generally dispensable for constitutive nuclear shuttling of STAT3. Our findings are in

agreement with previously published observations that N- and C-terminal domains are not essential for constitutive nucleocytoplasmic shuttling of STAT1, STAT3 and STAT5 [218] and that inactivating mutations in the SH2 domain do not alter the subcellular distribution of the mutated fusion proteins in resting cells compared to wild-type [50]. Moreover, constitutive nuclear import of unphosphorylated Stat1 has been shown to be mediated by direct interactions with nucleoporin 153 and nucleoporin 214 of the nuclear pore and STAT3 competed for the same NPC-binding sites with STAT1 and importin- β , suggesting similarity between STAT1 and STAT3 latent nuclear import mechanisms [218].

6. STAT3 downregulates gp130/STAT1 signaling via target gene expression

STAT1 and STAT3 despite their very similar structures very often have opposing effects on cellular processes. While STAT3 exerts anti-inflammatory functions, stimulates cell survival and proliferation downstream of several cytokine or growth factor receptors, STAT1 inhibits proliferation and promotes innate and adaptive immune responses. In addition, both transcription factors appear to play opposite roles in tumorigenesis, STAT3 being beneficial for tumor progression and immune evasion, while STAT1 is often described as a tumor suppressor. Apart from often reported functional antagonism, STAT1 and STAT3 activation are reciprocally regulated and imbalances in their expression or activation levels may re-direct cytokine or growth factor signals from proliferative to apoptotic, or from inflammatory to anti-inflammatory [88-90]. In the second part of this thesis, we have investigated STAT3-mediated downregulation of atypical IL-6-induced STAT1 activation and analysed the role of the NTD and transcriptional activity of STAT3 in this process.

In the absence of STAT1, STAT3 phosphorylation on tyrosine 705 is enhanced following IFN γ treatment, which can replace STAT1 in STAT1-deficient MEF cells to induce GAS-dependent gene transcription [94]. Similarly, in STAT3 null MEFs, STAT1 expression and activation are increased following IL-6 stimulation and this re-directs IL-6 signaling to an IFN γ -like response [100]. To verify these observations, we stimulated WT, STAT3 $-/-$ and STAT1 $-/-$ MEF cell lines with IL-6 and IFN γ for different time points and analyzed endogenous STAT activation and nuclear

translocation. Indeed, the absence of STAT3 led to abnormal Y701 phosphorylation of STAT1 after IL-6 stimulation without significantly affecting IFN γ -induced STAT1 activation (Fig. 3.14A). This mimics increased STAT1 activation observed in MEF Δ/Δ (Δ N)STAT3-FP and (mSNICQ)STAT3-FP cells (Fig. 3.4A). Furthermore, IL-6-induced atypical STAT1 activation resulted in nuclear accumulation in STAT3 null MEFs (Fig. 3.15B). In contrast, despite slightly increased tyrosine 705 phosphorylation of STAT3 in STAT1-deficient cells (Fig. 3.14B) there was no nuclear translocation of endogenous STAT3 observed in STAT1 $-/-$ MEF upon IFN γ stimulation (Fig. 3.15C).

Abnormal activation and expression of STATs in STAT-deficient cells has been previously described in different systems. In line with our observations, in MEFs neither STAT1 nor Erk1/2 activation were affected downstream of IFN γ signaling by STAT3 absence, whereas upon IL-6 type cytokine (OSM) stimulation STAT1 activation is much stronger and more prolonged in STAT3 $-/-$ MEFs [199]. Furthermore, the activation of STAT1 in human neoplastic T lymphocytes after IFN γ stimulation was generally unaffected by STAT3 silencing, while IL-6 stimulation of the same cells correlated with prolonged STAT1 activation and the induction of major histocompatibility complex (MHC) class I expression [227].

Depletion of STAT1 resulted in an enhanced early STAT3 activation upon IL-6 stimulation (Fig. 3.14A). Constitutively active STAT1C mutant has been shown to attenuate IL-6-induced STAT3 activation and the expression of pro-apoptotic genes [102], whereas gain-of-function STAT1 mutations impair STAT3 activity in patients with chronic mucocutaneous candidiasis [228], suggesting that the presence of STAT1 might downregulate IL-6/STAT3 signaling in a similar manner to STAT3, which has been shown to negatively regulate STAT1-dependent gene activation [101, 229]. However, our preliminary data showed that *socs3* upregulation is not further increased in STAT1 $-/-$ MEFs upon IL-6 treatment (data not shown).

On the other hand, the absence of nuclear accumulation of endogenous STAT3 in STAT1 $-/-$ cells upon IFN γ treatment does not support the previously reported ability of STAT3 to replace STAT1 in inducing GAS-dependent gene expression [94]. Of note, although strong and sustained IFN γ -induced STAT3 activation in STAT1 $-/-$ fibroblasts has been reported by several groups [94, 198], one group could not

reproduce these results with the cells of the same origin [230]. Moreover, in the human fibrosarcoma cell line U3A STAT1 deficiency did not affect STAT3 Y705 phosphorylation and nuclear translocation upon OSM stimulation [97], but IFN γ treatment did not activate STAT3 at all in the same cells [198], suggesting that IFN γ -induced STAT3 activation is cell-type specific. STAT1 and STAT3 depletion effects on one another found in the literature are summarized in tables 4.1 and 4.2.

Tab. 4.1: STAT3 depletion consequences on STAT1 signaling. BM – bone marrow, CRC – colorectal carcinoma

Cell type	Depletion	Effect on STAT1	Ref.
Murine embryonic fibroblasts	Genetic knockout	IL-6 induced increased and prolonged Y701 phosphorylation and increased (?) enhanced type I IFN-gene expression	100, 101, 199
Murine BM-derived hematopoietic cells	Genetic knockout	Increased Y701 phosphorylation and total STAT1 expression	231-233
Murine peritoneal macrophages	Genetic knockout	Constitutive Y701 phosphorylation and increased STAT1 expression	234
Murine intestinal epithelial cells	Genetic knockout	Increased STAT1 expression	235
Murine CD4 ⁺ T cells	STAT3 mRNA destabilization	Increased and prolonged Y701 phosphorylation upon Th17 differentiation	236
Human lung MRC-5	siRNA knockdown	Increased (?) IL-6 induced STAT1 gene expression	229
Human monocytic cell line THP-1	shRNA knockdown	Enhanced type I IFN-gene expression	227
Human T cells	shRNA knockdown	IL-6 induced increased and prolonged Y701 phosphorylation and increased (?) STAT1 gene expression;	237
Human CRC HT-29	shRNA knockdown	IL-6 induced increased Y701 phosphorylation, increased STAT1 expression	238
Human CRC LS174T,	shRNA knockdown	Increased STAT1 expression	238
Human CRC SW620, HCT116	shRNA knockdown	Reduced STAT1 expression	238

Tab. 4.2: STAT1 depletion consequences on STAT3 signaling.

Cell type	Depletion	Effect on STAT3	Ref.
Murine embryonic fibroblasts	Genetic knockout	IFN γ -induced increased and prolonged Y705 phosphorylation, increased STAT3 and STAT1 gene expression;	94, 198
Murine lung type II epithelial cells	Genetic knockout	Increased and prolonged Y705 phosphorylation and total STAT3 expression	239
Murine plasmacytoid dendritic cells	Genetic knockout	Increased STAT3 expression	240
Murine macrophages	Genetic knockout	IFN β - and IFN γ -induced prolonged Y705 phosphorylation	241
Murine naive CD4 $^{+}$ T cells	Genetic knockout	IL-6 + IL-27-induced increased Y705 phosphorylation	242
Human fibrosarcoma U3A cell line	Chemical mutagenesis	No observed effect on STAT3 signaling	97, 198
Human isolated CD4 $^{+}$ T cells	Autosomal deficiency	IL-21-induced increased Y705 phosphorylation and STAT1 gene expression;	243

Based on literature data and our own observations, we conclude that reciprocal crossregulation of IFN γ /STAT1 and IL-6/STAT3 signaling pathways is cell-type specific and asymmetric in MEFs. Asymmetric functions for STAT1 and STAT3 have also been demonstrated in T cells, where STAT3 is responsible for the overall transcriptional output driven by both IL-6 and IL-27 cytokines, whereas STAT1 regulates the specific cytokine signatures and cannot compensate for STAT3 absence [244].

The ratio of phosphorylated STAT1 to phosphorylated STAT3 in naive CD4 $^{+}$ cells determines whether the combination of IL-6 and IL-27 inhibits or induces Th17 cell differentiation [242], whereas gain-of-function STAT1 mutations recapitulated the impact of dominant-negative STAT3 mutations on Tfh and Th17 cells, confirming a putative inhibitory effect of hypermorphic STAT1 over STAT3 [245]. Moreover, total

ratio of STAT1 to STAT3 expression is proposed as a key determinant of colorectal tumor progression [237], while lower *stat1* and *stat3* transcript levels correlated with a particularly high survival rate in patients with acute lymphoid leukemia [246]. Finally, human cytomegalovirus has been recently shown to re-direct gp130 signaling from an IL-6 type response to an IFN γ -like response via viral IE1 protein [236], which mimics the phenotype observed in STAT3-deficient MEFs [100]. Thus, understanding the exact mechanisms of mutual crossregulation between STAT1 and STAT3 in different cell types and tissues will foster therapeutic progress in treating several pathological conditions.

Using STAT-deficient cells we have demonstrated, that STAT3 intracellular presence negatively regulates STAT1 activation upon IL-6 stimulation. Although the exact mechanism of STAT3-mediated downregulation of STAT1 signaling has not been clarified to date, three non-mutually exclusive explanations have been proposed. First, the absence of STAT3 may release competition for the common receptor docking sites, favoring recruitment and activation of STAT1 by gp130 upon IL-6 treatment. Second, in STAT3 $-/-$ cells STAT3 does not sequester STAT1 into heterodimers, thereby increasing the efficacy or strength of STAT homodimer signals [97, 229]. Third, specific STAT3 target gene(s) such as *socs3* are involved in differential activation of STAT3 and STAT1 downstream of gp130 [176].

In line with our previous observations, increase in total intracellular STAT3 levels was accompanied with further decrease in STAT1 Y701 phosphorylation following IL-6, but not IFN γ treatment (Fig. 3.16). Furthermore, N-terminal deletion and transcriptionally dead R609Q mutants could not reproduce this effect, suggesting that STAT3 transcriptional activity is involved in this process. Interestingly, NTD of STAT3 alone was sufficient for STAT3-mediated downregulation of STAT1-dependent genes [101]. Given that STAT1 activation after IL-6 treatment was markedly increased in cells stably transfected with (Δ N)STAT3-FP constructs (Fig. 3.4A), it may be possible that the NTD of STAT3 is responsible for negative regulation of STAT1 activity upon IL-6 activation.

To test this hypothesis, we analyzed IL-6-induced STAT1 activation in STAT3 $-/-$ MEFs stably transfected with (WT)STAT3-FP and found that stable reconstitution of

full-length STAT3 could reverse the effect, confirming the role of wild-type STAT3 in this regulation mechanism (Fig. 3.17A). Afterwards, the activation of endogenous STAT1 upon both IL-6 and IFN γ treatment was compared across WT, STAT3 $-/-$ and STAT3 $-/-$ MEFs stably expressing (WT)STAT3-FP or (Δ N)STAT3-FP. The (L78R)STAT3-FP construct only lacks preformed dimer formation in latent state with all other STAT3 properties intact and the isolated NTD of STAT3 has been previously shown by our group to have an effect on STAT3-regulated gene transcription [53]. In order to analyze whether STAT3 preformed dimer absence or isolated STAT3 NTD presence have an effect on IL-6 induced STAT1 activation, MEF STAT3 $-/-$ stable transfected with (L78R)STAT3-FP and (NTD)STAT3-FP constructs were added to the experiment. As expected, STAT3-deficient and (Δ N)STAT3-FP showed similar upregulation of STAT1 phosphorylation at tyrosine 701 upon IL-6 stimulation, while both (WT)STAT3-FP and (L78R)STAT3-FP could rescue abnormal STAT1 signaling, indicating that lack of preformed dimer formation does not prevent STAT3 to regulate STAT1 activation (Fig. 3.17B). Furthermore, stable expression of the isolated STAT3 NTD in STAT3 $-/-$ could not rescue atypical STAT1 activation in IL-6-treated cells. Given that in cells stably expressing (Δ N)STAT3-FP and (NTD)STAT3-FP STAT1 demonstrated strong nuclear accumulation after IL-6 treatment (Fig. 3.18) in the same manner as in STAT3 null MEFs, we conclude that N-terminal deletion mutant could not regulate STAT1 signaling, but this effect was not due to absence of the NTD itself.

In summary, the mechanisms that enable STAT3 to regulate STAT1 activation upon gp130 signaling involve its transcriptional activity. Since NTD alone could not reverse the abnormal STAT1 activation, we conclude that (Δ N)STAT3-FP cannot regulate STAT1 due to its defect in target gene expression (Fig. 3.4A) (such as *socs3*, as reported previously [176]) and not specific NTD properties. SOCS3 deficiency led to increased activation of STAT1 and STAT3 after IL-6 treatment but normal activation of STAT1 after stimulation with IFN γ . Conversely, IL-6-induced STAT1 and STAT3 activation is normal in SOCS1 deficient cells, whereas STAT1 activation induced by IFN γ is prolonged, indicating SOCS protein family involvement in reciprocal regulation of IL-6 and IFN γ signaling [56]. In agreement with these data, cells expressing the DNA-binding deficient (mSNICQ)STAT3 mutant with intact NTD but

incapable of proper socs3 induction also showed enhanced STAT1 phosphorylation after IL-6 treatment (Fig. 3.4A).

Given that STAT1 abnormal activation is still present despite proper (Δ N)STAT3-FP activation at the receptor, competition for receptor binding could not account for STAT3-mediated downregulation of gp130-mediated STAT1 signaling. In line with these observations, despite the ability of constitutively active gp130 to activate both STAT1 and STAT3 without ligand stimulation [247], abnormal activation of STAT1 via mutated gp130 was not sufficient for the induction of STAT1-dependent genes in endothelial cells [99], in contrast to IFN γ -like response observed in STAT3-deficient MEFs [100].

Of note, abnormally activated STAT1 in (Δ N)STAT3-FP expressing cells existed predominantly as a (Δ N)STAT3-FP/heterodimer (Fig.3.4A), while in STAT3 $-/-$ MEFs only STAT1/STAT1 homodimers are formed. STAT heterodimers have been described to have functions distinct from homodimers [248], however in mice expressing exclusively dominant negative STAT3 β isoform most of the activated STAT1 molecules formed heterodimers with STAT3 β and induction of IFN- γ targets correlated with STAT-deficient MEFs [176]. Potentially different gene expression profiles between STAT3 $-/-$ and (Δ N)STAT3-FP expressing cells require further investigation.

7. Canonical signaling of STAT3 and NF- κ B are independent of each other but NF- κ B supports expression and activation of STAT1 and STAT3

STAT3 and NF- κ B are pleiotropic transcription factors that are involved in various physiological processes, such as development, differentiation, immunity and metabolism. Both proteins are often constitutively activated in numerous cancers due to upregulation of upstream signaling pathways in response to autocrine and paracrine signals present within the tumor microenvironment. STAT3 and NF- κ B activation pathways differ in their activation mechanisms. STAT3 activation is characterized by an activating phosphorylation followed by dimerization, while canonical NF- κ B signaling involves proteasome-mediated degradation of inhibitory proteins resulting in the release of DNA-binding subunits. However, once activated,

both factors control the expression of several groups of genes, including anti-apoptotic, proliferative and immune response genes. Some of these genes overlap and are activated via transcriptional cooperation between the two factors. Other forms of crosstalk between NF- κ B and STAT3, such as physical interaction, cooperation at gene promoters or negative regulation of each other, have been described [60]. In the next part of this thesis, we show that STAT3 has no direct influence on canonical TNF α -induced NF- κ B signaling, while the p65 subunit of NF- κ B positively affects STAT3 and STAT1 signaling.

We first defined optimal sample preparation conditions for simultaneous visualization of both p65 and STAT3 in cultured cells via immunofluorescence using combined paraformaldehyde/methanol treatment. The choice of the processing method is most important for appearance of the immunostainings and the interpretation of the results may vary depending on the protocol used [249]. In our hands, NF- κ B p65 subunit nuclear accumulation upon TNF α treatment is clearly detectable after paraformaldehyde fixation but hardly visible after methanol fixation (Fig. 3.19A). Our findings are in agreement with previously published data that methanol treatment results in a perinuclear localization of p65 in human dendritic cells upon stimulation [177]. Paraformaldehyde preparation also preserved the intracellular and membrane structures better than methanol and resulted in a more accurate localization of Fas and FasL proteins in liver cells [250].

In turn, several reports describing the visualization of STAT3 nuclear translocation by microscopy have used different methods of fixation [52, 81, 157]. Our data demonstrates that paraformaldehyde fixation leads to a predominant nuclear localization of endogenous STAT3 both in resting and IL-6-stimulated cells, while methanol fixation and combined protocols lead to a more uniform distribution of STAT3 in unstimulated cells and a significant increase in nuclear STAT3 after cytokine treatment (Fig. 3.19B). These observations could explain the previously reported prominent nuclear localization of endogenous STAT3 in both resting and activated states in different cell lines [157], which is contradictory to live-cell imaging of ectopically expressed STAT3 fluorescent fusion proteins showing predominant cytoplasmic localization of STAT3 in resting cells and rapid nuclear accumulation upon stimulation [52, 53]. Paraformaldehyde fixation has been shown previously to

cause misinterpretation of the subcellular localization of plant proteins causing dissociation of these proteins from metaphase chromosomes [251]. While paraformaldehyde preserves structural elements at the expense of reduced antigen accessibility, fixation with methanol can disturb structural integrity of the cells [252]. We found a combined paraformaldehyde/methanol fixation protocol to be optimal for parallel p65 and STAT3 visualization in cultured cells by immunofluorescence (Fig. 3.19C). In line with our observations, combined treatment has been reported previously to be more useful for proper visualization of transmembrane and soluble cytoplasmic proteins than paraformaldehyde or methanol fixation alone [253, 254].

To assess the role of STAT3 in canonical NF- κ B signaling, we compared TNF α -induced pathway activation in wild-type and STAT3^{-/-} cells. Our results demonstrate that the absence of STAT3 has no significant effect on total p65 levels, p65 phosphorylation on serine 536, I κ B α phosphorylation and degradation, as well as subsequent p65 nuclear translocation and *ikba* gene induction (Fig. 3.20 A and B, 3.21A and B). At least five kinases converge on p65 phosphorylation at serine 536 [255], which is one of the most extensively studied p65 posttranslational modifications [104], suggesting that all molecular steps upstream of p65 S536 phosphorylation remained unaffected upon STAT3 deletion.

In contrast to previously published data [136], the absence of STAT3 had no detrimental effects on TNF α -induced nuclear translocation of NF- κ B p65 and target gene expression, as demonstrated by our optimized immunostaining protocol and subcellular fractionation experiments (Fig. 3.21A, B). I κ B α is a classical NF- κ B target gene, which is linked with p65 in a regulatory feedback loop [256]. Deletion of p65, but not STAT3, had detrimental effects on *ikba* expression and this effect can be rescued by p65 reconstitution, confirming the dependence of I κ B α expression on the NF- κ B p65 subunit. Since the regulation of several other target genes has been reported to require both p65 and STAT3 DNA association [132-134], genes other than *ikba* may have been influenced by STAT3 deletion. However, proper *ikba* upregulation indicates that canonical NF- κ B signaling is intact in STAT3^{-/-} cells. Furthermore, overexpression of STAT3 also had no effect on p65 activation and nuclear translocation in HeLa cells (Fig. 3.25).

These data indicate that STAT3 has no direct influence on canonical NF- κ B signaling upon TNF α stimulation, suggesting that previously published observations of STAT3 silencing being beneficial for NF- κ B activation in cancer or primary cells [137-139] are not universal, but rather cell-type or stimulus specific, along with the impact of oncogenesis or the extracellular microenvironment.

Knockout of endogenous p65 in MEF led to downregulation of total STAT3 and STAT1 levels and this effect was rescued in p65-YFP-complemented p65^{-/-} cells (Fig. 3.22B) confirming the involvement of p65 in controlling total STAT3 and STAT1 levels [257, 258]. Interestingly, total STAT5 levels were unaffected upon deletion and subsequent reconstitution of p65-YFP. Furthermore, several serine to alanine mutations affecting p65 transcriptional activity were tested in order to further elucidate critical residues in p65-mediated regulation of STAT3 and STAT1 expression (Fig. 3.23). Our results revealed, that serine 276 substitution to alanine in p65 led to a similar decrease in STAT1 and partially STAT3 amounts observed in p65-deficient cells, while S311A, S468A and S536A mutants demonstrated only a minor decrease. In contrast to classical single tyrosine phosphorylation of STAT proteins, several serine residues of the p65 subunit are phosphorylated and phosphorylation of these residues affects the activity of NF- κ B and its interaction with co-regulators differently [259]. Phosphorylation of p65 at serine 276 regulates a subset of NF- κ B target genes with specific *cis*-acting elements in their promoters, such as those encoding IL-6, IL-8, Gro- β , and ICAM-1 [259], as well as allowing for binding of CREB-binding protein (CBP)/p300 [121]. In contrast phosphorylation of serine 536 favors binding of TATA-binding protein-associated factor II31, a component of TFIID [255]. Our data indicate, that expression of STAT1 and STAT3 depends on p65 activity and S276A mutation of p65 had the most detrimental effect on total levels of STAT1 and to a lesser extent STAT3 compared to wild-type p65.

Despite lower total amounts of protein, cytokine-induced nuclear import of STAT3 remained intact in p65^{-/-} cells (Fig. 3.24 A, B) suggesting that IL-6 induced signaling itself was less affected. Interestingly, reconstitution of p65^{-/-} cells with p65-YFP led to an increased *socs3* upregulation in response to IL-6 (Fig. 3.22C). Several reports suggest a positive association between NF- κ B transcriptional activity and STAT3

activation. Direct activation of NF- κ B led to increased STAT3 expression in cardiomyocytes, which could be abrogated by a NF- κ B inhibitor [260]. In the absence of tumour suppressor p53, both NF- κ B and STAT3 were constitutively activated and depleting p65 suppressed constitutive activation of STAT3 [257]. Similarly, suppression of NF- κ B activity by p65R siRNA in Sirt1-null MEF reduced mitochondrial function and the expression of STAT3 [258]. In turn, in human hypopharyngeal epithelium cells acidic-bile salts induced a substantial increase in total p65 amounts, which was subsequently correlated with upregulation of STAT3 [261]. Moreover, in our hands inducible overexpression of p65-dsRed in HeLa cells led to an increased STAT3 activation and nuclear accumulation along with abnormal STAT1 nuclear presence (Fig. 3.26A). Therefore we conclude that p65 supports expression and activation of STAT3 and STAT1.

STAT3 and STAT1 have been demonstrated to separately associate with NF- κ B in the cytoplasm resulting in various effects [113, 262]. While both NF- κ B and STAT3 signaling pathways, but not MAPKs, were dysregulated by interferons in STAT1-null macrophages, overactivation of STAT3 was the key mechanism in downregulation of NF- κ B signaling [241]. Additionally, deficiency of one of the major NF- κ B activating receptors TLR4 led to enhanced STAT1-driven Th1 differentiation and suppressed STAT3-driven Th17 expansion [263], whereas IL-27, a crucial cytokine for bridging innate and adaptive immunity, has been shown to rely on all three transcription factors for its proper signaling [264]. Taking this into account, a triple collaboration of STAT1, STAT3 and NF- κ B in immunological and pathological processes is worth exploring further. Taken together, our results suggest that TNF α -induced canonical NF- κ B signaling does not rely on STAT3, while expression of the NF- κ B p65 subunit positively correlate with total STAT3 and STAT1 levels and augments their activation.

Physical interaction between the p65 and STAT3 has also been described, both in cytoplasm [113, 128] and nucleus [133, 134, 180, 265-269]. Importantly, STAT3 is known to directly bind to the transactivation domain of NF- κ B through its DNA-binding domain [134, 269]. Given that we have successfully used a GFP antibody in co-immunoprecipitation experiments with MEF Δ/Δ STAT3-FP cells to study STAT3/STAT1 heterodimer formation (Fig. 3.4A), we decided to analyze physical association between STAT3 and p65. Both NF- κ B activation alone and combined

activation of NF- κ B and STAT3 have been reported to result in STAT3/p65 complex formation [128, 180], therefore the cells stably expressing (WT)STAT3-FP were treated with IL-6, TNF α and a combination of both cytokines (Fig. 3.27).

Co-immunoprecipitation revealed STAT3/p65 physical binding upon TNF α treatment and prolonged IL-6 + TNF α stimulation, but not IL-6 treatment alone. This is in agreement with previously published observations [128, 180]. However, compared to STAT3/STAT1 binding, this association was much weaker and more transient. Since our data from STAT3 $-/-$ MEFs indicate that STAT3 is dispensable for canonical NF- κ B signaling, this interaction might be relevant only for induction of some specific genes that require complex formation of both STAT3 and p65, *ikba* being not one of them.

8. STAT3-YFP knock-in mice have been successfully generated

In the past, fluorescent fusion proteins of STAT3 have been successfully used by our group to study subcellular localization and intracellular dynamics of STAT3 [49, 52, 53, 58]. STAT3-YFP nuclear translocation upon activation with IL-6 can be observed in living cells using confocal microscopy. Nuclear accumulation peaks after 20 minutes and thereafter decreases within 120 minutes, demonstrating STAT3 feedback inhibition via SOCS3 [49]. In order to utilize this tool *in vivo*, we have created in collaboration with Valeria Poli group a STAT3-YFP knock-in mice, expressing fluorescently-labeled STAT3 α -isoform under control of the endogenous STAT3 promoter. In the last part of this thesis, we genotyped and characterized STAT3-YFP knock-in mice in order to verify correct STAT3-YFP expression and to validate the transgenic murine model for further research.

The fluorescent tag insertion did not influence the biological activity of STAT3-YFP, because both heterozygous and homozygous mice were obtained at a Mendelian ratio and seemed to be normal and fertile (Fig. 3.28). We did not observe any differences with respect to their wild-type littermates in many biological parameters, such as life expectancy and body weight. The insertion of YFP at the end of the *stat3* gene leads to sole presence of the STAT3 α isoform without expression of the truncated STAT3 β isoform that is normally generated through alternative splicing.

Although mice expressing exclusively STAT3 α isoform displayed no significant differences compared to wild-type concerning fertility and survival [176], these STAT3 β null mice exhibited reduced recovery from endotoxic shock and hyperresponsiveness of endotoxin-inducible genes in the liver [270]. Moreover, peritoneal macrophages from STAT3 β -deficient mice showed impaired IL-10 production [176], thus indicating an important role for STAT3 β in STAT3-mediated anti-inflammatory responses. These observations should be kept in mind during future experiments with this *in-vivo* model.

To analyze the expression of STAT3-YFP, we prepared whole cell lysates from spleen and analyzed them by immunoblotting. Endogenous STAT3 was the only band detected in wild-type mice, but two bands corresponding to both native STAT3 and STAT3-YFP transgene have been observed in heterozygous animals (Fig. 3.29B). Furthermore, homozygous mice showed only STAT3-YFP signals, as expected. Confocal microscopy of splenic cells and freshly prepared primary hepatocytes confirmed the presence of STAT3-YFP and signal intensity correlates with the genotype (Fig. 3.29A and C). In summary, our characterization of the STAT3-YFP knock-in murine model verified the proper expression of functional STAT3-YFP without any observed adverse effects, which makes STAT3-YFP knock-in mice a very promising tool to study STAT3 dynamics *in vivo*.

V. Summary and Outlook

Signal transducer and activator of transcription 3 (STAT3) is a pleiotropic transcription factor that is activated by a variety of cytokines and is involved in many physiological processes including embryonic development, haematopoiesis and immunity. Activation of STAT3, which involves its phosphorylation at Y705 and nuclear accumulation, has been observed in several pathophysiological conditions such as cancer, chronic inflammation and autoimmunity. Besides canonical activation at the receptor by JAK kinases and subsequent dimerization and nuclear translocation, STAT3 forms latent dimers and constitutively shuttles in and out of the nucleus or unstimulated cells. Moreover, functional crosstalks with other transcription factors, such as STAT1 and NF- κ B, have been studied in the context of immune response and cancer progression. During this doctoral thesis we investigated non-canonical aspects of STAT3 signaling and analysed its interplay with STAT1 and NF- κ B signaling pathways. For this purpose, we used STAT3-deficient MEFs stably transfected with several fluorescently labeled STAT3-FP constructs. In our hands, stably expressing wild-type STAT3-FP reproduces endogenous STAT3 signaling including phosphorylation of tyrosine 705, nuclear translocation, specific GAS-element binding and induction of the target gene *socs3*.

The first part of this work elucidates the functions of the N-terminal domain and GAS-site recognition in STAT3 nuclear trafficking, as well as functional difference between cytokine-induced and latent nucleocytoplasmic shuttling of STAT3. Our results show that GAS-element-specific DNA recognition is dispensable for nuclear accumulation of STAT3, because (mSNICQ)STAT3-FP still underwent nuclear translocation upon IL-6 treatment despite its inability to bind a radioactively labelled DNA probe in EMSA assay. Interestingly, although (mSNICQ)STAT3-FP still binds STAT1 in IL-6 stimulated cells, phosphorylated (mSNICQ)STAT3-FP/STAT1 heterodimers are also not able to bind specific GAS sequence, indicating that both monomeric partners in STAT3/STAT1 heterodimers must be able to recognize and associate with specific GAS-sequences in order to exert their functions. The functional relevance and mechanistic features of STAT heterodimers *in vivo* are still not fully understood [248],

therefore further analysis of DNA recognition by STAT heterodimers could help to understand the molecular basis for STAT heterodimer formation and function *in vivo*, revealing novel therapeutic approaches to treat dysfunctional STAT signaling.

In contrast to DNA-recognition mutant, the STAT3 N-terminal domain deletion mutant remains in the cytoplasm in the form of activated dimers capable of GAS-element binding after IL-6 stimulation. We conclude that the observed prolonged phosphorylation and reduced expression of STAT3-regulated genes after deletion of the NTD is a result of defective nuclear accumulation, which cannot be rescued via CRM1-mediated nuclear export inhibition. Based on our observations of (Δ N)STAT3-FP and (mSNICQ)STAT3-FP signaling we determined that nuclear accumulation and GAS-recognition during cytokine-induced STAT3 signaling are two separate processes that does not depend on each other. Nevertheless, both mechanisms are required for full STAT3 target expression, as demonstrated by defective early *socs3* induction by these mutants. Of note, at later time points both mutants showed upregulation of *socs3*, which can be attributed either to delayed action of mutated STAT3 constructs or to possible STAT3 replacing mechanism, such as STAT1 or other unidentified proteins. Given that MEFA/ Δ proliferate and thrive in culture, it is worthwhile to define which mechanisms compensate for STAT3 absence. Most prominent candidates are STAT1 and MAPK pathways, which are continuously activated upon IL-6 type cytokine treatment as described previously [199].

The exact mechanisms impeding (Δ N)STAT3-FP nuclear translocation upon cytokine treatment remains to be elucidated. In contrast to STAT1, STAT3 NTD is not required for binding to various importin- α isoforms (α 3, α 5 and α 7), as demonstrated by our *in-vitro* pulldown experiments. Moreover, the importin- α 5 mutant Y476G that does not bind STAT1 is still able to bind endogenous STAT3, indicating that there are molecular and mechanistic differences between STAT1 and STAT3 active nuclear import. Although *in-vitro* pulldown experiments with bacterially expressed proteins have been widely used to study nuclear trafficking of STATs [155, 157-160, 175], the expression of recombinant proteins might produce unwanted biological artifacts or lead to incorrect conformation of desired proteins. Furthermore, the relatively large size of the GST-tag attached to importin molecules may interfere with the activity or

impose dimerization of recombinant proteins [271, 272]. Thus, other systems for studying intracellular STAT-importin interactions must be employed.

Lack of cytokine-induced nuclear accumulation or defective dephosphorylation of (Δ N)STAT3-FP observed in this work can be attributed to abolished protein-protein interaction due to either direct absence of the NTD or an indirect allosteric effect on integrity of the STAT3 molecule. Data from the literature showed many STAT3 interacting partners as potential candidates important for both nuclear translocation and subsequent deactivation of STAT3. First, several proteins apart from classical receptor/JAK complexes have been identified to enhance and facilitate STAT3 phosphorylation and nuclear translocation. Most prominent examples are Src [94, 273-275], p300 [81, 171], c-Jun/JunB [276], SMAD1/4 [277], Rac1 via MgcRacGap [219], STAP-2 [278], ZIPK [279], Y14 [280], Brk [281] and ARL3 [282]. On the other hand, other than SOCS3 proteins are tightly involved in STAT3 negative regulation by promoting dephosphorylation and STAT3 degradation via direct interactions. These include several phosphatases, such as TC-PTP (PTPN2) [206], DUSP2 [210], Meg2 (PTPN9) [283] and SHP2 (PTPN11) [284], as well as other proteins, including HDAC1 [285], PIAS3 [286], GdX [208], SIPAR [209], ARHI [220], PDLIM2 [287], cyclin D [288], Daxx [289], KAP-1 [290], ECHS1 [291], Tip60 [292], HIC1 [293], Sin3A [294], PML [295], MyOD [296], p21WAF1 [297], STATIP1 [298], LMW-DSP2 [299], GATA-1 and GATA-2 [300]. Out of these, DUSP2, HDAC1, ECHS1, ARHI and PDLIM2 interacted with the NTD of STAT3. Further analysis of consequences of NTD deletion on association with different activating and suppressing factors can reveal potential mechanism required for STAT3 active nuclear import or dephosphorylation. Recent advances in STAT3 interactome analysis identified 136 proteins as putative interaction partners of STAT3 in Hek293 cells [301], yielding new potential candidates for further research.

Inhibition of CRM1-mediated nuclear export by LMB results in nuclear accumulation of latent STAT3 and prolonged nuclear presence of STAT3 after cytokine-induced nuclear translocation. Nevertheless, dephosphorylation kinetics of both (WT)STAT3-FP and (Δ N)STAT3-FP remained unchanged upon LMB treatment in IL-6 treated cells. These results revealed that nuclear export is not required for STAT3 dephosphorylation after cytokine activation and main phosphatases involved in

STAT3 deactivation are localized in the nucleus. TC45 [206] and DUSP2 [210] nuclear phosphatases have been described previously as important STAT3 negative regulators.

Our data also showed that presence of functional SH2 or N-terminal domains, as well as preformed dimers and GAS-element-specific DNA recognition are all dispensable for constitutive nucleocytoplasmic shuttling of latent STAT3, supporting the idea that basal nuclear import of STAT3 employs different transport mechanisms than cytokine-induced active nuclear translocation similarly to STAT1 [224]. Studying the interactions of STAT3 with nucleoporins such as Nup153 and Nup214, previously reported to interact with STAT1 [218], may help to clarify the exact mechanism of latent nucleocytoplasmic shuttling for STAT3.

STAT3 null MEFs stably expressing mutated (Δ N)STAT3-FP and (mSNICQ)STAT3-FP constructs also demonstrated increased STAT1 activation upon IL-6 stimulation in comparison to (WT)STAT3-FP expressing cells. Previous reports demonstrated that in the absence of STAT1, STAT3 phosphorylation is enhanced following IFN γ treatment and that STAT3 activation can replace STAT1 in GAS-dependent gene induction [94]. Likewise, in the absence of STAT3, STAT-1 activation is increased following IL-6 stimulation and this leads to an IFN γ -like responses, suggesting mutual cross-regulation mechanisms [100]. In the second part of this work we demonstrate, that mutual regulation of STAT1 and STAT3 is not symmetric. While the absence of STAT3 led to enhanced phosphorylation and nuclear accumulation of endogenous STAT1, IFN γ stimulation of STAT1 null MEFs resulted only in a slight increase in STAT3 phosphorylation without subsequent nuclear translocation. The expression of target genes for both factors (for example *socs3*, *cfos* and *junB* as STAT3 targets and *irf1*, *gbp2*, *stat1* as STAT1-dependent genes) under these conditions will further clarify transcriptional activity for atypically activated STAT1 and STAT3.

In order to further clarify the exact mechanism by which STAT3 can downregulate non-canonical STAT1 activation upon IL-6 treatment, we used cell lines stably expressing wild-type and mutated STAT3-FP constructs. Our data reveal that stable restoration of wild-type STAT3-FP in STAT3-deficient MEFs rescued the abnormal STAT1 phosphorylation, while STAT3-FP overexpression further decreased IL-6-

induced activation of STAT1 in HeK293 cells. IFN γ -induced STAT1 activation was unaffected across all conditions. Furthermore, NTD deletion and transcriptionally defective STAT3 mutants (R609Q and mSNICQ) could not reproduce this effect, indicating that transcriptional activity and, possibly, unique functions of STAT3 NTD are responsible for modulating atypical STAT1 signaling. The comparison of several mutants stably expressed in STAT3-null MEFs showed that preformed dimer formation, competition for receptor docking sites and unique functions of the isolated STAT3 NTD are not involved in STAT3-mediated regulation of gp130/STAT1 signaling. It has been reported that in IL-6-treated cells, STAT1 dephosphorylation required *de novo* protein synthesis when STAT3 is present [176], while SOCS3 $^{-/-}$ macrophages and hepatocytes induce IFN γ -responsive genes in response to IL-6, similarly to IFN γ -like response observed in STAT3 $^{-/-}$ MEFs [56, 57, 302]. Conclusively, our data together with previously published results indicate that STAT3 target gene expression, such as *socs3*, is negatively regulating IL-6-induced STAT1 activation under normal conditions. Hence, stable transfection of (Δ N)STAT3-FP and (mSNICQ)STAT3-FP mutants that are defective in *socs3* gene expression did not rescue abnormal STAT1 activation in STAT3-null cells as (WT)STAT3-FP did.

NF- κ B and STAT3 are essential transcription factors in immunity and act at the interface of the transition from chronic inflammation to cancer. Different functional crosstalks between NF- κ B and STAT3 have been recently described arguing for a direct interaction of both proteins. In the third part of this work, we systematically analysed canonical NF- κ B p65 and STAT3 signaling in p65 $^{-/-}$ and STAT3 $^{-/-}$ cells. Our data demonstrated that the fixation procedure has a strong influence on the appearance of the subcellular distribution of STAT3 and NF- κ B subunit p65 having important implications for the interpretation of published data. The consistent parallel analysis of endogenous p65 and STAT3 subcellular distribution by immunofluorescence required an optimized fixation protocol with 3.7% PFA treatment followed by short ice-cold methanol incubation.

Using p65 $^{-/-}$ or STAT3 $^{-/-}$ MEFs, we have found that STAT3 does not interfere directly with canonical TNF α -induced NF- κ B signalling. However, expression of NF- κ B positively correlates with total STAT3 and STAT1 levels and supports STAT3 and STAT1 activation. Given that stable reconstitution of wild-type p65-YFP but not the

S276A mutant in p65-deficient cells restored normal STAT1 and STAT3 levels, we conclude that transcriptional activity of p65 controls the expression of total STAT1 and STAT3, but not STAT5, without affecting canonical IL-6-induced STAT3 signaling. Analysis of p65 binding to STAT1 and STAT3 promoters and initiation of transcription will further clarify the role of NF- κ B in STAT signaling. Taken together, our findings indicate that previously reported functional cross-talks between both pathways are not universal but rather cell-type specific.

In the last part of this thesis we generated and characterized STAT3-YFP knock-in mice as a potentially powerful tool to study STAT3 dynamics *in-vivo*. Our data show that STAT3-YFP knock-in mice were successfully generated. The animals do not show any obvious abnormal phenotype. The YFP fluorescence can be detected by flow cytometry and confocal microscopy. STAT3-YFP knock-in mice will be a valuable tool for deciphering the functions and dynamics of STAT3 in many physiological and pathological processes *in-vivo* using different murine disease models and advanced microscopy techniques.

VI. References

1. **Lodish H, Berk A, Kaiser CA, Krieger M, Bretscher A, Ploegh H, Amon A, Scott MP.** *Molecular cell biology*, 7th edition. 2013, New York: W. H. Freeman and Company.
2. **Alberts B, Johnson A, Lewis J, Raff M, Roberts K, Walter P.** *Molecular Biology of the Cell. 4th edition.* 2002, New York: Garland Science.
3. **Bradshaw RA, Dennis EA.** *Handbook of Cell Signaling (Second Edition).* 2010, Academic Press.
4. **Isaacs A, Lindenmann J.** Virus interference. I. The interferon. *Proc. R. Soc. Lond. B Biol. Sci.* 1957, 147,258-267
5. **Darnell JE, Kerr IM, Stark GR.** Jak-STAT pathways and transcriptional activation in response to IFNs and other extracellular signaling proteins. *Science*, 1994, 264, 1415-21.
6. **Stark GR, Darnell JE Jr.** The JAK-STAT pathway at twenty. *Immunity*. 2012, 36(4):503-14.
7. **Levy DE, Kessler DS, Pine R, Reich N, Darnell JE Jr.** Interferon-induced nuclear factors that bind a shared promoter element correlate with positive and negative transcriptional control. *Genes Dev.* 1988, 2(4):383-93.
8. **Schindler C, Fu XY, Imbrota T, Aebersold R, Darnell JE Jr.** Proteins of transcription factor ISGF-3: one gene encodes the 91-and 84-kDa ISGF-3 proteins that are activated by interferon alpha. *Proc Natl Acad Sci U S A.* 1992, 89(16):7836-9.
9. **Decker T, Lew DJ, Mirkovitch J, Darnell JE Jr.** Cytoplasmic activation of GAF, an IFN-gamma-regulated DNA-binding factor. *EMBO J.* 1991, 10(4):927-32.
10. **Shuai K, Schindler C, Prezioso VR, Darnell JE Jr.** Activation of transcription by IFN-gamma: tyrosine phosphorylation of a 91-kD DNA binding protein. *Science.* 1992, 258(5089):1808-12.
11. **Schindler C, Shuai K, Prezioso VR, Darnell JE Jr.** Interferon-dependent tyrosine phosphorylation of a latent cytoplasmic transcription factor. *Science.* 1992, 257(5071):809-13
12. **Lütticken C, Wegenka UM, Yuan J, Buschmann J, Schindler C, Ziemiecki A, Harpur AG, Wilks AF, Yasukawa K, Taga T, Kishimoto T, Barbieri G, Pellegrini S, Sendtner M, Heinrich PC, Horn F.** Association of transcription factor APRF and protein kinase Jak1 with the interleukin-6 signal transducer gp130. *Science.* 1994, 263(5143):89-92.
13. **Akira S, Nishio Y, Inoue M, Wang XJ, Wei S, Matsusaka T, Yoshida K, Sudo T, Naruto M, Kishimoto T.** Molecular cloning of APRF, a novel IFN-stimulated gene factor 3 p91-related transcription factor involved in the gp130-mediated signaling pathway. *Cell.* 1994, 77(1):63-71.
14. **Wegenka UM, Lütticken C, Buschmann J, Yuan J, Lottspeich F, Müller-Esterl W, Schindler C, Roeb E, Heinrich PC, Horn F.** The interleukin-6-activated acute-phase response factor is antigenically and

- functionally related to members of the signal transducer and activator of transcription (STAT) family. *Mol Cell Biol.* 1994, 14(5):3186-96.
15. **Campbell GS, Meyer DJ, Raz R, Levy DE, Schwartz J, Carter-Su C.** Activation of acute phase response factor (APRF)/Stat3 transcription factor by growth hormone. *J Biol Chem.* 1995, 270(8):3974-9.
 16. **Zhong Z, Wen Z, Darnell JE Jr.** Stat3 and Stat4: members of the family of signal transducers and activators of transcription. *Proc Natl Acad Sci U S A.* 1994, 91(11):4806-10.
 17. **Jacobson NG, Szabo SJ, Weber-Nordt RM, Zhong Z, Schreiber RD, Darnell JE Jr, Murphy KM.** Interleukin 12 signaling in T helper type 1 (Th1) cells involves tyrosine phosphorylation of signal transducer and activator of transcription (Stat)3 and Stat4. *J Exp Med.* 1995, 181(5):1755-62.
 18. **Mui AL, Wakao H, O'Farrell AM, Harada N, Miyajima A.** Interleukin-3, granulocyte-macrophage colony stimulating factor and interleukin-5 transduce signals through two STAT5 homologs. *EMBO J.* 1995, 14(6):1166-75.
 19. **Liu X, Robinson GW, Gouilleux F, Groner B, Hennighausen L.** Cloning and expression of Stat5 and an additional homologue (Stat5b) involved in prolactin signal transduction in mouse mammary tissue. *Proc Natl Acad Sci U S A.* 1995, 92(19):8831-5.
 20. **Hou J, Schindler U, Henzel WJ, Ho TC, Brasseur M, McKnight SL.** An interleukin-4-induced transcription factor: IL-4 Stat. *Science.* 1994, 265(5179):1701-6.
 21. **Levy DE, Darnell JE.** STATs: transcriptional control and biological impact. *Nat Rev.* 2002, 3, 651-62.
 22. **Schindler C, Levy DE, Decker T.** JAK-STAT signaling: from interferons to cytokines. *J Biol Chem.* 2007, 282(28):20059-63.
 23. **O'Shea JJ, Gadina M, Kanno Y.** Cytokine signaling: birth of a pathway. *J Immunol.* 2011, 187(11):5475-8.
 24. **Mohr A, Chatain N, Domszalai T, Rinis N, Sommerauer M, Vogt M, Müller-Newen G.** Dynamics and non-canonical aspects of JAK/STAT signalling. *Eur J Cell Biol.* 2012, 91(6-7):524-32.
 25. **Braunstein, J, Brutsaert, S, Olson, R, and Schindler, C.** STATs dimerize in the absence of phosphorylation. *J Biol Chem.* 2003, 278: 34133-34140.
 26. **Meyer T, Gavenis K, Vinkemeier U.** Cell type-specific and tyrosine phosphorylation-independent nuclear presence of STAT1 and STAT3. *Exp Cell Res.* 2002, 272(1):45-55.
 27. **Meyer T, Vinkemeier U.** Nucleocytoplasmic shuttling of STAT transcription factors. *Eur J Biochem.* 2004, 271(23-24):4606-12.
 28. **Cheon H, Yang J, Stark GR.** The functions of signal transducers and activators of transcriptions 1 and 3 as cytokine-inducible proteins. *J Interferon Cytokine Res.* 2011, 31(1):33-40.
 29. **Li WX.** Canonical and non-canonical JAK-STAT signaling. *Trends Cell Biol.* 2008, 18(11):545-51
 30. **Park HJ, Li J, Hannah R, Biddie S, Leal-Cervantes AI, Kirschner K, Flores Santa Cruz D, Sexl V, Göttgens B, Green AR.** Cytokine-induced megakaryocytic differentiation is regulated by genome-wide loss of a uSTAT transcriptional program. *EMBO J.* 2016, 35(6):580-94.

31. **Paukku K, Silvennoinen O.** STATs as critical mediators of signal transduction and transcription: lessons learned from STAT5. *Cytokine Growth Factor Rev.* 2004, 15(6):435-55.
32. **Wegrzyn J, Potla R, Chwae YJ, Sepuri NB, Zhang Q, Koeck T, Derecka M, Szczepanek K, Szelag M, Gornicka A, Moh A, Moghaddas S, Chen Q, Bobbili S, Cichy J, Dulak J, Baker DP, Wolfman A, Stuehr D, Hassan MO, Fu XY, Avadhani N, Drake JI, Fawcett P, Lesnefsky EJ, Larner AC.** Function of mitochondrial Stat3 in cellular respiration. *Science.* 2009, 323(5915):793-7.
33. **Ng DC, Lin BH, Lim CP, Huang G, Zhang T, Poli V, Cao X.** Stat3 regulates microtubules by antagonizing the depolymerization activity of stathmin. *J Cell Biol.* 2006, 172(2):245-57.
34. **Lim CP, Cao X.** Structure, function, and regulation of STAT proteins. *Mol Biosyst.* 2006, 2(11):536-50
35. **Domoszlai T.** Dimerization of the transcription factor STAT3 analyzed by single-molecule fluorescence spectroscopy and advanced microscopy. Doctoral Thesis. *RWTH Aachen University*, 2013.
36. **O'Shea JJ, Plenge R.** JAK and STAT signaling molecules in immunoregulation and immune-mediated disease. *Immunity.* 2012, 36(4):542-50.
37. **Levy DE.** Physiological significance of STAT proteins: investigations through gene disruption in vivo. *Cell Mol Life Sci.* 1999, 55(12):1559-67.
38. **Takeda K, Noguchi K, Shi W, Tanaka T, Matsumoto M, Yoshida N, Kishimoto T, Akira S.** Targeted disruption of the mouse Stat3 gene leads to early embryonic lethality. *Proc Natl Acad Sci U S A.* 1997, 94(8):3801-4.
39. **Levy DE, Lee CK.** What does Stat3 do? *J Clin Invest.* 2002, 109(9):1143-8.
40. **Heinrich PC, Behrmann I, Haan S, Hermanns HM, Müller-Newen G, Schaper F.** Principles of interleukin (IL)-6-type cytokine signalling and its regulation. *Biochem J.* 2003, 374(Pt 1):1-20.
41. **Görtz D.** Development and optimization of receptor fusion proteins for the inhibition of IL-6-type cytokines in vivo. Doctoral Thesis. *RWTH Aachen University*, 2016.
42. **Heinrich PC, Behrmann I, Müller-Newen G, Schaper F, Graeve L.** Interleukin-6-type cytokine signalling through the gp130/Jak/STAT pathway. *Biochem J.* 1998, 334 (Pt 2):297-314.
43. **Garbers C, Hermanns HM, Schaper F, Müller-Newen G, Grötzinger J, Rose-John S, Scheller J.** Plasticity and cross-talk of interleukin 6-type cytokines. *Cytokine Growth Factor Rev.* 2012, 23(3):85-97.
44. **Müller-Newen G.** The cytokine receptor gp130: faithfully promiscuous. *Sci STKE.* 2003, 2003(201):PE40.
45. **Stancato LF, David M, Carter-Su C, Larner AC, Pratt WB.** Preassociation of STAT1 with STAT2 and STAT3 in separate signalling complexes prior to cytokine stimulation. *J Biol Chem.* 1996, 271(8):4134-7.
46. **Novak U, Ji H, Kanagasundaram V, Simpson R, Paradiso L.** STAT3 forms stable homodimers in the presence of divalent cations prior to activation. *Biochem Biophys Res Commun.* 1998, 247(3):558-63.

47. **Haan S, Kortylewski M, Behrmann I, Müller-Esterl W, Heinrich PC, Schaper F.** Cytoplasmic STAT proteins associate prior to activation. *Biochem J.* 2000, 345 Pt 3:417-21.
48. **Bhattacharya S, Schindler C.** Regulation of Stat3 nuclear export. *J Clin Invest.* 2003, 111(4):553-9.
49. **Pranada AL, Metz S, Herrmann A, Heinrich PC, Müller-Newen G.** Real time analysis of STAT3 nucleocytoplasmic shuttling. *J Biol Chem.* 2004, 279(15):15114-23
50. **Kretzschmar AK, Dinger MC, Henze C, Brocke-Heidrich K, Horn F.** Analysis of Stat3 (signal transducer and activator of transcription 3) dimerization by fluorescence resonance energy transfer in living cells. *Biochem J.* 2004, 377(Pt 2):289-97.
51. **Guschin D, Rogers N, Briscoe J, Witthuhn B, Watling D, Horn F, Pellegrini S, Yasukawa K, Heinrich P, Stark GR, Ihle JN, Kerr IM.** A major role for the protein tyrosine kinase JAK1 in the JAK/STAT signal transduction pathway in response to interleukin-6. *EMBO J.* 1995, 14(7):1421-9.
52. **Vogt M, Domoszlai T, Kleshchanok D, Lehmann S, Schmitt A, Poli V, Richtering W, Müller-Newen G.** The role of the N-terminal domain in dimerization and nucleocytoplasmic shuttling of latent STAT3. *J Cell Sci.* 2011, 124(Pt 6):900-9.
53. **Domoszlai T, Martincuks A, Fahrenkamp D, Schmitz-Van de Leur H, Küster A, Müller-Newen G.** Consequences of the disease-related L78R mutation for dimerization and activity of STAT3. *J Cell Sci.* 2014, 127(Pt 9):1899-910.
54. **Wegenka UM, Buschmann J, Lütticken C, Heinrich PC, Horn F.** Acute-phase response factor, a nuclear factor binding to acute-phase response elements, is rapidly activated by interleukin-6 at the posttranslational level. *Mol Cell Biol.* 1993, 13(1):276-88.
55. **Yuan J, Wegenka UM, Lütticken C, Buschmann J, Decker T, Schindler C, Heinrich PC, Horn F.** The signalling pathways of interleukin-6 and gamma interferon converge by the activation of different transcription factors which bind to common responsive DNA elements. *Mol Cell Biol.* 1994, 14(3):1657-68.
56. **Crocker BA, Krebs DL, Zhang JG, Wormald S, Willson TA, Stanley EG, Robb L, Greenhalgh CJ, Förster I, Clausen BE, Nicola NA, Metcalf D, Hilton DJ, Roberts AW, Alexander WS.** SOCS3 negatively regulates IL-6 signaling in vivo. *Nat Immunol.* 2003, 4(6):540-5
57. **Lang R, Pauleau AL, Parganas E, Takahashi Y, Mages J, Ihle JN, Rutschman R, Murray PJ.** SOCS3 regulates the plasticity of gp130 signaling. *Nat Immunol.* 2003, 4(6):546-50.
58. **Herrmann A, Vogt M, Mönningmann M, Clahsen T, Sommer U, Haan S, Poli V, Heinrich PC, Müller-Newen G.** Nucleocytoplasmic shuttling of persistently activated STAT3. *J Cell Sci.* 2007, 120(Pt 18):3249-61.
59. **Decker T, Kovarik P, Meinke A.** GAS elements: a few nucleotides with a major impact on cytokine-induced gene expression. *J Interferon Cytokine Res.* 1997, 17(3):121-34
60. **Grivennikov S., Karin M.** Dangerous liaisons: STAT3 and NF-kB collaboration and crosstalk in cancer. *Cytokine & Growth Factor Reviews,* 2010, 21, 11-9.

61. **Hirano T, Ishihara K, Hibi M.** Roles of STAT3 in mediating the cell growth, differentiation and survival signals relayed through the IL-6 family of cytokine receptors. *Oncogene*. 2000, 19(21):2548-56.
62. **Réb   C, V  gran F, Berger H, Ghiringhelli F.** STAT3 activation: A key factor in tumor immunoescape. *JAKSTAT*. 2013, 2(1):e23010
63. **Chen Z, Laurence A, Kanno Y, Pacher-Zavisin M, Zhu BM, Tato C, Yoshimura A, Hennighausen L, O'Shea JJ.** Selective regulatory function of Socs3 in the formation of IL-17-secreting T cells. *Proc Natl Acad Sci U S A*. 2006, 103(21):8137-42
64. **Yang XO, Panopoulos AD, Nurieva R, Chang SH, Wang D, Watowich SS, Dong C.** STAT3 regulates cytokine-mediated generation of inflammatory helper T cells. *J Biol Chem*. 2007, 282(13):9358-63.
65. **Chou WC, Levy DE, Lee CK.** STAT3 positively regulates an early step in B-cell development. *Blood*. 2006, 108(9):3005-11.
66. **Zhou Z, Gushiken FC, Bolgiano D, Salsbery BJ, Aghakasiri N, Jing N, Wu X, Vijayan KV, Rumbaut RE, Adachi R, Lopez JA, Dong JF.** Signal transducer and activator of transcription 3 (STAT3) regulates collagen-induced platelet aggregation independently of its transcription factor activity. *Circulation*. 2013, 127(4):476-85.
67. **Aggarwal BB, Kunnumakkara AB, Harikumar KB, Gupta SR, Tharakan ST, Koca C, Dey S, Sung B.** Signal transducer and activator of transcription-3, inflammation, and cancer: how intimate is the relationship? *Ann N Y Acad Sci*. 2009, 1171:59-76.
68. **Yu H, Pardoll D, Jove R.** STATs in cancer inflammation and immunity: a leading role for STAT3. *Nat Rev Cancer*. 2009, 9(11):798-809.
69. **Darnell JE.** Validating Stat3 in cancer therapy. *Nat. Med.*, 2005, 11, 595-6
70. **Musteanu M, Blaas L, Mair M, Schleder M, Bilban M, Tauber S, Esterbauer H, Mueller M, Casanova E, Kenner L, Poli V, Eferl R.** Stat3 is a negative regulator of intestinal tumor progression in Apc(Min) mice. *Gastroenterology*. 2010, 138(3):1003-11.e1-5.
71. **Zammarchi F, de Stanchina E, Bournazou E, Supakorndej T, Martires K, Riedel E, Corben AD, Bromberg JF, Cartegni L.** Antitumorigenic potential of STAT3 alternative splicing modulation. *Proc. Natl. Acad. Sci.*, 2011, 108, 17779-84.
72. **de la Iglesia N, Puram SV, Bonni A.** STAT3 regulation of glioblastoma pathogenesis. *Curr Mol Med*. 2009, 9(5):580-90.
73. **Fagard R, Metelev V, Souissi I, Baran-Marszak F.** STAT3 inhibitors for cancer therapy: Have all roads been explored? *JAKSTAT*. 2013, 2(1):e22882
74. **Timofeeva OA, Gaponenko V, Lockett SJ, Tarasov SG, Jiang S, Michejda CJ, Perantoni AO, Tarasova NI.** Rationally designed inhibitors identify STAT3 N-domain as a promising anticancer drug target. *ACS Chem Biol*. 2007, 2(12):799-809.
75. **Wang Y, Levy DE.** Comparative evolutionary genomics of the STAT family of transcription factors. *JAKSTAT*. 2012, 1(1):23-33.
76. **Timofeeva OA, Tarasova NI.** Alternative ways of modulating JAK-STAT pathway: Looking beyond phosphorylation. *JAKSTAT*. 2012, 1(4):274-84.

77. **Wenta N, Strauss H, Meyer S, Vinkemeier U.** Tyrosine phosphorylation regulates the partitioning of STAT1 between different dimer conformations. *Proc Natl Acad Sci U S A.* 2008, 105(27):9238-43.
78. **Ota N, Brett TJ, Murphy TL, Fremont DH, Murphy KM.** N-domain-dependent nonphosphorylated STAT4 dimers required for cytokine-driven activation. *Nat Immunol.* 2004, 5(2):208-15.
79. **Zhang X, Darnell JE Jr.** Functional importance of Stat3 tetramerization in activation of the alpha 2-macroglobulin gene. *J Biol Chem.* 2001, 276(36):33576-81
80. **Zhang L, Badgwell DB, Bevers JJ 3rd, Schlessinger K, Murray PJ, Levy DE, Watowich SS.** IL-6 signaling via the STAT3/SOCS3 pathway: functional analysis of the conserved STAT3 N-domain. *Mol Cell Biochem.* 2006, 288(1-2):179-89
81. **Ray S, Boldogh I, Brasier AR.** STAT3 NH2-terminal acetylation is activated by the hepatic acute-phase response and required for IL-6 induction of angiotensinogen. *Gastroenterology.* 2005, 129(5):1616-32.
82. **Ray S, Lee C, Hou T, Bhakat KK, Brasier AR.** Regulation of signal transducer and activator of transcription 3 enhanceosome formation by apurinic/apyrimidinic endonuclease 1 in hepatic acute phase response. *Mol Endocrinol.* 2010, 24(2):391-401
83. **Ray S, Zhao Y, Jamaluddin M, Edeh CB, Lee C, Brasier AR.** Inducible STAT3 NH2 terminal mono-ubiquitination promotes BRD4 complex formation to regulate apoptosis. *Cell Signal.* 2014, 26(7):1445-55.
84. **Hou T, Ray S, Lee C, Brasier AR.** The STAT3 NH2-terminal domain stabilizes enhanceosome assembly by interacting with the p300 bromodomain. *J Biol Chem.* 2008, 283(45):30725-34.
85. **Hu T, Yeh JE, Pinello L, Jacob J, Chakravarthy S, Yuan GC, Chopra R, Frank DA.** Impact of the N-terminal domain of STAT3 in STAT3-dependent transcriptional activity. *Mol Cell Biol.* 2015, 35(19):3284-300.
86. **Mohr A, Fahrenkamp D, Rinis N, Müller-Newen G.** Dominant-negative activity of the STAT3-Y705F mutant depends on the N-terminal domain. *Cell Commun Signal.* 2013, 11:83.
87. **Timofeeva OA, Tarasova NI, Zhang X, Chasovskikh S, Cheema AK, Wang H, Brown ML, Dritschilo A.** STAT3 suppresses transcription of proapoptotic genes in cancer cells with the involvement of its N-terminal domain. *Proc Natl Acad Sci U S A.* 2013, 110(4):1267-72
88. **Stephanou A, Latchman DS.** Opposing actions of STAT-1 and STAT-3. *Growth Factors.* 2005, 23(3):177-82.
89. **Regis G, Pensa S, Boselli D, Novelli F, Poli V.** Ups and downs: the STAT1:STAT3 seesaw of Interferon and gp130 receptor signalling. *Semin Cell Dev Biol.* 2008, 19(4):351-9.
90. **Avalle L, Pensa S, Regis G, Novelli F, Poli V.** STAT1 and STAT3 in tumorigenesis: A matter of balance. *JAKSTAT.* 2012, 1(2):65-72.
91. **Platanias LC.** Mechanisms of type-I- and type-II-interferon-mediated signalling. *Nat Rev Immunol.* 2005, 5(5):375-86.
92. **Schroder K, Hertzog PJ, Ravasi T, Hume DA.** Interferon-gamma: an overview of signals, mechanisms and functions. *J Leukoc Biol.* 2004, 75(2):163-89.

93. **Bromberg JF, Wrzeszczynska MH, Devgan G, Zhao Y, Pestell RG, Albanese C, Darnell JE Jr.** Stat3 as an oncogene. *Cell*. 1999, 98(3):295-303.
94. **Qing Y, Stark GR.** Alternative activation of STAT1 and STAT3 in response to interferon-gamma. *J Biol Chem*. 2004, 279(40):41679-85.
95. **Wiederkehr-Adam M, Ernst P, Müller K, Bieck E, Gombert FO, Ottl J, Graff P, Grossmüller F, Heim MH.** Characterization of phosphopeptide motifs specific for the Src homology 2 domains of signal transducer and activator of transcription 1 (STAT1) and STAT3. *J Biol Chem*. 2003, 278(18):16117-28.
96. **Stephens JM, Lumpkin SJ, Fishman JB.** Activation of signal transducers and activators of transcription 1 and 3 by leukemia inhibitory factor, oncostatin-M, and interferon-gamma in adipocytes. *J Biol Chem*. 1998, 273(47):31408-16.
97. **Haan S, Keller JF, Behrmann I, Heinrich PC, Haan C.** Multiple reasons for an inefficient STAT1 response upon IL-6-type cytokine stimulation. *Cell Signal*. 2005, 17(12):1542-50.
98. **Kim J, Yoon Y, Jeoung D, Kim YM, Choe J.** Interferon- γ stimulates human follicular dendritic cell-like cells to produce prostaglandins via the JAK-STAT pathway. *Mol Immunol*. 2015, 66(2):189-96.
99. **Mahboubi K, Pober JS.** Activation of signal transducer and activator of transcription 1 (STAT1) is not sufficient for the induction of STAT1-dependent genes in endothelial cells. Comparison of interferon-gamma and oncostatin M. *J Biol Chem*. 2002 Mar 8;277(10):8012-21.
100. **Costa-Pereira AP, Tininini S, Strobl B, Alonzi T, Schlaak JF, Is'harc H, Gesualdo I, Newman SJ, Kerr IM, Poli V.** Mutational switch of an IL-6 response to an interferon-gamma-like response. *Proc Natl Acad Sci U S A*. 2002, 99(12):8043-7.
101. **Wang WB, Levy DE, Lee CK.** STAT3 negatively regulates type I IFN-mediated antiviral response. *J Immunol*. 2011, 187(5):2578-85.
102. **Dimberg LY, Dimberg A, Ivarsson K, Fryknäs M, Rickardson L, Tobin G, Ekman S, Larsson R, Gullberg U, Nilsson K, Öberg F, Wiklund HJ.** Stat1 activation attenuates IL-6 induced Stat3 activity but does not alter apoptosis sensitivity in multiple myeloma. *BMC Cancer*. 2012, 12:318.
103. **Karin M, Ben-Neriah Y.** Phosphorylation meets ubiquitination: the control of NF- κ B activity. *Annu Rev Immunol*. 2000;18:621-63.
104. **Schmitz ML, Mattioli I, Buss H, Kracht M.** NF- κ B: A Multifaceted Transcription Factor Regulated at Several Levels. *ChemBiochem*. 2004, 5, 1348 – 1358.
105. **Hayden MS, Ghosh S.** Shared principles in NF- κ B signaling. 2008, *Cell* 132: 344-362.
106. **Neumann M, Naumann M.** Beyond I κ Bs: alternative regulation of NF- κ B activity. *FASEB J*. 2007, 21(11):2642-54.
107. **Vallabhapurapu S, Karin M.** Regulation and function of NF- κ B transcription factors in the immune system. *Annu Rev Immunol*. 2009, 27:693-733.
108. **Hoffmann A, Natoli G and Ghosh G.** Transcriptional regulation via the NF- κ B signaling module. *Oncogene*, 2006, 25, 6706-6716.
109. **Wietek C and O'Neill LA.** Diversity and regulation in the NF- κ B system. *Trends Biochem. Sci.*, 2007, 32, 311-319.

110. **Arenzana-Seisdedos F, Turpin P, Rodriguez M, Thomas D, Hay RT, Virelizier JL, Dargemont C.** Nuclear localization of I kappa B alpha promotes active transport of NF-kappa B from the nucleus to the cytoplasm. *J Cell Sci.* 1997, 110 (Pt 3):369-78.
111. **Chen Lf, Fischle W, Verdin E, Greene WC.** Duration of nuclear NF-kappaB action regulated by reversible acetylation. *Science.* 2001, 293(5535):1653-7.
112. **Birbach A, Gold P, Binder BR, Hofer E, de Martin R, Schmid JA.** Signaling molecules of the NF-kappa B pathway shuttle constitutively between cytoplasm and nucleus. *J Biol Chem.* 2002, 277(13):10842-51
113. **Yang J, Liao X, Agarwal MK, Barnes L, Auron PE, Stark GR.** Unphosphorylated STAT3 accumulates in response to IL-6 and activates transcription by binding to NFkappaB. *Genes Dev.* 2007, 21, 1396-408.
114. **Oeckinghaus A, Ghosh S.** The NF-kB Family of Transcription Factors and Its Regulation. *Cold Spring Harb. Perspect. Biol.*, 2009, 1, a000034.
115. **Baud V, Karin M.** Is NF-kB a good target for cancer therapy? Hopes and pitfalls. *Nat Rev Drug. Discov.* 2009, 8, 33-40.
116. **Klein U and Ghosh S.** The Two Faces of NF-kB Signaling in Cancer Development and Therapy. *Cancer Cell*, 2011, 20, 556-8.
117. **Basseres DS and Baldwin AS.** Nuclear factor-kB and inhibitor of kB kinase pathways in oncogenic initiation and progression. *Oncogene*, 2006, 25, 6817-30.
118. **Ryan KM, Ernst MK, Rice NR, Vousden KH.** Role of NF-kappaB in p53-mediated programmed cell death. *Nature*, 2000, 404, 892-7.
119. **Hoffman A, Baltimore D.** Circuitry of nuclear factor kB signaling. *Immunological Reviews* 2006, 210, 171-86.
120. **Perkins ND.** Post-translational modifications regulating the activity and function of the nuclear factor kappa B pathway. *Oncogene*, 2006, 25, 6717-6730.
121. **Zhong H, Voll RE, and Ghosh S.** Phosphorylation of NF-kappa B p65 by PKA stimulates transcriptional activity by promoting a novel bivalent interaction with the coactivator CBP/p300. *Mol. Cell*, 1998, 1, 661-71.
122. **Vermeulen L, De Wilde G, Van Damme P, Vanden Berghe W and Haegeman G.** Transcriptional activation of the NF-kappaB p65 subunit by mitogen and stress-activated protein kinase-1 (MSK1). *Embo. J.*, 2003, 22, 1313-24.
123. **Dong J, Jimi E, Zhong H, Hayden MS, Ghosh S.** Repression of gene expression by unphosphorylated NF-kappaB p65 through epigenetic mechanisms. *Genes Dev.* 2008, 22(9):1159-73.
124. **Duran A, Diaz-Meco MT, Moscat J.** Essential role of RelA Ser311 phosphorylation by zetaPKC in NF-kappaB transcriptional activation. *EMBO J.* 2003, 22(15):3910-8.
125. **Mattioli I, Geng H, Sebald A, Hodel M, Bucher C, Kracht M, Schmitz ML.** Inducible phosphorylation of NF-kappa B p65 at serine 468 by T cell costimulation is mediated by IKK epsilon. *J Biol Chem.* 2006 Mar, 281(10):6175-83.
126. **Schwabe RF, Sakurai H.** IKKbeta phosphorylates p65 at S468 in transactivation domain 2. *FASEB J.* 2005, 19(12):1758-60.

127. **Hu J, Haseebuddin M, Young M, Colburn NH.** Suppression of p65 phosphorylation coincides with inhibition of I κ B α polyubiquitination and degradation. *Mol Carcinog.* 2005, 44(4):274-84.
128. **Bode JG, Albrecht U, Häussinger D, Heinrich PC, Schaper F.** Hepatic acute phase proteins--regulation by IL-6- and IL-1-type cytokines involving STAT3 and its crosstalk with NF- κ B-dependent signaling. *Eur J Cell Biol.* 2012 Jun-Jul;91(6-7):496-505.
129. **Bollrath J, Greten FR.** IKK/NF- κ B and STAT3 pathways: central signalling hubs in inflammation-mediated tumour promotion and metastasis. *EMBO Rep.* 2009, 10(12):1314-9
130. **He G, Karin M.** NF- κ B and STAT3 – key players in liver inflammation and cancer. *Cell Research,* 2011, 21, 159-68.
131. **Yang J, Stark GR.** Roles of unphosphorylated STATs in signaling. *Cell Res.* 2008 Apr;18(4):443-51.
132. **Agrawal A, Cha-Molstad H, Samols D, Kushner I.** Overexpressed nuclear factor- κ B can participate in endogenous C-reactive protein induction, and enhances the effects of C/EBP β and signal transducer and activator of transcription-3. *Immunology.* 2003, 108(4):539-47.
133. **Hagihara K, Nishikawa T, Sugamata Y, Song J, Isobe T, Taga T, Yoshizaki K.** Essential role of STAT3 in cytokine-driven NF- κ B-mediated serum amyloid A gene expression. *Genes Cells.* 2005, 10(11):1051-63.
134. **Yu Z, Zhang W, Kone BC.** Signal transducers and activators of transcription 3 (STAT3) inhibits transcription of the inducible nitric oxide synthase gene by interacting with nuclear factor κ B. *Biochem J.* 2002 Oct 1;367(Pt 1):97-105.
135. **Debidda M, Wang L, Zang H, Poli V, Zheng Y.** A role of STAT3 in Rho GTPase-regulated cell migration and proliferation. *J Biol Chem.* 2005, 280(17):17275-85.
136. **Zouein FA, Duhé RJ, Arany I, Shirey K, Hosler JP, Liu H, Saad I, Kurdi M, Booz GW.** Loss of STAT3 in mouse embryonic fibroblasts reveals its Janus-like actions on mitochondrial function and cell viability. *Cytokine.* 2014, 66(1):7-16.
137. **Kulesza DW, Carré T, Chouaib S, Kaminska B.** Silencing of the transcription factor STAT3 sensitizes lung cancer cells to DNA damaging drugs, but not to TNF α - and NK cytotoxicity. *Exp Cell Res.* 2013, 319(4):506-16.
138. **McFarland BC, Gray GK, Nozell SE, Hong SW, Benveniste EN.** Activation of the NF- κ B pathway by the STAT3 inhibitor JSI-124 in human glioblastoma cells. *Mol Cancer Res.* 2013, 11(5):494-505.
139. **Grabner B, Schramek D, Mueller KM, Moll HP, Svinka J, Hoffmann T, Bauer E, Blaas L, Hruschka N, Zboray K, Stiedl P, Nivarthi H, Bogner E, Gruber W, Mohr T, Zwick RH, Kenner L, Poli V, Aberger F, Stoiber D, Egger G, Esterbauer H, Zuber J, Moriggl R, Eferl R, Györfy B, Penninger JM, Popper H, Casanova E.** Disruption of STAT3 signalling promotes KRAS-induced lung tumorigenesis. *Nat Commun.* 2015, 6:6285.
140. **Stewart M.** Molecular mechanism of the nuclear protein import cycle. *Nat Rev Mol Cell Biol.* 2007, 8(3):195-208.

141. **Görlich D, Kutay U.** Transport between the cell nucleus and the cytoplasm. *Annu Rev Cell Dev Biol.* 1999, 15:607-60.
142. **Feldherr CM, Akin D, Cohen RJ.** Regulation of functional nuclear pore size in fibroblasts. *J Cell Sci.* 2001, 114(Pt 24):4621-7.
143. **Cronshaw JM, Krutchinsky AN, Zhang W, Chait BT, Matunis MJ.** Proteomic analysis of the mammalian nuclear pore complex. *J Cell Biol.* 2002, 158(5):915-27.
144. **Turner JG, Sullivan DM.** CRM1-mediated nuclear export of proteins and drug resistance in cancer. *Curr Med Chem.* 2008, 15(26):2648-55.
145. **Turner JG, Dawson J, Cubitt CL, Baz R, Sullivan DM.** Inhibition of CRM1-dependent nuclear export sensitizes malignant cells to cytotoxic and targeted agents. *Semin Cancer Biol.* 2014, 27:62-73.
146. **Fung HY, Chook YM.** Atomic basis of CRM1-cargo recognition, release and inhibition. *Semin Cancer Biol.* 2014, 27:52-61
147. **Meissner T, Krause E, Vinkemeier U.** Ratjadone and leptomycin B block CRM1-dependent nuclear export by identical mechanisms. *FEBS Lett.* 2004 Oct 8;576(1-2):27-30.
148. **Pumroy RA, Cingolani G.** Diversification of importin- α isoforms in cellular trafficking and disease states. *Biochem J.* 2015, 466(1):13-28.
149. **Kobe B.** Autoinhibition by an internal nuclear localization signal revealed by the crystal structure of mammalian importin alpha. *Nat Struct Biol.* 1999, 6(4):388-97.
150. **Lange A, Mills RE, Lange CJ, Stewart M, Devine SE, Corbett AH.** Classical nuclear localization signals: definition, function, and interaction with importin alpha. *J Biol Chem.* 2007, 282(8):5101-5
151. **Goldfarb DS, Corbett AH, Mason DA, Harreman MT, Adam SA.** Importin alpha: a multipurpose nuclear-transport receptor. *Trends Cell Biol.* 2004, 14(9):505-14.
152. **Matsuura Y, Stewart M.** Nup50/Npap60 function in nuclear protein import complex disassembly and importin recycling. *EMBO J.* 2005, 24(21):3681-9.
153. **Sekimoto T, Imamoto N, Nakajima K, Hirano T, Yoneda Y.** Extracellular signal-dependent nuclear import of Stat1 is mediated by nuclear pore-targeting complex formation with NPI-1, but not Rch1. *EMBO J.* 1997, 16(23):7067-77
154. **Liang P, Zhang H, Wang G, Li S, Cong S, Luo Y, Zhang B.** KPNB1, XPO7 and IPO8 mediate the translocation of NF- κ B/p65 into the nucleus. *Traffic.* 2013, 14(11):1132-43.
155. **Nardozzi J, Wenta N, Yasuhara N, Vinkemeier U, Cingolani G.** Molecular basis for the recognition of phosphorylated STAT1 by importin alpha5. *J Mol Biol.* 2010, 402(1):83-100
156. **Xu W, Edwards MR, Borek DM, Feagins AR, Mittal A, Alinger JB, Berry KN, Yen B, Hamilton J, Brett TJ, Pappu RV, Leung DW, Basler CF, Amarasinghe GK.** Ebola virus VP24 targets a unique NLS binding site on karyopherin alpha 5 to selectively compete with nuclear import of phosphorylated STAT1. *Cell Host Microbe.* 2014, 16(2):187-200.
157. **Liu L, McBride KM, Reich NC.** STAT3 nuclear import is independent of tyrosine phosphorylation and mediated by importin-alpha3. *Proc Natl Acad Sci U S A.* 2005, 102(23):8150-5

158. **Ushijima R, Sakaguchi N, Kano A, Maruyama A, Miyamoto Y, Sekimoto T, Yoneda Y, Ogino K, Tachibana T.** Extracellular signal-dependent nuclear import of STAT3 is mediated by various importin alphas. *Biochem Biophys Res Commun.* 2005, 330(3):880-6.
159. **Ma J, Cao X.** Regulation of Stat3 nuclear import by importin alpha5 and importin alpha7 via two different functional sequence elements. *Cell Signal.* 2006, (8):1117-26.
160. **Huang S, Chang IS, Lin W, Ye W, Luo RZ, Lu Z, Lu Y, Zhang K, Liao WS, Tao T, Bast RC Jr, Chen X, Yu Y.** ARHI (DIRAS3), an imprinted tumour suppressor gene, binds to importins and blocks nuclear import of cargo proteins. *Biosci Rep.* 2009, 30(3):159-68.
161. **Suthaus J, Tillmann A, Lorenzen I, Bulanova E, Rose-John S, Scheller J.** Forced homo- and heterodimerization of all gp130-type receptor complexes leads to constitutive ligand-independent signaling and cytokine-independent growth. *Mol Biol Cell.* 2010, 21(15):2797-807.
162. **Moreno R, Sobotzik JM, Schultz C, Schmitz ML.** Specification of the NF-kappaB transcriptional response by p65 phosphorylation and TNF-induced nuclear translocation of IKK epsilon. *Nucleic Acids Res.* 2010, 38(18):6029-44.
163. **Wallner B, Leitner NR, Vielnascher RM, Kernbauer E, Kolbe T, Karaghiosoff M, Rülcke T, Decker T, Müller M.** Generation of mice with a conditional Stat1 null allele. *Transgenic Res.* 2012, 21(1):217-24.
164. **Arcone R, Pucci P, Zappacosta F, Fontaine V, Malorni A, Marino G, Ciliberto G.** Single-step purification and structural characterization of human interleukin-6 produced in *Escherichia coli* from a T7 RNA polymerase expression vector. *Eur J Biochem.* 1991, 198(3):541-7.
165. **Weiergräber O, Hemmann U, Küster A, Müller-Newen G, Schneider J, Rose-John S, Kurschat P, Brakenhoff JP, Hart MH, Stabel S, Heinrich PC.** Soluble human interleukin-6 receptor. Expression in insect cells, purification and characterization. *Eur J Biochem.* 1995, 234(2):661-9.
166. **Livak KJ, Schmittgen TD.** Analysis of relative gene expression data using real-time quantitative PCR and the 2⁻(Delta Delta C(T)) Method. *Methods.* 2001, 25(4):402-8.
167. **Ketteler R, Glaser S, Sandra O, Martens UM, Klingmüller U.** Enhanced transgene expression in primitive hematopoietic progenitor cells and embryonic stem cells efficiently transduced by optimized retroviral hybrid vectors. *Gene Ther.* 2002, 9(8):477-87.
168. **Takeda K, Kaisho T, Yoshida N, Takeda J, Kishimoto T, Akira S.** Stat3 activation is responsible for IL-6-dependent T cell proliferation through preventing apoptosis: generation and characterization of T cell-specific Stat3-deficient mice. *J Immunol.* 1998, 161(9):4652-60.
169. **Alonzi T, Maritano D, Gorgoni B, Rizzuto G, Libert C, Poli V.** Essential role of STAT3 in the control of the acute-phase response as revealed by inducible gene inactivation [correction of activation] in the liver. *Mol Cell Biol.* 2001, 21(5):1621-32.
170. **Gerhartz C, Heesel B, Sasse J, Hemmann U, Landgraf C, Schneider-Mergener J, Horn F, Heinrich PC, Graeve L.** Differential activation of acute phase response factor/STAT3 and STAT1 via the cytoplasmic domain of the interleukin 6 signal transducer gp130. I.

- Definition of a novel phosphotyrosine motif mediating STAT1 activation. *J Biol Chem*. 1996 May 31;271(22):12991-8.
171. **Yuan ZL, Guan YJ, Chatterjee D, Chin YE.** Stat3 dimerization regulated by reversible acetylation of a single lysine residue. *Science*. 2005, 307(5707):269-73.
172. **Becker S, Groner B, Müller CW.** Three-dimensional structure of the Stat3beta homodimer bound to DNA. *Nature*. 1998, 394(6689):145-51.
173. **Shuai K, Liao J, Song MM.** Enhancement of antiproliferative activity of gamma interferon by the specific inhibition of tyrosine dephosphorylation of Stat1. *Mol Cell Biol*. 1996, 16(9):4932-41.
174. **Strehlow I, Schindler C.** Amino-terminal signal transducer and activator of transcription (STAT) domains regulate nuclear translocation and STAT deactivation. *J Biol Chem*. 1998, 273(43):28049-56.
175. **Meissner T, Krause E, Lödige I, Vinkemeier U.** Arginine methylation of STAT1: a reassessment. *Cell*. 2004, 119(5):587-9
176. **Maritano D, Sugrue ML, Tininini S, Dewilde S, Strobl B, Fu X, Murray-Tait V, Chiarle R, Poli V.** The STAT3 isoforms alpha and beta have unique and specific functions. *Nat Immunol*. 2004, 5(4):401-9.
177. **Blaecke A, Delneste Y, Herbault N, Jeannin P, Bonnefoy JY, Beck A, Aubry JP.** Measurement of nuclear factor-kappa B translocation on lipopolysaccharide-activated human dendritic cells by confocal microscopy and flow cytometry. *Cytometry*. 2002, 48(2):71-9.
178. **Adli M, Baldwin AS.** IKK-i/IKKepsilon controls constitutive, cancer cell-associated NF-kappaB activity via regulation of Ser-536 p65/RelA phosphorylation. *J Biol Chem*. 2006, 281(37):26976-84
179. **Okazaki T, Sakon S, Sasazuki T, Sakurai H, Doi T, Yagita H, Okumura K, Nakano H.** Phosphorylation of serine 276 is essential for p65 NF-kappaB subunit-dependent cellular responses. *Biochem Biophys Res Commun*. 2003, 300(4):807-12.
180. **Dhar K, Rakesh K, Pankajakshan D, Agrawal DK.** SOCS3 promotor hypermethylation and STAT3-NF-kB interaction downregulate SOCS3 expression in human coronary artery smooth muscle cells. *Am J Physiol Heart Circ Physiol*. 2013, 304(6):H776-85.
181. **Borkham-Kamphorst E, Huss S, Van de Leur E, Haas U, Weiskirchen R.** Adenoviral CCN3/NOV gene transfer fails to mitigate liver fibrosis in an experimental bile duct ligation model because of hepatocyte apoptosis. *Liver Int*. 2012, 32(9):1342-53.
182. **Araki T, Kawata T, Williams JG.** Identification of the kinase that activates a nonmetazoan STAT gives insights into the evolution of phosphotyrosine-SH2 domain signaling. *Proc Natl Acad Sci U S A*. 2012, 109(28):E1931-7.
183. **Debnath B, Xu S, Neamati N.** Small molecule inhibitors of signal transducer and activator of transcription 3 (Stat3) protein. *J Med Chem*. 2012, 55(15):6645-68
184. **Herrmann A, Sommer U, Pranada AL, Giese B, Küster A, Haan S, Becker W, Heinrich PC, Müller-Newen G.** STAT3 is enriched in nuclear bodies. *J Cell Sci*. 2004, 117(Pt 2):339-49.
185. **Köster M, Hauser H.** Dynamic redistribution of STAT1 protein in IFN signaling visualized by GFP fusion proteins. *Eur J Biochem*. 1999, 260(1):137-44.

186. **Frahm T, Hauser H, Köster M.** IFN-type-I-mediated signaling is regulated by modulation of STAT2 nuclear export. *J Cell Sci.* 2006, 119(Pt 6):1092-104.
187. **Huang YM, Wen YP, Li XA, Yuan Y, Luo QZ, Li M.** [Amino acids 395-416 in DNA binding domain of STAT4 is involved in IL-12-induced nuclear import of STAT4]. [Article in Chinese]. *Sheng Li Xue Bao.* 2012 Aug 25;64(4):372-8.
188. **Fahrenkamp D, de Leur HS, Küster A, Chatain N, Müller-Newen G.** Src family kinases interfere with dimerization of STAT5A through a phosphotyrosine-SH2 domain interaction. *Cell Commun Signal.* 2015, 13:10.
189. **Zeng R, Aoki Y, Yoshida M, Arai K, Watanabe S.** Stat5B shuttles between cytoplasm and nucleus in a cytokine-dependent and -independent manner. *J Immunol.* 2002, 168(9):4567-75.
190. **Chen HC, Reich NC.** Live cell imaging reveals continuous STAT6 nuclear trafficking. *J Immunol.* 2010, 185(1):64-70
191. **Auernhammer CJ, Bousquet C, Melmed S.** Autoregulation of pituitary corticotroph SOCS-3 expression: characterization of the murine SOCS-3 promoter. *Proc Natl Acad Sci U S A.* 1999, 96(12):6964-9.
192. **Lillemeier BF, Köster M, Kerr IM.** STAT1 from the cell membrane to the DNA. *EMBO J.* 2001, 20(10):2508-17.
193. **Herrington J, Rui L, Luo G, Yu-Lee LY, Carter-Su C.** A functional DNA binding domain is required for growth hormone-induced nuclear accumulation of Stat5B. *J Biol Chem.* 1999, 274(8):5138-45.
194. **Chandrasekaran P, Zimmerman O, Paulson M, Sampaio EP, Freeman AF, Sowerwine KJ, Hurt D, Alcántara-Montiel JC, Hsu AP, Holland SM.** Distinct mutations at the same positions of STAT3 cause either loss or gain of function. *J Allergy Clin Immunol.* 2016, pii: S0091-6749(16)30356-6.
195. **Pelham SJ, Lenthall HC, Deenick EK, Tangye SG.** Elucidating the effects of disease-causing mutations on STAT3 function in autosomal-dominant hyper-IgE syndrome. *J Allergy Clin Immunol.* 2016, pii: S0091-6749(16)30282-2.
196. **Buettner R, Corzano R, Rashid R, Lin J, Senthil M, Hedvat M, Schroeder A, Mao A, Herrmann A, Yim J, Li H, Yuan YC, Yakushijin K, Yakushijin F, Vaidehi N, Moore R, Gugiu G, Lee TD, Yip R, Chen Y, Jove R, Horne D, Williams JC.** Alkylation of cysteine 468 in Stat3 defines a novel site for therapeutic development. *ACS Chem Biol.* 2011 May 20;6(5):432-43
197. **Teng P, Zhang X, Wu H, Qiao Q, Sebt SM, Cai J.** Identification of novel inhibitors that disrupt STAT3-DNA interaction from a γ -AApeptide OBOC combinatorial library. *Chem Commun (Camb).* 2014, 50(63):8739-42.
198. **Ramana CV, Kumar A, Enelow R.** Stat1-independent induction of SOCS-3 by interferon-gamma is mediated by sustained activation of Stat3 in mouse embryonic fibroblasts. *Biochem Biophys Res Commun.* 2005, 327(3):727-33
199. **Schiavone D, Avalle L, Dewilde S, Poli V.** The immediate early genes Fos and Egr1 become STAT1 transcriptional targets in the absence of STAT3. *FEBS Lett.* 2011, 585(15):2455-60.

200. **Pakala SB, Rayala SK, Wang RA, Ohshiro K, Mudvari P, Reddy SD, Zheng Y, Pires R, Casimiro S, Pillai MR, Costa L, Kumar R.** MTA1 promotes STAT3 transcription and pulmonary metastasis in breast cancer. *Cancer Res.* 2013, 73(12):3761-70.
201. **Meyer T, Marg A, Lemke P, Wiesner B, Vinkemeier U.** DNA binding controls inactivation and nuclear accumulation of the transcription factor Stat1. *Genes Dev.* 2003, 17(16):1992-2005.
202. **Xu L, Ji JJ, Le W, Xu YS, Dou D, Pan J, Jiao Y, Zhong T, Wu D, Wang Y, Wen C, Xie GQ, Yao F, Zhao H, Fan YS, Chin YE.** The STAT3 HIES mutation is a gain-of-function mutation that activates genes via AGG-element carrying promoters. *Nucleic Acids Res.* 2015, pii: gkv911 .
203. **Mertens C, Zhong M, Krishnaraj R, Zou W, Chen X, Darnell JE Jr.** Dephosphorylation of phosphotyrosine on STAT1 dimers requires extensive spatial reorientation of the monomers facilitated by the N-terminal domain. *Genes Dev.* 2006, 20(24):3372-81.
204. **Meyer T, Hendry L, Begitt A, John S, Vinkemeier U.** A single residue modulates tyrosine dephosphorylation, oligomerization, and nuclear accumulation of stat transcription factors. *J Biol Chem.* 2004 Apr 30;279(18):18998-9007.
205. **Sgrignani J, Olsson S, Ekonomiuk D, Genini D, Krause R, Catapano CV, Cavalli A.** Molecular Determinants for Unphosphorylated STAT3 Dimerization Determined by Integrative Modeling. *Biochemistry.* 2015, 54(35):5489-501.
206. **ten Hoeve J, de Jesus Ibarra-Sanchez M, Fu Y, Zhu W, Tremblay M, David M, Shuai K.** Identification of a nuclear Stat1 protein tyrosine phosphatase. *Mol Cell Biol.* 2002, 22(16):5662-8.
207. **Yamamoto T, Sekine Y, Kashima K, Kubota A, Sato N, Aoki N, Matsuda T.** The nuclear isoform of protein-tyrosine phosphatase TC-PTP regulates interleukin-6-mediated signaling pathway through STAT3 dephosphorylation. *Biochem Biophys Res Commun.* 2002, 297(4):811-7.
208. **Wang Y, Ning H, Ren F, Zhang Y, Rong Y, Wang Y, Su F, Cai C, Jin Z, Li Z, Gong X, Zhai Y, Wang D, Jia B, Qiu Y, Tomita Y, Sung JJ, Yu J, Irwin DM, Yang X, Fu X, Chin YE, Chang Z.** GdX/UBL4A specifically stabilizes the TC45/STAT3 association and promotes dephosphorylation of STAT3 to repress tumorigenesis. *Mol Cell.* 2014, 53(5):752-65.
209. **Ren F, Geng Y, Minami T, Qiu Y, Feng Y, Liu C, Zhao J, Wang Y, Fan X, Wang Y, Li M, Li J, Chang Z.** Nuclear termination of STAT3 signaling through SIPAR (STAT3-Interacting Protein As a Repressor)-dependent recruitment of T cell tyrosine phosphatase TC-PTP. *FEBS Lett.* 2015, 589(15):1890-6.
210. **Lu D, Liu L, Ji X, Gao Y, Chen X, Liu Y, Liu Y, Zhao X, Li Y, Li Y, Jin Y, Zhang Y, McNutt MA, Yin Y.** The phosphatase DUSP2 controls the activity of the transcription activator STAT3 and regulates TH17 differentiation. *Nat Immunol.* 2015, 16(12):1263-73.
211. **Rohan PJ, Davis P, Moskaluk CA, Kearns M, Kruttsch H, Siebenlist U, Kelly K.** PAC-1: a mitogen-induced nuclear protein tyrosine phosphatase. *Science.* 1993, 259(5102):1763-6.

212. **Rushworth LK, Kidger AM, Delavaine L, Stewart G, van Schelven S, Davidson J, Bryant CJ, Caddy E, East P, Caunt CJ, Keyse SM.** Dual-specificity phosphatase 5 regulates nuclear ERK activity and suppresses skin cancer by inhibiting mutant Harvey-Ras (HRasQ61L)-driven SerpinB2 expression. *Proc Natl Acad Sci U S A*. 2014, 111(51):18267-72.
213. **Lang R, Hammer M, Mages J.** DUSP meet immunology: dual specificity MAPK phosphatases in control of the inflammatory response. *J Immunol*. 2006, 177(11):7497-504
214. **Oh YM, Kim JK, Choi Y, Choi S, Yoo JY.** Prediction and experimental validation of novel STAT3 target genes in human cancer cells. *PLoS One*. 2009, 4(9):e6911.
215. **Hügel S.** Individual functions and substrate specificities of importin α subtypes. Doctoral Thesis. *University of Lübeck*, 2013.
216. **Ben-Yaakov K, Dagan SY, Segal-Ruder Y, Shalem O, Vuppalachandi D, Willis DE, Yudin D, Rishal I, Rother F, Bader M, Blesch A, Pilpel Y, Twiss JL, Fainzilber M.** Axonal transcription factors signal retrogradely in lesioned peripheral nerve. *EMBO J*. 2012, 31(6):1350-63.
217. **Cimica V, Chen HC, Iyer JK, Reich NC.** Dynamics of the STAT3 transcription factor: nuclear import dependent on Ran and importin- β 1. *PLoS One*. 2011;6(5):e20188
218. **Marg A, Shan Y, Meyer T, Meissner T, Brandenburg M, Vinkemeier U.** Nucleocytoplasmic shuttling by nucleoporins Nup153 and Nup214 and CRM1-dependent nuclear export control the subcellular distribution of latent Stat1. *J Cell Biol*. 2004, 165(6):823-33.
219. **Kawashima T, Bao YC, Minoshima Y, Nomura Y, Hatori T, Hori T, Fukagawa T, Fukada T, Takahashi N, Nosaka T, Inoue M, Sato T, Kukimoto-Niino M, Shirouzu M, Yokoyama S, Kitamura T.** A Rac GTPase-activating protein, MgcRacGAP, is a nuclear localizing signal-containing nuclear chaperone in the activation of STAT transcription factors. *Mol Cell Biol*. 2009, 29(7):1796-813.
220. **Nishimoto A, Yu Y, Lu Z, Mao X, Ren Z, Watowich SS, Mills GB, Liao WS, Chen X, Bast RC Jr, Luo RZ.** A Ras homologue member 1 directly inhibits signal transducers and activators of transcription 3 translocation and activity in human breast and ovarian cancer cells. *Cancer Res*. 2005, 65(15):6701-10.
221. **Muthu K, Panneerselvam M, Topno NS, Jayaraman M, Ramadas K.** Structural perspective of ARHI mediated inhibition of STAT3 signaling: an insight into the inactive to active transition of ARHI and its interaction with STAT3 and importin β . *Cell Signal*. 2015, 27(4):739-55.
222. **Langenfeld F, Guarracino Y, Arock M, Trouvé A, Tchertanov L.** How Intrinsic Molecular Dynamics Control Intramolecular Communication in Signal Transducers and Activators of Transcription Factor STAT5. *PLoS One*. 2015, 10(12):e0145142
223. **Namanja AT, Wang J, Buettner R, Colson L, Chen Y.** Allosteric Communication across STAT3 Domains Associated with STAT3 Function and Disease-Causing Mutation. *J Mol Biol*. 2016, 428(3):579-89.

224. **Meyer T, Begitt A, Lödige I, van Rossum M, Vinkemeier U.** Constitutive and IFN-gamma-induced nuclear import of STAT1 proceed through independent pathways. *EMBO J.* 2002, (3):344-54.
225. **Ma J, Zhang T, Novotny-Diermayr V, Tan AL, Cao X.** A novel sequence in the coiled-coil domain of Stat3 essential for its nuclear translocation. *J Biol Chem.* 2003, 278(31):29252-60.
226. **Hemmman U, Gerhartz C, Heesel B, Sasse J, Kurapkat G, Grötzinger J, Wollmer A, Zhong Z, Darnell JE Jr, Graeve L, Heinrich PC, Horn F.** Differential activation of acute phase response factor/Stat3 and Stat1 via the cytoplasmic domain of the interleukin 6 signal transducer gp130. II. Src homology SH2 domains define the specificity of stat factor activation. *J Biol Chem.* 1996; 271(22):12999-3007.
227. **Regis G, Icardi L, Conti L, Chiarle R, Piva R, Giovarelli M, Poli V, Novelli F.** IL-6, but not IFN-gamma, triggers apoptosis and inhibits in vivo growth of human malignant T cells on STAT3 silencing. *Leukemia.* 2009, 23(11):2102-8.
228. **Zheng J, van de Veerdonk FL, Crossland KL, Smeekens SP, Chan CM, Al Shehri T, Abinun M, Gennery AR, Mann J, Lendrem DW, Netea MG, Rowan AD, Lilic D.** Gain-of-function STAT1 mutations impair STAT3 activity in patients with Chronic Mucocutaneous Candidiasis (CMC). *Eur J Immunol.* 2015, 45(10):2834-46
229. **Ho HH, Ivashkiv LB.** Role of STAT3 in type I interferon responses. Negative regulation of STAT1-dependent inflammatory gene activation. *J Biol Chem.* 2006, 281(20):14111-8.
230. **Gough DJ, Sabapathy K, Ko EY, Arthur HA, Schreiber RD, Trapani JA, Clarke CJ, Johnstone RW.** A novel c-Jun-dependent signal transduction pathway necessary for the transcriptional activation of interferon gamma response genes. *J Biol Chem.* 2007, 282(2):938-46.
231. **Lee CK, Raz R, Gimeno R, Gertner R, Wistinghausen B, Takeshita K, DePinho RA, Levy DE.** STAT3 is a negative regulator of granulopoiesis but is not required for G-CSF-dependent differentiation. *Immunity.* 2002, 17(1):63-72.
232. **Grisouard J, Shimizu T, Duek A, Kubovcakov L, Hao-Shen H, Dirnhofer S, Skoda RC.** Deletion of Stat3 in hematopoietic cells enhances thrombocytosis and shortens survival in a JAK2-V617F mouse model of MPN. *Blood.* 2015
233. **Yan D, Jobe F, Hutchison RE, Mohi G.** Deletion of Stat3 enhances myeloid cell expansion and increases the severity of myeloproliferative neoplasms in Jak2V617F knock-in mice. *Leukemia.* 2015
234. **Matsukawa A, Kudo S, Maeda T, Numata K, Watanabe H, Takeda K, Akira S, Ito T.** Stat3 in resident macrophages as a repressor protein of inflammatory response. *J Immunol.* 2005, 175(5):3354-9.
235. **Musteanu M, Blaas L, Mair M, Schleder M, Bilban M, Tauber S, Esterbauer H, Mueller M, Casanova E, Kenner L, Poli V, Eferl R.** Stat3 is a negative regulator of intestinal tumor progression in Apc(Min) mice. *Gastroenterology.* 2010, 138(3):1003-1
236. **Masuda K, Ripley B, Nyati KK, Dubey PK, Zaman MM, Hanieh H, Higa M, Yamashita K, Standley DM, Mashima T, Katahira M, Okamoto T, Matsuura Y, Takeuchi O, Kishimoto T.** Arid5a regulates

- naive CD4⁺ T cell fate through selective stabilization of Stat3 mRNA. *J Exp Med*. 2016, 213(4):605-19.
237. **Harwardt T, Lukas S, Zenger M, Reitberger T, Danzer D, Übner T, Munday DC, Nevels M, Paulus C.** Human Cytomegalovirus Immediate-Early 1 Protein Rewires Upstream STAT3 to Downstream STAT1 Signaling Switching an IL6-Type to an IFN γ -Like Response. *PLoS Pathog*. 2016, 12(7):e1005748.
 238. **Nivarthi H, Gordziel C, Themanns M, Kramer N, Eberl M, Rabe B, Schleder M, Rose-John S, Knösel T, Kenner L, Freund P, Aberger F, Han X, Kralovics R, Dolznig H, Jennek S, Friedrich K, Moriggl R.** The ratio of STAT1 to STAT3 expression is a determinant of colorectal cancer growth. *Oncotarget*. 2016
 239. **Ramana CV, DeBerge MP, Kumar A, Alia CS, Durbin JE, Enelow RI.** Inflammatory impact of IFN- γ in CD8⁺ T-cell-mediated lung injury is mediated by both Stat1-dependent and -independent pathways. *Am J Physiol Lung Cell Mol Physiol*. 2015
 240. **Capitini CM, Nasholm NM, Chien CD, Larabee SM, Qin H, Song YK, Klover PJ, Hennighausen L, Khan J, Fry TJ.** Absence of STAT1 in donor-derived plasmacytoid dendritic cells results in increased STAT3 and attenuates murine GVHD. *Blood*. 2014, 124(12):1976-86.
 241. **Kim HS, Kim DC, Kim HM, Kwon HJ, Kwon SJ, Kang SJ, Kim SC, Choi GE.** STAT1 deficiency redirects IFN signalling toward suppression of TLR response through a feedback activation of STAT3. *Sci Rep*. 2015, 5:13414
 242. **Peters A, Fowler KD, Chalmin F, Merkler D, Kuchroo VK, Pot C.** IL-27 Induces Th17 Differentiation in the Absence of STAT1 Signaling. *J Immunol*. 2015
 243. **Wan CK, Andraski AB, Spolski R, Li P, Kazemian M, Oh J, Samsel L, Swanson PA, McGavern DB, Sampaio EP, Freeman AF, Milner JD, Holland SM, Leonard WJ.** Opposing roles of STAT1 and STAT3 in IL-21 function in CD4⁺ T cells. *Proc Natl Acad Sci U S A*. 2015, 112(30):9394-9.
 244. **Hirahara K, Onodera A, Villarino AV, Bonelli M, Sciumè G, Laurence A, Sun HW, Brooks SR, Vahedi G, Shih HY, Gutierrez-Cruz G, Iwata S, Suzuki R, Mikami Y, Okamoto Y, Nakayama T, Holland SM, Hunter CA, Kanno Y, O'Shea JJ.** Asymmetric Action of STAT Transcription Factors Drives Transcriptional Outputs and Cytokine Specificity. *Immunity*. 2015, 42(5):877-89.
 245. **Ma CS et al.** Unique and shared signaling pathways cooperate to regulate the differentiation of human CD4⁺ T cells into distinct effector subsets. *J Exp Med*. 2016, pii: jem.20151467.
 246. **Adamaki M, Tsotra M, Vlahopoulos S, Zampogiannis A, Papavassiliou AG, Moschovi M.** STAT transcript levels in childhood acute lymphoblastic leukemia: STAT1 and STAT3 transcript correlations. *Leuk Res*. 2015, pii: S0145-2126(15)30379-9.
 247. **Rinis N, Küster A, Schmitz-Van de Leur H, Mohr A, Müller-Newen G.** Intracellular signaling prevents effective blockade of oncogenic gp130 mutants by neutralizing antibodies. *Cell Commun Signal*. 2014, 10;12:14
 248. **Delgoffe GM, Vignali DA.** STAT heterodimers in immunity: A mixed message or a unique signal? *JAKSTAT*. 2013, 2(1):e23060

249. **Schnell U, Dijk F, Sjollem KA, Giepmans BN.** Immunolabeling artifacts and the need for live-cell imaging. *Nat Methods*. 2012, 9(2):152-8
250. **Vekemans K, Rosseel L, Wisse E, Braet F.** Immuno-localization of Fas and FasL in rat hepatic endothelial cells: influence of different fixation protocols. *Micron*. 2004, 35(4):303-6.
251. **Li MW, Zhou L, Lam HM.** Paraformaldehyde Fixation May Lead to Misinterpretation of the Subcellular Localization of Plant High Mobility Group Box Proteins. *PLoS One*. 2015, 10(8):e0135033.
252. **Smith-Clerc J, Hinz B.** Immunofluorescence detection of the cytoskeleton and extracellular matrix in tissue and cultured cells. *Methods Mol Biol*. 2010, 611:43-57.
253. **Pollice AA, McCoy JP Jr, Shackney SE, Smith CA, Agarwal J, Burholt DR, Janocko LE, Hornicek FJ, Singh SG, Hartsock RJ.** Sequential paraformaldehyde and methanol fixation for simultaneous flow cytometric analysis of DNA, cell surface proteins, and intracellular proteins. *Cytometry*. 1992;13(4):432-44.
254. **Brock R, Hamelers IH, Jovin TM.** Comparison of fixation protocols for adherent cultured cells applied to a GFP fusion protein of the epidermal growth factor receptor. *Cytometry*. 1999, 35(4):353-62.
255. **Buss H, Dörrie A, Schmitz ML, Hoffmann E, Resch K, Kracht M.** Constitutive and interleukin-1-inducible phosphorylation of p65 NF- κ B at serine 536 is mediated by multiple protein kinases including I κ B kinase (IKK)- α , IKK β , IKK ϵ , TRAF family member-associated (TANK)-binding kinase 1 (TBK1), and an unknown kinase and couples p65 to TATA-binding protein-associated factor II31-mediated interleukin-8 transcription. *J Biol Chem*. 2004 Dec 31;279(53):55633-43.
256. **Scott ML, Fujita T, Liou HC, Nolan GP, Baltimore D.** The p65 subunit of NF-kappa B regulates I kappa B by two distinct mechanisms. *Genes Dev*. 1993, 7(7A):1266-76.
257. **Guo AK, Hou YY, Hirata H, Yamauchi S, Yip AK, Chiam KH, Tanaka N, Sawada Y, Kawauchi K.** Loss of p53 enhances NF- κ B-dependent lamellipodia formation. *J Cell Physiol*. 2014, 229(6):696-704.
258. **Bernier M, Paul RK, Martin-Montalvo A, Scheibye-Knudsen M, Song S, He HJ, Armour SM, Hubbard BP, Bohr VA, Wang L, Zong Y, Sinclair DA, de Cabo R.** Negative regulation of STAT3 protein-mediated cellular respiration by SIRT1 protein. *J Biol Chem*. 2011 Jun 3;286(22):19270-9.
259. **Anrather J, Racchumi G, Iadecola C.** cis-acting, element-specific transcriptional activity of differentially phosphorylated nuclear factor-kappa B. *J Biol Chem*. 2005, 280(1):244-52
260. **Lu Y, Zhou J, Xu C, Lin H, Xiao J, Wang Z, Yang B.** JAK/STAT and PI3K/AKT pathways form a mutual transactivation loop and afford resistance to oxidative stress-induced apoptosis in cardiomyocytes. *Cell Physiol Biochem*. 2008, 21(4):305-14.
261. **Sasaki CT, Issaeva N, Vageli DP.** In vitro model for gastroduodenal reflux-induced nuclear factor-kappaB activation and its role in hypopharyngeal carcinogenesis. *Head Neck*. 2015

262. **Krämer OH, Baus D, Knauer SK, Stein S, Jäger E, Stauber RH, Grez M, Pfitzner E, Heinzel T.** Acetylation of Stat1 modulates NF-kappaB activity. *Genes Dev.* 2006, s20(4):473-85.
263. **Xu QQ, Zhou Q, Xu LL, Lin H, Wang XJ, Ma WL, Zhai K, Tong ZH, Su Y, Shi HZ.** Toll-Like receptor 4 signaling inhibits malignant pleural effusion by altering Th1/Th17 responses. *Cell Biol Int.* 2015
264. **Guzzo C, Che Mat NF, Gee K.** Interleukin-27 induces a STAT1/3- and NF-kappaB-dependent proinflammatory cytokine profile in human monocytes. *J Biol Chem.* 2010, 285(32):24404-11.
265. **Uskokovic A, Dinić S, Mihailović M, Grdović N, Arambašić J, Vidaković M, Bogojević D, Ivanović-Matić S, Martinović V, Petrović M, Poznanović G, Grigorov I.** STAT3/NF-kB interactions determine the level of haptoglobin expression in male rats exposed to dietary restriction and/or acute phase stimuli. *Mol Biol Rep*, 2012, 39, 167-76
266. **Lee H, Deng J, Xin H, Liu Y, Pardoll D, Yu H.** A requirement of STAT3 DNA-binding precludes Th-1 immunostimulatory gene expression by NF-kB in tumors. *Cancer Res*, 2011, 71(11):3772-80.
267. **Lee H, Herrmann A, Deng JH, Kujawski M, Niu G, Li Z, Forman S, Jove R, Pardoll DM, Yu H.** Persistently Activated Stat3 Maintains Constitutive NF-kB Activity in Tumors. *Cancer Cell*, 2009, 15, 283-93.
268. **Zhang Z, Fuller GM.** The Competitive Binding of STAT3 and NF-kB on an Overlapping DNA Binding Site. *Biochem Biophys Res Commun*, 1997, 237, 90-4.
269. **Kesanakurti D, Chetty C, Rajasekhar Maddirela D, Gujrati M, Rao JS.** Essential role of cooperative NF-kB and Stat3 recruitment to ICAM-1 intronic consensus elements in the regulation of radiation-induced invasion and migration in glioma. *Oncogene.* 2013, 32(43):5144-55.
270. **Yoo JY, Huso DL, Nathans D, Desiderio S.** Specific ablation of Stat3beta distorts the pattern of Stat3-responsive gene expression and impairs recovery from endotoxic shock. *Cell.* 2002, 108(3):331-44.
271. **Structural Genomics Consortium; China Structural Genomics Consortium; Northeast Structural Genomics Consortium.** Protein production and purification. *Nat Methods.* 2008 Feb;5(2):135-46
272. **Gopal GJ, Kumar A.** Strategies for the production of recombinant protein in Escherichia coli. *Protein J.* 2013, 32(6):419-25.
273. **Yu CL, Meyer DJ, Campbell GS, Larner AC, Carter-Su C, Schwartz J, Jove R.** Enhanced DNA-binding activity of a Stat3-related protein in cells transformed by the Src oncoprotein. *Science.* 1995 Jul 7;269(5220):81-3.
274. **Cirri P, Chiarugi P, Marra F, Raugei G, Camici G, Manao G, Ramponi G.** c-Src activates both STAT1 and STAT3 in PDGF-stimulated NIH3T3 cells. *Biochem Biophys Res Commun.* 1997, 239(2):493-7.
275. **Wang YZ, Wharton W, Garcia R, Kraker A, Jove R, Pledger WJ.** Activation of Stat3 preassembled with platelet-derived growth factor beta receptors requires Src kinase activity. *Oncogene.* 2000, 19(17):2075-85.
276. **Ginsberg M, Czeko E, Müller P, Ren Z, Chen X, Darnell JE Jr.** Amino acid residues required for physical and cooperative transcriptional interaction of STAT3 and AP-1 proteins c-Jun and c-Fos. *Mol Cell Biol.* 2007, 27(18):6300-8.

277. **Nakashima K, Yanagisawa M, Arakawa H, Kimura N, Hisatsune T, Kawabata M, Miyazono K, Taga T.** Synergistic signaling in fetal brain by STAT3-Smad1 complex bridged by p300. *Science*. 1999, 284(5413):479-82.
278. **Minoguchi M, Minoguchi S, Aki D, Joo A, Yamamoto T, Yumioka T, Matsuda T, Yoshimura A.** STAP-2/BKS, an adaptor/docking protein, modulates STAT3 activation in acute-phase response through its YXXQ motif. *J Biol Chem*. 2003, 278(13):11182-9.
279. **Sato N, Kawai T, Sugiyama K, Muromoto R, Imoto S, Sekine Y, Ishida M, Akira S, Matsuda T.** Physical and functional interactions between STAT3 and ZIP kinase. *Int Immunol*. 2005, 17(12):1543-52.
280. **Ohbayashi N, Taira N, Kawakami S, Togi S, Sato N, Ikeda O, Kamitani S, Muromoto R, Sekine Y, Matsuda T.** An RNA binding protein, Y14 interacts with and modulates STAT3 activation. *Biochem Biophys Res Commun*. 2008, 372(3):475-9.
281. **Ikeda O, Sekine Y, Mizushima A, Nakasuji M, Miyasaka Y, Yamamoto C, Muromoto R, Nanbo A, Oritani K, Yoshimura A, Matsuda T.** Interactions of STAP-2 with Brk and STAT3 participate in cell growth of human breast cancer cells. *J Biol Chem*. 2010, 285(49):38093-103.
282. **Togi S, Muromoto R, Hirashima K, Kitai Y, Okayama T, Ikeda O, Matsumoto N, Kon S, Sekine Y, Oritani K, Matsuda T.** A New STAT3-binding Partner, ARL3, Enhances the Phosphorylation and Nuclear Accumulation of STAT3. *J Biol Chem*. 2016, 291(21):11161-71.
283. **Su F, Ren F, Rong Y, Wang Y, Geng Y, Wang Y, Feng M, Ju Y, Li Y, Zhao ZJ, Meng K, Chang Z.** Protein tyrosine phosphatase Meg2 dephosphorylates signal transducer and activator of transcription 3 and suppresses tumor growth in breast cancer. *Breast Cancer Res*. 2012, 14(2):R38.
284. **Gunaje JJ, Bhat GJ.** Involvement of tyrosine phosphatase PTP1D in the inhibition of interleukin-6-induced Stat3 signaling by alpha-thrombin. *Biochem Biophys Res Commun*. 2001, 288(1):252-7.
285. **Ray S, Lee C, Hou T, Boldogh I, Brasier AR.** Requirement of histone deacetylase1 (HDAC1) in signal transducer and activator of transcription 3 (STAT3) nucleocytoplasmic distribution. *Nucleic Acids Res*. 2008, 36(13):4510-20.
286. **Chung CD, Liao J, Liu B, Rao X, Jay P, Berta P, Shuai K.** Specific inhibition of Stat3 signal transduction by PIAS3. *Science*. 1997, 278(5344):1803-5.
287. **Tanaka T, Yamamoto Y, Muromoto R, Ikeda O, Sekine Y, Grusby MJ, Kaisho T, Matsuda T.** PDLIM2 inhibits T helper 17 cell development and granulomatous inflammation through degradation of STAT3. *Sci Signal*. 2011, 4(202):ra85.
288. **Bienvenu F, Gascan H, Coqueret O.** Cyclin D1 represses STAT3 activation through a Cdk4-independent mechanism. *J Biol Chem*. 2001, 276(20):16840-7.
289. **Muromoto R, Nakao K, Watanabe T, Sato N, Sekine Y, Sugiyama K, Oritani K, Shimoda K, Matsuda T.** Physical and functional interactions between Daxx and STAT3. *Oncogene*. 2006, 25(14):2131-6.
290. **Tsuruma R, Ohbayashi N, Kamitani S, Ikeda O, Sato N, Muromoto R, Sekine Y, Oritani K, Matsuda T.** Physical and functional

- interactions between STAT3 and KAP1. *Oncogene*. 2008, 27(21):3054-9.
291. **Chang Y, Wang SX, Wang YB, Zhou J, Li WH, Wang N, Fang DF, Li HY, Li AL, Zhang XM, Zhang WN.** ECHS1 interacts with STAT3 and negatively regulates STAT3 signaling. *FEBS Lett*. 2013, 587(6):607-13.
292. **Xiao H, Chung J, Kao HY, Yang YC.** Tip60 is a co-repressor for STAT3. *J Biol Chem*. 2003, 278(13):11197-204
293. **Lin YM, Wang CM, Jeng JC, Leprince D, Shih HM.** HIC1 interacts with and modulates the activity of STAT3. *Cell Cycle*. 2013, 12(14):2266-76
294. **Icardi L, Mori R, Gesellchen V, Eyckerman S, De Cauwer L, Verhelst J, Vercauteren K, Saelens X, Meuleman P, Leroux-Roels G, De Bosscher K, Boutros M, Tavernier J.** The Sin3a repressor complex is a master regulator of STAT transcriptional activity. *Proc Natl Acad Sci U S A*. 2012, 109(30):12058-63.
295. **Kawasaki A, Matsumura I, Kataoka Y, Takigawa E, Nakajima K, Kanakura Y.** Opposing effects of PML and PML/RAR alpha on STAT3 activity. *Blood*. 2003, 101(9):3668-73.
296. **Kataoka Y, Matsumura I, Ezoe S, Nakata S, Takigawa E, Sato Y, Kawasaki A, Yokota T, Nakajima K, Felsani A, Kanakura Y.** Reciprocal inhibition between MyoD and STAT3 in the regulation of growth and differentiation of myoblasts. *J Biol Chem*. 2003, 278(45):44178-87
297. **Coqueret O, Gascan H.** Functional interaction of STAT3 transcription factor with the cell cycle inhibitor p21WAF1/CIP1/SDI1. *J Biol Chem*. 2000, 275(25):18794-800.
298. **Collum RG, Brutsaert S, Lee G, Schindler C.** A Stat3-interacting protein (StIP1) regulates cytokine signal transduction. *Proc Natl Acad Sci U S A*. 2000, 97(18):10120-5.
299. **Sekine Y, Tsuji S, Ikeda O, Sato N, Aoki N, Aoyama K, Sugiyama K, Matsuda T.** Regulation of STAT3-mediated signaling by LMW-DSP2. *Oncogene*. 2006, 25(42):5801-6
300. **Ezoe S, Matsumura I, Gale K, Satoh Y, Ishikawa J, Mizuki M, Takahashi S, Minegishi N, Nakajima K, Yamamoto M, Enver T, Kanakura Y.** GATA transcription factors inhibit cytokine-dependent growth and survival of a hematopoietic cell line through the inhibition of STAT3 activity. *J Biol Chem*. 2005, 280(13):13163-70
301. **Blumert C, Kalkhof S, Brocke-Heidrich K, Kohajda T, von Bergen M, Horn F.** Analysis of the STAT3 interactome using in-situ biotinylation and SILAC. *J Proteomics*. 2013 Dec 6;94:370-86.
302. **Yasukawa H, Ohishi M, Mori H, Murakami M, Chinen T, Aki D, Hanada T, Takeda K, Akira S, Hoshijima M, Hirano T, Chien KR, Yoshimura A.** IL-6 induces an anti-inflammatory response in the absence of SOCS3 in macrophages. *Nat Immunol*. 2003, 4(6):551-6.

VII. Abbreviations

+/+	Homozygous knock-in ESC
+/-	Heterozygous knock-in ESC
± SD	Standard deviation
ΔIBB	Lacking IBB domain
ΔN	Lacking N-domain
ΔNES	Lacking NES
ΔNLS	Lacking NLS
ΔTAD	Lacking TAD
°C	Degree Celsius
μg, μl, μm	Micrograms, microliters, micrometers
α-32P	Radioactively labeled with Phosphorus-32

A

A	Adenine
A549	Adenocarcinomic human lung epithelial cells.
APE1	Apurinic/apyrimidinic endonuclease 1
APRF	Acute phase response factor (STAT3)
APS	Ammonium persulfate
ARHI	Aplysia ras homology member I
ARL3	ADP-ribosylation factor-like protein 3
ARM	Armadillo repeats

B

BIRC5	Baculoviral inhibitor of apoptosis repeat-containing5
BRD4	Bromodomain-containing protein 4
Brk	Breast tumor kinase
BSA	Bovine serum albumin

C

C	Cytosine
C57BL/6	C57 black 6 inbred strain of laboratory mouse
CAS	Cellular apoptosis susceptibility protein
CCD	Coiled-coil domain
cDNA	Complementary DNA
<i>cfos</i>	Cellular Fos proto-oncogene gene
CFP	Cyan fluorescent protein
c-Jun	Jun proto-oncogene
CLC	Cardiotrophin-like cytokine
CNTF	Ciliary neurotrophic factor
CO ₂	Carbon dioxide
Co-IP	Co-immunoprecipitation
CRM1	Chromosomal maintenance 1
CRP	C-reactive protein
CT-1	Cardiotrophin-1
C-terminal	Carboxy-terminal

D

dATP	Deoxyadenosine triphosphate
Daxx	Death-associated protein 6
DBD	DNA-binding domain
dCTP	Deoxycytidine triphosphate
ddH ₂ O	Double distilled water
dGTP	Deoxyguanosine triphosphate
DMEM	Dulbecco's modified Eagle's medium
DMSO	Dimethyl sulfoxide
DNA	Deoxyribonucleic acid

dNTPs	Deoxyribose-containing nucleoside triphosphates
dsRed	Red fluorescent protein
DTT	Dithiothreitol
dTTP	Deoxythymidine triphosphate
DUSP	Dual-specificity phosphatase

E

<i>E.Coli</i>	<i>Escherichia coli</i>
ECHS1	Enoyl Coenzyme A hydratase short chain 1
EDTA	Ethylenediaminetetraacetic acid
eGFP	Enhanced green fluorescent protein
EMSA	Electrophoretic mobility shift assay
ESC	Embryonic stem cells, murine

F

FACS	Fluorescence-activated cell sorting
FCS	Fetal calf serum
FLP	Flippase recombinase
FP	Fluorescent protein, forward primer
FRT	Flippase recognition target

G

G	Guanine
GAPDH	Glyceraldehyde 3-phosphate dehydrogenase
GAS	Gamma IFN-activated site
GATA	Transcription factors that bind to "GATA" sequence
<i>gfp2</i>	Interferon-induced guanylate-binding protein 2 gene
G-CSF	Granulocyte colony-stimulating factor
gDNA	Genomic DNA
gp130	Glycoprotein 130
gp80	Glycoprotein 80

GPCRs	G protein–coupled receptors
GST	Glutathione S-transferases

H

HDAC1	Histone deacetylase 1
Hek293	Human embryonic kidney 293 cells
HeLa	Henrietta Lacks, human cervical cancer cells
HIC1	Hypermethylated in cancer 1 protein
HRP	Horseradish peroxidase
HUVEC	Human umbilical vein endothelial cells

I

IB	Immunoblot
IBB	Importin-beta binding
ICAM-1	Intercellular adhesion molecule 1
IE1	Immediate-early 1 protein
IF	Immunofluorescence
IFN	Interferon
IFNGR	Interferon gamma receptor
IgG	Immunoglobulin G
IKK	I κ B kinase
IL	Interleukin
IL-6R α	Interleukin-6 receptor alpha subunit
iNOS	Nitric oxide synthase, inducible isoform
<i>irf1</i>	Interferon regulatory factor 1 gene
ISGF	Interferon-stimulated gene factor 3
ISRE	Interferon-stimulated response element
I κ B α	Inhibitor of kappa beta alpha
<i>ikba</i>	I κ B α gene

J

JAK	Janus kinase
JunB	Jun B Proto-Oncogene
<i>junB</i>	Jun B Proto-Oncogene gene

K

K48-linked	Lysine 48 linked
KAP-1	KRAB-associated protein-1
kDa	Kilodaltons

L

LD	Linker domain
LIF	Leukemia inhibitory factor
LIFR	LIF receptor
LMB	Leptomycin B
LMW-DSP2	Dual specificity protein phosphatase 22
LPS	Lipopolysaccharide
LSM	Laser scanning microscopy

M

MAPK	Mitogen-activated protein kinases
MEF	Mouse embryonic fibroblasts
MEF Δ/Δ	STAT3-deficient MEFs
Meg2	Tyrosine-protein phosphatase non-receptor type 9
MgcRacGAP	Rac GTPase activating protein
<i>mGUSB</i>	Murine beta-glucuronidase gene
min	Minutes
ml	Mililiters
mm	Milimeters
mRNA	Messenger RNA
MSK1	Mitogen- and stress-activated protein kinase-1

mSNICQ	Mutated SNICQ amino acid sequences
MyOD	Myogenic differentiation 1 protein

N

n	Amount
NaVO ₃	Sodium orthovanadate
NEMO	NF-Kappa-B essential modulator
NES	Nuclear export signal
NF-κB	Nuclear factor kappa beta
ng, nm	Nanograms, nanometers
NLS	Nuclear localization signal
NPCs	Nuclear pore complexes
NTD	N-terminal domain
Nup	Nucleoporin
N-terminal	Amino-terminal

O

OD	Optical density
OSM	Oncostatin M
OSMR	OSM receptor

P

p21WAF	Cyclin-dependent kinase inhibitor 1
p300	Histone acetyltransferase p300
p65	NF-κB subunit p65, RelA
p65 -/-	p65-deficient
PCR	Polymerase chain reaction
PDLIM2	PDZ and LIM domain protein 2
PFA	Paraformaldehyde
PIAS3	Protein inhibitor of activated STAT 3

PML	Promyelocytic leukemia protein
pmol	picomol
PMSF	Phenylmethanesulfonyl fluoride
Poly(dI-dC)	Poly(deoxyinosinic-deoxycytidylic) acid
PTEFb	Positive transcription elongation factor
PTPN	Protein tyrosine phosphatases, non-receptor type
PVDF	Polyvinylidene fluoride

Q

qPCR	Quantitative real-time PCR
------	----------------------------

R

Rac1	Ras-related C3 botulinum toxin substrate 1
Ran	Ras-related nuclear protein
RanBP1	Ran-specific binding protein 1
RanGAP	Ran GTPase-activating protein
RanGTP	Guanosine-5'-triphosphate-bound Ran
RANTES	Regulated on activation, normal T cell expressed and secreted protein
RATs	Ratjadones
RelA	NF- κ B subunit RelA, p65
RHD	Rel homology domain
RhoA	Ras homolog gene family, member A
RIPA	Radioimmune precipitation assay
RNA	Ribonucleic acid
RNA Pol II	RNA polymerase II
RP	Reverse primer
RPM	Rounds per minute
RTKs	Receptor tyrosine kinases

S

S1/S1	STAT1 homodimers
S3/S1	STAT3/STAT1 heterodimers
S3/S3	STAT3 homodimers
SAA	Serum amyloid A
SCF- β TrCP	Multi-protein E3 ubiquitin ligase
SDS	Sodium dodecyl sulfate
SDS-PAGE	SDS polyacrylamide gel electrophoresis
SH2	Src Homology 2 domain
SHP2	Src homology-2 domain containing protein tyrosine phosphatase-2
SIE	sis-inducible element
Sin3A	Paired amphipathic helix protein
SIPAR	STAT3-Interacting Protein As a Repressor
SMAD	Sma and Mad (Mothers against decapentaplegic) protein
SOCS3	Suppressor of cytokine signaling 3
<i>socs3</i>	SOCS3 gene
Src	Rous sarcoma oncogene cellular homologue
STAP-2	Signal-transducing adaptor protein 2
STAT	Signal transducer and activator of transcription
STAT1 -/-	STAT1-deficient
STAT1C	Constitutively active STAT1
STAT3 -/-	STAT3-deficient
STATIP1	STAT3-interacting protein 1

T

T	Thymine
TAD	Transactivation domain
TAK1	TGF β -activated kinase 1
TC45	Nuclear isoform of TC-PTP
TC-PTP	Tyrosine-protein phosphatase non-receptor type 2
TEMED	Tetramethylethylenediamine
Tfh	Follicular B helper T cells

Th1	T helper cell subset 1
Th17	T helper cell subset 17
Th2	T helper cell subset 2
Tip60	60 kDa Tat-interactive protein
TNF α	Tumor necrosis factor alpha
TRAF	TNF receptor associated factors
T-Rex	Tetracycline repressor protein expressing cells
Tris	Tris(hydroxymethyl)aminomethane
TYK2	Non-receptor tyrosine kinase 2

U

U4C-JAK1	Mutant fibrosarcoma cell line reconstituted with JAK1
UBL4A	Ubiquitin-like protein 4A
U-STATs	Unphosphorylated STAT proteins

V

VP24	Viral protein 24
------	------------------

W

WT	Wild type
----	-----------

Y

YFP	Yellow fluorescent protein
YXXQ	Tyrosin-any two amino acids-glutamine motif

Z

ZIPK	Zipper interacting protein kinase
------	-----------------------------------

Acknowledgements

First and foremost, I would like to express an enormous gratitude to my supervisor Prof. Dr. Gerhard Müller-Newen for his excellent guidance, critical and careful review of my research and an opportunity to work in his group. He has truly become a mentor of mine during the years and a person, who I always looked up to.

A special thanks to Prof. Dr. Martin Zenke for being both my master thesis and doctoral thesis supervisor, as well as for his kind support and review of this dissertation.

I am grateful to Prof. Dr. Bernhard Lüscher for being the third supervisor of this thesis and his vast help during my years at the Institute of Biochemistry and Molecular Biology, RWTH Aachen University.

In particular, I would like to say “Thank you very much” to Andrea Küster for her constant support, helpful advice and useful technical assistance.

Many thanks to Hildegard Schmitz-Van de Leur for sharing her vast experience and providing needed technical support.

Also I would like to thank all my current and ex-colleagues in Laboratory 13 for creating a nice working atmosphere: Sabrina Ernst, Anne Liong, Dirk Fahrenkamp, Nicolas Chatain, Anne Mohr, Dieter Görtz, Tamas Domoszlai, Natalie Rinis, Kasia Andryka, Vera Alexandrova, Marco Hoffmann, Corina Zimmermann and Sara Zafarnia.

I would like to thank also colleagues from the floor 42 (3. Etage des Flures 42), who have always been helpful and supportive, as well as all people from the Institute of Biochemistry and Molecular Biology for helpful advice and critical discussion during my research.

In addition, extra special thanks to my friends for their constant support and just being there for me: Nikolajs Tkacenko, Oxana Khamidova, Gufron Atokhojaev, Gulparis Atokhojaeva, Artjoms Kosovs, Natalja Pavlicenko.

Last, but not least, I would like to thank my mother Svetlana Martincuka and my grandmother Ludmila Zueva for their never-ending help and love. I owe all my accomplishments to them.

Curriculum Vitae (Deutsch)

Vor- und Zuname: Antons Martincuks
Studium Anschrift: Heinrichsallee 39
52062, Aachen
Geburtsdatum/–ort: 11.05.1987. Riga, Lettland.
Familienstand: ledig
Staatsangehörigkeit: Lettland

Schulbildung

09.1994 - 06.2006 Allgemeine Mittelschule (Rigaer Herderschule) in Riga, Lettland. Abschluss: Abitur, Deutsches Sprachdiplom der Kultusministerkonferenz

Hochschulbildung

09.2006 - 06.2009 Studium der Pharmazie an der Universität Lettlands in Riga, Lettland. Abschluss: Bachelor - Grad der Medizinwissenschaften auf dem Gebiet der Pharmazie
02.2009 - 05.2009 Aufenthalt an der Hogeschool Utrecht University of Applied Sciences im Rahmen der "ERASMUS" Austauschprogramms in Utrecht, Niederlande.
09.2009 – 01.2012 Studium an der Universität RWTH Aachen, Deutschland. Studienfach: Biotechnologie, Abschluss: Master of Science
Seit 04.2012 Promotion am Institut für Biochemie und Molekularbiologie an der Universität RWTH Aachen, Deutschland.

Berufspraxis

10.2011 – 12.2011 Wiss. Hilfskraft am Institut für Biochemie und Molekularbiologie an der Universität RWTH Aachen
04.2012 – 12.2012, Seit 01.2016 Wiss. Mitarbeiter am Institut für Biochemie und Molekularbiologie an der Universität RWTH Aachen

Ehrenamt

Seit 11.2012	Mitgründer und Vorstandsmitglied, Vereinigung Russischsprechender Studenten Aachens (VeRSA), Aachen
01.2014 – 03.2015	Präsident, Vereinigung Russischsprechender Studenten Aachens (VeRSA), Aachen

Weiterbildung

Sonstige Kenntnisse	Führerschein Klasse 3 FELASA-B Kurs, Aachen 2013 Seminar "Scientific Writing", Aachen, 2015 Seminar "Scientific Presenting", Aachen, 2016
---------------------	--

Sonstiges

Stipendien/ Studienfinanzierungen	01.08.2010 – 01.09.2011 Studienfinanzierung durch Bildungsfonds von Career Concept AG 01.10.2010 – 31.03.2012 Stipendium aus dem Bildungsfonds der RWTH Aachen 01.01.2013 – 31.12.2015 Promotionsstipendium durch die Studienstiftung des deutschen Volkes
Ehrenurkunden	Im Studienjahr 2010 gehörte ich zu den 3% der Besten des Jahrgangs (Deans List RWTH Aachen) DAAD-Preis 2015 für ausländische Studierende
Sprachkenntnisse	Gute Deutschkenntnisse in Wort und Schrift, Gute Englischkenntnisse in Wort und Schrift, Gute Lettischkenntnisse (Muttersprache) Gute Russischkenntnisse (Muttersprache)
EDV-Kenntnisse	MS Word, Excel, PowerPoint, Adobe Photoshop, Illustrator, GraphPad Prism

Curriculum Vitae (English)

Name: Antons Martincuks
Address: Heinrichsallee 39
52062, Aachen, Germany
Date and place of birth: 11.05.1987. Riga, Latvia
Family status: Single
Citizenship: Latvia

School education

09.1994 - 06.2006 Public high school (Rigaer Herderschule) in Riga, Latvia.
Certificate: German Language Certificate of the Education
Ministers Conference

Higher education

09.2006 - 06.2009 Pharmacy bachelor program at Latvian University in Riga,
Latvia. Degree: Bachelor of Science.
02.2009 - 05.2009 ERASMUS stay at Hogeschool Utrecht University of Applied
Sciences in Utrecht, Netherlands.
09.2009 – 01.2012 Biotechnology master program at RWTH Aachen University,
Germany. Degree: Master of Science.
Since 04.2012 Biology doctoral studies (Dr. rer. nat.) at the Institute of
Biochemistry and Molecular Biology, RWTH Aachen University,
Germany.

Relevant professional experience

10.2011 – 12.2011 Academic help at the Institute of Biochemistry and Molecular
Biology, RWTH Aachen University, Germany.
04.2012 – 12.2012, Research assistant at the Institute of Biochemistry and
Since 01.2016 Molecular Biology, RWTH Aachen University, Germany.

Honorary post

Since 11.2012	Co-founder and student board member, Vereinigung Russischsprechender Studenten Aachens (VeRSA), Aachen
01.2014 – 03.2015	Student Chairman, Vereinigung Russischsprechender Studenten Aachens (VeRSA), Aachen

Advanced training

Learned skills/certificates	Driving licence category b FELASA-B course, Aachen 2013 Seminar "Scientific Writing", Aachen, 2015 Seminar "Scientific Presenting", Aachen, 2016
-----------------------------	---

Miscellaneous

Scholarships/ Funding	01.08.2010 – 01.09.2011 Student funding via Career Concept AG 01.10.2010 – 31.03.2012 Scholarship from Education Fund, RWTH Aachen 01.01.2013 – 31.12.2015 PhD research fellowship from German National Academic Foundation
Honorary certificates	Deans List RWTH Aachen 2010 DAAD 2015 Award for Outstanding Achievements and Extraordinary Volunteer Involvement of International Students
Language skills	German: Advanced English: Fluent Latvian: Fluent Russian: Mother tongue
Computer literacy	MS Word, Excel, PowerPoint, Adobe Photoshop, Illustrator, GraphPad Prism

Eidesstattliche Erklärung

Hiermit erkläre ich an Eides statt, dass ich die vorliegende Dissertation:

„Role of STAT3 N-terminal domain and GAS-site recognition in signaling and crosstalk with STAT1 and NF- κ B”

selbstständig verfasst habe und dabei nur die angegebenen Quellen und Hilfsmittel benutzt verwendet habe.

Antons Martincuks
Aachen, 14.02.2017